Terms and Conditions of Use of Digitised Theses from Trinity College Library Dublin

Copyright statement

All material supplied by Trinity College Library is protected by copyright (under the Copyright and Related Rights Act, 2000 as amended) and other relevant Intellectual Property Rights. By accessing and using a Digitised Thesis from Trinity College Library you acknowledge that all Intellectual Property Rights in any Works supplied are the sole and exclusive property of the copyright and/or other IPR holder. Specific copyright holders may not be explicitly identified. Use of materials from other sources within a thesis should not be construed as a claim over them.

A non-exclusive, non-transferable licence is hereby granted to those using or reproducing, in whole or in part, the material for valid purposes, providing the copyright owners are acknowledged using the normal conventions. Where specific permission to use material is required, this is identified and such permission must be sought from the copyright holder or agency cited.

Liability statement

By using a Digitised Thesis, I accept that Trinity College Dublin bears no legal responsibility for the accuracy, legality or comprehensiveness of materials contained within the thesis, and that Trinity College Dublin accepts no liability for indirect, consequential, or incidental, damages or losses arising from use of the thesis for whatever reason. Information located in a thesis may be subject to specific use constraints, details of which may not be explicitly described. It is the responsibility of potential and actual users to be aware of such constraints and to abide by them. By making use of material from a digitised thesis, you accept these copyright and disclaimer provisions. Where it is brought to the attention of Trinity College Library that there may be a breach of copyright or other restraint, it is the policy to withdraw or take down access to a thesis while the issue is being resolved.

Access Agreement

By using a Digitised Thesis from Trinity College Library you are bound by the following Terms & Conditions. Please read them carefully.

I have read and I understand the following statement: All material supplied via a Digitised Thesis from Trinity College Library is protected by copyright and other intellectual property rights, and duplication or sale of all or part of any of a thesis is not permitted, except that material may be duplicated by you for your research use or for educational purposes in electronic or print form providing the copyright owners are acknowledged using the normal conventions. You must obtain permission for any other use. Electronic or print copies may not be offered, whether for sale or otherwise to anyone. This copy has been supplied on the understanding that it is copyright material and that no quotation from the thesis may be published without proper acknowledgement.

THE MODELLING OF ELECTRIC VEHICLE DRIVING CYCLES, USAGE PATTERNS AND AN INVESTIGATION OF THE ENVIRONMENTAL AND ECONOMIC IMPACTS OF ELECTRIC VEHICLES

John Brady

A dissertation submitted to the University of Dublin in the partial fulfilment of the requirements for the degree Doctor of Philosophy.

Department of civil, Structural & Environmental Engineering
Trinity College Dublin

May 2013

Abstract

The European Union has set a number of policy objectives to achieve a sustainable energy future through measures to tackle climate change and to ensure energy security. Electricity as fuel for vehicle propulsion offers the possibility to substitute fossil fuels with a wide diversity of primary energy sources. Recognising the potential benefits of electric vehicles, governments worldwide have established clear deployment goals for electric vehicles and have introduced consumer incentives. These sustainable energy objectives are clearly reflected in Ireland with targets to have 10% of the private car fleet powered by electricity and to generate 40% electricity from renewable energy sources by 2020.

The environmental and socioeconomic impacts of electric vehicles on society and the additional demand placed on the electricity grid need to be understood in order to support policy decisions. However, realistic environmental, economic and electricity grid impact studies can only be evaluated if the energy economy, the travel and charging patterns of electric vehicles operating in the real-world are understood. In addition, in order to enable the continued development of powertrains and energy storage systems for electric vehicles and to evaluate these developments a better understanding of real-world driving conditions are required. The purpose of this research is to study the environmental, economic and technical challenges of the mass market penetration of electric vehicles.

The use of electric vehicles for commuting is particularly favourable as driving range restrictions and long charging cycles are not major constraints. The potential reduction in road traffic related emissions due to commuting in the Greater Dublin Area in 2020 under different electric vehicle market penetration scenarios are evaluated. The results indicate that the introduction of electric vehicles presents an advantage over a business as usual scenario in terms of reducing emissions. Under the most likely scenario (10% market penetration by the year 2020) the results indicate a net reduction of 3% in CO_2 emissions relative to the business as usual scenario could be achieved, which will represent approximately 2% of the CO_2 emissions from the transport sector in 2020. The analysis supports existing international evidence that electric vehicles will contribute to emissions reductions however, the time required for electric vehicles to acquire a significant share of the national fleet, suggests that they will have a limited impact on climate change and urban air quality for at least the next decade.

Electric vehicles present policy makers worldwide with competing goals, the goal to support and encourage the adoption of electric vehicles, while on the other hand to tackle climate change and provide a sustainable transportation system. The loss in tax revenue as a consequence of incentive schemes is a debateable topic. An analysis of the socioeconomic costs and benefits of Ireland's

electric vehicle policy is conducted by comparing the environmental benefits, expressed in monetary value, with the associated reduction in tax revenues and the cost of the Irish government's electric vehicle incentive scheme. The analysis indicates that by 2020 the 10% market penetration of electric vehicles will result in a social marginal net loss of €324 million or €1,408 per vehicle. The primary reason for this loss is due to losses in all sources of tax revenue compared with the market penetration rates required to achieve a significant reduction in emissions. The findings of this analysis are in line with a number of international studies which have found that the mass market penetration of electric vehicles will result in losses in transportation related tax revenues.

In relation to the design of drivetrains and the subsequent evaluation of the environmental and lifecycle costs of existing and emerging vehicular technologies, it is important to have an understanding of real-world driving conditions in terms of velocity and acceleration profiles. Driving cycles have been developed to provide a velocity-time profile that are intended to be representative of real-world driving conditions and hence are used to assimilate driving conditions on a laboratory chassis dynamometer. However, existing driving cycles do not emulate real-world driving conditions particularly well and the requirement for realistic real-world driving cycles to be developed has been cited in the literature. A four-step modelling approach for developing driving cycles is presented and a set of driving cycles for the Greater Dublin Area are developed. It was determined that electric vehicles almost entirely operate in urban driving conditions and that the energy economy of an electric vehicle is highest on short journeys and in urban stop-start driving conditions. The developed driving cycles outperform a selection of existing well-established worldwide driving cycles with respect to representing real-world driving conditions in the Greater Dublin Area. It was found that real-world driving patterns differ from existing certification driving cycles developed for emissions testing in Europe, America and Japan. They generally consist of lower velocity driving and higher acceleration rates. The developed driving cycles would aid in the design of electric vehicles that are operating in the Greater Dublin Area and would allow electricity grid analysis, economic and lifecycle studies to be conducted with a higher degree of confidence.

In the past the scientific community have used deterministic approaches to model the travel and charging patterns of electric vehicles in order to evaluate the impacts of electric vehicles on the electricity grid and to support policy decisions. However, given the complexity and stochastic nature of these behaviours, a stochastic model would be more beneficial. A stochastic simulation approach to simulate the travel patterns and charging profiles of electric vehicles is developed. The model uses an iterative method of conditional distributions with a Bayesian inference to generate journey schedules by synthesising journey distances, journey times and parking times. At each destination a probabilistic charging decision model is used to simulate charging decision making behaviour and hence charging profiles for a fleet of electric vehicles. Additional factors such as

battery characteristics, the probability of charging point availability at destinations and plugging-in behaviour are included in the model. The charging aspect of the overall model performs satisfactorily, however, the inherent errors due to the complexity of the underlying travel pattern model has implications for the simulated charging profiles. Therefore, further development of the underlying travel pattern model is needed in order for the model to be a viable tool for analysing the impacts on the electricity grid of large scale electric vehicle deployment.

Acknowledgements

The completion of this doctoral dissertation was possible with the support of several people. I would like to express my sincere gratitude to all of them. First of all, I would like to express my immense gratitude to my supervisor Prof. Margaret O'Mahony, for her valuable guidance, scholarly inputs and consistent encouragement. She has been an excellent supervisor. Her links to industry and other researchers have been invaluable.

I would also like to thank Mr. Senan Mcgrath of ESB ecars for providing access to data from electric vehicles, without which this research would not have been possible.

To my family and friends, whose support over the past few years has been immense. My younger siblings, Catriona, Conor and Cathal have been a constant source of encouragement. To my parents, Pat and Pauline, who instilled a great interest in learning in me from an early age, and to whom I am always grateful.

Table of Contents

Declaration

I declare that this thesis has not been submitted as an exercise for a degree at this or any other university and it is entirely my own work.

I agree to deposit this thesis in the University's open access institutional repository or allow the library to do so on my behalf, subject to Irish Copyright Legislation and Trinity College Library conditions of use and acknowledgement

May 2013

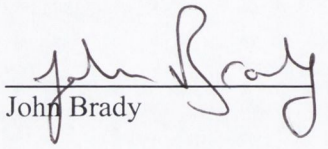

John Brady

List of Acronyms

AEIG Atmospheric Emissions Inventory Guidebook

AMT Annual Motor Tax

BAU Business as Usual

BEV Battery electric vehicle

CAN Control Area Network

CBA Cost Benefit Analyses

CDF Cumulative distribution function

CO Carbon Monoxide

CO_2 Carbon Dioxide

CO_{2eq} Carbon Dioxide Equivalent

COV Coefficient of variation

CSO Central Statistics Office

DCSMV Driving Cycle Statistical Metrics Vector

DEHLG Department of Environment Heritage and Local Government

DEI Driving Environment Identifier

DERT Driving environment recognition tool

DIE Driving Information Extractor

EAEV European Association for Electric Vehicles

ED Electric Driving

EEA European Environment Agency

EPA Environmental Protection Agency

EPRI Electrical Power Research Institute

ESB Electricity Supply Board

ESRI Economic and Social Research Institute

EUDC Extra Urban Driving Cycle

FTP Federal Test Procedure

FTP File Transfer Protocol

GDA Greater Dublin Area

GHG Greenhouse Gas

GPS Global Positioning System

HBS Household Budget Survey

HEV Hybrid electric vehicle

HFV Hydrogen Fuel cell Vehicles

HWFET Highway Fuel Economy Test cycle

ICE Internal combustion engine

ICEV Internal Combustion Engine Vehicles

LDVs Light-duty vehicles

LOS Level of service

LVQ Learning Vector Quantisation

MER Minimum Energy Requirement

MLE Maximum likelihood estimation

MNB Marginal Net Benefit

MOU Memorandums Of Understanding

NCCS National Climate Change Strategy

NEC National Emissions Ceiling

NEDC New European Driving Cycle

NN Neural networks

NO_X Oxides of nitrogen

NRDC Natural Resources Defence Council

NYCC New York City cycle

OECD Organisation for Economic Co-operation and Development

OMSP Open Market Selling Price

PCA Principle Component Analysis

PDF Probability density functions

PER Primary Energy Requirement

PHEV Plug in hybrid electric vehicle

PKE Positive acceleration kinetic energy

PM_{10} Particular Matter, diameter less than 10 microns

$PM_{2.5}$ Particular Matter, diameter less than 2.5 microns

POWCAR Place of work Census of Anonymised Records

SAFD Speed and acceleration distribution

SEAI Sustainable Energy Authority Ireland

TAD Total absolute second to second difference

TPM Transition probability matrix

UDC Urban Driving Cycle

UDDS Urban Dynamometer Driving Schedule

UNECE United Nations Economic Commission for Europe

UNECE United Nations Economic Commission for Europe

UNFCCC United Nations Framework Convention on Climate Change

V2G Vehicle to grid

VAT Value Added Tax

VOC Volatile Organic Compounds

VRT Vehicle Registration Tax

WLTP Worldwide harmonised Light vehicles Test Procedures

List of Publications

1. Brady, J. and O'Mahony, M. 2011. Introduction of electric vehicles to Ireland: Socioeconomic analysis. *Transportation Research Record: Journal of the Transportation Research Board*, 64-71.

2. Brady, J. and O'Mahony, M. 2011. Travel to work in Dublin. The potential impacts of electric vehicles on climate change and urban air quality. *Transportation Research Part D: Transport and Environment,* 16, 188-193.

List of Tables

List of Figures

1 Introduction

Globally, in 2010, the transport sector consumed approximately 2,200 million tons of oil equivalent (mtoe), which constituted about 19% of global energy supplies (World Energy Council, 2010). Road transport accounted for the majority (76%) of the transportation energy consumption of which light-duty vehicles (LDVs) accounted for 52% (World Energy Council, 2010). Correspondingly, the CO_2 emissions from the transport sector accounted for 23% of global CO_2 emissions of which emissions from LDVs accounted for 41% (World Energy Council, 2010). Over the period 1990 to 2007, CO_2 emissions from transport have grown globally by 45%, led by emissions from the road sector in terms of volume and by shipping and aviation in terms of highest growth rates (OECD, 2010). This growth in energy consumption and emissions closely follows the global economic and population growth in the last decade. According to the World Bank, growth in the Gross Domestic Product (GDP) between 2000 and 2006 for Organisation for Economic Co-operation and Development (OECD) and non-OECD countries was 2.5% and 4.9% per year respectively. With regards to population growth, over the same period, the World Bank states that the OECD's population grew by 0.7% per year, while the non-OECD population grew by approximately 1.5% per year. Globally, the transportation sector will face several unprecedented challenges in the coming decades. The world's population is expected to increase by 2.2 billion, reaching 9.2 billion by 2050, with more than two-thirds of the population living in cities (World Energy Council, 2010). Correspondingly energy consumption in the transport sector is forecast to increase by between 80%-130% (World Energy Council, 2010) and the Joint Research Centre (2008) forecasts the emissions from transport will increase by 19%.

With these challenges in mind, electricity as fuel for vehicle propulsion offers the possibility to substitute oil with a wide diversity of primary energy sources. This could ensure security of energy supply and a broad use of renewable and carbon-free energy sources in the transport sector which could assist global CO_2 emissions reduction targets.

In Europe, the electrification of transport has been made a priority in the Community Research Programme (European Commission, 2013b) and it also figures prominently in the European Economic Recovery Plan (European Commission, 2008) within the framework of the Green Car Initiative (European Commission, 2013a). The policy related to battery-powered vehicles is mainly focused on technological optimisation and market development. As such, the European Commission is supporting a Europe-wide electromobility initiative, Green eMotion (European Commission, 2013c), which is a partnership of forty-three partners from industry, utilities, vehicle manufacturers, municipalities, universities and research institutions. The objective of the initiative is to facilitate the mass market roll-out of electric vehicles (EV) in Europe. Individually, a number

of European governments have established clear deployment goals for EVs and have introduced consumer incentives. Norway, Denmark, and England have set targets to have approximately 50,000, 200,000 and 1.7 million EVs respectively deployed by 2020 (Houses of Parliament, 2010, Avere, 2012). In Ireland a target for 10% (230,000 vehicles) of the private car fleet to be powered by electricity by 2020 was announced in 2008 (Dempsey, 2008). Many countries offer subsidies of approximately €5,000 towards the retail price to early purchasers of EVs in an attempt to grow their EV markets. The highest incentives are in Norway and Denmark, where EVs are exempt from vehicle registration tax, which can be in excess of €10,000 (Houses of Parliament, 2010). Several other governments worldwide have announced ambitious targets for EV uptake. The Japanese government has set a target of 20% EVs, including hybrids, plug-in hybrids, battery-electric and fuel cell vehicles (Electric Vehicles Initiative, 2013). In America, the Recovery Act of 2009 (United States Congress, 2009) included $2.4 billion funding to support the research and design of vehicles and infrastructure with a target to deploy one millions EVs by 2015 was announced in 2011 (Department of Energy, 2011). To achieve this target and to accelerate EV adoption, a number of incentives including tax credits up to $7,500 towards the purchase price of EVs have been introduced.

During the last decade a large body of literature concerning the economic and environmental analysis of alternative fuels in vehicle propulsion systems has been published (Granovskii et al, 2006, Samaras and Meisterling, 2008, Shiau et al, 2009). The electrification of commuter vehicles seems particularly favourable as driving range restrictions and long charging cycles are not major constraints. Doyle and Adomaitis (2013) report that up to 10,000 EVs have been sold in Norway and many are used for commuting in Oslo due to incentives such as free parking and charging, road tolls and the use of bus lanes which equates to a saving of approximately $8,200 per year. Hughes and Sundaram (2011) analysed the potential reduction in greenhouse gas (GHG) emissions by substituting commuter internal combustion engine vehicles (ICEV) with EVs in Nova Scotia in Canada and found that whilst the vehicles rely on carbon-based fuel for their propulsion the cumulative decadal GHG emissions reduction could be up to 31%. In Ireland, a number of studies have found that there is extensive short and long distance car-based commuting in the Greater Dublin Area (GDA) (Commins and Nolan, 2008, Horner, 1999, Morgenroth, 2001, Morgenroth, 2002). Therefore, the first objective of this thesis it to estimate the potential reduction in road traffic related emissions due to commuting in the GDA under different EV market penetration scenarios.

Common to all new technologies, EVs face barriers to adoption, such as lack of knowledge by potential users, low consumer risk tolerance and high initial costs (Diamond, 2009). In an attempt to address some of these market barriers it has become common for governments to introduce financial consumer incentives to encourage the purchase of EVs. However, the arrival of EVs

presents policy makers worldwide with competing goals. On one hand there are policy goals that support and encourage the adoption of EVs, while on the other hand there is a need to continue to fund the transportation system. Hence, incentive programmes are often the subject of public and political debate. Herynkova (2009) conducted a social cost benefit analysis of the market penetration of EVs in Denmark for the year 2020 and found that from a purely financial perspective EVs are not socially profitable as the reduction in environmental costs is by far offset by the decrease in tax revenues. In America, the Congressional Budget Office (2012) estimates that federal policies to promote the manufacture and purchase of EVs will cost $7.5 billion up to 2019 of which tax credits for purchasing EVs will account for $1.8 billion. For the European Union (EU), Essen and Kampman (2011) estimate that under the most realistic scenario of 3.3 million EVs by 2020 and 50 million EVs by 2030, a net loss in tax revue of €18 billion in 2030 would be realised.

In consideration of these international studies and in order to investigate new options for transportation funding it is first necessary to understand the impact that EVs could have on tax revenue. Therefore, the second objective of this thesis is to estimate the socioeconomic costs and benefits of the 10% market penetration of EVs in Ireland, by comparing the environmental benefits, expressed in monetary value, with the associated reduction in tax revenues and the cost of the Irish government's EV grant scheme.

In relation to the design of drivetrains and the subsequent evaluation of the environmental and lifecycle costs of existing and emerging vehicular technologies, it is important to have an understanding of real-world driving conditions in terms of velocity and acceleration profiles. Driving cycles have been developed to provide a velocity-time profile that are intended to be representative of real-world driving conditions and hence are used to assimilate driving conditions on a laboratory chassis dynamometer. In addition to playing an important role in design they also serve as a standardised measurement procedure for the certification of a vehicle's fuel economy, emissions and driving range.

However, research has shown that there is poor correlation between existing driving cycles and real-world driving conditions with regards to estimating fuel consumption and emissions, particularly in relation to modal driving cycles (Eva, 2000, Tzirakis et al, 2006). There are significant variations in real-world operating conditions compared to test procedures and this variation causes a significant difference in emissions and fuel economy in real-world operating conditions. The German Ministry of Transport, Building and Urban Development recently demonstrated that the majority of cars consume around 25% more fuel and thus emit more CO_2 emissions than certified (Helmers and Marx, 2012). Of the one hundred cars investigated 40% exceeded their certified limit, while a couple of percent of the vehicles had a fuel consumption of

up to 70% higher than certified. Real-world driving in America has also recently been analysed, and it has been shown that the American certification driving cycles, the Urban Dynamometer Driving Schedule (UDDS) cycle and the Highway Fuel Economy Test cycle (HWFET) are much less aggressive than real-world driving conditions, thus leading to the significant under prediction of peak power demands and energy economy (Fellah et al, 2009, Patil et al, 2009, E. D. Tate et al, 2009). Existing driving cycles are intuitive choices for the design of vehicles because they are the driving cycles that are used for the certification of emissions and fuel economy. However, designing vehicles to a fixed driving cycle, especially EVs, results in a suboptimal vehicle for any driving environment that varies significantly from the driving cycles used in the design. Discrepancies between existing driving cycles and real-world driving conditions exist due to a number of factors such as insufficient data, inadequate driving cycle development methodologies and methods to assess the representativeness of developed driving cycles of real-world driving conditions.

The literature demonstrates that existing driving cycles do not emulate real-world driving conditions particularly well and cites the requirement for realistic real-world driving cycles to be developed (Ashtari et al, 2012a, Helmers and Marx, 2012, Rask and Rousseau, 2012). In addition, regulatory agencies worldwide are seeking to update testing procedures to account for real-world driving conditions in order to certify and assess the lifecycle costs of emerging vehicular technologies. In an attempt to address the limitations of existing driving cycles, the next objective of this thesis is to undertake a review of existing driving cycle development methodologies and to conduct an analysis of real-world driving cycles in order to contribute to the knowledge regarding the real-world operating conditions and energy demands of EVs. A modelling approach for the development of real-world driving cycles will be proposed and set of real-world driving cycles for the Greater Dublin Area will be developed and evaluated.

The environmental and economic impacts of EVs are linked to the times and energy mix of the electricity grid from which they are charged. In addition, policy decisions in relation to investment in electricity grid infrastructure are linked to the perceived societal benefits of EVs and the impacts that EVs could have on the electricity grid. It is generally accepted that the charging of a large population of EVs will have two major effects on the grid; it will increase the overall power load needed and it will increase the load on local distribution networks. Either of these could become the limiting factor but it is believed that the local load distribution problems will become prevalent sooner than the more general overall power supply issue (Hill et al, 2012). However, the uncontrolled charging of a large population of EVs could increase peak demand substantially. System operators must largely rely on conventional generators (fossil fuels) to meet this demand. This would reduce potential GHG emissions reduction benefits and increases in the peak demand could require transmission capacity expansion.

Therefore, in order to support policy decisions, the impact of EVs on the power system needs to be evaluated. In order to achieve this, reliable models capable of translating the travel and charging patterns of a large population of EVs into their respective power demand are needed. The complexity and stochastic nature of travel and charging patterns point to a stochastic model to satisfactorily model these behaviours. In the past couple of years, the scientific community has been more focused on the analysis of the potential impact of charging EVs. The effect of the large-scale integration of EVs into the power grid has been studied in several papers (Dallinger et al, 2011, Di et al, 2011, Kristoffersen et al, 2011, Lojowska et al, 2012) and issues such as peak load, network losses and cost minimisation have been analysed. However, the majority of the early studies have used a deterministic approach to model travel patterns, using collected data directly or expected values and averages (Di et al, 2011, Mullan et al, 2011, Weiller, 2011). This approach fails to capture the stochastic nature of travel behaviour. Observed vehicle travel patterns have been reported in many studies (Golob and Gould, 1998) but the stochastic modelling of driving patterns has received little attention until recently (Ashtari et al, 2012b, Green et al, 2010, Hill et al, 2012, Lojowska et al, 2011, Lojowska et al, 2012). In addition, EV electricity grid integration studies either assume definite charging whilst a vehicle is parked or charging is conditioned upon a set of rules usually related to the state of charge (SOC) and/or the length of time that the vehicle is parked. Therefore, the final objective of this thesis is to review exiting EV travel pattern and charging modelling approaches and to develop a stochastic travel pattern and charging model capable of generating representative schedules of daily journeys and hence charging profiles for a population of EVs.

The Place of work Census of Anonymised Records (POWCAR) dataset (Central Statistics Office, 2007a), which is derived from the data gathered in the 2006 Irish census and the ISus private car stock model developed by the Economic and Social Research Institute (ESRI) (Hennessy and Tol, 2010) are the primary sources of data for the environmental and socioeconomic research presented in this thesis. In 2010, a nationwide EV demonstration project was launched in Ireland. Fifteen EVs were trialled in households of ESB (an Irish electricity utility company) employees for periods of four months over a two year period. Data collected by data logging equipment installed in the vehicles is the primary source of data for the driving cycle, travel and charging pattern models presented in this thesis.

To summarise, the objectives of this research are as follows:

1. To estimate the potential reduction in road traffic related emissions due to commuting in the Greater Dublin Area under different EV market penetration scenarios.

2. To estimate the socio-economic costs and benefits of the 10% market penetration of EVs in Ireland, by comparing the environmental benefits, expressed in monetary value, with the associated reduction in tax revenues and the cost of the Irish government's EV grant scheme.

3. To undertake a review of existing driving cycle development methodologies and to conduct an analysis of real-world driving cycles to contribute to the knowledge regarding the real-world operating conditions and energy demands of EVs.

4. To propose a modelling approach for the development of real-world driving cycles, to develop and evaluate a set of real-world driving cycles for the GDA.

5. To review exiting EV travel pattern modelling approaches and to develop a stochastic travel pattern model to synthesise a representative schedule of daily journeys for a population of EVs.

6. To review existing EV charging models and to develop and integrate a charging model into the travel pattern model to simulate the charging profiles of a population of EVs.

The remainder of this thesis is structured as follows:

Chapter 2 evaluates the potential reduction in road traffic related emissions due to commuting in the GDA in 2020 under different EV market penetration scenarios. The POWCAR dataset is used as the source of origin-destination commuting patterns. The ISus private car stock model is used to make assumptions about the future size and breakdown of the private car fleet. Assumptions regarding the number of people in employment and commuting in the GDA are based on future employment projections by the ESRI. The potential reduction in tailpipe emissions is calculated using the COPERT 4 tailpipe emissions model (European Environment Agency, 2009). This chapter concludes with a discussion of the findings.

Chapter 3 presents a social cost-benefit analysis of the 10% market penetration of EVs in Ireland by 2020. It employs the same datasets and modelling techniques used in Chapter 2. It analyses the socioeconomic costs and benefits of this policy by comparing the environmental benefits, expressed in monetary value, with the associated reduction in tax revenues and the cost of the government's EV grant scheme. This chapter concludes with a discussion of the findings and areas for further research.

Chapter 4 forms the basis of the research presented in Chapter 5. This chapter provides an overview of driving cycles and reviews existing driving cycle development methodologies for ICEVs and EVs. An overview of a proposed four-step modelling approach for developing a set of

real-world driving cycles for the GDA is presented. The EV demonstration project and the data collection techniques are outlined. The remainder of the chapter details the first step in the modelling approach. A description of the employed data processing techniques which were implemented to remove erroneous data points is presented. The simulation of an EV drivetrain to estimate the energy economy of EVs over the recorded real-world driving cycles is explained. Finally, a driving environment recognition tool is developed to determine and classify the driving conditions in terms of road-types and levels of congestion that the EVs in the demonstration project operated in. This facilitates an analysis of the energy economy of EVs in different driving environments and allows the proportion of time spent operating in different driving environments to be determined. This chapter concludes with a discussion of the findings and introduces the research presented in Chapter 5.

In Chapter 5 the remaining three-steps of the proposed modelling approach to developing driving cycles are outlined. Firstly, a Markov-chain driving cycle model developed with real-world data is presented. The purpose of the model is to synthesis candidate driving cycles. Secondly, a driving cycle assessment procedure is outlined. A regression analysis is presented which identifies driving cycle parameters that are statistically significant in terms of influencing the energy economy of an EV over a driving cycle. When synthesising driving cycles with the Markov-chain model multiple iterations of the process are performed until the statistical parameters of the synthesised driving cycles, identified by the regression analysis, match the mean of the statistical parameters of real-world driving cycles within certain error bounds. This ensures that a developed driving cycle is representative of the real-world driving cycles in the dataset. In the final step, two methodologies are used to assess the representativeness of the developed driving cycles and a selection of well-established worldwide driving cycles of the original real-world driving cycle dataset. Two methodologies are also used to compare the developed driving cycles to the selection of worldwide cycles. This chapter concludes with a discussion of the merits of the developed driving cycles and areas for further research.

Chapter 6 forms the basis of the research presented in Chapter 7. In this chapter a stochastic travel pattern model that simulates a schedule of daily journeys for a population of EVs is presented. GPS travel data collected during the EV demonstration project are used to derive distributions of travel pattern related variables. The dependence structure between six variables is modelled using a non-parametric copula function. The model uses an iterative method of conditional distributions with a Bayesian inference to generate journey schedules by synthesising journey distances, journey times and parking times. This chapter concludes with a discussion of the performance of the model and options for the further development of the model. The research presented in Chapter 5 is also introduced. Finally, areas for further research in relation to the modelling of the travel patterns of EVs are also discussed.

Chapter 7 extends the model presented in Chapter 6. The developed model translates the transportation patterns of a population of EVs into the respective power demand of the EVs. At the end of each journey scheduled by the travel pattern model a decision is required as to whether or not to charge the battery. A number of different methods of modelling charging decision making behaviour are investigated and a probabilistic charging model is incorporated into the travel pattern model. Additional factors such as battery characteristics, the probability of charging point availability at destinations and plugging-in behaviour are included in the model. The chapter concludes with a discussion of the performance of the model and areas for further research.

The final chapter, Chapter 8, concludes with a discussion of the main findings and the contribution to knowledge. This chapter summarises the main findings of the thesis.

2 Travel to work in Dublin. The potential impacts of electric vehicles on climate change and urban air quality

As discussed in Chapter 1, the Irish government has outlined plans for 10% of the national road fleet to be powered by electricity by 2020. Typically, EVs are seen as viable substitutes for commuter vehicles due to the repetitive nature and fixed distances of their trips and because the vehicles can be charged during daytime and overnight. This chapter evaluates the potential reduction in road traffic related emissions due to commuting in the Greater Dublin Area under different EV market penetration scenarios. The results indicate that the introduction of EVs offers the potential for reductions in all road traffic related emissions. However, the time required for EVs to acquire a significant share of the fleet, suggests that they will have a limited impact on climate change and urban air quality for at least the next decade. The contents of this chapter are published in Brady and O'Mahony (2011).

This chapter is organised as follows: Section 2.1 provides an overview of the Irish transport sector and emission levels in Ireland. Section 2.2 includes a literature review of (i) travel to work patterns in Dublin, (ii) the Irish private car fleet, (iii) urban air quality in Dublin and (iv) the potential of EVs to reduce emissions. Section 2.3 describes the dataset used and Section 2.4 presents the methodology implemented to estimate the potential reduction in emissions. In Section 2.5 the results are presented and analysed and Section 2.6 concludes the chapter.

2.1 Overview of the transport sector and emission levels

The transport sector contributes greatly to global GHG emissions and is responsible for approximately 23% of carbon dioxide (CO_2) emissions worldwide (IPCC, 2007). In Ireland, under the National Climate Change Strategy (NCCS), the Environmental Protection Agency (EPA) is the designated agency for developing national annual emission projections. The Department of Environment Heritage and Local Government (DEHLG) report the annual GHG emissions to the United Nations Framework Convention on Climate Change (UNFCCC), the European Environment Agency (EEA) and the United Nations Economic Commission for Europe (UNECE) to determine emissions ceilings under the EU National Emissions Ceiling (NEC) directive and the United Nations Economic Commission for Europe (UNECE) Gothenburg Protocol.

In 2008, transport emissions in Ireland accounted for 21.3% (14,255 $MtCO_{2eq}$) of the national total, which represents an increase of 176% on 1990 levels (Environmental Protection Agency, 2009c). This upsurge can be attributed to a period of unprecedented economic growth, which led to an increase in vehicle numbers, the purchase of larger vehicles and the reliance on private cars for commuting to and from work (Environmental Protection Agency, 2009c). Due to the economic slowdown, the annual growth rate of transport emissions is projected to slow significantly, however continued growth is expected. Based on recent economic projections by the Economic and Social

Research Institute (ESRI) of Ireland and incorporating additional energy efficiency savings as described in Ireland's National Energy Efficiency Plan (Department of Communications Energy and Natural Resources, 2007), Sustainable Energy Authority Ireland (SEAI) forecast an average annual growth in transport energy demand of 3.1% per annum for 2012-2020 (Environmental Protection Agency, 2009b, Howley et al, 2009b). This forecast includes EV deployment and additional measures outlined in the Department of Transport's Sustainable Travel and Transport Action Plan (Department of Transport, 2008). The SEAI's energy demand forecast is based the ESRI's 2008 Medium-Term Review and only takes into account the ESRI's Autumn 2008 Quartly Economic Commentary. This assumes a recession in the short term (2008-2009) and that the economy will return to its position where it otherwise would have been by 2020 (Environmental Protection Agency, 2009b). Derived from these projections and coupled with an economic shock analysis, which takes account of the further deterioration of the economy since Autumn 2008, transport emissions are expected to increase by 11% (16 $MtCO_{2eq}$) over the period 2007-2020 (Environmental Protection Agency, 2009b).

Ireland's transport sector is highly dependent on imported fossil fuels. In 2009 over 99% of the energy use in transport was dependant on imported oil as a fuel (Howley et al, 2009b). This reliance makes Ireland very vulnerable to the supply and price of oil. The price of crude oil doubled between July 2007 and July 2008, leading to peak petrol and diesel prices of €1.34 and €1.44 per litre (Howley et al, 2009b). It is difficult to forecast future crude oil prices as international demand patterns are dependent on a wide variety of factors such as the strength of the global economy and future oil discoveries. However, oil is a limited natural resource hence it is expected that the demand and price will continue to increase.

2.2 Review of the literature

This section reviews the literature in relation to travel to work patterns in Dublin, the Irish private car fleet, urban air quality in Dublin and the potential of EVs in reducing emissions

2.2.1 Travel to work patterns in the GDA

Due to the rapid economic development, employment and household incomes have increased significantly in Ireland over the last decade. This has subsequently led to a substantial increase in the level of car dependence and private car registrations in the country. These trends are particularly noticeable in Greater Dublin Area (GDA), which saw an increase in employment by 48.9% and private car registrations by over 60% over the period 1996-2006 (Central Statistics Office, 2007b). In 2006, 51.8% of commuters in the GDA travelled to work by car, an increase of 5% on 1996 levels (Commins and Nolan, 2008). The GDA is defined as Dublin City and the surrounding counties of Fingal, Dun Laoghaire-Rathdown, South Dublin, Kildare, Wicklow and Meath.

During the period of economic growth, a number of studies focusing on the extent on commuting and travel patterns in Ireland have been conducted. Horner (1999) employed data from the 1991-1996 Census. The analysis revealed greater car usage for short journeys and a significant increase in long-distance car-based commuting across the country. Overall, there was a 42% increase in car-based commuting over the period 1991-1996. In 1996, 52.6% of commuters travelling under 10 miles to work did so by car. Furthermore, the car was the mode of choice for 80% of those travelling more than 10 miles. Morgenroth (2001) used data supplied by the Irish Revenue Commissioners to estimate the extent of the commuting belt around Dublin. In 2000, 54.1% of commuters in Ireland travelled to work by car, an increase of nearly 8% since 1996. It was concluded that in fact the commuter belt extends beyond the GDA and that a substantial number of individuals commute long distances from counties outside the GDA. This is referred to as the "Outer Belt" region in Figure 2.1.

Figure 2.1. Commuter belt for Dublin City Morgenrath (2001).

Morgenroth (2002) drew on data from the 1991-1996 Census and the Central Statistics Office's (CSO) quarterly national household travel to work survey, to analyse the determinants of inter-county commuting flows. An increasing reliance on cars for long distance commuting, which is prevalent in rural counties surrounding major urban centres was revealed. In 1996, over 140,000 workers commuted more than 15 miles to work, a 52% increase on 1996 levels. Walsh et al (2006) used 2002 Census data to estimate commuter catchment areas around gateways and hubs outlined in the National Spatial Strategy. They too identified extensive long-distance car based commuting (greater than 30 kilometres) associated with large towns and cities, such as Cork, Limerick and

Galway but particularly Dublin City. A larger proportion of individuals were found to commute to Dublin from areas of North Wexford, Carlow, Laois, East Offaly, Westmeath, South Cavan and Louth. This supports the findings of Morgenroth (2002).

Similar travel patterns in relation to commuting have been observed in other European metropolitan areas. Kendall (2008) states that worldwide commuter distances are below 50 km as well as most other daily trips. On average 84% of all car trips in London are less than 20 km and 95% of individuals travel less than 75 km per day (Mayor of London, 2009). Nagelhout and Ros (2009) argue the EVs appear to be most suited for short to medium-range distance trips, a trait shared by the majority of Irish commuters. The European Association for Electric Vehicles (EAEV) also refer to the high potential of EVs as a small, low-powered second car that could be used for short trips and daily commuting (European Association for Electric Vehicles, 2009).

2.2.2 The private car fleet in Ireland

As a result of the rapid economic and social change in Ireland over the last decade the number of private cars in Ireland rose from 990,000 in 1995 to just under 1.9 million in 2007, an increase of 90% (Department of Transport, 2009). The reliance on the passenger car for inland transport accounted for 76.1% of the total inland passenger kilometres, considerably below the EU 27 average of 83.4% (Eurostat, 2009a).

Another aspect of the economic growth is the increase in car density. The two most commonly used indicators to measure car density are the private-car ownership level per 1,000 of the population and the number of cars per household. The level of car ownership influences an individual's mode of travel to work and in 2006 the rate of car ownership was 412 per 1000 habitants, slightly below the EU 27 average of 466 per 1000 habitants (Eurostat, 2009b). This suggests that there is room for continued growth of the private car fleet in Ireland. Between 2002 and 2006, the number of households that owned at least two cars increased from 478,660 to 1,242,839, representing 68% of all households. Increasing car ownership levels have been a trend of the last two decades. Between 1991 and 2002 the proportion of households with at least two cars increased more than five times from 87,174 to 478,660 (Horner, 1999).

In addition to the growth in the number of private cars, there have also been considerable changes in the structure of the fleet. Figure 2.2 shows how the purchasing trends of private vehicles with respect to engine size have changed over the period 1990-2008. It demonstrates a shift in purchasing trend towards cars of larger engine sizes. Cars with an engine size of 1.2 litres or less are showing steadily declining numbers, whereas cars with an engine size greater than 1.2 litres are all showing increasing trends. Cars with an engine size in the 1.2-1.5 litre range are the fastest growing range and accounted for 38% of the total fleet in 2008. The 1.5-1.7 litre, the 1.7-1.9 litre

and the greater than 1.9 litre bands are also steadily increasing, accounting for 15.9%, 13.8% and 16.8% of the total fleet in 2008 respectively (Howley et al, 2009b).

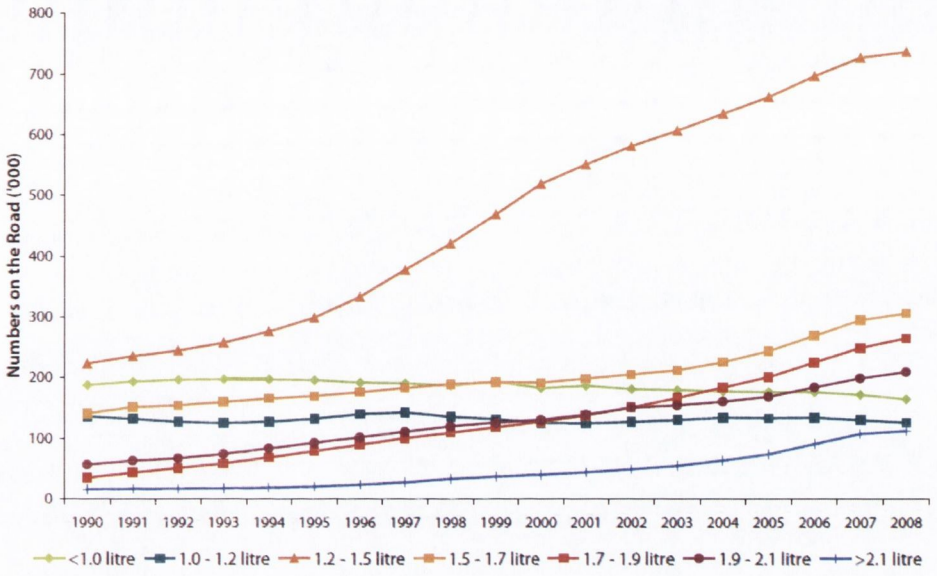

Figure 2.2. Trends in the private car fleet structure (Howley et al, 2009b).

In 2009, the average annual mileage of passenger vehicles in Ireland was 16,708 kilometres, with a higher average mileage for diesel cars (15,054 km) than petrol cars (9,486 km). Typically passenger vehicles with an engine size less than 1.2 litres have a lower than average annual mileage for both petrol and diesel vehicles.

2.2.3 Air quality in Dublin

The contribution of road traffic to levels of air pollutants can vary dramatically in urban areas. A recent study indicates that Dublin's air quality is extremely favourable when compared to 26 other European cities and in 2008 the levels of all pollutants were within the legal parameters (Boldo et al, 2006, O'Leary, 2009).

When considering urban air quality, six major pollutants are considered. Two classifications of particular matter, one having a diameter less than 10 microns (PM_{10}) and one of diameter less than 2.5 microns ($PM_{2.5}$), which is generally considered to be the most harmful to human health (Kantor et al, 2009). This small particular matter can penetrate deep into the respiratory system increasing the frequency and severity of respiratory disorders. In 2008, the annual mean concentrations measured at all stations in Ireland were below the 40 $\mu g/m^3$ limit value for annual mean. $PM_{2.5}$ is only measured at one station in Ireland and in 2008 it was within than annual mean limit for $PM_{2.5}$ of 25 $\mu g/m^3$ (Environmental Protection Agency, 2009a). Carbon monoxide (CO) is a colourless and odourless gas, formed when carbon in fuel is not completely oxidised. It enters the bloodstream thought the lungs and reduces oxygen delivery to the body's organs and tissues (Boldo et al, 2006). The highest maximum 8-hour CO level of 6.2 mg/m^3 was recorded at Coleraine Street in Dublin,

which is within the permitted daily 8-hour CO level of 10 mg/m^3. The short term exposure to Nitogen dioxide (NO_2) is associated with reduced lung function and airway responsiveness and increased reactivity to natural allergens. In 2008, the highest annual mean concentration of NO_2 (36 $\mu g/m^3$) was also recorded at Coleraine Street in Dublin, but this was within the annual mean limit for NO_2 of 40 $\mu g/m^3$ (Environmental Protection Agency, 2009a). Volatile organic compounds (VOCs) and oxides of nitrogen (NO_X) react with sunlight to form photochemical smog, which is generally the largest contributor to urban air pollution in industrialized cities. NO_X also contributes to the formation of acid rain and is a recognized ozone precursor.

2.2.4 Electric vehicle impact studies on emissions and air quality

Recently EVs have been gaining a lot of attention around the world due to their ability to reduce the reliance on diesel/gasoline and thus reducing tailpipe emissions. The concept of an EV has been around since the late 1890s long before global warming became a global concern (Electric Auto Association, 2005). As battery technology advances, EVs are becoming a more realistic option in the battle against global warming. The International Energy Agency (IEA) state that EVs and hybrids are "*likely to garner support because of their broad ability to consistently reduce negative externalities with respect to energy imports, GHGs and air quality*" (Passier et al, 2007).

The net reduction in GHGs realised by replacing conventional internal combustion engine vehicles (ICEV) with EVs is the difference between the GHG emissions avoided by reducing fuel consumption, the GHG emissions produced by generating electricity and any additional GHG emissions emitted during the manufacturing of an EV rather than an ICEV (Samaras and Meisterling, 2008). Recent studies in North America indicate that a net reduction in GHG emissions can be achieved by replacing ICEVs with PHEVs. The Electrical Power Research Institute (2007) and the Natural Resources Defence Council (NRDC) compared PHEVs to HEVs and ICEVs using specific electricity generating technologies. The results concluded that regardless of the electricity supply, PHEVs and HEVs would result in a net decrease in GHG emissions (between 28-67%) relative to ICEVs (Electric Power Research Institute, 2007). Lilienthal and Brown (2007) estimated the potential CO_2 emissions reduction through the introduction of PHEVs into individual states in North America. It was determined that use of PHEVs would provide CO_2 emissions reductions in 49 states and on average a CO_2 reduction of 42% per mile driven. However, the author notes that majority of the U.S electricity generation comes from coal, which implies that greater reductions would be possible if the electricity generation was more efficient. Parks et al (2007) considered the emissions associated with PHEVs in the Xcel Energy Colorado service territory under various PHEV charging scenarios. The analysis revealed significant CO_2 emissions reductions in all cases. In the case of Ireland, Smith (2010) examined the potential benefits of PHEVs in terms of reducing the primary energy requirement (PER) and CO_2 emissions

of passenger cars in Ireland. The analysis found that the electrification of the Irish passenger car fleet could reduce the PER and CO_2 emissions by 50% for each km travelled in electric mode.

Only a limited number of studies have been carried out which investigate the impact of EVs on urban air quality. When an EV is operating in electric driving mode, it does not produce any tailpipe emissions. Therefore it can be expected that all traffic related emissions would significantly improve, since electricity is generated mostly outside urban areas where air pollutants are usually concentrated. Passier et al (2007) argues that since tailpipe emissions are 'displaced' from densely populated areas to remote sites, considerable population exposure benefits can be realised. Kantor et al (2009) investigated the air quality impacts of alternative vehicle technologies in Ontario, Canada. In the overall scenario the results showed the adoption of PHEVs would result in insignificant decreases in PM and sulphur oxides (SO_X) emissions, based on the current generation mix in Ontario. However, the author noted that "*reductions in the urban environment could have slightly positive impacts on the population*".

2.3 Data sources

The primary source of travel data for this analysis was the Place of work Census of Anonymised Records (POWCAR). It derives from the data gathered in the 2006 Irish census and details information on 1,834,472 regular work trips of the entire population (Central Statistics Office, 2007a). It is the only source of disaggregate origin-destination travel to work data in Ireland.

2.3.1 The ISus private car stock model

The ISus private car stock model developed by the ESRI, was used to make assumptions about the future size and breakdown of the private car fleet. The model, which is driven by forecasts on the economy and the population, is constructed from a long history of data on vehicle sales and has been calibrated to recent data on the actual private car stock. The model distinguishes cars by fuel type, engine size and age. The current composition of the Irish private car fleet is presented in Table 2.1. A detailed description of the ISus model and the data sources used in the development of the model are available in Hennessy and Tol (2010). An overview of the model summarised from Hennessy and Tol (2010) is outlined here.

Table 2.1. The Irish private car fleet composition.

Fuel	CC bands	Number of vehicles	Private car fleet (%)
Gasoline	**< 1.4 Litre**	963,044	49.9
	1.4 – 2.0 Litre	543,080	28.1
	>2.0 Litre	53,251	2.8
Diesel	**<2.0 Litre**	320,073	16.6
	>2.0 Litre	50,571	2.6
Total		1,930,019	100

The Prevalence of Car Ownership

The saturation of the private car market is important in forecasting the future level of the private car stock. At the saturation point, changes in the car stock are directly proportional to the changes in the population or its demographic components. HERMES a macroeconomic model (Fitzgerald et al, 2002), used for making forecasts about the Irish economy, including a forecast of the car stock C at time t, saturates the rate of car ownership at 0.8 cars per adult population and uses an error correction procedure to predict the car stock according to Equation 2.1:

$$\Delta ln \frac{0.8}{C_t/P_t - 1} = \alpha + \beta \frac{Y_t}{P_t} \tag{2.1}$$

where Y is the level of disposable income and P is the population aged between 15 and 64 years. The model forecasts the stock of private cars up to 2025.

Type of Car

Once the future level of car ownership was determined, the share of the stock in terms of engine size was estimated. Information from the Household Budget Survey (HBS) on expenditure on motor tax was used to establish the engine sizes of the cars owned in the country. Then a multi-nominal logit regression with 9 categories of engine size as the dependent variables was performed and income elasticities for each engine size were estimated. A separate regression by fuel type was then performed and the income elasticities were aggregated. These income elasticities were then used to forecast the number of cars per engine size using information on future levels of disposable income determined by the HERMES model (Bergin et al, 2009).

The historical progression of the diesel car stock was tracked in the model but it was not possible for the authors to extrapolate this trend to predict the future size of the diesel car stock due to recent policy changes. This essentially caused a structural break in the series. To overcome this, the authors applied a breakeven distance methodology along with information on the mileage distribution by engine size, to forecast the diesel car stock by engine size. According to the authors, the theory of the breakeven distance methodology is as follows, diesel cars are more expensive to buy and to own, but cheaper to drive. Therefore, a diesel car is more attractive to people who drive long distances (more than the break-even distance). The mileage distribution function specifies the fraction of the population who drive more than a particular distance, and therefore allowed the market share of diesel cars to be determined. The authors reported that this methodology has been used previously to determine the share of diesel car sales in Mayeres and Proost (2001) and Rouwendal and de Vries (1999) but with the added advantage that the ISus model is disaggregated by engine size. Unspecified data sources were used to compute the break-even distance values for

each engine size class and mileage distribution data were used to compute diesel market shares. This approach allowed the market share for each engine size class to be determined.

Stock Demographics

The model distinguishes 10 engine sizes and 25 age classes. The dynamic equations for the model are

$$C_{t,l,s,f} = S_{t,l,s,f} \tag{2.2}$$

$$C_{t,a,s,f} = (1 - \rho_{t,a,s,f})C_{t-1,a-1,s,f} : a = 2,3,\dots,24 \tag{2.3}$$

$$C_{t,24,s,f} = (1 - \rho_{t,24,s,f})C_{t-1,24,s,f} + (1 - \rho_{t,25,s,f})C_{t-1,25,s,f} \tag{2.4}$$

where $C_{t,a,s,f}$ is the stock of private cars in year t, of age a, of engine size s and of fuel f; S represents sales and $\rho_{t,a,s,f}$ is the probability of scrapping which is independent of time, size and fuel according to Equation 2.4.

$$\rho_{t,a,s,f} = 1 - \frac{0.015(a-1)}{1 + 0.03(a-1)} \tag{2.4}$$

The demographic model was developed using historical data on new car registrations from 1965 and a scrappage parameter which affected the probability of scrappage. It was assumed that the life cycle of cars was no longer than 25 years. Therefore, the modelled car stock was representative of the real stock from the year 1990 onwards. The diesel car model was initialised from 1985. The same dynamic equations were used for the diesel car model and it was assumed that the lifecycle of diesel cars is 15 years. Therefore, the diesel car model was representative of the real stock from the year 2000 onwards. The stock of petrol cars was then calculated by differencing the two stock variables. Therefore, from the year 2000, the stock was representative of both fuel types. The scrappage parameter was calibrated to age distribution data taken from the Irish Bulletin of Vehicle Statistics (Department of Transport, 2009). The scrappage parameter in the model was time invariant and assumed that the durability of cars remains constant.

2.4 Methodology

2.4.1 Fleet emission calculation

The potential reduction in tailpipe GHG emissions was calculated using the COPERT 4 model. The COPERT 4 model is part of the EMEP/CORINAIR Atmospheric Emissions Inventory Guidebook (AEIG) (European Environment Agency, 2009) and is recommended by the European EEA to calculate national emission inventories (Kousoulidou et al, 2008). Over twenty European member states including Ireland use the COPERT 4 model. The COPERT 4 methodology is based

on average speeds and corresponding average speed emission factors to calculate vehicle emissions (Gkatzoflias et al, 2007). It includes 37 classes of gasoline passenger cars. A given car belongs to one of three ''subsectors'' depending on the cylinder volume (<1.4 L, 1.4–2.0 L and >2.0 L), and each subsector contains 12–14 ''technology classes'', reflecting the various stages of the EU exhaust regulations (EURO 1, EURO 2, etc.). For diesel cars there are two subsectors (<2.0 L and > 2.0 L), each containing seven technology classes. The vehicles were allocated to European emission standards on the basis of their age and application dates of the standards in Ireland. The percentage breakdown of the current fleet and the projected breakdown of the fleet in 2020 by technology class are detailed in Appendix A. A mix of urban (14% of distance), rural (9% of distance) and highway (76% of distance) driving was assumed with average speeds of 40 km/h (rural), 60 km/h (urban) and 100 km/h (highway).

The temperature data required for the COPERT models was sourced from the European Climate Assessment and Dataset (2010). Despite there being an advanced fuel specification provided by COPERT 4 for 2009 stage fuel, the fuel specifications which are defined in the Air Pollution Act 1987 are used instead (Irish Statute Book, 2003). The only difference being that the 2009 stage fuel specifications, has a reduced sulphur content from 50 parts per million (ppm) to 10 ppm. The unit used to express the polycyclic aromatic hydrocarbon value in the Irish Statutes is in % m/m. COPERT 4 requires the unit to be % v/v, therefore the default value was used instead.

2.4.2 Employment and passenger car kilometres in the GDA

In 2006, it is estimated that 223,578 individuals travelled to work in Dublin by car. Based on the Central Statistics Office (2010) employment statistics for the nation between 2006 and 2009 and future employment projections by the ESRI (Bergin et al, 2010), the number of individuals who will potentially travel to work in Dublin by car in 2020 was forecast. Under a low growth scenario, the ESRI predict that annual employment will increase by 1.9% and 0.9% between 2011 and 2015 and between 2015 and 2020 respectively. By applying the national employment statistics to the GDA, it was estimated that approximately 226,300 people will travel to work in Dublin by car in 2020, of which approximately 156,800 will belong to households with two or more vehicles.

As this study is concerned with annual emissions, the daily trip kilometres were calculated on an annual level. Annual work trips was based on a 220 day year daily return trip. The average distance travelled to work in Dublin was 15.3 km in 2006, which equates to an average annual distance of 6,732 km per individual. Table 2.2 details the projected number of individuals who will travel to work in Dublin by car.

Table 2.2. Estimated number of individuals who travel to work by car.

Year	Forecasted ESRI employment growth (low growth scenario)	Total number of individuals who travel to work by car	No. of households likely to own 2 cars or more who travel to work by car
2006	-	223,578	154,940
2007	-	231,791	160,631
2008	-	231,670	160,547
2009	-8.6	211,746	146,740
2010	-4.2	202,853	140,577
2011	1.3	205,490	142,405
2012	1.3	208,161	144,256
2013	1.3	210,868	146,131
2014	1.3	213,609	148,031
2015	1.3	216,386	149,955
2016	0.9	218,333	151,305
2017	0.9	220,298	152,667
2018	0.9	222,281	154,041
2019	0.9	224,281	155,427
2020	0.9	226,300	156,826

2.4.3 Potential electric vehicle market penetration

The main uncertainty of this analysis is without doubt the estimation of the future market penetration of EVs into the motor industry. The accurate prediction of the market penetration includes great uncertainties and depends on a multitude of influencing factors (i.e. fossil fuel price, national incentive schemes and new developments in EV technology). In this analysis the rate of market penetration was estimated using a logistic S-curve. This methodology is in keeping with other studies, which have used S-curves to predict the market penetration of new technologies. These include Hollinshead et al (2005), who used S-curves to predict the market penetration of fuel cells in transportation and Draper et al (2008), who used S-curves to predict the economic impact of EV adoption in the United States (U.S.).

The shape of the curve is determined according to the Equation 2.1 (Brandewinder, 2008).

$$f(t) = \frac{1}{1 + e^{-\alpha(t-T_0)}} \tag{2.1}$$

Where:

$$\alpha = \frac{\ln\left(\frac{1}{f_1} - 1\right) - \ln(\frac{1}{f_2} - 1)}{t_2 - t_1} \tag{2.2}$$

$$T_0 = \frac{\ln(\frac{1}{f_1} - 1)}{\alpha} + t_1 \tag{2.3}$$

Two years, denoted t_1 and t_2 and the expected market penetration of EVs, denoted f_1 and f_2 at those particular years and the long-term market share t were required to be specified. Assuming that EV sales commence in 2011 and that 90% market penetration is achieved by 2035, the reduction in emissions under three different market penetration scenarios, 'high', 'medium' and 'low' (Figure 2.3) was analysed. Note, market penetration refers to the penetration of annual sales - penetration of the entire car fleet would take significantly longer. Under the 'high' penetration scenario it was assumed that EVs will achieve 25% market share by 2020; under the 'medium' and 'low' scenarios, a share of 15% and 10% respectively. A Business as Usual (BAU) or baseline scenario was also investigated.

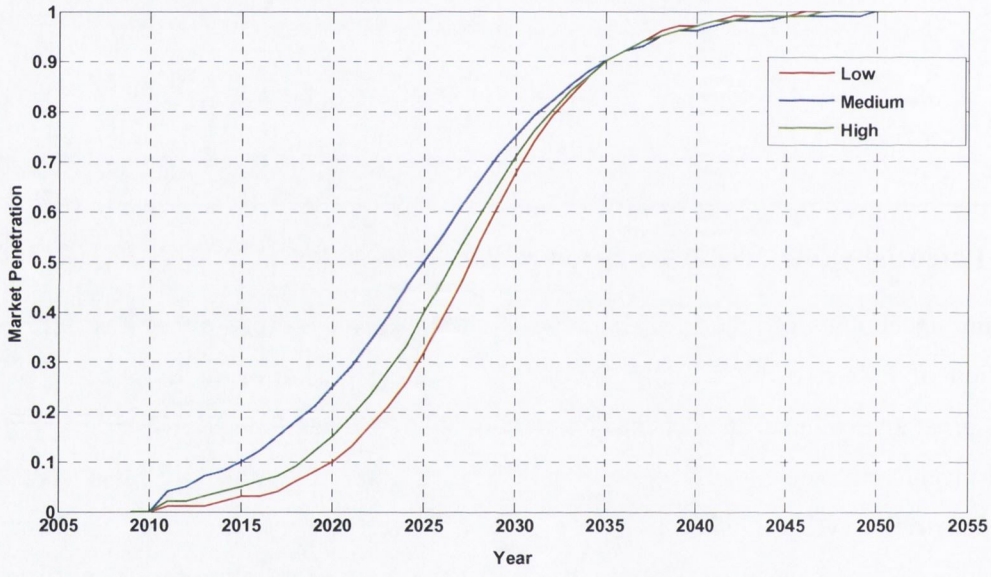

Figure 2.3. Projected EV market penetration under three scenarios 'high', 'medium' and 'low'.

From the analysis of the Society of the Irish Motor Industry (2010b) new vehicle registration statistics over the period 2000-2007, an average of 79,512 new cars were registered in the GDA per annum. Due to the deterioration of the economy, new car registrations significantly decreased to 63,557 (-8%) and 26,265 (-59%) in 2008 and 2009 respectively. Early indications in 2010 suggested a recovery in the industry with a 42% increase in sales (30,040) on the same period in 2009 (Society of the Irish Motor Industry, 2010a). For the purposes of this analysis, it was assumed that the industry will return to its position where it otherwise would have been by 2020, prior to the global economic recession and that there will be approximately 79,500 new cars registered in the GDA each year up to and including 2020.

Numerous studies have shown that the proportion of households with at least two cars is considerably higher in rural areas than in urban areas largely due to the fact that individuals living in urban areas have access to a more frequent public transport system (Commins and Nolan, 2008, Scottish Executive, 2005). Only 65% of households own two or more vehicles in the GDA. Based on the technical features such as the driving range achievable by current EV models it was assumed that only households with two or more cars would consider purchasing an EV. This reduced the potential market to approximately 51,700 sales per year.

Due to the extended driving range achievable by PHEVs, it was assumed that PHEVS are viable substitutes for all ICEVs with an engine size between 1.4 and 2.0 litres, but that BEVs will only replace ICEVs with an engine size less than 1.4 litres, which have a lower than average annual mileage (Howley et al, 2009b). Furthermore, it was assumed that the EVs will only displace vehicles which comply with the Euro V exhaust standards (2010) and then Euro VI exhaust standards (2015).

In the reviewed studies the range of conceivable market penetration scenarios varies widely (Clement-Nyns et al, 2010, Hadley and Tsvetkova, 2008, Simpson, 2006). The majority of studies estimate the market penetration of EVs, but few differentiate between PHEVs and BEVs. It was assumed that PHEVs will become widely available in the near future and that rapid growth will lead to mass commercialisation. However, it is expected that there will not be mass market penetration of BEVs for a number of years due to the premium price and limited consumer acceptance with regard to charging times and driving range. The Irish electricity utility company, the Electricity Supply Board (ESB), who is responsible for the development of the national EV charging infrastructure, forecast that in 2020 the EV fleet in Ireland will consist of 70% PHEVs and 30% BEVs (Mulvaney, 2010b). Table 2.3 presents the projected composition of the commuter fleet in 2020 under each of the investigated scenarios.

Table 2.3. Projected composition of the commuter passenger car fleet under each market penetration scenario.

Technology	BAU	Low	Medium	High
ICEV	156,826	136,712	123,563	91,924
BEV	0	14,080	23,284	45,431
PHEV	0	6,034	9,979	19,471
Total	156,826	156,826	156,826	15,6826

2.4.4 The fraction of a journey completed in electric driving mode

BEVs produce zero tailpipe emissions when in operation. In the case of PHEVs, the fraction of a trip that would be completed in electric driving mode is difficult to determine. Vehicle driving ranges are variable and so is the instantaneous fraction of drive energy derived from the battery. PHEVs have several operating strategies. One mode of operation is where a PHEV operates up to a specified range on electrical power before switching to the internal combustion engine (ICE). This

is referred to as a serial PHEV. For instance the PHEV-20 nomenclature implies that the vehicle drives for the first 20 km powered by the battery and then switches to the ICE for the remainder of the journey. PHEVs can also be powered by both energy sources simultaneously, where the electric motor generally supplies power at low speeds and is supplemented by the ICE at high speeds. This is referred to as parallel PHEV. The fraction of a trip completed in electric driving mode or the fraction of kilometres displaced by electricity is difficult to determine. According to Smith (2010) and Parks et al (2007) the fraction of the trip completed in electric driving mode is dependent on the trip length, the driving profile, driving habits and the PHEV operational mode. Smith (2010) reports that some current PHEV models such as the Chevrolet Volt and the Volkswagen VW "twindrive" have 100% performance capacity in electric driving mode and are capable of travelling 40 km or more in electric driving mode (Tate et al, 2009, Volkswagen, 2008). It is expected that in the future all PHEV models will have 100% performance capacity in electric driving mode and that the combustion engine will only serve as a means of extending the driving range (Smith, 2010). In 2006, 93% of commuters travelled less than 40 km to work in Dublin. Therefore, it was assumed that all trips to work are completed in electric driving mode and hence produce no tailpipe emissions.

2.4.5 Electrical energy requirement of electric vehicles and the carbon intensity of the national grid

In estimating the potential GHG and urban air quality benefits from the deployment of EVs, it was necessary to account for the emissions impact of electricity generation. In order to quantify the potential energy requirement of the EV fleet, it was first necessary to quantify the energy economy of a vehicle. Smith (2010) developed a model to determine the minimum theoretical energy required to move a given vehicle a fixed distance over a specific driving cycle. The model was then used to calculate the minimum energy requirement (MER) (Wh km^{-1}), of a range of vehicles representative of the Irish passenger car fleet, operating over a selection of legislative and real-world driving cycles. A MER of 105 Wh km^{-1} for a PHEV on a single recorded Irish driving cycle was calculated. Allowing for inefficiencies between the wall socket/tyre-road interface (75%) and efficiency gains through regenerative braking (60%), this increased to 140 Wh km^{-1} and was referred to as the wall socket electrical energy requirement (WSER). Losses that occur during the generation, transmission and distribution of electricity were also taken into account. The Irish electricity supply efficiency is expected to be 67% in 2020 (Smith, 2010). Therefore, the WSER translated to an estimated primary energy requirement (PER) of 0.209 kWh km^{-1} (Smith, 2010).

In a review of transport options to alleviate the effects of climate change, urban air pollution and oil dependence, Sandy (2009) reports that under optimum conditions, the average fuel economy of a BEV is 2.6 times greater than that of an ICEV, giving an energy economy of 0.26 kWh km^{-1}. However, Foley et al (2009) report that under real world driving conditions the specific energy

economy is 10-25 kWh/70 km. It was assumed that the electric energy requirement of a PHEV and a BEV are 0.209 kWh km^{-1} and 0.25 kWh km^{-1} respectively.

In 2008 the carbon intensity of the Irish electricity supply was 582 g CO_2/kWh (Howley et al, 2009a). Wind generation is steadily growing and accounted for 10% of electricity generation in 2009 and overall, the share of electricity generated from renewable energy sources accounted for 14.4% (Dennehy et al, 2010). This suggests that Ireland has surpassed the mandatory EU interim target of 13.2% for 2010 as outlined in the EU Directive (2009/28/EC) (European Commission, 2009). The high levels of growth in wind generation are expected to continue into the next decade as the Irish government have set a national target of deriving 40% of electricity from renewable resources by 2020 (Eirgrid, 2009). Taking into account the combined measures of increasing the share of renewable generation and improvements in the overall efficiency of the electricity supply, it was assumed that the carbon intensity of the electricity supply will be 393 g CO_2/kWh in 2020.

2.5 Results and analysis

Emissions levels for 2010 and the projected emissions under three EV market penetration scenarios and a BAU scenario for the year 2020 were estimated in this analysis. Table 2.4 presents both the estimated tailpipe emissions and the emissions due to electricity generation for each of the scenarios investigated. The results show that each of the EV market penetration scenarios examined would realise a net reduction in CO_2 emissions and tailpipe air pollutants. BAU or baseline CO_2 emissions for 2020 are projected to be 318 kilo tonnes (kt) CO_2 (a 5% reduction on 2010 levels). The 'high' and 'medium' market penetration scenarios demonstrate that a net reduction in CO_2 emissions of 10% and 5% respectively could be achieved. Under the most likely scenario of 10% market penetration, the findings show that a net reduction of 3% in CO_2 emissions could be achieved.

The results for the BAU scenario suggest that there will be significant reductions in CO, VOC, PM, NO_2 and NO_x emissions in 2020, without the introduction of EVs to the fleet. These reductions can be attributed to two factors, the introduction of Euro 5 and Euro 6 emissions standards, which have stricter limits on pollutant emissions and the retirement of older higher pollutant emitting vehicles from the fleet. The highest reduction is, consequently, predicted for CO (76%) and VOCs have a similar expected evolution (70%). The results also showed considerable reductions of 68% and 54% for NO_2 and CH_4 emissions respectively. The Euro 5 and Euro 6 emissions standards will require NO_X emissions to be reduced by 25-50%. Therefore a 29% reduction in NO_X emissions is in line with expectations.

Table 2.4. Emission results.

Pollutant	2010	BAU 2020	% Change from 2010	High	% Change from BAU 2020	Medium	% Change from BAU 2020	Low	% Change from BAU 2020
Tailpipe	337,102	318,700	-6	248,678	-22	282,316	-11	296,296	-7
Grid CO_2	-	-	-	37,999	-	19,475	-	11,776	-
Net CO_2	337,102	318,700	-6	286,677	-10	301,791	-5	308,072	-3
CH_4	28.54	13.02	-54	11.38	-13	12.18	-6	12.51	-4
N_2O	5.24	7.03	34	4.42	-37	5.69	-19	6.22	-11
CO	3,385.65	828.60	-76	713.85	-14	769.75	-7	792.99	-4
VOC	376.71	113.37	-70	94.26	-17	103.57	-9	107.44	-5
NO_X	283.79	200.50	-29	148.80	-26	172.38	-14	182.19	-9
NO_2	41.46	13.30	-68	13.16	-1	13.23	-0.54	13.25	-0.34
$PM_{2.5}$	29.93	21.3	-29	15.90	-25	18.53	-13	19.62	-8
PM_{10}	42.31	35.12	-17	25.76	-27	30.32	-14	32.22	-8

Note: All values are in tonnes.

The introduction of EVs exhibits superiority in further reducing all road traffic related emissions. A comparison between the EV adoption scenarios examined demonstrates that the 'high' adoption scenario would result in the largest decrease in overall emissions. Under the most probable scenario (10% market penetration by the year 2020) the results indicate a modest reduction in emissions. A further 8% reduction on the BAU scenario for $PM_{2.5}$ and PM_{10} is observed. Globally, VOCs contribute to the formation of ozone (O_3) which can lead to the production of photochemical smog in urban areas. Whilst Ireland does not experience smog pollution, the introduction of EVs could further reduce emissions by 5%. By 2020, NO_x emissions are expected to decrease by a further 9% relative to the BAU scenario. Projected reductions in CO and NO_2 emissions are the lowest at 4% and <1% respectively.

2.6 Summary and conclusions

Ireland has experienced unprecedented economic growth and employment over the last decade, particularly in the Greater Dublin Area. Subsequently household incomes and car ownership levels have increased accordingly. The electrification of commuter vehicles seems particularly favourable as driving range restrictions and long charging cycles are not major constraints. This analysis focused on the near term evaluation of the potential reduction in road traffic related emissions due to commuting in the Greater Dublin Area.

The results of this analysis showed that the introduction of EVs presents an advantage over the BAU case in every aspect of their emissions. Under the most likely scenario (10% market penetration by the year 2020) the results indicate a net reduction of 3% in CO_2 emissions relative to the BAU case could be achieved. These results are mildly encouraging as this reduction in CO_2 emissions will most likely only account for approximately 2% of the CO_2 emissions from the transport sector in 2020. Urban air pollutants are individually projected to decrease by up to 11% under the most likely 'low' market penetration scenario. Due to the displacement of tailpipe emissions from densely populated areas to remote electricity generation sites, moderate pollution exposure benefits could be realised.

When examining the results presented one must be mindful of the limitations of the approach followed in this study. The analysis presented assumed that all trips are completed in electric driving mode, hence produce no tailpipe emissions. The COPERT 4 model is based upon international averages and as such may be subject to some error in the emissions calculated. The vehicle population and activity data may also be subject to some scrutiny, in that they were based on 2006 Census data and the ESRI's 2009 Medium Term employment forecast. The evolution of the vehicle fleet with respect to engine size was based on the author's assumptions having observed the trends of the last decade. Future analysis should seek to evaluate the impact of governmental policies on the adoption of EVs in Ireland and the reduction in road traffic related emissions should be re-evaluated.

As a conclusion of this analysis, the results obtained indicate that the time required for EVs to acquire a significant share of the fleet, suggests that they will have a limited impact on climate change and urban air quality for at least the next decade but supports existing evidence that EVs can contribute to emissions reductions.

3 The introduction of electric vehicle to Ireland: A socioeconomic analysis

It has become common for governments to introduce financial consumer incentives in an attempt to stimulate the EV market. However, EVs present policy makers worldwide with competing goals, the goal to encourage the adoption of EVs, while on the other hand to tackle climate change and provide a sustainable transportation system. The loss in tax revenue as a consequence of incentive schemes is becoming a debateable topic. The objective of this chapter is to undertake a social cost-benefit analysis of the 10% market penetration of EVs in Ireland by 2020. It analyses the socio-economic costs and benefits of this policy by comparing the environmental benefits, expressed in monetary value, with the associated reduction in tax revenues and the cost of the government's EV grant scheme. The analysis concludes that the 10% adoption of EVs in Ireland will result in a monetary loss in the region of €324 million for the government (in the order of 0.5-1% of total tax revenue expressed at 2009 levels). The primary reason for this is due to losses in all sources of tax revenue due to the EV penetration rates required to achieve an appreciable reduction in GHGs. The contents of this chapter are published in Brady and O'Mahony (2011).

This chapter is organised as follows: Section 3.1 introduces the concept of cost benefit analyses (CBA) and outlines the objective of the analysis. Section 3.2 reviews previous research on socioeconomic CBAs of EVs. Section 3.3 provides an overview of the vehicle tax system in Ireland. Section 3.4 details the methodology and key assumptions of the analysis. In Section 3.5 the results are presented and analysed. Section 3.6 discusses the limitations of the analysis. Section 3.7 concludes the chapter and recommends areas for further research.

3.1 Introduction to cost benefit analyses and the objective of the analysis

In order to ensure the early availability of EVs for the Irish market, the Irish government have signed memorandums of understanding (MOU) with a Renault-Nissan alliance and Mitisubishi. Under the terms of the agreements, the car manufactures will supply EVs, while the government will introduce policies and incentives to support the widespread adoption of EVs and they will support the development of a nationwide charging infrastructure.

Common to all new technologies, EVs face barriers to adoption, such as lack of knowledge by potential users, low consumer risk tolerance and high initial production costs (Diamond, 2009). In an attempt to address some of these market barriers it has become common for governments to introduce financial consumer incentives to encourage the purchase of EVs. Despite the proliferation of such incentive programmes, their efficiency in actually promoting the purchase of EVs is unclear and the programs are often the subject of public and political debate. One argument put forward by Carlsson and Johansson-Stenman (2003) is that "*even though EVs may not be*

socially beneficial today, they probably will be tomorrow and that the introduction of EVs is a long process that must start today".

A CBA is a useful tool for comparing the positive and negative effects of different activities or projects. Large uncertainties and simplified assumptions are generally associated with a CBA. A common criticism of published research in this area is the outdated data on EV technology and the electrical generation mix on which they are based. However, Carlsson and Johansson-Stenman (2003) argue that CBAs can be a valuable tool for policy making decisions provided that a detailed presentation of the assumptions made is outlined.

The objective of this chapter is to examine the socio-economic costs and benefits of the proposed deployment of EVs in Ireland in 2020. This objective is achieved by comparing the environmental benefits, expressed in monetary value, with the associated reduction in tax revenues and the cost of the government's EV grant scheme. This comparison is particularly important in countries with high fuel taxes, as is the case with most European countries.

3.2 Cost benefit analysis of electric vehicles

The concept of a social cost-benefit analysis is commonly used by policy decision-makers to attempt to measure the social benefits of a proposed project in monetary terms and to compare them with its costs. Carlsson and Johansson-Stenman (2003) attempted to calculate the costs and benefits of both EVs and HEVs and the private and societal costs attached to them. The study was conducted from a Swedish perspective for year 2010 and the primary objective was to estimate all relevant costs elements whilst simultaneously highlighting the effect of changed tax revenues, rather than focusing on manufacturing and maintenance costs. The social benefit/costs of replacing ICEVs with EVs was defined as the "*difference between the benefit in terms of decreased external costs and the cost in terms of reduced taxation.*" In this context "external costs" refers to environmental costs. Consequently, the social marginal net benefit (MNB) can be calculated according to the following equation derived by Carlsson and Johansson-Stenman (2003):

$$MNB = \Delta MD - \Delta R \tag{3.1}$$

Where, ΔMD refers to the decrease in marginal damage, or external costs from replacing one ICEV with an EV, and ΔR is the associated decrease in tax revenues. The analysis revealed that BEVs would be socially unprofitable primarily because the taxes applied to them are heavily subsidised compared to ICEVs. HEVs were found to be socially and privately profitable without subsidies, especially for city based delivery trucks. Herynkova (2009) conducted a similar analysis for Denmark for the year 2020, based on Carlsson and Johansson-Stenman's (2003) social cost benefit analysis equation. It was found that from a purely financial perspective EVs are not socially

profitable as their reduction in environmental costs is by far offset by the decrease in tax revenues. However, vehicles in Denmark are subject to a particularly high registration tax of 180% and VAT of 25%. Forkenbrock (2006) points out that the rising fuel efficiency of vehicles such as HEVs will result in reduced revenue from motor fuel taxes and as motor fuel tax becomes less productive, governments will have to change the ways in which they finance road infrastructure. In Vermot, the Vermot Energy Investment Corporation (2012) calculated that the if the target to have 25% of the vehicle fleet powered by renewable energy by 2030 is achieved, it would result in a loss in all sources of tax revenue of $21 million. In America, a study by Hall (2012) suggests that as EVs gain a greater market share and the fuel efficiency of ICEVs increases up 2050, federal fuel taxes could decline by up to 41.5%. A study by Gonder et al (2007) suggests that PHEVs will also result in "substantial petroleum displacement", which further strengthens the concept that motor fuel taxes will be significantly reduced as a result of the deployment of EVs into national private vehicle fleets. Earlier research by Delucchi and Lipman (2001) presented a detailed life-cycle cost analysis for BEVs and found that the performance and cost of batteries must be significantly reduced in order for BEVs to become competitive. More recently Granovskii et al (2006) preformed an economic and environmental comparison of ICEVs, BEVs and hydrogen fuel cell vehicles (HFV). It was shown that if electricity generated by a gas turbine engine with an efficiency of 50-60% was used to charge a BEV with a high capacity battery, then a BEV would be advantageous. Lipman and Delucchi (2006) provide a detailed and comprehensive lifecycle cost analysis of HEVs based on significant modifications to a previous model presented in Delucchi and Lipman (2001). It was found that combining advanced vehicle improvements with mild vehicle hybridisation provides the least cost hybrid vehicle option, with life cycle costs close to those of baseline vehicles.

3.3 The Irish vehicle tax system

In 2006, the total contribution from all motor related sources to the Irish exchequer was over €5.5 billion. The main contributors were vehicle registration tax (VRT), annual motor taxes (AMT) and excise duty on fuels, which accounted for €1,257.5 million, €879.7 million and €2,042.3 million respectively (The Society of Irish Motor Industry, 2010). Income from value added tax (VAT) receipts and revenue from road tolls also contributed significantly. Since July 2008, VRT and AMT rates are linked directly to the specific CO_2 emissions (CO_2 g/km) of the vehicle and are applied as a percentage of the open market selling price (OMSP), as shown in Table 3.1. In addition, as shown by the range applied across the bands, the purchasing signal promoting lower emitting cars is strong. VRT rates vary from 14% on the purchase price for cars with CO_2 emissions of up to 120g/km to 36% for cars with CO_2 emissions greater than 225g/km. However, under current legislation, BEVs are exempt from vehicle registration tax and PHEVs are entitled to up to €2,500 off the VRT payable upon a new vehicle registration. Vehicles with emissions in the 0-120g/km category are subject to an annual motor tax of €104.

Table 3.1. CO_2 based vehicle registration and road tax bands.

Emission Band	Specific CO_2 Emissions (g/km)	VRT (%OMSP)	AMT (€)
A	≤ 120	14%	104
B	> 120 - 140	16%	156
C	> 140 -155	20%	302
D	> 155 - 170	24%	447
E	>170 - 190	28%	630
F	>190 – 225	32%	1,050
G	> 225	36%	2,100

Since April 2010, a government grant has been available towards the purchase price of BEVs and PHEVs. BEVs with an OMSP greater than €20,000 are eligible for a €5,000 governmental grant, whereas PHEVs with an OMSP greater than €18,000 are eligible for a €2,500 grant (Sustainable Energy Authority Ireland, 2010). The incentive for BEVs with an OMSP less than €20,000 ranges from €2,000 for vehicles priced between €14,000 and €15,000 up to €4,500 for those priced between €19,000 and €20,000. Excise duties of 54.34 cent/litre and 44.95 cent/litre are applied to unleaded petrol and diesel fuelled vehicles respectively. These duties include the new carbon tax introduced in 2010 and are subject to VAT at 21%. A reduced VAT rate of 13.5% is levied on electricity utility bills.

3.4 Methodology and key assumptions

Two different scenarios were explored, a Business as Usual (BAU) scenario and an EV scenario, in which the 10% market penetration target is achieved and 230,000 vehicles are purchased. Carlsson and Johansson-Stenman (2003) social cost benefit analysis equation was employed, however an additional parameter was included to account for the Irish government's EV grant scheme. Thus, the equation was expanded to the following:

$$MNB = \Delta MD - \Delta R\text{-G} \tag{3.2}$$

Where, ΔMD is the total decrease in marginal damage, or external costs from replacing ICEVs with EVs, ΔR is the associated decrease in tax revenues and G represents the cost of the EV grant scheme. This section also details the general assumptions made in this analysis. These assumptions provided a natural benchmark case, since it is not known whether economic or technical parameters such as prices, taxes and vehicle characteristics will fluctuate over the next decade.

3.4.1 Vehicle parameters

Two particular vehicles, which are due to be released in 2011 and 2012 respectively were taken as representative of EV vehicles; the Nissan Leaf (BEV) and the Toyota Prius Plug-in hybrid (PHEV). Fourteen ICEV models were taken to represent conventional vehicles. Each of the seven road tax

bands (A-G) were allocated two representative vehicles, one petrol and one diesel vehicle. The characteristics of each vehicle were based on published specifications. However the price of the PHEV has yet to be released and was assumed to be competitive with a similar-sized car. Table 3.2 lists both the actual and assumed technical and economic parameters of each vehicle. It is recognised that the future passenger vehicle requirements are difficult to predict and so these values are hypothetical indicators that enable the calculation of resource consumption in a range of areas such as fuel and electricity consumption. This calculation in turn allowed the estimation of projected tax revenue from a variety of sources.

Table 3.2. Technical and economic parameters of the representative vehicles.

	Emission Band	Fuel Type	Engine Size (L)	CO_2 Emissions (g/km)	Fuel consumption (l/100 km)	OSMP (€)	Battery Capacity (kWh)
Toyota Aygo	A	Petrol	1.0	106	4.5	10,670	-
Volkswagen Polo Trendline	A	Diesel	1.2	92	3.4	17,000	-
Nissan Leaf	A	Electric	-	0	0	29,995	24
Toyota Plug-in Prius	A	Electric/Petrol	1.8	89	3.9	30,000	5.2
Toyota Auris	B	Petrol	1.3	139	5.9	18,945	-
Volkswagen Jetta Trendline	B	Diesel	1.6	122	4.7	21,700	-
Toyota Avensis	C	Petrol	1.6	152	6.5	24,165	-
Volkswagen Passat CC	C	Diesel	2.0	146	6.1	38,520	-
Toyota Verso	D	Petrol	1.6	161	6.8	29,040	-
Volkswagen Tiguan	D	Diesel	2.0	164	6.4	35,760	-
Toyota RAV4	E	Petrol	2.0	174	7.4	28,695	-
Nissan X-Trail	E	Diesel	2.0	179	6.8	37,170	-
Mercedes-Benz S-Clas	F	Petrol	3.0	200	7.6	98,600	-
Nissan Qashai+2	F	Diesel	2.0	209	7.9	38,785	-
Mercedes-Benz SL-Clas	G	Petrol	3.5	236	8.8	136,635	-
Toyota Land Cruiser	G	Diesel	3.0	243	9.1	36,735	-

Note: - = not applicable.

3.4.2 Emissions estimation

The potential reduction in tailpipe GHG emissions was estimated using the COPERT 4 model described in Section 2.4.1. A mix of urban (30% of total distance), rural (50% of total distance) and highway (20% of total distance) driving was considered with average speeds of 40 km/hr (rural), 60 km/hr (urban) and 100 km/hr (highway). The same temperature and fuel specification listed in Section 2.41 were also assumed for this analysis.

The GHGs considered were CO_2, CH_4, and nitrous oxide, which can each be described in the form of carbon dioxide equivalent (CO_{2eq}), where CO_2 is given the value of 1 CO_{2eq} (Intergovernmental Panel on Climate Change, 2007). The actual weighting used to convert methane and nitrous oxide to CO_{2eq} depends on the particular global warming potential lifetime used. In this study it is taken as 100 years, and as such methane and nitrous oxide assumed weightings of 25 and 298 (Intergovernmental Panel on Climate Change, 2007). The other main pollutants related to traffic (PM, NMVOCs, and NOx) were also evaluated. The external costs of the tailpipe emissions in euros per tonne were estimated on the basis of the European Commission's handbook of external costs in the transport sector (Maibach et al, 2009).

3.4.3 The future size and breakdown of the private car fleet

In 2008 there were 1,924,281 private cars registered in Ireland, of which 3,579 (0.15%) were classified as EVs (Department of Transport, 2009). The ISus private car stock model described in Section 2.3 was used to make assumptions about the future size and breakdown of the private car fleet (Hennessy and Tol, 2010). The model projects that there will be approximately 2.2 million private cars in Ireland in 2020. As taxation levels are calculated based on emissions per kilometre rather than engine size, concordances constructed by the ESRI were used to transform engine sizes into emissions bands. The concordance table used was based on actual sales in 2008-2009 (Hennessy and Tol, 2010). The table is available in Appendix B.

From new-vehicle registration statistics of the Society of Irish Motor Industry over the period 2000 to 2007, approximately 158,309 new cars are registered in Ireland each year. Due to the deterioration of the economy, new car registrations significantly decreased to 151,607 (-18%) and 57,460 (-62%) in 2008 and 2009 respectively. Early indications in 2010 (June) suggested a recovery in the industry with a 45% increase in sales (67,864) on the same period in 2009 (Society of the Irish Motor Industry, 2010a). In this analysis, it was assumed that the industry will return to its position where it otherwise would have been by 2020, prior to the global economic recession and that there will be approximately 158,000 new cars registered in Ireland in 2020.

3.4.4 Annual passenger car kilometres and energy economy of electric vehicles

In 2009, the average annual passenger car kilometers for passenger cars was 16,708 km (Howley et al, 2009b). Cars with a small engine size typically tend to travel less than the average annual mileage. For example, cars with an engine size of less than 1.4 litres travelled approximately 13,000 km in 2009. The ESRI's distance model, which projects the distance travelled for each engine size for a given year was used to determine the annual mileage of passenger cars (Hennessy and Tol, 2010). The model accounts for changes in the composition of the car stock and is driven by the elasticity estimate and change in the relative price of fuel. The distance driven per year takes account of changes in the composition of the private car fleet according to Equation 3.3 (Hennessy and Tol, 2010):

$$D_{t+1} = \left(1 + \varepsilon_{i,t}\left(1 - \frac{P_{t+1}}{P_t}\right)\right) D_t \Delta \frac{C_{i,jt}}{C_t} \tag{3.3}$$

where $C_{i,jt}$ is the number of cars of size i and fuel j at time t; $\varepsilon_{i,t}$ is the price elasticity of the distance travelled for engine size i in the time period t. The model was calibrated against data on distance travelled from the years 2000-2008. The authors report that the elasticities used were similar to those reported in Hayashi et al (2001). This equation is weighted by the change in new car sales per engine class, which essentially takes into account that changing consumer preferences for cars does not equal different preferences for vehicle kilometres travelled (Hennessy and Tol, 2010).

It was assumed that PHEVs are viable substitutes for all ICEVs with an engine size between 1.4 and 2.0 litres, but that BEVs will only replace engine sizes less than 1.4 litres because of their limited driving range. It was assumed that the EVs are distributed evenly across both fuel types and engine sizes and hence will have a similar annual mileage.

According to Smith (2010), the fraction of passenger car kilometres completed by a PHEV in electric driving mode is dependent on the trip length, fleet penetration, kinematic profile and the vehicles characteristics such as its all-electric range. From an analysis of Irish passenger car trip length distributions and assuming one overnight charge per twenty four hour period, Smith (2010) estimates that 67% of passenger car kilometres could be completed by PHEVs with all all-electric range of 40 km. The same estimate was used in this analysis. As outlined in Section 2.4.5, it was assumed that the electric energy requirement of a PHEV and a BEV are 0.209 kWh km^{-1} and 0.25 kWh km^{-1} respectively.

3.4.5 Size of the electric vehicle fleet

The rate of market penetration of EVs was estimated using the logistic S-curve described in Section 2.4.3 (Brandewinder, 2008). Assuming that EV sales commence in 2011, that 28% and 90% market penetration is achieved by 2020 and 2035 respectively and that the average number of vehicle sales per year is 158,000, 44,240 EV sales were estimated in 2020 (Figure 3.1). Cumulative sales over the period 2011-2020, were calculated to be 231,474, which compares with the government target of 230,000. Note that market penetration refers to the penetration of annual sales.

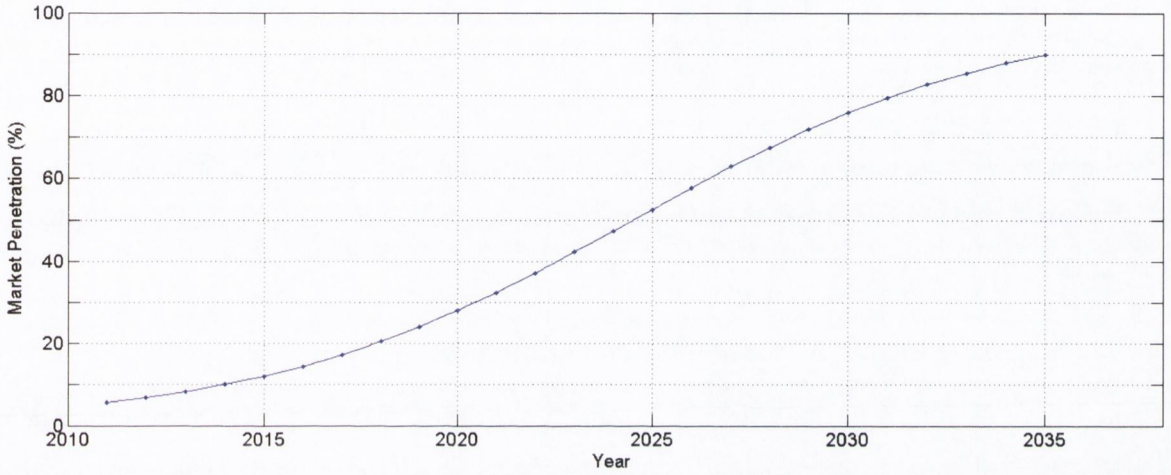

Figure 3.1. Projected EV market penetration.

As discussed in Section 2.4.3 it was assumed that sales of EVs in the Ireland over the period 2011-2020 will consist of 70% PHEVs and 30% BEVs (Mulvaney, 2010b).

3.4.6 Tax and electricity rates

As discussed in Section 3.3, under current legislation PHEVs are entitled to up €2,500 off the VRT payable upon a new vehicle registration and BEVs are exempt from VRT. It was assumed that this policy will be extended to 2020. The excise duties and VAT applied to fuels were assumed to remain unchanged in 2020. Furthermore, it was assumed that annual motor tax rates will be similar to those in 2010.

It is likely that electricity utilities will introduce a special night time electricity rate under which customers will be able to charge their vehicles. However since details of such rates have yet to be released it was assumed that the rate will be similar to the ESB's current "Night Saver Tariff". Under this rate customers are charged a reduced rate of €0.0745 (excluding VAT) per kWh of electricity consumed.

3.5 Results

3.5.1 Monetary cost of CO_2 emissions from electricity generation

Assuming that the electrical power requirement of a PHEV and a BEV are 0.209 $kWhkm^{-1}$ and 0.25 $kWhkm^{-1}$ respectively and that 67% of the annual passenger car kilometres of a PHEV will be completed in electric driving mode, the total electrical power requirement of EVs in 2020 is estimated to be 244 GWh. In calculating the emissions produced from electricity generation, it is assumed that 40% of the electricity mix will come from renewables and that the electricity CO_2 emission intensity factor will be 393 g/kWh in 2020 (Mulvaney, 2010a). On the basis of these assumptions, the total energy-related CO_2 emissions associated with electricity generation is projected to be 235 kt.

The European Commission prescribes a monetary value of €40/tonne of CO_2. This value equates to a monetary loss of €9.39 million for CO_2 emissions emitted from the generation of the electricity required to power EVs.

3.5.2 Monetary benefit of reduced tailpipe emissions

Table 3.3 presents the estimate of total emissions (CO_{2eq}, PM, NMVOCs, NO_x) for each scenario and the calculated monetary benefit. The largest benefit will be as a result of decreased CO_{2eq} emissions. The BAU or baseline CO_{2eq} emissions for 2020 from the private car feet are projected to be 5.93 mega tonnes (Mt) CO_{2eq}. Under the EV scenario it is expected that this will decrease to 5.36 Mt CO_{2eq}, a saving of 570,000 t CO_{2eq}, a monetary benefit of €22.8 million. Overall, the total reduction in CO_2 emissions and other types of pollutants equates to a monetary benefit of €31.27 million.

Table 3.3. Emission results.

Pollutant	External cost (€/tonne)	EV scenario		BAU scenario		Monetary benefit (million €)
		Emissions	Monetary cost (million €)	Emissions	Monetary cost (million €)	
CO_{2eq} (Mt)	40	5.36	214.4	5.93	237.2	22.80
NO_x (t)	3,800	5920	22.50	6394	24.30	1.80
NMVOC (t)	700	1361	0.95	1530	1.07	0.13
$PM_{2.5}$ (t)	126,200	391	49.34	422	53.26	3.92
PM_{10} (t)	50,500	623	31.46	675	34.09	2.63
Total			318.65		349.92	31.27

3.5.3 Estimated vehicle registration and motor tax revenue

The 2020 vehicle procurement was based on an average of a 158,000 new registrations per year and the progressive development in sales of EVs between 2010 and 2020. The expected VRT revenue in 2020 under the BAU scenario and EV scenario are projected to be €857 million and €759 million respectively.

The annual motor tax rates for each road tax band are presented in Table 3.1. Currently the annual motor tax rate for both BEVs and PHEVs is €104. Under the EV scenario, the figure is calculated assuming that the PC fleet consists of 230,000 EVs and that the remainder of the fleet consists of ICEVs. Taking these factors into account, the expected AMT revenue in 2020 under the BAU scenario and EV scenario are projected to be €859 million and €824 million respectively. From the introduction of EVs, the calculations indicate a monetary loss of €98 million and €35 million in VRT and annual motor tax revenue respectively.

3.5.4 Estimated cost of the governmental EV grant scheme

In a worst case scenario the OMSP of all BEVs and PHEVs purchased in 2020 will be greater than €20,000 and €18,000 respectively. Under this scenario, the EV grant scheme could potentially cost the government €143.77 million.

3.5.5 Estimated fuel tax revenue

The fuel economy of the vehicles is based on the specifications provided in Table 3.2. BEVs are powered solely by electricity. Hence they consume no fossil fuel and it is assumed that 67% of the annual passenger car kilometres of a PHEV will completed in electric driving mode. On the basis of these factors, approximately 875 and 1,235 mega litres of petrol and diesel respectively will be consumed in 2020 under the EV scenario. Assuming that excise duties of 54.34 cent/litre and 44.95 cent/litre are applied to unleaded petrol and diesel fuelled vehicles respectively, the corresponding fuel tax revenues in 2020 under the BAU scenario and EV scenario are projected to be €1.09 billion and €1.03 billion respectively. The calculations indicate a potential loss in fuel tax revenue of €60 million.

3.5.6 Estimated VAT revenue

In July 2010, the average price per litre of petrol and diesel in Ireland was 133.3 cents and 124.9 cents per litre respectively (AA Ireland, 2010). Assuming similar prices in 2020 and that fuel will be subject to VAT at 21%, the expected VAT revenue from fuel consumption under the BAU scenario and EV scenario are projected to be €308.95 million and €291.43 million respectively. The calculations indicate that the reduced fuel consumption associated with the introduction of EVs will result in a reduction of €17.52 million in VAT revenue.

The operation of EVs will result in increased electricity consumption and hence increased VAT revenue. With a VAT rate of 13.5% levied on electricity utility bills, this increased consumption will yield approximately €6.00 million in VAT revenue.

3.5.6.1 Total social marginal net benefit of electric vehicles

Table 3.4 presents a summary of the benefits of reduced environmental damage with the costs associated with the losses in fuel tax revenue and the government EV grant scheme. From the results, it is clear that the deployment of EVs in Ireland will lead to a net benefit in terms of environmental costs (€26 million). However, this benefit will be offset by the projected losses in tax revenue and the cost of the government's EV grant scheme. The total tax revenue is projected to decrease by 6.6% from €3,116 million to €2,910 million under the BAU and EV scenarios respectively, a loss of €206 million. However, the total exchequer taxation receipts for 2009 were €32,570 million (The Department of Fiance, 2009), which indicates that this loss will likely only be in the region of 0.5% to 1% of the government's total tax revenue, based on 2009 levels. Including the likely cost of the EV grant scheme (€144 million), the overall indication is that the deployment of EVs is not socioeconomically beneficial and results in a social marginal net loss of €324 million. The potential loss per EV is approximately €1,408.

3.6 Study limitations

This study is relatively narrow in scope, in that it does not include a full life cycle analysis of an EV. Rather this study is meant to contribute to a better understanding of the potential implications that the replacement of ICEs with EVs could have on tax revenue whilst estimating the environmental benefits. The results are based on a number of critical assumptions, some of which are rather uncertain. Above all, the analysis only focuses on the year 2020, as this year has been identified by the Irish government as a significant target year to have 230,000 EVs deployed. Whilst emissions benefits may not be significant by this time, they will continue to increase post 2020 whereas social costs in terms of incentives and VRT tax breaks will most likely have been discontinued. In addition, only a single market penetration scenario was run in which a certain percentage of new car sales each year are electric. The model does not allow one to examine whether EVs replace old high emissions emitting vehicles or whether they are only purchased by environmentally concerned consumers who already own a vehicle with relatively low emissions. A discrete choice model of consumer preferences to assess the impact of the consumer on EV purchases similar to Brownstone and Train (1999) would be required. Instead assumptions are made about the vehicle engine sizes that EVs will replace and how certain targets will be reached in terms of market share of sales.

Table 3.4. Summary of the socioeconomic cost benefit analysis.

	Total marginal (environmental) damage (MD)		Tax revenue (R) (Million €)
BAU scenario			
CO_2 emissions from electricity generation	n/a		
Tailpipe emissions (CO_{2eq}, NO_x, NMVOC, $PM_{2.5}$, PM_{10})	350		
VRT revenue			857
Motor tax revenue			859
Fuel tax revenue			1,091
VAT from fuel sales			309
VAT from electricity consumption			n/a
Total	350		3,116
EV scenario			
CO_2 emissions from electricity generation	9		
Tailpipe emissions (CO_{2eq}, NO_x, NMVOC, $PM_{2.5}$, PM_{10})	319		
VRT revenue			759
Motor tax revenue			824
Fuel tax revenue			1,030
VAT from fuel sales			291
VAT from electricity consumption			6
Total	324		2,910
Total marginal benefit of reduced emissions (ΔMD)		26	
Total tax revenue loss (ΔR)		206	
Cost of governmental EV grant scheme (G)		144	
Total social marginal net benefit (MND) MNB = ΔMD - ΔR - G		-324	
Total social marginal net benefit per EV (€)		-1,408	

The market penetration of EVs was estimated using a logistic S-curve, but in reality it is likely to be a function of a number of factors such as fuel price, the purchase price of the vehicles after government subsidies and the relative utility of EVs compared to ICEVs. The last factor would have been difficult to estimate at the time that this analysis was undertaken as EVs were not available on the market. Due to fuel price volatility no projections were attempted for the future price of fuel or electricity. Current incentives and tax rates, were assumed to remain static. However, vehicle production may become commercially viable before 2020 leading to a reduction in retail prices, which in turn may lead to the termination of government incentives and VRT tax

breaks prior to 2020. In addition, the future composition of the EV fleet was assumed to consist of 30% BEVs and 70% PHEVs. This is important because each vehicle type is entitled to different incentives and have different performance characteristics in relation to fuel consumption and their electrical power requirements. The CO_2 emission intensity of the electrical generation system in 2020 was taken to be 393 g/kWh assuming that the government target of 40% electricity generation from renewable sources by 2020 is achieved. The COPERT 4 model used to estimate emissions from the passenger car fleet is based upon international averages and as such may be subject to some error in the emissions calculated.

3.7 Conclusions

This chapter presents a social cost-benefit analysis of the adoption of EVs in Ireland. The analysis found that by 2020 the 10% market penetration of EVs will result in a social marginal net loss of €324 million or €1,408 per EV. The primary reason for this loss is due to losses in all sources of tax revenue compared with the EVs' penetration rates required to achieve an appreciable reduction in emissions. This loss of €206 million is in the region of 0.5% to 1% of total tax revenue in Ireland at 2009 levels. However, this result should be interpreted carefully in light of the assumptions and study limitations outlined in the previous section. Critically this analysis focuses on the year 2020, which would be in the early stages of a transition from ICEVs to EVs. At this time costs in terms of incentives and VRT tax breaks are highest to encourage adoption whilst the benefits in terms of reduced emissions are lowest due to low fleet penetration. A similar analysis conducted over a longer time frame could possibly yield a positive social net benefit. Furthermore, it is difficult to predict when the current government incentive scheme and VRT tax break will be terminated. Combined these account for 77% (€242 million) of losses, which if discontinued prior to 2020 could result is a positive outcome in the short term. However, the analysis suggests that even if current government incentives and VRT tax breaks are continued to 2020 the short term social costs of EVs will be close to that of the business-as-usual scenario. The transition from ICEVs to EVs will be lengthy process, therefore, post 2020 assuming reasonable anticipated technological progress, increased market penetration and the termination of government incentives, the full social lifetime costs of EVs will most likely surpass the short term losses and could well be lower than the full social lifetime costs of ICEvs. However, as both new EV and ICEV designs and concepts continue to emerge, continued research is needed in this area.

3.7.1 Areas for future study

This study provides a host of possible new directions for future research. First, it could be extended as noted earlier, by including a comprehensive analysis of the full life cycle costs to society of EVs. Additionally the extent of emissions reductions depends on what vehicles types are replaced by EVs. A discrete choice model of consumer preferences would facilitate a more realistic representation of market penetration.

There is a need to quantify the disutility to the consumer associated with the usability of an EV in terms of the limited driving range and lack of recharging infrastructure. As a starting point, one could estimate the disutility of the costs associated with the installation of home recharging equipment and garage space requirements.

A further analysis would be possible when EVs come to market. It would be useful to integrate a more careful assessment of travel patterns. This would be possible through EV trials and would allow a better analysis of the emissions and fuel consumption savings. Additional sensitivity analysis on the assumed fuel efficiency of EVs, fuel and electricity prices would also provide insights and eliminate ambiguity. A comparison of multiple time frames of different lengths would benefit an analysis of this type to monitor how the social net benefit changes over time.

4 An introduction to driving cycles and an analysis of real-world driving conditions

Understanding real-world driver behaviour in the form of driving cycles is instrumental in the design of efficient powertrains and energy storage systems for EVs. In addition, driving cycles serve as a standardised measurement procedure for the certification of a vehicle's fuel economy, emissions and driving range. In relation to the research presented in Chapters 2 and 3, driving cycles also facilitate the evaluation of the economic and lifecycle costs of emerging vehicular technologies. However, discrepancies between existing driving cycles and real-world driving conditions exist due to a number of factors such as insufficient data, inadequate driving cycle development methodologies and methods to assess the representativeness of developed driving cycles.

This chapter forms the basis of the research presented in Chapter 5. A review of existing driving cycles and driving cycle development methodologies for ICEVs and EVs is conducted. Then a four-step modelling approach for developing a set of real-world driving cycles for the GDA is presented. An EV demonstration project and the data collection and processing techniques are outlined. The remainder of the chapter details the first step in the modelling approach. The energy economy of the vehicles is estimated by simulating a modelled powertrain over recorded real-world driving cycles using an advanced vehicle simulation software. An analysis of real-world driving cycles is conducted to contribute to the knowledge regarding the real-world operating conditions and energy demands of EVs. A driving environment recognition tool based on a neural network is developed to determine and classify the driving conditions in terms of road-types and levels of congestion that the EVs in the demonstration project operated in. It was established that EVs primarily operate in urban driving conditions and that the energy economy of EVs is largest on short journeys and in urban stop-start driving conditions. This initial analysis of the energy economy and operating conditions of EVs in the real-world forms the basis of the development of a set of driving cycles for the GDA in Chapter 5.

This chapter is organised as follows: Sections 4.1 and 4.2 provide an overview of driving cycles and existing cycles in different countries respectively. A review of existing driving cycle development methodologies is conducted in Section 4.3. An overview of the proposed four-step modelling approach for developing a set of real-world driving cycles is presented in Section 4.4. A description of the EV demonstration project and the pre-processing, filtering and smoothing of the logged data is outlined in Section 4.5. The simulation of a modelled drivetrain over recorded driving cycles is presented in Section 4.6. The data is segmented by journey distance in Section 4.7. The driving environment recognition tool is presented and validated in Sections 4.8 and 4.9 respectively. The entire dataset is then segmented and classified using the driving environment recognition tool in Section 4.10. An analysis of the energy economy of EVs in different driving

environments and the proportion of time spent operating in different driving environments is presented in Section 4.11. Section 4.12 concludes the chapter with a discussion of the findings and introduces the research presented in Chapter 5.

4.1 An overview of driving cycles

Traditionally, the design, evaluation and certification of a vehicle's fuel economy are determined by using driving cycles. Driving cycles have been developed to provide a velocity-time profile that is representative of real-world driving conditions. They are used to assimilate driving conditions on a laboratory chassis dynamometer (Figure 4.1). These tests have been designed such that they can be applied to a variety of vehicles irrespective of the vehicle's performance or the intended operating conditions of the vehicle in the real-world.

Figure 4.1. Images of the dynamometer testing of vehicles (Rask and Rousseau, 2012).

There are two types of driving cycles - transient cycles such as the Federal Test Procedure (FTP-75) (Figure 4.2 (a)) (United States Environmental Protection Agency, 1993) and modal cycles such as the New European Driving Cycle (NEDC) (Figure 4.2 (b)) (United Nations Economic Commission for Europe, 2005). The primary difference is that modal cycles are a compilation of constant acceleration and constant velocity periods, whereas transient cycles involve many velocity variations, typical of on-road driving conditions.

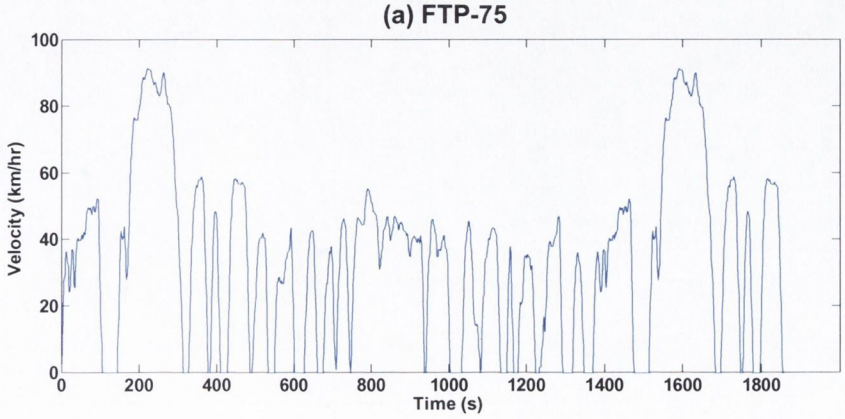

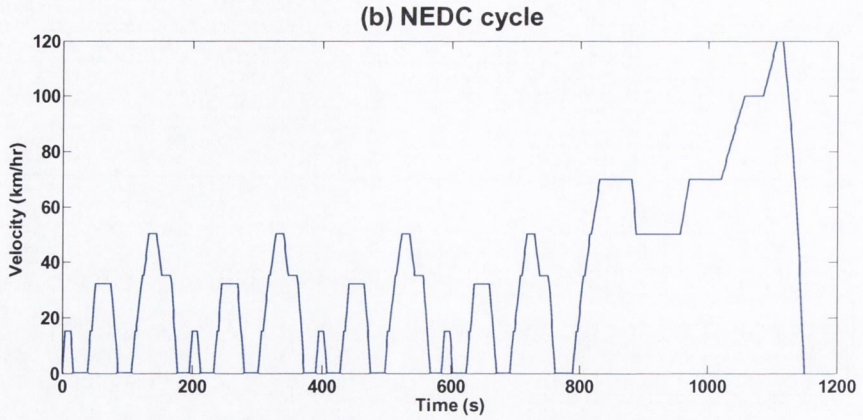

Figure 4.2. (a) The FTP-75 driving cycle and (b) the NEDC driving cycle (United Nations Economic Commission for Europe, 2005, United States Environmental Protection Agency, 1993).

There are two main categories of driving cycles, legislative and non-legislative. Legislative driving cycles such as the NEDC, the FTP-75 and the Japanese 10-15 Mode cycle (dieselnet, 2013b) are used by regulatory authorities to certify a vehicle's emissions, fuel economy and driving range (in the case of EVs) within their respective jurisdictions. Non-legislative driving cycles such as the Hong Kong cycle (Hung et al, 2007), the Edinburgh cycle (Esteves-Booth et al, 2001) and the Athens cycle (Tzirakis et al, 2006) have broad applications in research from vehicle design to life cycles analyses.

Regulation UN ECE 101 stipulates the current method by which the electric energy economy of EVs is estimated and certified in Europe (United Nations Economic Commission for Europe, 2005). The test procedure uses the NEDC cycle. The NEDC consists of four repeated Urban Driving Cycles (UDC) and one Extra Urban Driving Cycle (EUDC). The overall distance of the test is 11 km and it reaches a peak velocity of 50 km/hr in the urban segment and a peak velocity of 120 km/hr in the extra-urban segment of the cycle.

A peculiar situation arises in the case of an EV, since certification tests have to be repeated ten to fifteen times in order to evaluate the driving range of the vehicle (the distance of the NEDC is 11 km and driving range of an EV is approximately 160 km). When the cycle is repeated a number of times, it implies that the vehicle is driven in low-velocity urban conditions for approximately 65% of the time and in high velocity extra urban driving conditions for 35% of the time. It will be demonstrated in this thesis that in a real-world journey, an EV does not typically operate at high velocity for such a large proportion of time.

In 2014, under the guidelines of the UNECE World Forum for Harmonisation of Vehicle Regulations, the Worldwide harmonised Light vehicles Test Procedures (WLTP) will replace Regulation UN ECE 101 (dieselnet, 2013e). It aims to establish a worldwide test procedure to

measure LDV emissions and energy economy. New driving cycles and a test procedure will be introduced to address off-cycle emissions. Further details of the WLTP driving cycles will be provided in the next section.

Driving cycles provide an estimation of fuel economy and are useful for comparison purposes. However, there is poor correlation with real-world driving conditions and their effects on fuel consumption and emissions, particularly in relation to modal cycles. There are significant variations in real-world usage compared to test procedures and this variation causes a significant difference in emissions and fuel economy in real-world operating conditions (Eva, 2000, Tzirakis et al, 2006). Tzirakis et al (2006) developed a driving cycle for Athens using data collected from an ICEV. Dependent on the vehicle tested fuel consumption and emissions were found to be 9-79% and up to 300% higher respectively than that observed on the NEDC.

Real-world driving in America has recently been analysed, and it has been shown that the American certification cycles, the Urban Dynamometer Driving Schedule (UDDS) cycle and the Highway Fuel Economy Test cycle (HWFET) are much less aggressive than real-world driving conditions, thus leading to the significant under prediction of the peak power demands and energy economy of vehicles in the real-world (Fellah et al, 2009, Patil et al, 2009, E. D. Tate et al, 2009). Combinations of different cycles have been used in EV analysis to overcome parts of this deficiency (Fellah et al, 2009), as well as scaling of the UDDS (Duoba et al, 2009). Gonder et al (2007) used GPS driving cycle data collected from a fleet of 227 vehicles in the State of Missouri to simulate the fuel and electricity consumption of PHEVs. The results were compared against the HWFET and the FTP-75 cycles. The modelled fuel consumption was lower for real-world driving cycles than the certification cycles whereas the electricity consumption was higher for the real-world cycles than the certification cycles. The author noted that these findings suggest that the US EPA's driving cycles do not capture the range of speeds and accelerations typical of real-world driving and that these differences can significantly affect the energy economy of PHEVs. Shahidinejad et al (2010) states that there are many concerns about the problems inherent in existing driving cycles such as the underestimation of cruise, acceleration and stop-and-go activities in different brackets of velocities. They concluded that existing cycles do not completely emulate the real-world power demands of PHEVs.

Driving cycles also play an important role in the analysis and design of vehicle propulsion systems. There are various PHEV powertrains configurations such as serial, parallel and serial–parallel. The vehicle's power management strategy provides the propulsion energy by blending the power sources from the electric motor and the ICE. Each type of powertrain configuration requires a substantially different power blending optimisation technique. The energy economy of blended PHEVs are particularly sensitive to driving cycles (Rask and Rousseau, 2012), therefore the

optimum power management strategy is best determined by design using realistic driving cycles (Ali Ashtari, 2012, Qiuming et al, 2008).

Namdoo et al (2010) analysed the impact of driving cycle aggressiveness on the energy economy of a vehicle using a simulation of a midsize parallel hybrid PHEV. The author evaluated the outcome of sizing the electric motor and battery to follow the UDDS cycle and six additional standard driving cycles. The results demonstrated that a PHEV's design is directly influenced by the choice of driving cycle.

Design optimisation studies in America have typically used either a single federal drive cycle such as the FTP-75 or a weighted sum of two driving cycles, such as the FTP-75 and the HWFET (Fellini et al, 1999, Whitefoot et al, 2010). These are intuitive choices because they are the driving cycles that are used for U.S. federal emissions and fuel economy certification. However, designing vehicles to a fixed driving cycle results in a suboptimal vehicle for any driving environment that varies significantly from the driving cycles used in the design. Dubarry et al (2007) suggest that the lack of comprehensive driving cycles to allow for the benchmarking of vehicle and battery performance could undermine the development of EVs and this could also have significant impacts on the calculated life of the battery.

From the review of the literature it can be concluded that driving cycles play an important role in the design, certification and evaluation of vehicular technologies and that existing driving cycles do not completely emulate real-world driving conditions. Hence, analysing real-world driving cycles and conditions and developing representative real-world driving cycles are essential for EV design. Worldwide, regulatory agencies are seeking to update testing procedures to account for real-world usage. In addition, research has shown that the benefit of a particular vehicle technology is dependent on the cycle that it was evaluated on (Rask and Rousseau, 2012). Therefore, real-world driving cycles are required for realistic economic and life cycle studies.

The next section presents a selection of common driving cycles and their key statistical features that are used in different countries.

4.2 An overview of driving cycles used in different countries

Barlow et al (2009) published a reference handbook for the Department of Transport in the UK detailing the statistical parameters of 256 worldwide driving cycles. The driving cycles from Barlow et al (2009) were used in the work presented in this thesis. This section presents an overview of a selection of legislative and common non-legislative cycles used in different geographical areas. This will be followed by a discussion on the different approaches used in development of driving cycles.

4.2.1 European driving cycles

4.2.1.1 The NEDC

As discussed in Section 4.1, the NEDC is used as a reference cycle for certifying vehicles in Europe under Regulation UN ECE 101. The NEDC consists of four repeated Urban Driving Cycles (UDC) and one Extra Urban Driving Cycle (EUDC). The main characteristics of the cycle are listed in Table 4.1.

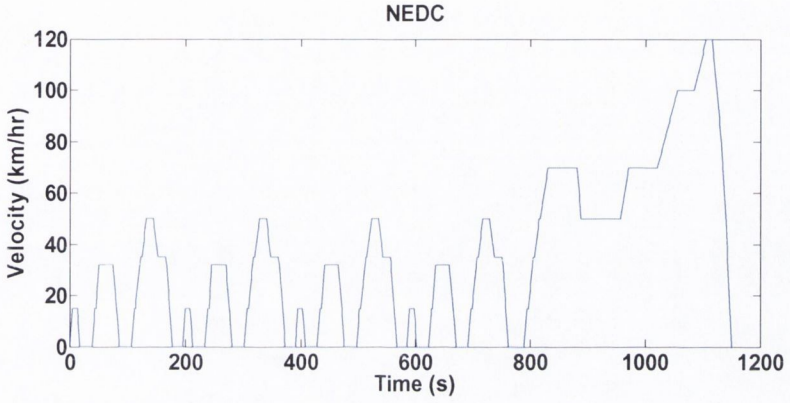

Figure 4.3. The NEDC.

Table 4.1. Characteristics of the NEDC.

Characteristic	NEDC
Distance	11,023 m
Duration	1180 s
Average speed	33.6 km/hr

4.2.1.2 The worldwide harmonised light vehicles test procedures

As discussed in Section 4.1, the WLTP is a test currently being developed under the guidelines of the UNECE World Forum for Harmonisation of Vehicle Regulations. In 2014, it is expected that the WLTP test will replace Regulation UN ECE 101 (dieselnet, 2013e) and hence the NEDC for the certification LDVs.

The test procedure will provide strict guidance on the conditions under which dynamometer tests should be performed in relation to road load, gear shifting, car weight, fuel quality, ambient temperature, tire selection and pressure. The WLTP procedure will include three test cycles applicable to vehicle categories of different power to mass (PMR) ratios. The PMR parameter will be defined as the ratio of rated power (W) to kerb mass (kg). The main characteristics of the cycles are listed in Table 4.2.

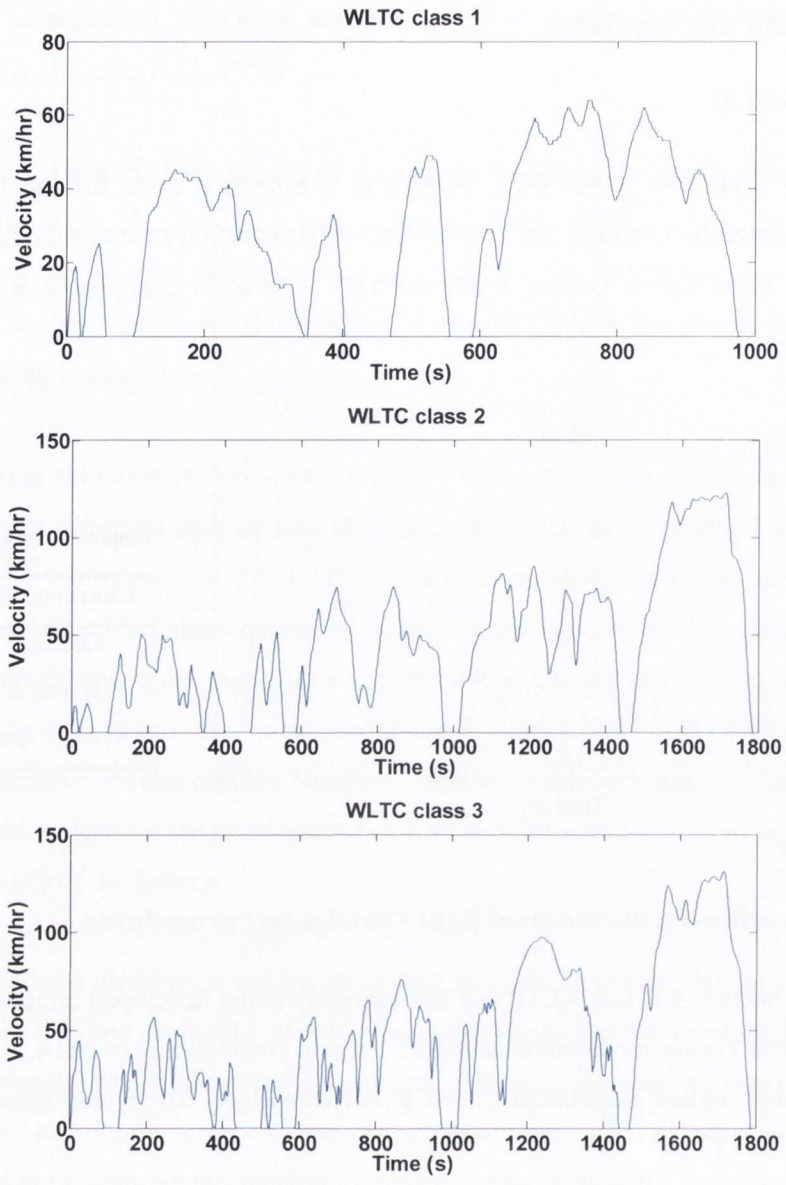

Figure 4.4. The WLTP cycles.

Table 4.2. Characteristics of the WLTP cycles.

Characteristic	WLTP class 1	WLTP class 2	WLTP class 3
Distance	8,091 m	14,664 m	23,262
Duration	1022 s	1,477 s	1,800
Average speed	17.6 km/hr	54.0 km/hr	92 km/hr

4.2.1.3 The Artemis driving cycles

The Artemis cycles were developed during a European research project, Artemis (André, 2004). There are 3 different cycles, an urban cycle, a rural cycle and, and a motorway cycle. The Artemis cycles are not used for certification of emissions or fuel consumption. However, car manufacturers would use these real-world cycles in the design of vehicles and to assess the real-world performance of vehicles. The main characteristics of the cycles are listed in Table 4.3.

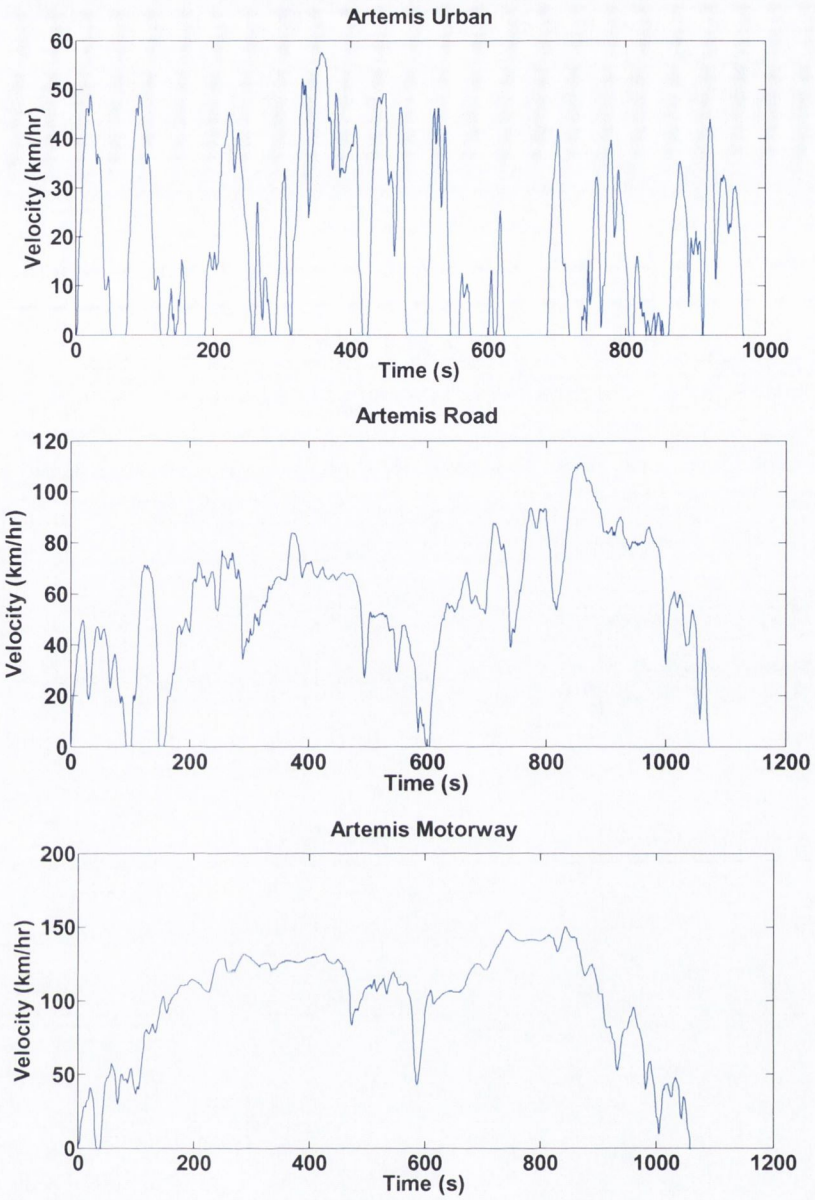

Figure 4.5. The Artemis driving cycles.

Table 4.3. Characteristics of the Artemis cycles.

Characteristic	Urban	Rural	Motorway
Distance	4,874 m	17,275 m	28,737
Duration	993 s	1,082 s	1,068 s
Average speed	17.7 km/hr	57.5 km/hr	96.9 km/hr

4.2.2 American driving cycles

4.2.2.1 The FTP-75 cycle

The FTP-75 cycle is one of the cycles defined in the U.S. EPA's federal test procedures and in Title 40 of the U.S. Code of Federal Regulations, Protection of the Environment (United States Environmental Protection Agency, 2013). It is intended to represent a commuting cycle with a

section of urban driving and a section of motorway driving. The main characteristics of the cycle are listed in Table 4.4.

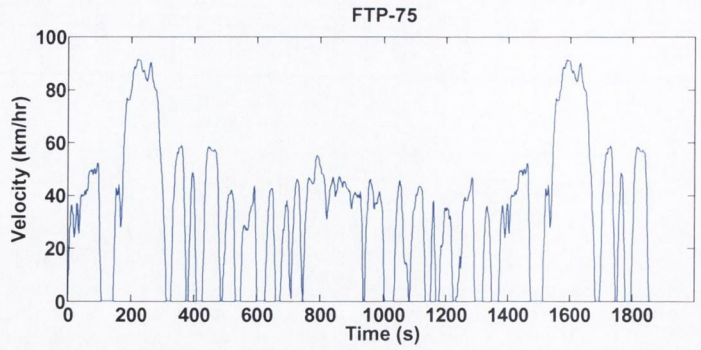

Figure 4.6. The FTP-75 cycle.

Table 4.4. Characteristics of the FTP-75 cycle.

Characteristic	FTP-75
Distance	17,787 m
Duration	1874 s
Average speed	34.2 km/hr

4.2.2.2 The Highway Fuel Economy cycle

The HWFET cycle is also defined in the U.S. EPA's federal test procedures and in Title 40 of the U.S. Code of Federal Regulations, Protection of the Environment (United States Environmental Protection Agency, 2013). It is intended to represent highway driving. The main characteristics of the cycle are listed in Table 4.5.

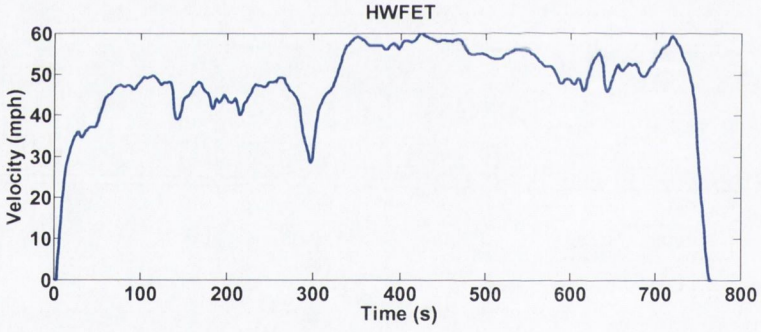

Figure 4.7. The HWFET cycle.

Table 4.5. Characteristics of the HWFET cycle.

Characteristic	FTP-75
Distance	14,045 m
Duration	765 s
Average speed	77.7 km/hr

4.2.2.3 The New York City cycle

The New York City cycle (NYCC) is not part of the U.S. EPA's federal test procedures but it is commonly used to assess fuel economy in low speed urban driving conditions with frequent stops (dieselnet, 2013a). The main characteristics of the cycle are listed in Table 4.6.

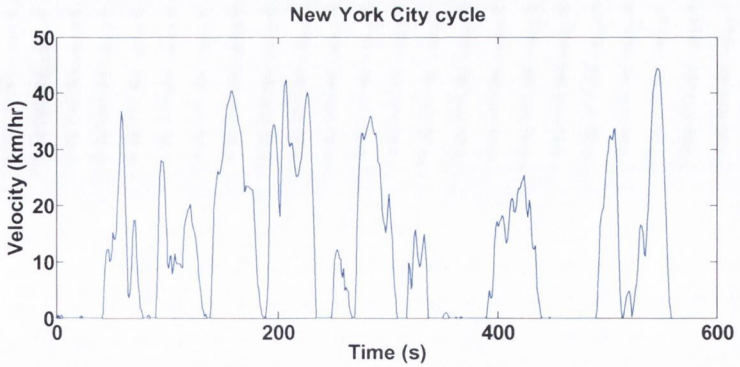

Figure 4.8. The New York city cycle.

Table 4.6. Characteristics of the NYCC.

Characteristic	NYCC
Distance	1,093 m
Duration	598 s
Average speed	11.4 km/hr

4.2.3 Japanese driving cycles

4.2.3.1 The Japanese 10-15 Mode cycle

The Japanese 10-15 mode cycle is used in Japan for emission certification and fuel economy for light duty vehicles (dieselnet, 2013b). The main characteristics of the cycle are listed in Table 4.7. In 2015, the Japanese 10-15 model cycle will be replaced by the JC08 cycle which is a longer and more aggressive cycle. The cycle is intended to represent driving in congested city traffic, including idling periods and frequently alternating acceleration and deceleration events (Dieselnet, 2013c). The main characteristics of the JCO8 cycle are listed in Table 4.8.

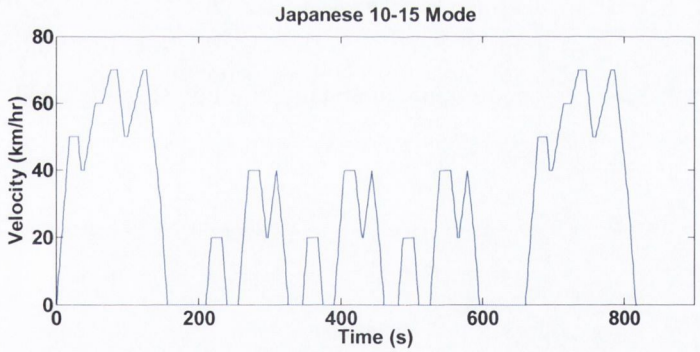

Figure 4.9. The Japanese 10-15 Mode cycle.

Table 4.7. Characteristics of the Japanese 10-15 Mode cycle.

Characteristic	10-15 Mode
Distance	4,016 m
Duration	660 s
Average speed	28 km/hr

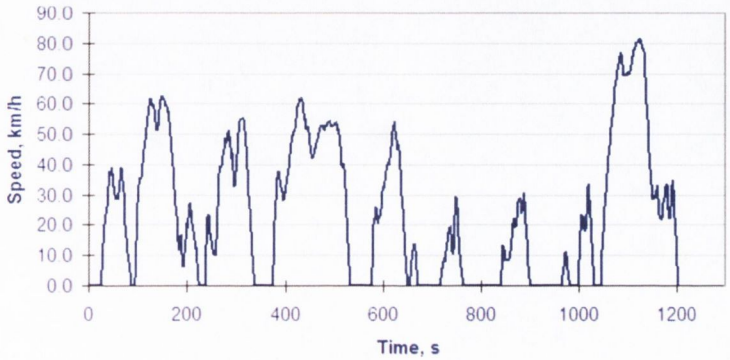

Figure 4.10. The Japanese JC08 cycle (Dieselnet, 2013c).

Table 4.8.Characteristics of the JC08 cycle.

Characteristic	JC08 Mode
Distance	8,171 m
Duration	1204 s
Average speed	24.4 km/hr

4.3 A review of driving cycle development methodologies

There are two distinct approaches used to develop driving cycles. In the first approach modal driving cycles are developed from a number of constant acceleration and constant velocity phases.

The second approach uses collected on-road driving data to develop transient driving cycles. Typically, the first step is to record real-world driving cycles and then divide the collected speed-time traces into smaller sections termed micro-trips or micro-segments which have been defined according to certain rules. These terms are discussed in more detail in the next section. These micro-trips/segments are then separated into various groups. The groups represent collections of similar traffic conditions (e.g. average speed) and/or road types (e.g. motorway and urban). After the data have been classified into groups, micro-trips/segments are chosen according to certain criteria and then joined together to form a complete driving cycle. The basic logic in choosing micro-trips is to ensure that they closely replicate the trends and characteristics of the entire logged driving cycle dataset. The final step requires a single driving cycle to be selected from among the developed candidate driving cycles based on a set of target statistical measures. The objective is to match the assessment criteria of a candidate cycle with those derived from the whole driving cycle database (i.e. target statistics). It is important to define a suitable set of assessment criteria. Speed and acceleration related parameters, idling time, cruising time, the number of stops and the speed and acceleration distribution (SAFD) of cycles are the most frequently used measures as they have a strong influence on emissions (Chen et al, 2007, Tong and Hung, 2010). A SAFD expresses the amount of time spent in specific speed and acceleration bins and provides quantitative information about the operating characteristics of the roads in the geographical area under study (Figure 4.11).

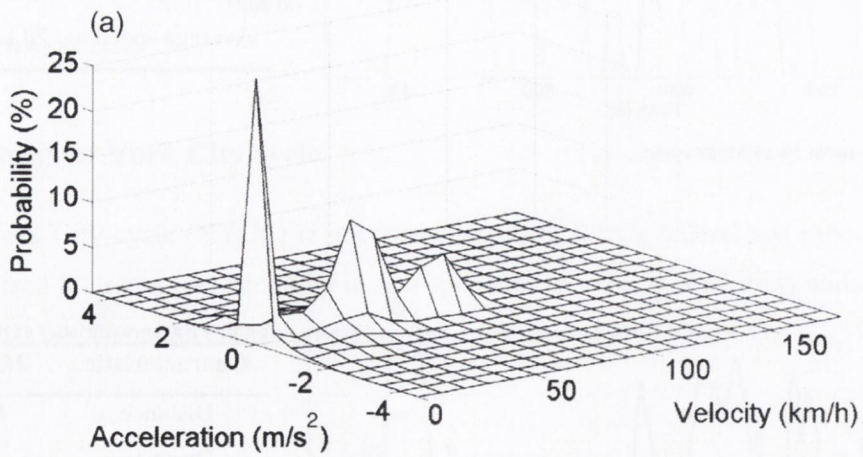

Figure 4.11. Example of a speed-acceleration frequency distribution plot (Shahidinejad et al, 2010).

The general method for developing transient driving cycles is illustrated by the flowchart in Figure 4.12. Andre (1996) and Lin and Niemeier (2003) discuss the effectiveness of existing

methodologies used in developing driving cycles to represent the characteristics of logged driving cycle data. Tong and Hung (2010) conducted a review of 101 worldwide transient driving cycles and proposed a framework for developing driving cycles. The recommendations of the review were that "traffic activity patterns and quantitative statistics should be considered when selecting the test routes" and that "the tendency of zero change in acceleration, which has been commonly ignored in the literature, and the application of succession probability at a second-by-second level should be further explored".

Typically, existing driving cycle development methodologies can be generalised into four types: micro-trip based cycle development, micro-segment based cycle development, cycle development based on pattern classification and modal cycle development (Lin and Niemeier, 2003). A review of driving cycle development methodologies is presented in the next section

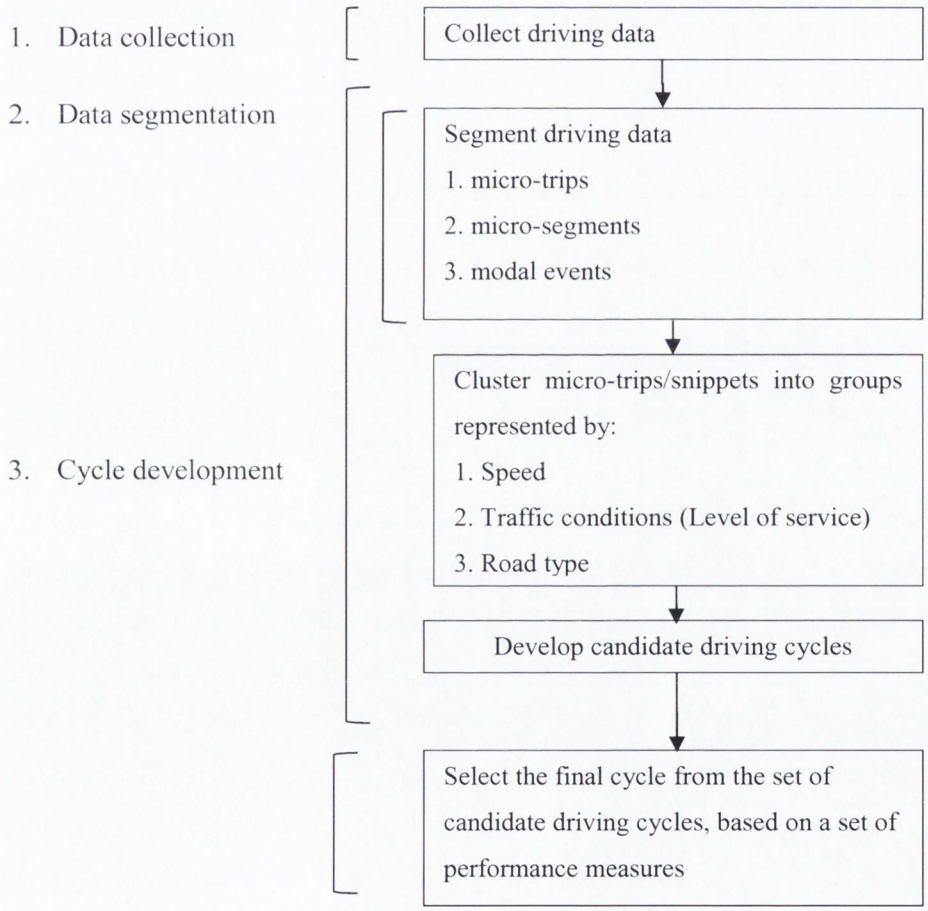

Figure 4.12. Simplified driving cycle development process.

4.3.1 Micro-trip based cycle development

One approach to develop a driving cycle is to chain micro-trips, which are defined as the driving activity between adjacent stops, including the leading period of idle time (Figure 4.13) (Austin et al, 1993).

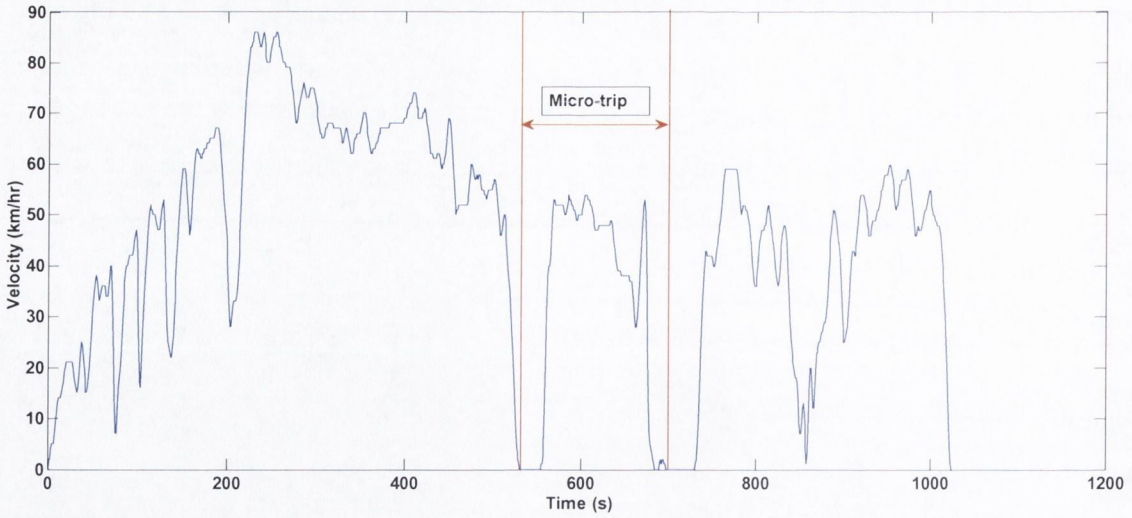

Figure 4.13. Micro-trip illustration.

Cycles such as the Sydney cycle (Kent et al, 1978), the Hong Kong cycle (Hung et al, 2007) the China cycle set (Wang et al, 2008) and the Pune cycle (Kamble et al, 2009) were developed using a micro-trip method. Using the micro-trip method the driving cycle data are segmented into micro-trips and then the micro-trips are generally partitioned into different pools of driving conditions by clustering methods. A driving cycle is then constructed by chaining representative micro-trips with the goal that the cycle closely matches the logged driving cycle dataset. Micro-trips are usually selected using one of three methods: random selection; 'best incremental', meaning incrementally searching for and adding a micro-trip with specific driving characteristics that improve and match the target statistics; or a hybrid of both approaches (Austin et al, 1993). Candidate cycles are assessed using parameters such as mean speed, maximum speed, minimum speed, mean acceleration, mean deceleration and a SAFD plot (Dai et al, 2008). Different variations of the micro-trip based approach are the most frequently used methods. The major limitation to the micro-trip based method is that a micro-trip does not differentiate various types of driving conditions such as roadway type or level of service (LOS) (Dai et al, 2008). LOS refers to the categorisation of traffic flow on a road network (i.e. free flowing). As a result, replicating driving activities under a particular driving condition is difficult (André, 2004). For example, under smooth traffic conditions, a vehicle seldom stops and a single micro-trip may cover different road segments or different traffic conditions. The micro-trip method has been criticised that the parameters and criteria used for cycle development are not directly related to emissions (Tong and Hung, 2010). The next section reviews the micro-segment based cycle development methodology.

4.3.2 Micro-segment based cycle development

A trip-segment is obtained, as illustrated in Figure 4.14, by partitioning vehicle speed-time profiles using changes in roadway type or LOS, in addition to stops (Carlson and Austin, 1997).

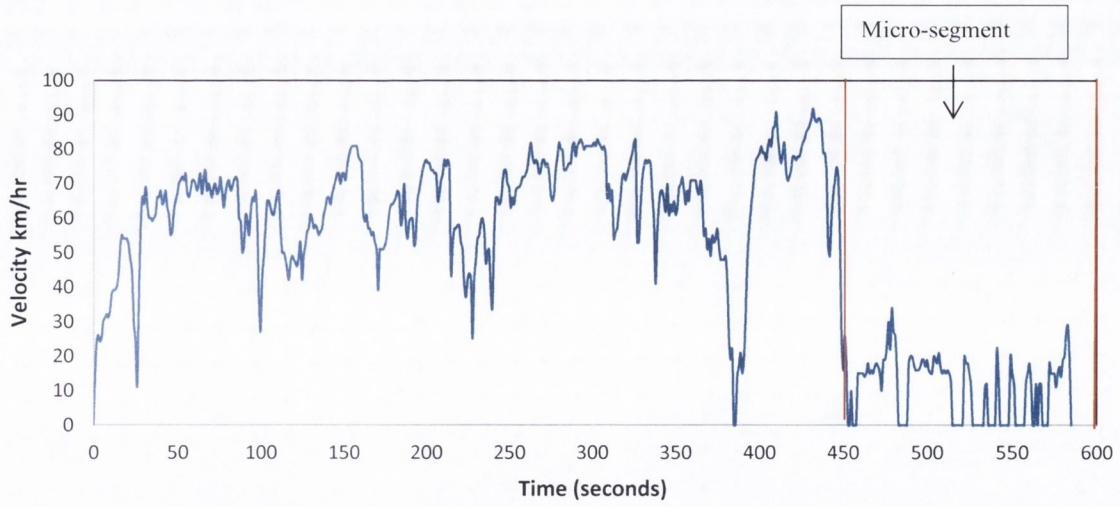

Figure 4.14. Micro-segment illustration.

The driving cycles can be segmented by roadway type or LOS and cycles can be developed to represent driving profiles for specific road-types and traffic conditions. One application of the segment-based cycle development method was the development of the U.S. EPA's facility-specific speed correction cycles (Dai et al, 2008). The MOBILE 6 vehicle emission modelling software (U.S. Environmental Protection Agency, 2012) was updated in 2001 to account for differences in driver behaviour on different roadway types and aggressive driving behaviour by using real-world driving cycles and a micro-segment development method (Brzezinski et al, 2001). Similar to the micro-trip based method, trip segments are selected and connected using a hybrid of random and best-incremental logic. However, unlike a micro-trip, trip segments can start and end at any speed. Therefore, the chaining of segments requires certain constraints on speed and acceleration between the two connecting seconds of the previous and succeeding micro-segments. For example, in developing the U.S. EPA's facility specific cycles, the differences in speeds between two connecting segments was required to be within 0.5 mph, and the difference in acceleration within 0.5 mph/sec (Carlson and Austin, 1997). The 'best' cycle was then selected using two primary parameters: 1) the sum of the difference in the SAFD between the developed candidate cycle and the entire logged driving cycle dataset, and 2) the amount of operation occurring in high power mode (Carlson and Austin, 1997). To this author's knowledge micro-segment based methodologies have only been used for developing driving cycles for ICEVs for emission estimation purposes. The next section reviews cycle development with pattern classification.

4.3.3 Cycle development with pattern classification

Andre (1996) and Andre et al (1995) developed cycles in Europe using pattern classification (Andre, 1996, Andre et al, 1995). In this approach, 'kinematic sequences' (similar to micro-trips) were classified into heterogeneous classes using statistical methods. The approach used succession probabilities to estimate the likelihood that one class of activity precedes or follows a particular activity class. Driving cycles were synthesised by connecting kinematic sequences randomly

selected from each of the activity classes in accordance with the probability and chronology of kinematic sequences (Andre et al, 1995).

In developing the European Urban Cycles, the kinematic sequences were described by 20 variables such as duration, idle time, distance and the mean, the maximum, the minimum and the standard deviation of speed and acceleration. Principle Component Analysis (PCA) was applied to the 20 variables followed by a cluster analysis on the kinematic sequences. Four classes were identified, representing congested, free-flow urban traffic, extra-urban and motorway driving conditions. Next, a trip was viewed as a series of kinematic sequences. The recorded driving cycles were classified based on the frequency of sequences in each kinematic sequence class and the number of transitions between two classes of kinematic sequences. Three types of trips were identified, urban trips, rural trips and motorway trips.

The method was further improved in the development of European driving cycles in the ARTEMIS project (Michel, 2004). To avoid bias due to the varying duration of sequences between two stops, speed-time traces were segmented into sequences of homogeneous size rather than partitioning by stops. Correspondence Analysis using chi-squared distance and cluster analysis were applied to classify the sequences into 12 driving conditions. Urban, rural and motorway cycles were developed based on the observed composition of driving conditions. To this author's knowledge the methodology described in this section has only been used for developing driving cycles for ICEVs for emission estimation purposes. The next section reviews cycle development based on vehicle operation modes.

4.3.4 Modal cycle based development

A study by Lin and Niemeier (2002) applied a mode-based cycle development method for estimating emissions, where real-world driving was viewed as a sequence of acceleration, deceleration, cruise, and idle modes. Studies show that running emissions are related to vehicle modal operation (Barth et al, 1996a, Fomunung et al, 1999). Therefore, for emission estimation purposes, it was logical to analyse and replicate driving activities from a modal perspective. Assuming that the likelihood of a particular modal event (e.g. acceleration, cruise, or deceleration) occurring depends only on the mode of the previous modal event, driving activities were modelled as a Markov chain.

Lin and Niemeier's (2002) modal cycle development comprised of four steps. Firstly, the real-world driving cycle data were partitioned into snippets of various durations based on acceleration using a maximum likelihood estimation (MLE) clustering method. Secondly, the snippets were classified into different modal bins, again using the MLE clustering method. However in that case, the clustering variables included mean, minimum, and maximum speeds and acceleration rates. The

third step was to create a transition probability matrix (TPM) that contained the succession probabilities between different modes. A cycle was then developed as a Markov chain. The snippet selection algorithm required that the selected snippet improved the match to the observed SAFD of the logged driving cycles, and that the start speed of the snippet matched the end speed of the previous snippet within 0.2 km/hr. Snippet selection was repeated until the desired cycle length was achieved. A number of other studies have used stochastic approaches for developing driving cycles for EVs and are reviewed in the next section.

4.3.5 Driving cycles and electric vehicle applications

An extensive literature review revealed little reference to the development of driving cycles for BEVs, taking into account energy economy as the primary requirement for representing real-world driving cycle data. The driving cycles studies referred to in the previous sections primarily focused on developing urban driving cycles using snippets extracted from recorded speed-time traces to estimate vehicular emissions and fuel economy in different geographical areas.

A simplified methodology for generating driving cycles was reported in Qiuming et al (2008) in the development of a power management strategy for PHEVs. The methodology was based on the assumption of constant acceleration and deceleration rates, along with the consideration of the speed limits on different road segments in the area under study. However, a single representative driving cycle was not developed. Alessandrini and Orecchini (2003) collected 3,100 km of real-world driving cycle data from an electric Citroen Saxo. A driving cycle for BEVs in the city of Rome was synthesised by tracking a path through a joint velocity and acceleration matrix. A random number generator was used to simulate the probability component in which a time sequence of velocities was produced. A representative driving cycle was developed for Rome. The cycle was compared to a number of existing cycles. The author noted that there was a requirement for the developed cycle in order to represent the driving conditions of EVs in Rome because the developed cycle had a lower value of acceleration-speed product than the comparison cycles due to the limited power of the EV used in the study. It was also noted that there were frequent changes in acceleration, which is typical of traffic in a city.

Gong et al (2011) developed an iterative Markov chain approach for generating driving cycles for PHEVs. Logged driving cycle data from 673 journeys undertaken with a PHEV were first segmented into micro-trips, which were represented by a 1 x 18 element Driving Cycle Statistical Metrics Vector (DCSMV). PCA was then performed to reduce the 1 x 18 element vector into a 1 x 5 element vector. Four of the remaining variables, driving time, distance, maximum velocity and minimum velocity were selected to cluster the micro-trips into classes, each class representing a particular driving environment. TPMs were generated for each class with velocity and acceleration selected as the states and stochastic velocity profiles were then generated based on a stationary

Markov chain model. No statistical criteria were presented to ensure that a synthesised cycle was representative of the characteristics of the real-world driving cycles.

Similar to Gong et al (2011), Lee and Filipi (2011) also proposed a procedure for synthesising driving cycles for PHEVs using Markov chains. Real world driving cycles logged from 181 journeys in the city of Michigan were first categorised based on trip length and mean speed. The former was used to generally classify driving cycles as urban, suburban or long distance commutes and the latter to identify a particular driving style. TPMs were generated for each driving category in the form of two dimensional matrices. Based on an investigation of vehicle dynamic equations, the two states, velocity and acceleration, were also selected as states for the Markov chain. A discrete-time Markov chain was used to generate a large number of synthetic cycles. In a subsequent step, a regression analysis was performed to determine significant statistical criteria that had to be satisfied in order to confirm the representativeness of a synthesised candidate cycle. Cycles that best matched the logged driving cycles were considered to be representative of real-world driving. A representative driving cycle for the city of Michigan was not published.

Shahidinejad et al (2010) reported a driving cycle deployment methodology for PHEVs in the city of Winnipeg, Canada. Driving cycle data from 76 sedan type vehicles, sport utility vehicles and pickup trucks were collected over the course of a year. Twenty-five driving cycle parameters were computed for each driving cycle. A single most representative cycle was selected from the database of recorded cycles based on a comparison of the 25 driving cycle parameters of each cycle to the mean of the 25 driving cycle parameters of the entire dataset. Asharti et al (2012) also developed a driving cycle applicable to EVs in the city of Winnipeg using the same dataset reported in Shahidinejad et al (2010). The data was first clustered into different segments based on several driving parameters. Then, the probability of transitioning between different types of segments was calculated. The methodology used a snippet selection algorithm that optimised the selection of snippets with respect to 14 driving cycle parameters, which were not limited to SAFD matching. The iteration procedure continued until the desired cycle length was reached. A representative driving cycle, known as the Winnipeg driving cycle was developed and published to represent real-world driving conditions in the city of Winnipeg.

From the review of available literature it can be concluded that there does not exist a single widely accepted driving cycle for BEVs that represent typical real-world driving conditions in Ireland or Europe.

4.4 An overview of the proposed stochastic driving cycle development methodology

The literature review on driving cycles has resulted in a number of useful insights for this research. In this section an overview of a four-step methodology for developing driving cycles is presented. The cycles are developed over the course of this chapter and Chapter 5.

The ability of driving cycles to represent real-world driving conditions is enhanced by improving and combining four important steps in the driving cycle development process. In the first step a dynamic statistical analysis of logged driving cycles is conducted and the cycles are classified and segmented in terms of road-types and levels of congestion. In the second step a driving cycle model that synthesises cycles by the application of velocity and acceleration succession probabilities at a second by second level is developed. In the third step, a number of cycle assessment and evaluation procedures to ensure that the developed cycles are representative of the original dataset are performed. In the final step, an assessment of the representativeness of the developed driving cycles and a selection of well-established worldwide driving cycles of the recorded real-world driving cycles is conducted.

The goal of the first step, a statistical analysis, is to differentiate the recorded real-world driving cycle data into four different driving distance bins. At the end of the process a representative driving cycle of the real-world driving cycles in each bin will be developed. Next, a driving environment recognition tool is developed based on a statistical analysis of real-world driving cycle data. The tool uses a neural network to classify data. The tool is used to separate and classify the data into the four different bins, into different driving environments determined by road-types and levels of congestion. This allows the energy economy of EVs in different driving environments to be analysed. The development of this tool and the subsequent analysis of the data are presented in this chapter.

Existing driving cycles have been developed to represent driving conditions of particular road-types or traffic conditions for example the HWFET cycle was developed to represent motorway driving in the U.S. The road-type and traffic condition composition of driving cycles are dependent on the journey distance and it is important that this is taken into consideration and integrated into the development of the driving cycles. The driving environment recognition tool allows the proportion of time that EVs operate in specific driving environments to be determined. This analysis is also presented in this chapter.

The objective of the second step, driving cycle synthesis, is to develop a Markov-chain driving cycle model. A Markov chain, as a stochastic process, with the states velocity and acceleration has been demonstrated as being suitable to deal with the random property of cycles (Alessandrini and Orecchini, 2003, Gong et al, 2011, Lee and Filipi, 2011). Therefore, a TPM with velocity and

acceleration as the state variables is generated for each driving distance bin based on the recorded velocity and acceleration measurements in the bin. A TPM is then used to generate candidate driving cycles as a Markov chain for a given bin. The methodology of this step is presented in Chapter 5.

Since Markov chains are a stochastic process, there are no prior guarantees that a synthesised cycle will be representative of the real-world cycles in a given bin. As previously discussed, a developed driving cycle should resemble the overall characteristics of the original driving cycle dataset. At the same time, it has to preserve the naturalistic acceleration and deceleration events observed in real-world driving conditions. Hence a cycle assessment procedure is required. An overview of the cycle assessment procedure, the third step in the development process, is presented briefly in the next paragraph and in detail in Chapter 5.

A regression analysis is performed to determine the least number of statistically significant parameters that influence the energy economy of a vehicle over a driving cycle. The parameters identified in the regression analysis must be satisfied within certain error bounds in order to guarantee that a particular generated candidate cycle represents well the original driving cycle dataset. In addition to ensuring that the statistical parameters of the developed cycles match within certain error bounds the mean of the statistical parameters of the real-world driving cycles, the predicted energy economy of a developed driving cycle is assessed to ensure that it is representative of the real-world energy economy values in a given bin. Furthermore, the developed cycles are assessed to ensure that they consist of the same proportions of driving conditions in terms of road types and traffic conditions to those observed in real-world operating conditions.

In the final step, two methodologies are used to assess the representativeness of the developed driving cycles and a selection of well-established worldwide driving cycles of the original real-world driving cycles. An additional methodology is also used to compare the developed driving cycles to the selection of worldwide cycles. This allows the similarities or otherwise between the developed cycles and existing cycles to be determined. The methodology of this step is presented in Chapter 5.

The next section provides an overview of an EV demonstration project in Ireland. Following that the pre-processing, filtering and smoothing of the logged data is outlined.

4.5 Overview of the EV demonstration project and data collection techniques

Fifteen EVs were trialled in households of ESB (an Irish electricity utility company) employees for periods of four months July 2010-2012. The vehicles were Mitsubishi iMiEVs, a four-seater vehicle powered by a 16 kWh lithium ion battery pack. The electric motor provides 47kW of

power, a 180 Nm torque and is capable of reaching a top speed of 130 km/hr. A full charge of a battery takes about 8 hours and it has a typical driving range of 80 km.

4.5.1 Data collection

Data collected by data logging equipment installed in the vehicles is the primary source of data for the driving cycle analysis presented in this thesis. The data loggers were configured to read information from vehicle sensors available on the vehicle's CAN (Control Area Network) bus and to store these data in the logger's internal memory along with the vehicle's GPS (Global Positioning System) position. GPS data and CAN bus messages were logged every five seconds and every one second respectively when the vehicle ignition was on. Specifically the vehicle's velocity was logged every second from the Can bus. The data was automatically uploaded to a File Transfer Protocol (FTP) site every night. A graphical representation of the process is presented in Figure 4.15.

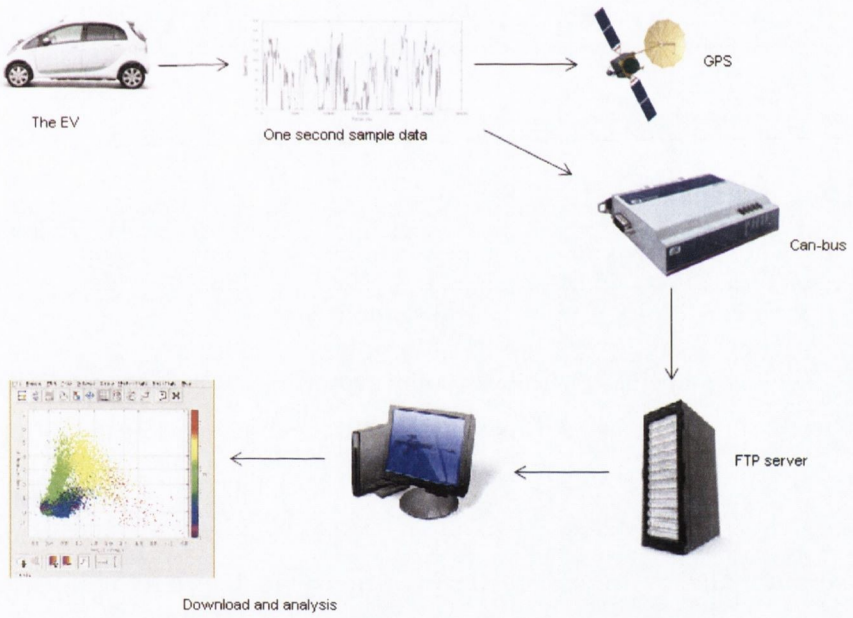

Figure 4.15. Overview of the EV data collection process.

The geographical areas in the GDA in which the data used for the development of the driving cycles were collected are shown in Figure 4.16. Data on a total of 1,485 journeys were collected for the analysis.

Figure 4.16. Map of the data collection region.

The next section, presents the data pre-processing, filtering and smoothing methods used to remove erroneous data points prior to the analysis of the data and the development of the driving cycles.

4.5.2 Velocity data processing: filtering and smoothing

At the end of the velocity data filtering and smoothing process the acceleration was computed directly from the measured velocity data using numerical differentiation (Equation 4.1). Hence, it was important the velocity data contained no erroneous data points. However, in practice the measured velocity data was found to contain intermitting periods of recording disruption typically between 2 and 8 seconds. The recording disruption was due to the limited technical capabilities of the data loggers in processing and storing data on a second by second basis. All the velocity data were subject to a series of pre-processing techniques described in this section.

$$a_t = \frac{S_t - S_{t-1}}{\Delta t} \tag{4.1}$$

Where:

a_t = the instantaneous acceleration at time t (m/s^2)

S_t = the measured velocity of the vehicle at time t (km/hr)

S_{t-1} = the measured velocity of the vehicle at t-1 (km/hr)

Δt = the duration between the velocity observations at time t and t-1 (seconds)

Firstly, all the recorded driving cycles were checked for periods of recording disruption and velocity measurements were linearly interpolated during the periods of disruption. However, the application of this technique could have resulted in unrealistic instantaneous acceleration values being computed depending on the time period of the disruption and the velocity measurements before and after the period of disruption. For example, consider Figure 4.17, which illustrates the instantaneous acceleration rate of a cycle, computed using Equation 4.1. The computed acceleration rate falls outside the feasible acceleration limits. Given that energy economy could be significantly influenced by acceleration values outside the feasible region, it was necessary to filter and smooth the raw velocity data after periods of velocity disruption were linearly interpolated. In the second step of the pre-processing of the velocity data, a smoothing algorithm was applied to all the driving cycles.

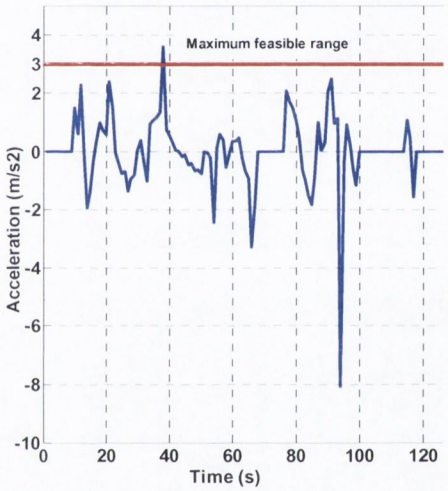

Figure 4.17. Acceleration rate computed from the raw velocity data.

Rakha et al (2001) investigated the suitability of a number of smoothing techniques on GPS velocity data. It was found that the Epanechnikov density kernel smoothing method performed well compared to the other methods. Hellinga (2011) also applied the Epanechnikov density kernel smoothing method to GPS velocity data when developing a fuel consumption and emissions model. Based on the literature, the Epanechnikov Kernel smoothing method was applied to the raw velocity data.

The Epanechnikov Kernel is computed as (Hellinga, 2011):

$$K(z_{ij}) = \begin{cases} 0.75(1 - z_{ij}^2) & |z_{ij}| \leq 1 \\ 0 & otherwise \end{cases} \quad (4.2)$$

Where for:

$z_{ij} = \frac{i-j}{\alpha}$

i = the current time interval (seconds)

j = the time interval j for which the density kernel is being computed (seconds)

α = duration of time period in the past and in the future considered within the smoothing (bandwidth)

When computing the smoothed velocity at time interval i, ($\hat{s}_i$), the weight associated with each velocity point in time interval j, (W_{ij}), is computed by

$$W_{ij} = \frac{K(z_{ij})}{\sum_{k=i-\alpha}^{i+\alpha} K(z_{ik})} \tag{4.3}$$

Then the smoothed velocity in interval i, ($\hat{s}_i$), is calculated by

$$\hat{s}_i = \sum_{j=i-a}^{i+a} W_{ij} S_i \tag{4.4}$$

And finally the acceleration is computed by

$$a_i = \frac{\hat{s}_i - \hat{s}_{i-\Delta}}{\Delta t} \tag{4.5}$$

where Δt is the time interval (1 second).

As indicated by Figure 4.18, the Epanechnikov kernel smoothing function provides parabolic weights that are dependent on the bandwidth (α).

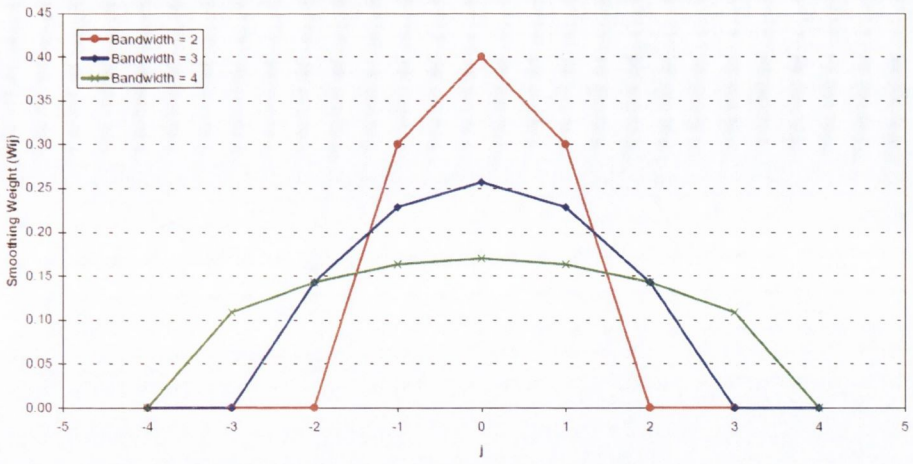

Figure 4.18. Epanechnikov Kernel smoothing weights for different bandwidths (Hellinga, (2011).

Figure 4.19 illustrates the application of Epanechnikov kernel smoothing with $\alpha = 3$ seconds to a recorded driving cycle. The smoothed velocity follows the measured velocity quite closely.

This smoothing algorithm was applied to each driving cycle and the smoothed velocity was rounded to the nearest whole number and the instantaneous acceleration rate was computed.

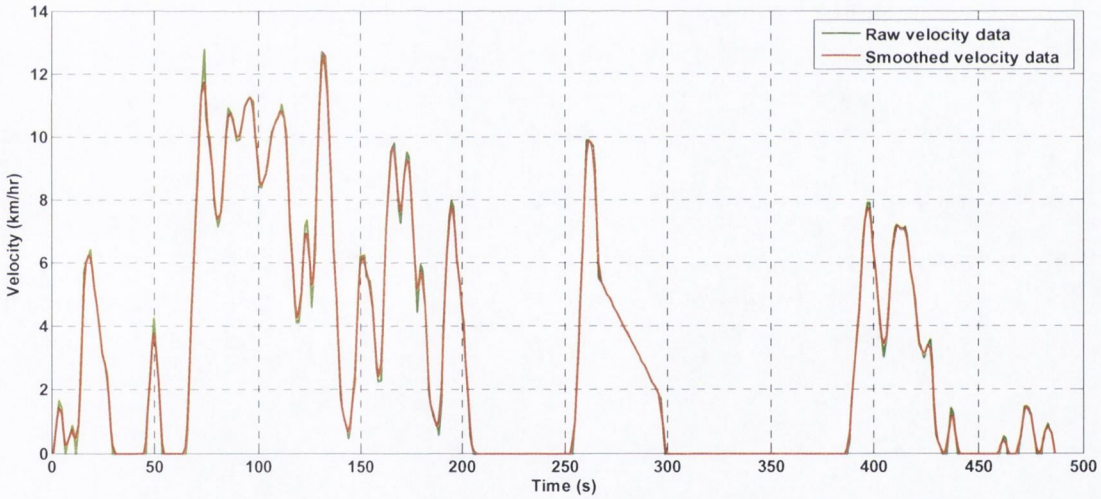

Figure 4.19. Raw velocity and Epanechnikov kernel smoothed velocity data ($\alpha = 3$ seconds).

However, on completion of the smoothing process, it was found that the application of the smoothing function did not absolutely guarantee that the computed acceleration fell within the feasible region. Therefore, in the third step of the pre-processing of the velocity data the acceleration values computed after the application of the smoothing technique were checked again for erroneous data points. The acceleration performance capabilities of the Mitsubishi iMiEV vehicle as a result of independent testing by Riches (2010) are listed in Table 4.9. All velocity and acceleration measurements for each journey were inspected and the driving cycle was excluded from the analysis if the rules listed in Table 4.10 were not adhered to.

Table 4.9. Acceleration performance capabilities of the Mitsubishi iMiEV vehicle (Riches, 2010).

Velocity (km/hr)	Time (s)	Acceleration (m/s^2)
0-48	4.5	2.98
48-72	3.4	1.97
72-96.5	13.5	1.19

Table 4.10. Rules for driving cycle exclusion.

1. An acceleration value greater than 3 m/s^2
2. A deceleration value less than 5 m/s^2
3. If an acceleration value occurred greater than the values listed in Table 1 in the corresponding velocity zone.

Figure 4.20 illustrates an example of a case in which the computed acceleration was greater than performance capability of the vehicle in the corresponding velocity zone. This driving cycle would have been removed from the database.

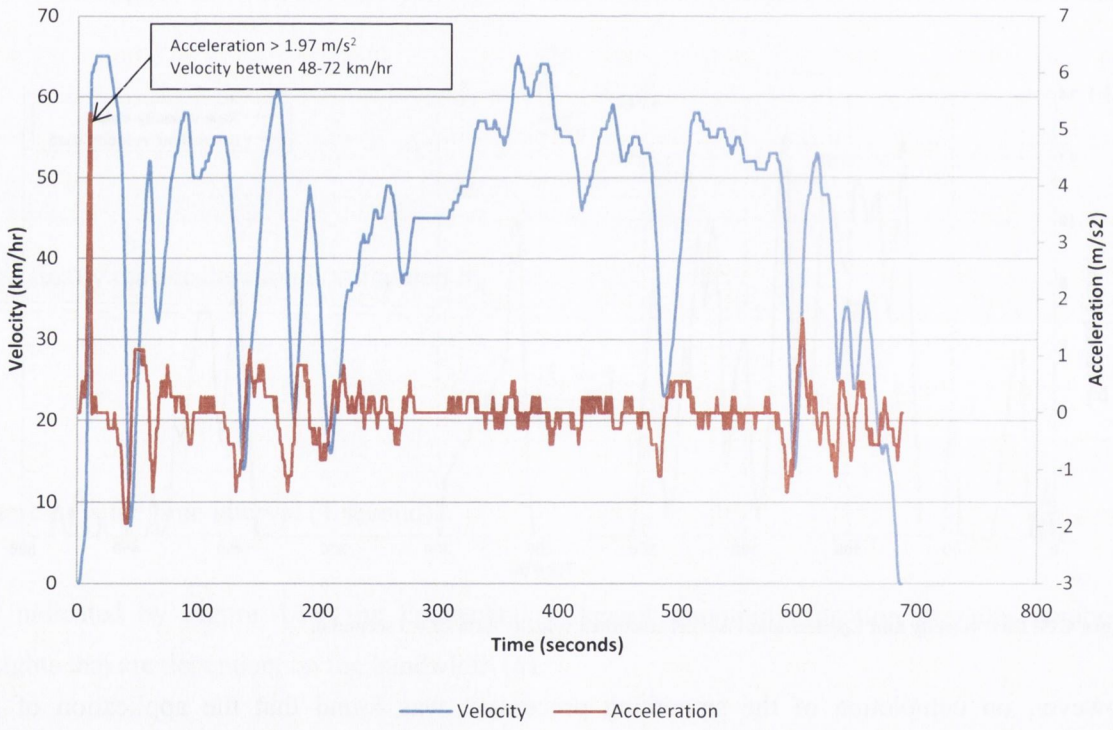

Figure 4.20. Example of an acceleration outlier after smoothing.

Readings from the battery such as voltage and current could not be detected on the Can-bus, hence the energy economy of the vehicles could not be computed from the logged data. After the velocity data was processed the next step was to simulate the energy economy of a vehicle over a driving cycle using an advanced vehicle simulation software, Autonomie (Argonne National Laboratory, 2012). The next section describes the simulation process.

4.6 Simulating the energy economy of an electric vehicle

This section describes the method used to simulate the energy economy of an EV over a driving cycle. Autonomie is a vehicle simulation tool developed by the Argonne National Laboratory (Argonne National Laboratory, 2012). The successor to the Powertrain System Analysis Toolkit (PSAT), Autonomie is a Matlab and Simulink-based program that is well suited to powertrain simulation because of its forward-facing architecture (Argonne National Laboratory, 2012).

Vehicle simulation typically follows one of two approaches: backward-facing of forward-facing (Argonne National Laboratory, 2012). Backward-facing tools such as the software program Advanced Vehicle Simulation (ADVISOR) (Big Ladder Software, 2013) begin with a desired vehicle speed and work backwards to determine how the powertrain and drive train should operate to meet the desired speed. A forward-facing vehicle model, on the other hand, simulates the flow of information as it actually occurs in a vehicle. It begins with a driving cycle which is fed into a driver model, which represents a human driver. The driver model responds to the velocity requests of the driving cycle by applying the accelerator and brake in appropriate measure. The accelerator commands are passed to a motor model which uses them to compute the amount of torque it will output and the amount of energy it will consume. The torque produced is passed to the transmission which factors in its own efficiency. Finally, the amount of torque that the vehicle can supply is passed to a model for the wheels which ultimately outputs the speed of the vehicle.

Forward-facing simulations rely on solving a system of ordinary differential equations to model the dynamic processes in the vehicle. The strength of a forward facing simulation is its ability to account for the dynamic processes taking place in the vehicle. A backward-facing approach is beneficial in simplicity and computation cost, while a forward-facing approach is advantageous in exploiting performance details (Musardo et al, 2005). Due to this capability, Autonomie was chosen as the simulation software for this study. Autonomie was validated by its developers by comparing its simulation results to empirical results for the Toyota Prius (Kim et al, 2012).

A Simulink diagram of the modelled drivetrain is presented in Figure 4.23. A default BEV powertrain which was available pre-programmed into Autonomie was modified to replicate the drivetrain of a Nissan Leaf vehicle using published technical specifications. The specifications of the modelled vehicle are available in Appendix C.

The model was validated by comparing the energy economy computed by the software to the certified energy economy of the Nissan Leaf. The energy economy is defined as the total energy consumed divided by the distance travelled (Wh/km). The published driving range and energy economy of the Nissan Leaf as stipulated by Regulation UN ECE 101 are 175 km and 173 Wh/km respectively (Nissan Ireland, 2012). This implies that it requires approximately 30.3 kWh (175 km

x 0.173 kWh/km) to fully charge the battery. The battery capacity of the Nissan Leaf is 24 kWh, which implies that the actual charging efficiency is approximately 80%. Ignoring the energy losses due to charging the energy economy of the Nissan Leaf is approximately 137 Wh/km (24 kWh / 175 km). The simulated energy economy of the modelled powertrain over the NEDC in Autonomie is 144 Wh/km, a 5% deviation from the certified energy economy. The modelled powertrain was simulated over all the recorded driving cycles to simulate the energy economy of the vehicles on a second by second basis.

After the energy economy of the vehicle was computed, the next step in the analysis was to segment the data by driving distance. Following this the data was segmented by road-type and level of congestion using a neural network tool. The next two sections describe these processes.

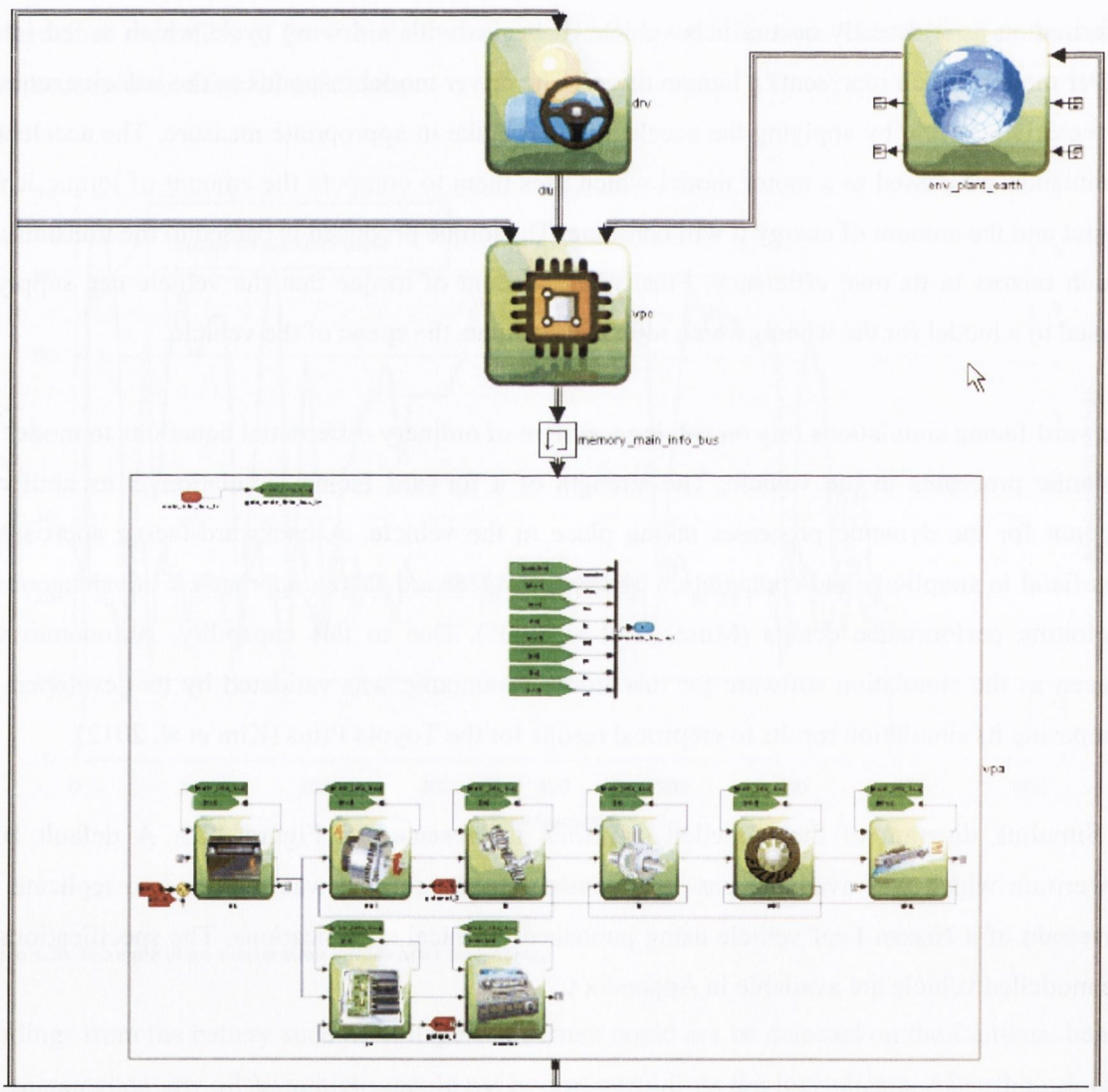

Figure 4.21. Simulink diagram of the modelled powertrain.

4.7 Data segmentation by journey distance

The driving cycle data was segmented into four driving distance bins. The binning of the data is significant because in Section 4.10 the energy economy of the driving cycles are analysed from the perspective of each bin and in Chapter 5 a representative driving cycle is developed for each bin.

The individual journey distance distribution is shown in Figure 4.22. Fifty five probability density functions (pdf), listed in Appendix D, which are available in a distribution fitting software package, EasyFitXL (EasyFitXL, 2013) were fitted iteratively to the individual journey distances to find the best fit. The three parameter fatigue life distribution (Equation 4.6) was found to be the best fit for the data based on the Kolmogorov Smirnov goodness of fit test, where $\alpha = 1.2698$, $\beta = 3346.6$ and $\gamma = 290.09$.

$$f(x) = \frac{\sqrt{(x-\gamma)/\beta} + \sqrt{\beta/(x-\gamma)}}{2\alpha(x-\gamma)} \cdot \emptyset\left(\frac{1}{\alpha}\left(\sqrt{\frac{x-\gamma}{\beta}} - \sqrt{\frac{\beta}{x-\gamma}}\right)\right) \tag{4.6}$$

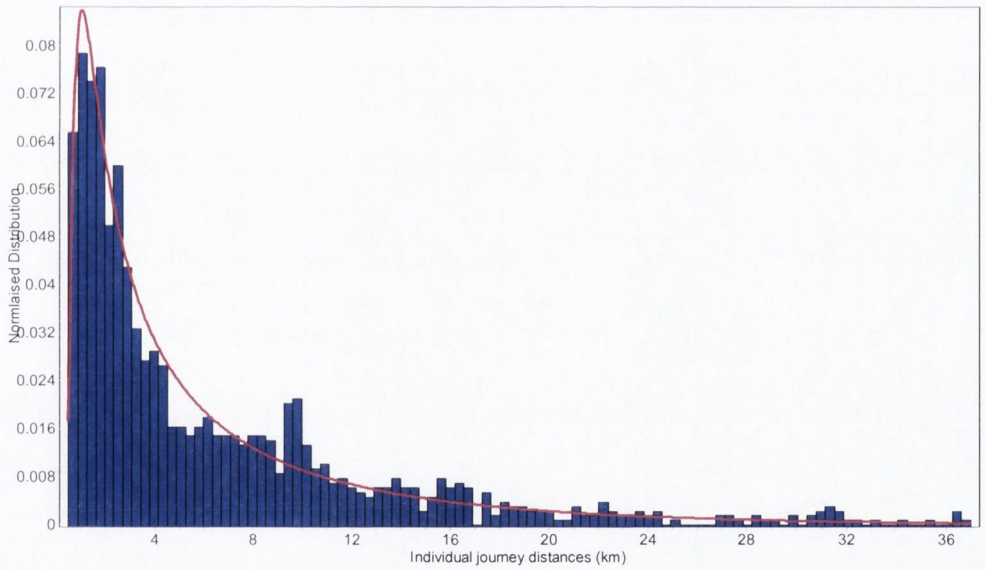

Figure 4.22. Individual driving distance distribution.

Figure 4.23 shows the cumulative distribution function (cdf) of the individual journey distances. The data were divided into four bins each having the same probability on the cdf.

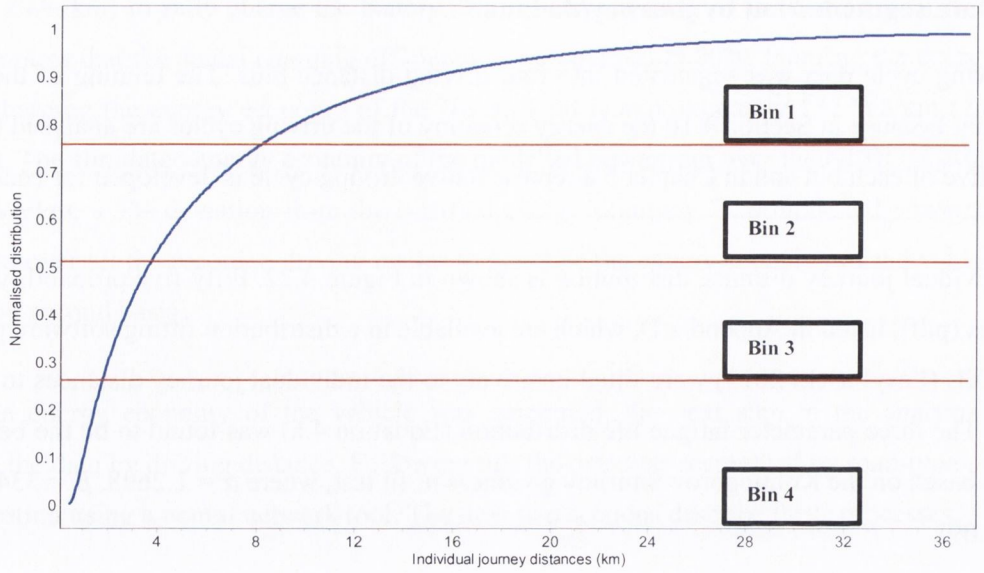

Figure 4.23. Cumulative distribution function of the individual journey distances.

The next section presents a driving environment recognition tool that was developed to segment and classify the driving cycle data in each bin by road-type and level of congestion.

4.8 Driving environment recognition tool

Driving cycles exhibited by real-world drivers are the product of the instantaneous decisions of the driver to cope with the physical driving environment. Research has shown that the driving environment of a vehicle has a strong influence on the fuel economy of the vehicle (Eva, 2000, Eva, 2001). Specifically road-type, level of congestion and driving style have varying degrees of impacts on a vehicle's fuel economy. These factors can generally be observed in the velocity profile of a vehicle.

In order to analyse the large amount of data collected in the form of driving cycles the solution was to split the driving cycles into small sections called micro-segments and to classify the micro-segments as one of six driving environments (e.g. congested urban driving or free-flowing motorway driving). This facilitated an analysis of the energy economy of the EVs in the different driving environments and allowed the proportion of time that EVs operated in each driving environment to be identified.

To this extent a driving environment recognition tool (DERT) was developed which divides a driving cycle into 30 second micro-segments. A wide range of descriptive parameters (29) based on a statistical analysis of the logged velocity and acceleration measurements are computed for each micro-segment and each micro-segment is then classified as a particular road-type and level of congestion.

The tool consists of two components, the Driving Information Extractor (DIE) and the Driving Environment Identifier (DEI). The functions of these components are as follows:

- Driving Information Extractor (DIE): The purpose of the DIE is to extract key statistical parameters from a logged driving cycle and these parameters are subsequently used to determine the road-type and the level of congestion.
- Driving Environment Identifier (DEI): The purpose of the DEI is to classify each micro segment as a particular road-type and the level of congestion.

The architecture and design methodology of the DIE component is presented in the next section. Following that, the DEI component is presented.

4.8.1 Driving Information Extractor (DIE)

As discussed previously, it has been shown that the driving environment (i.e. road types and levels of congestion) of a vehicle has a strong influence on its fuel consumption and that these driving environments can generally be observed in the velocity profile of a vehicle (Eva, 2000, Eva, 2001). The purpose of the DIE is to extract key statistical parameters from a driving cycle every 30 seconds (Figure 4.24).

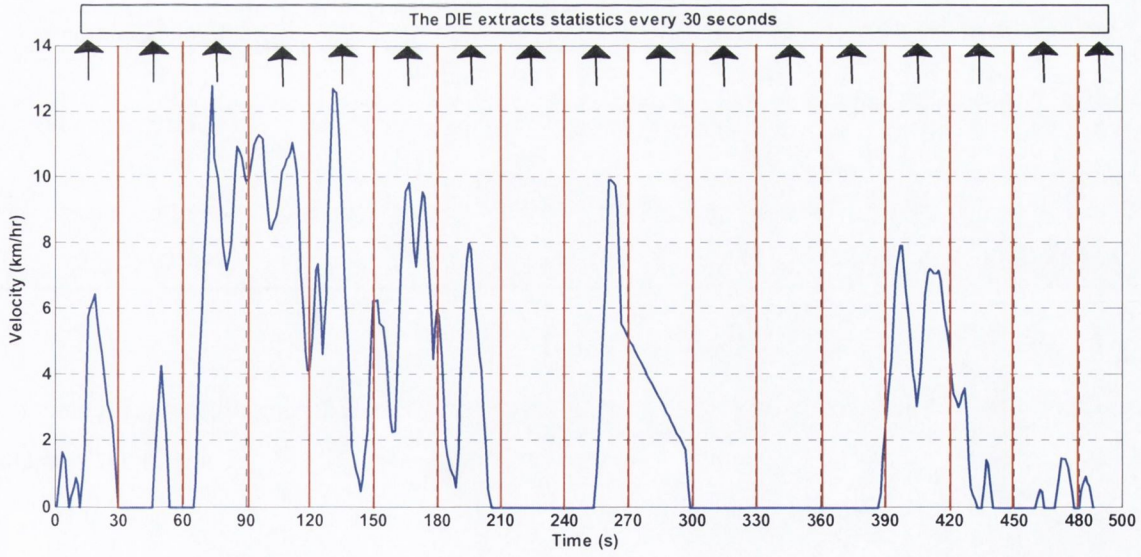

Figure 4.24. Illustration of the DIE extracting key statistics from the driving cycle every 30 seconds.

While there is no consensus among researchers as to a definite list of statistical parameters that should be extracted from a driving cycle, a number of studies have attempted to determine a list of such parameters (Eva, 2001, Jeon et al, 2002). A detailed description of 62 parameters that can be extracted from a driving cycle and their influence on fuel consumption and exhaust emissions were analysed by Ericsson (2001). Over 19,230 real-world driving cycles were collected. The author then used factorial analysis to reduce the initial 62 parameters to 16 independent parameters.

Furthermore, as noted in Ericsson (2002), 9 out of these 16 parameters critically affect fuel consumption and emissions. In Abdollahi (2006), 40 of the parameters identified by Ericsson (2001) were used in the design of an intelligent control strategy for a parallel hybrid EV to determine the driving environment that an EV is operating in. These 40 parameters affect the distribution of speed and acceleration and hence influence fuel consumption. Shankar et al (2012) used 29 of these parameters in the identification of driving conditions in a study to improve EV drivetrain component design. These parameters were solely based on speed and acceleration and hence were adopted in the development of the DIE component of the DERT tool. Table 4.11 lists the parameters which are extracted by the DIE. These parameters are used to identify the road-types and traffic conditions that the EVs in the demonstration trial operated on.

Table 4.11. Micro-segment parameters.

Parameter	Parameter	Parameter	Parameter
1. Average speed	8. Standard deviation of deceleration	15. % of time in speed interval 30-50 km/hr	23. % of time when (va) is 6-10
2. Standard deviation of speed	9. Maximum deceleration	16. % of time in speed interval 50-70 km/hr	24. % of time when (va) is 10-15
3. Maximum speed	10. Relative positive acceleration	17. % of time in speed 18. interval 70-90 km/hr	25. % of time when (va) is >15
4. Average acceleration	11. Number of stops per km	19. % of time in speed interval 90-110 km/hr	26. Total distance (m)
5. Standard deviation of acceleration	12. Stop duration per km	20. % of time in speed > 110 km/hr	27. Total duration
6. Maximum acceleration	13. % of time in speed interval 0-15	21. % of time when (va) < 0	28. Energy economy (Wh/km)
7. Average deceleration	14. % of time in speed interval 15-30	22. % of time when (va) is 3-6	29. Positive kinetic energy

4.8.2 Driving Environment Identifier (DEI)

After the statistical parameters of a driving cycle have been extracted, each 30 second segment of the driving cycle is classified as being of a particular road-type and level of congestion. The DEI uses a neural network to classify the micro-segments.

Neural networks (NN) are information processing systems that are a rough approximation and simplified simulation of the human brain. NNs have the ability to recognise complex patterns quickly with a high degree of accuracy (Ramgulam, 2006). They make no assumptions about the nature and distribution of the data and they are not biased in their analysis. In addition, NNs have non-linear tools and as such are good at predicting non-linear behaviour. NNs are used to solve many types of problems such as pattern classification, function approximation, forecasting, filtering and optimisation. They have been used in a wide range of applications such as speech recognition,

robotics, process control and telecommunications (Kumar et al, 2009, Lewis, 1996). NNs are an industry wide standard accepted tool for the classification of data. A theoretical background on the subject can be obtained in (Kohonen, 1990). A NN algorithm can be implemented in Matlab using its neural network toolbox.

Typically, the goal of a NN can be defined as a model which is able to map a set of training inputs to a set of training output variables. Then, the model should be able to accurately predict the output when new inputs are presented to the model. At a minimum a neural network is made up of three layers, the input layer, a hidden layer and an output layer. Each layer is made up of neurons. Figure 4.25 shows the structure of a simplified neural network. Each circle can be considered as a neuron. The connections between each neuron are known as synapses. In this example, there are three inputs into the network and two outputs from the network. Therefore, there are three input neurons in the first layer and two output neurons in the output layer. The optimum number of hidden layers and the number of neurons in these layers are generally determined by trial and error during the training/learning process.

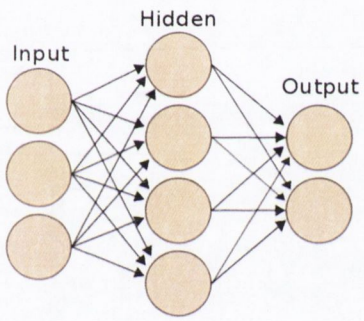

Figure 4.25. Illustration of a simplified neural network (Hovhannisyan, 2013).

There are different types of neural networks, but they are generally classified into feed-forward networks, feed-back networks and self-organising maps. Self-organising maps are typically used for pattern recognition (Kohonen, 1990) due to their effectiveness in the classification of complex and nonlinearly separable target classes (Hudson et al, 2012). Based on self-organising maps a network architecture called Learning Vector Quantisation (LVQ), formulated by Kohonen (1990), a widely used network for classification (Biehl et al, 2006) was used for the DEI component of the DERT tool.

Figure 4.26 illustrates the structure of a LVQ network. A LVQ network has a competitive layer and a second linear layer. The competitive layer learns to classify input vectors based on neural competitive learning, which allows the definition of a group of categories on the input data space using reinforced learning, either positive (reward) or negative (punishment). Specifically, if the winning node belongs to the same class of the input vector, its similarity to the input vector is positively reinforced by moving its weight vector closer to the input vector. However, if the

winning node does not belong to the class of the input vector, its weight vector is moved away from the input vector (Wang, 2013). The weight vectors of all the other nodes remain unchanged. The classes learned by the competitive layer are referred to as subclasses and the classes of the linear layer as target classes (Martín-Valdivia et al, 2007, Mathworks, 2012). The linear layer transforms the competitive layer's classes into target classes defined by the user. A detailed specification of the learning algorithm can be found in Kohonen (1990).

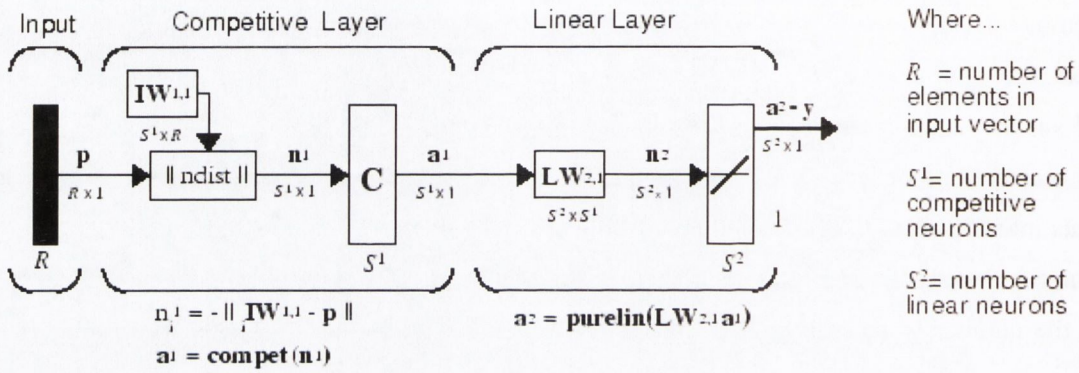

Figure 4.26. A learning vector quantisation network (Mathworks, 2012).

A method to assess how well a NN has been trained to correctly classify data is to examine the confusion plot of the NN. An example of a confusion plot with 3 target classes is illustrated in Figure 4.27. The confusion matrix shows the percentages of correct and incorrect classifications. Correct classifications are the green squares on the matrices diagonal. Incorrect classifications form the red squares. If the network has learned to classify properly, the percentages in the red squares should be very small, indicating few misclassifications.

The next section details how the network was trained to classify the driving cycle data. This will be followed by a discussion of the performance of the trained network.

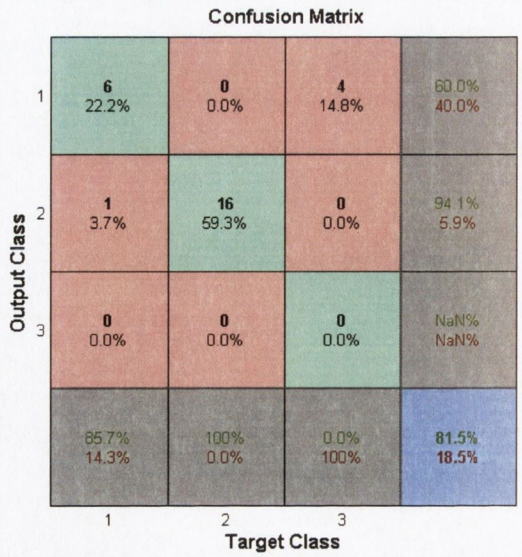

Figure 4.27. An example of a confusion matrix for a trained neural network (Mathworks, 2012).

4.8.2.1 Training the neural network

In order to classify the driving cycle data (i.e. the micro segments) as a particular road-type and level of congestion, a training dataset was required. Thirty different drivers were recruited to drive along a prescribed route at three different times of the day. The GPS data for each test route was plotted on Google Earth (Figure 4.28). Each driver completed the route once. The three different times of day (9:30 am, 1 pm and 4:30 pm) were chosen so that the vehicle would be driven in varying levels of congestion. It was found that when completing the trips, the traffic congestion was at its highest during the 4:45 pm trip and at its least during the 9:45 am trip. The route was chosen such that a variety of different road-types were encountered (i.e. urban, extra-urban and motorway).

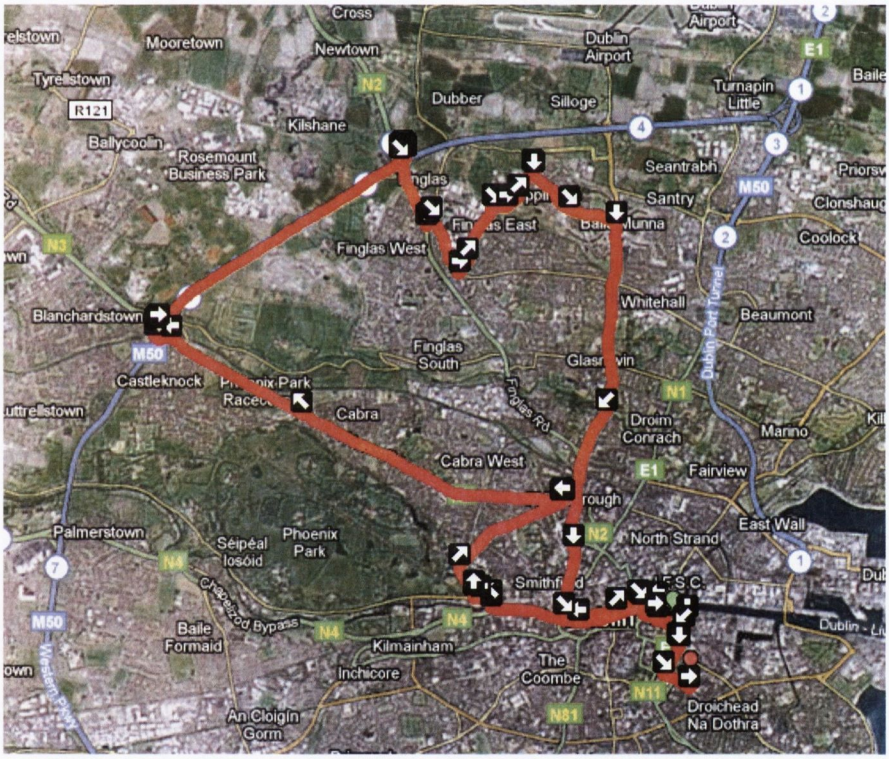

Figure 4.28. Route taken to generate training dataset for the neural network.

The resulting thirty trips were used as a training dataset for the NN. The training dataset consisted of 898 km of driving or 3,534 micro segments. The two sections that succeed this section illustrate how the road-type and level of congestion of each micro segment in the training dataset was determined.

After the training dataset was prepared the NN was trained. However, the weight of each parameter of a micro segment has a significant effect on the classification of a micro segment. Therefore, to give equal weight to each parameter, they were first normalised according to Equation 4.7, before being passed into the NN for training.

$$Normalised\ Input = \frac{X - \mu}{\sigma} \tag{4.7}$$

Where X is the input parameter, μ is the mean of the input parameter and σ is the standard deviation of the input parameter.

The competitive layer consisted of 15 neurons and the linear layer consisted of 6 neurons. The number of neurons in the competitive layer affects the accuracy of the network. However, if the number of neurons is dramatically increased, an over-training phenomena can occur. In this case the network learns not only the basic mapping associated with input and output data, but also the subtle nuances and even the errors specific to the training set. If too much training occurs, the network only memorises the training set and loses its ability to generalise to new data. From trial and error, it was found that 15 neurons produced the best outcome. This outcome was determined by examining the mean squared error of the trained neural network with respect to the testing samples. The overall performance of the network in terms of correctly classifying the training micro segments is discussed further in Section 4.8.

At the end of the process the NN was trained to identify and classify six different driving environments listed in Table 4.12:

Table 4.12. The six driving environments of the DERT tool

Driving environment	Driving environment
1. Stop-start Urban	4. Extra-urban
2. Congested Urban	5. Congested motorway
3. Free-flowing Urban	6. Free-flowing motorway

4.8.2.1.1 Neural network: road-type identification

This section illustrates how the road-type of each of the micro-segments of the test routes was determined. As illustrated in Figure 4.29 below, by examining the time stamps of the GPS data (bottom of the figure) and viewing the map, it was possible to assign each 30 second micro segment of a logged driving cycle from a test route as a particular road-type. This process was completed for each journey. The next section illustrates how the level of congestion of each micro segment was determined.

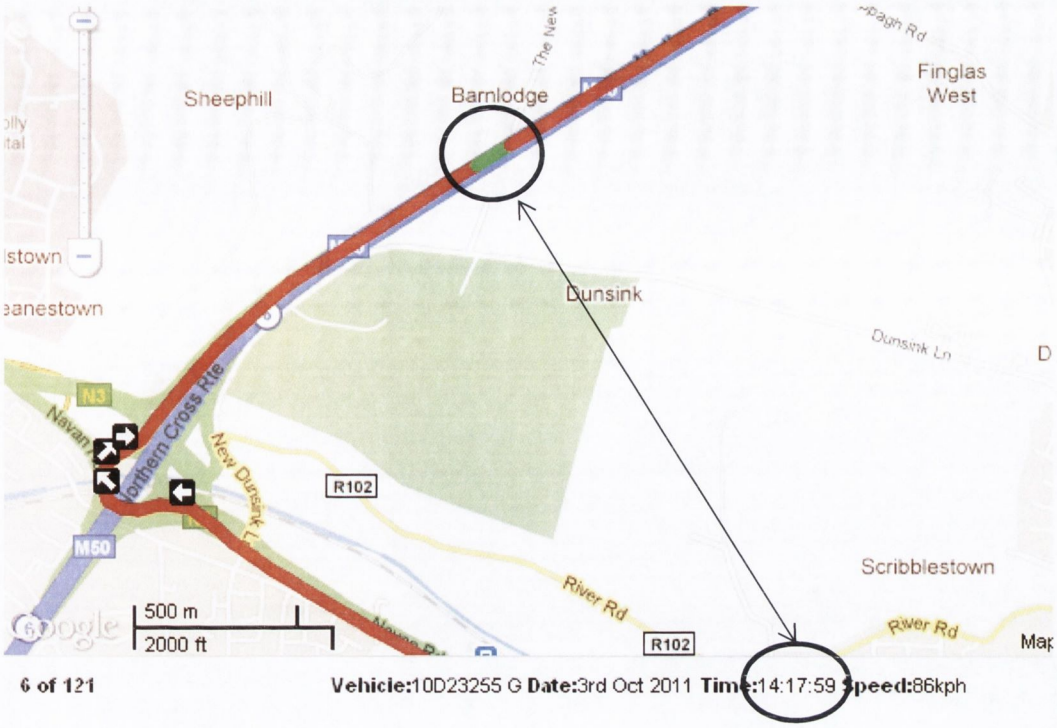

Figure 4.29. Illustration of road type identification.

4.8.2.1.2 Neural network: level of congestion identification

According to Smith (2006), the frequency and amplitude of instantaneous velocity changes, affects the fuel economy and emissions rates of vehicles. The quantification of speed fluctuation requires the analysis of second by second driving cycle data. Although measures of speed fluctuation are not commonly used as congestion indicators in practice, a number of studies based on empirical data show that they are related to other indicators of congestion. The use of speed fluctuation measures as congestion indicators can be justified by considering them as measures of smoothness of a driving profile. As the number of vehicles on the road increase, traffic becomes less smooth since vehicles are forced to decelerate and accelerate repeatedly. Driving profiles become increasingly unstable as drivers attempt to adjust in response to neighbouring vehicles and hence the level of speed fluctuation increases.

Barth et al (1996b) investigated the relationships between a number of microscopic speed fluctuation measures, which were calculated from driving cycles collected by a GPS-equipped instrumented vehicle and macroscopic traffic variables that were measured by traffic detectors on a motorway. The following measures for speed fluctuation were calculated:

- PKE (positive acceleration kinetic energy)
- TAD (total absolute second to second difference in speed per km)
- COV_{vt} (coefficient of variation of instantaneous speed)

PKE was expressed as m/s^2 and represents the work per done unit distance. It is defined as

$$PKE = \frac{\sum(v_{t,a}^2 - v_{t,b}^2)}{L} \qquad subject\ to\ a_t > 0\ m/s^2 \tag{4.8}$$

where $v_{t.a}$ and $v_{t.b}$ are the initial and final instantaneous velocities respectively in an acceleration manoeuvre and L is the distance travelled. Smooth driving profiles will have low PKE values, whereas driving profiles with large and frequent speed fluctuations will have high PKE values. It is noted that PKE increases only during positive acceleration manoeuvres. Strong acceleration events increase PKE substantially more than weak acceleration events, due to the quadratic form of the PKE equation.

TAD is defined as

$$TAD = \frac{\sum|v_{t,a} - v_{t,b}|}{L} \tag{4.9}$$

TAD is a measure of the overall change in speed per unit distance. Every time a vehicle changes speed (either up or down), TAD increases.

Finally, the coefficient of variation of speed COV_{vt} is defined as

$$COV_{vt} = \frac{\sigma_{vt}}{v_{avg}} \tag{4.10}$$

Where v_{avg} (km/hr) and σ represent the mean and the standard deviation of velocity of a particular driving profile respectively.

Smith (2006) demonstrated that for uninterrupted conditions the level of speed fluctuation increases with increasing density. All measures of speed fluctuation illustrated a consistent increase in their values with increasing levels of congestion. On the basis of this investigation, it was concluded that PKE, TAD and COV_{vt} are all good traffic congestion indicators.

It was decided to adopt COV_{vt} as the level of congestion indicator because it was best suited to the micro segment structure of the DERT tool. The mean and standard deviation of the velocity of a micro segment could be easily computed. The use of COV_{vt} facilitated the level of congestion to be expressed as a *congestion index*. Shankar et al (2012) used a similar index in the recognition of levels of congestion in an EV drivetrain component design study.

The boundaries of the congestion index in which the level of congestion of a micro segment could be classified as stop-start, congested or free-flowing is subjective. It was decided to use k-means clustering, a clustering algorithm, to cluster the micro segments of the training data into three clusters representing three levels of congestion, stop-start, congested and free-flowing respectively. The advantage of the k-means clustering algorithm is that it allows you to specify the number of clusters (i.e. 3). Montazeri-Gh and Fotouhi (2011) used a similar k-means clustering approach in a traffic condition recognition study in the development of an intelligent HEV control strategy. In that study the driving features 'idle time percentage' and 'average acceleration' of 150 second micro segments were clustered into three clusters.

Figure 4.30 illustrates the clustering of the micro segments classified as being of road-type urban in the collected training dataset. The average velocity and the computed congestion index for each micro segment are clustered into 3 clusters, which represent the three levels of congestion. The plot demonstrates as expected a decreasing average velocity as the congestion index increases. For example the 'free-flowing' level of congestion cluster (green) has a higher average velocity and lower congestion index than the 'congested' and 'stop-start' clusters. The training micro segments classified as 'motorway' were clustered into two clusters only, representing congested and free-flowing conditions because 'stop-start' traffic conditions were typically not experienced on the motorway portion of the test drives. The extra-urban micro segments were not clustered as the traffic conditions experienced during the test drives were primarily free-flowing. The next section describes the performance of the trained network in correctly classifying data.

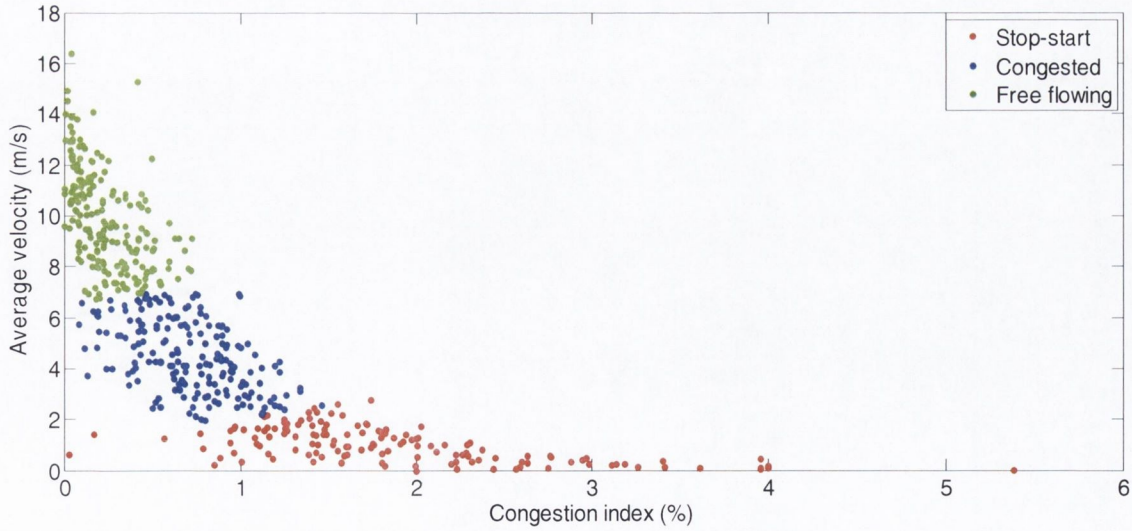

Figure 4.30. Result of k-means clustering for urban data.

4.9 Performance of the trained neural network

The performance of the NN with respect to identifying and classifying micro-segments as particular road-types is presented first. A visual comparison of the classification between the NN output and the training data is assessed by plotting the distribution of the mean velocity against the mean acceleration for each micro segment for both the training data (Figure 4.31 (a)) and the NN output (Figure 4.31 (b)). The figures demonstrate similar patterns in terms of the distribution of velocity and acceleration. The figures illustrate the misclassification of extra-urban segments. Some of the extra-urban data points (red) of the network output are misclassified as urban (blue) and motorway (green) when compared to the training data.

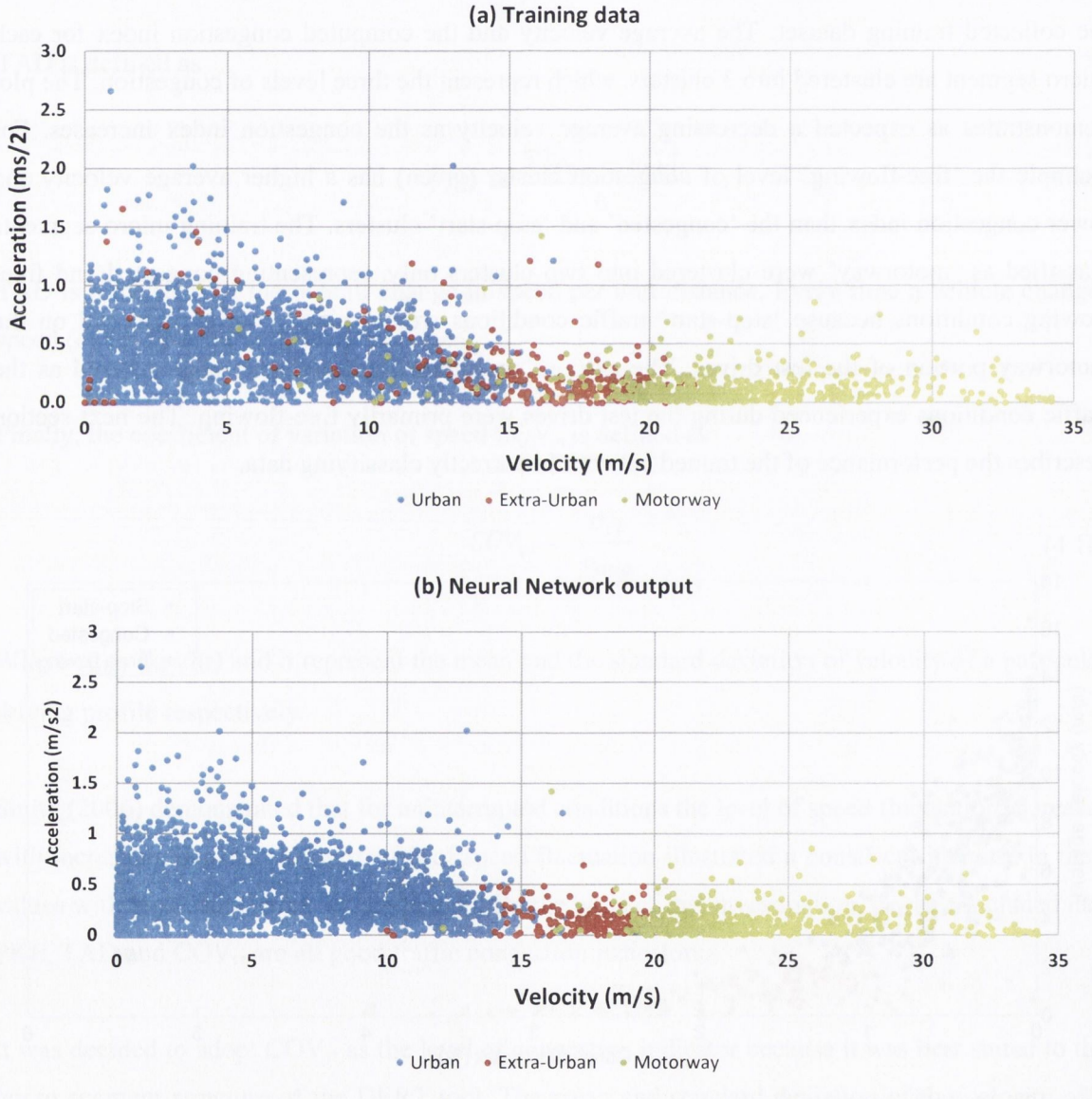

Figure 4.31. Comparison of (a) the training data and (b) the neural network output for the 3 target classes.

During the training process 15% of the training data is withheld in order to test the network after the training process. Figure 4.32 presents the confusion plot for the NN. The three target classes are

urban (1), extra-urban (2) and motorway (3). The overall percentage of correctly classified micro segments was 94%. The 6% of misclassified data was primarily due to the misclassification of 29% of the extra-urban micro-segments. This is due to the fact that slow speed extra-urban driving is similar to urban driving and high speed extra-urban driving is similar to motorway driving. The misclassification of urban driving and motorway driving micro segments are relatively low, less than 10% in both cases.

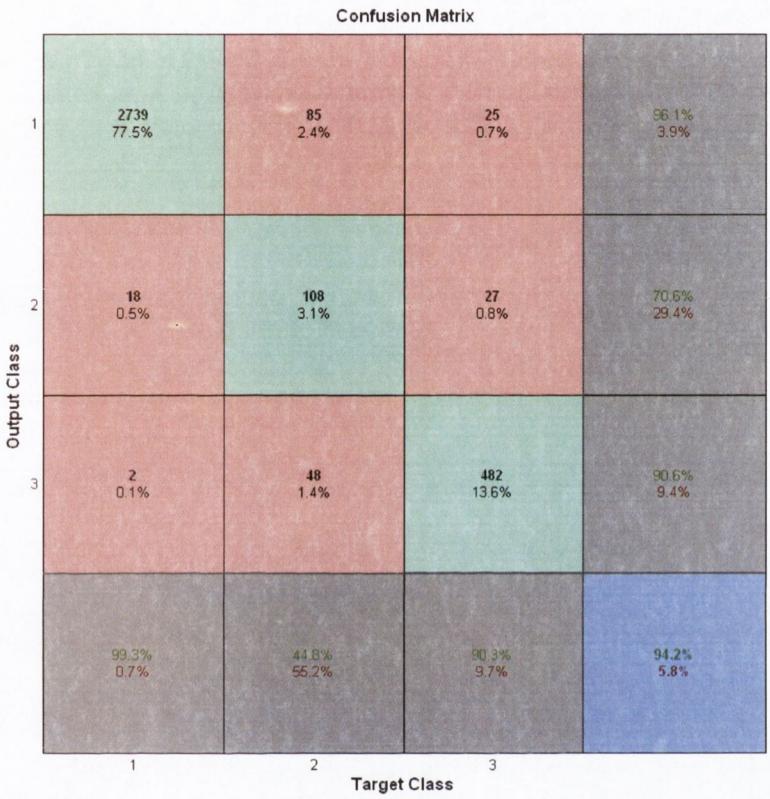

Figure 4.32. The confusion matrix for the NN containing 3 target classes.

The incorporation of the level of congestion into the NN resulted in a training dataset with the six driving environments (target classes) as illustrated Figure 4.33 (a). The output of the NN is illustrated in Figure 4.33 (b).

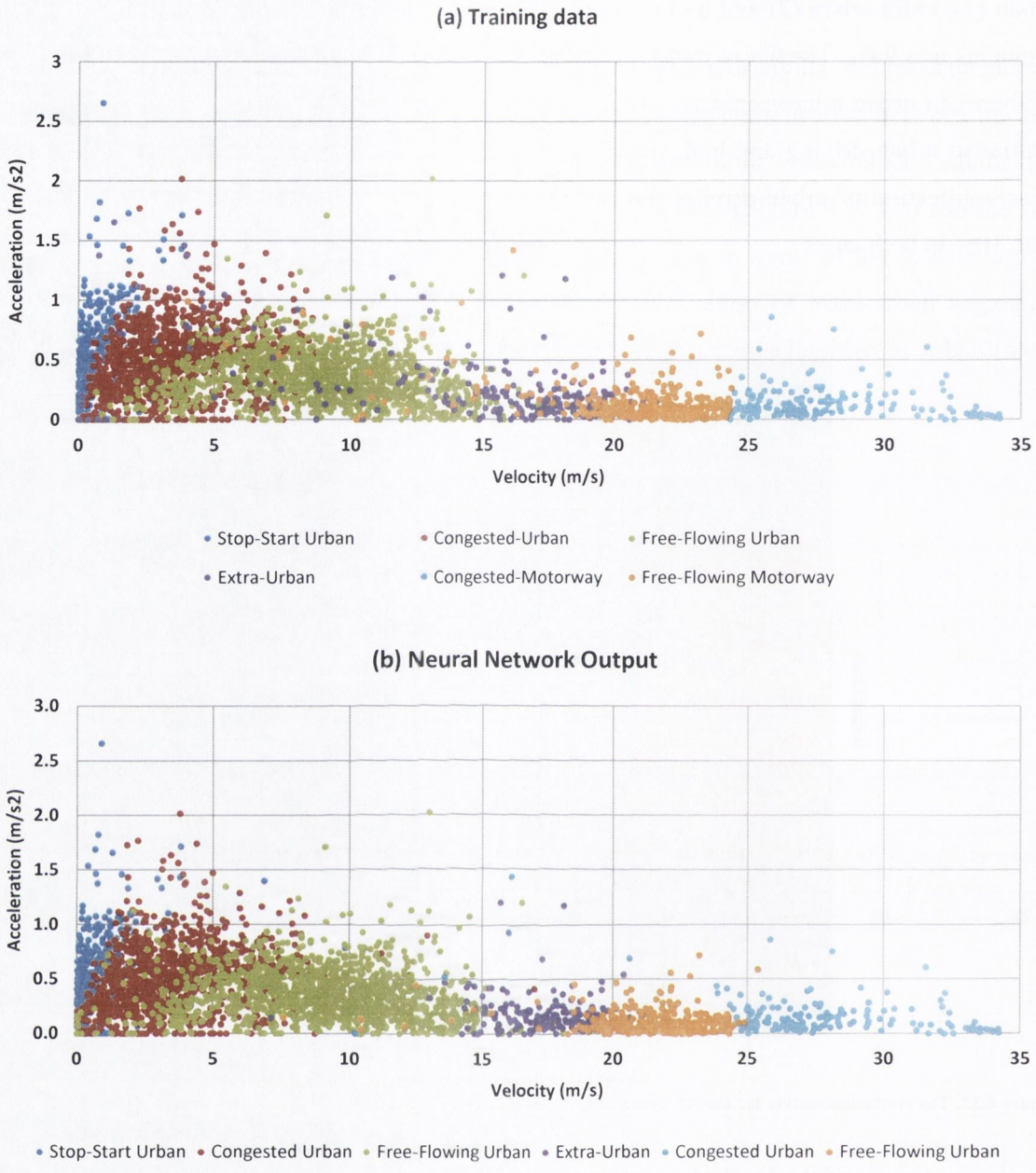

Figure 4.33. Comparison of (a) the training data and (b) the neural network output for the six driving environments.

Figure 4.34 presents the confusion plot for the NN with the six target classes. The six target classes are stop-start urban (1), congest urban (2), free-flowing urban (3), extra-urban (4), congested motorway (5) and free-flowing motorway (6). The overall percentage of correctly classified micro segments was 90%. The next section illustrates how the trained NN was used to classify all the collected driving cycle data.

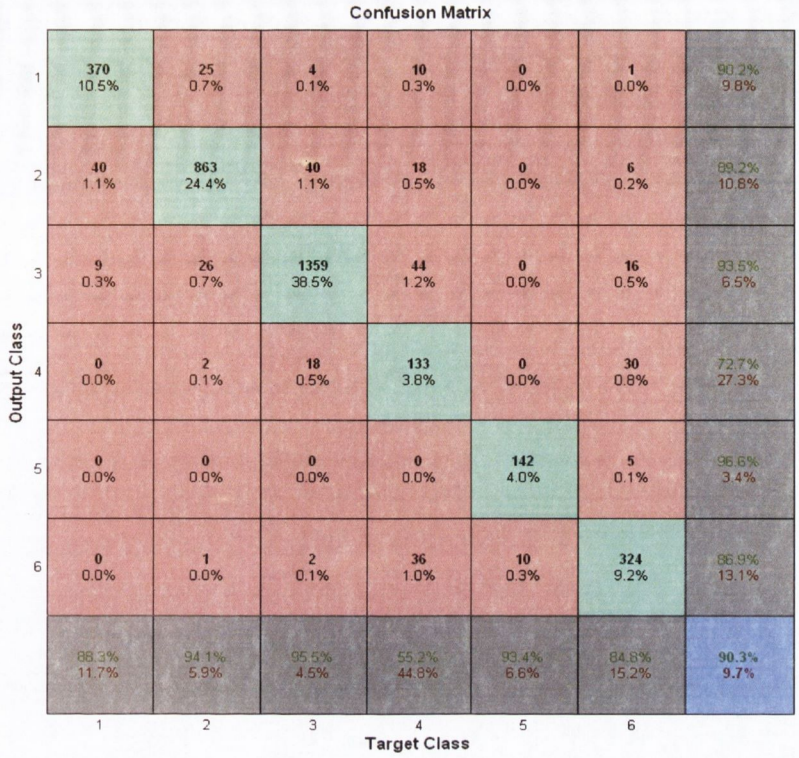

Figure 4.34. The confusion matrix for the neural network containing the 6 target classes.

4.10 The classification of all the recorded driving cycle data

The trained NN was used to classify the 6,952 km of logged driving cycle data. The classification of the entire dataset, shown in Figure 4.35, exhibits a similar pattern to the NN output in Figure 4.33 (b). The simulation of the modelled vehicle over the driving cycles and the subsequent binning of the driving cycles into four bins facilitated an analysis of the energy economy of an EV by driving distance. In addition, the classification of the entire driving cycle dataset (the micro segments) facilitated an analysis of the energy economy of an EV on various road types and in various levels of congestion. The next section presents these analyses.

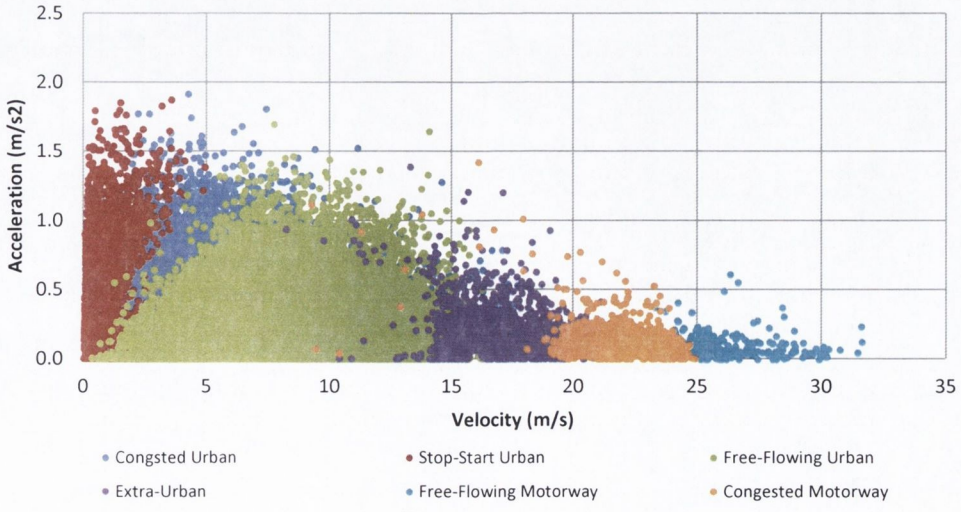

Figure 4.35. The classification of all the collected data.

4.11 The energy economy of EVs by driving distance and driving environment

This section presents an analysis of the energy economy of the EVs by driving distance and in the six different driving environments identified in the previous section. Figure 4.36 presents the distribution of the energy economy values in each of the four driving distance bins. The values are approximately normally distributed in each case and the spread of values decreases as the journey distance increases. Furthermore, the average energy economy decreases with increasing journey distance. An explanation of these trends is offered below. The average energy economy for bins 1 to bin 4 are 174 Wh/km, 165 Wh/km, 158 Wh/km and 155 Wh/km respectively.

At this point, it is important to note the predicted energy economy of a developed driving cycle should be representative of the observed energy economy values in a given bin. This will be discussed again in Chapter 5 in the evaluation of the developed driving cycles.

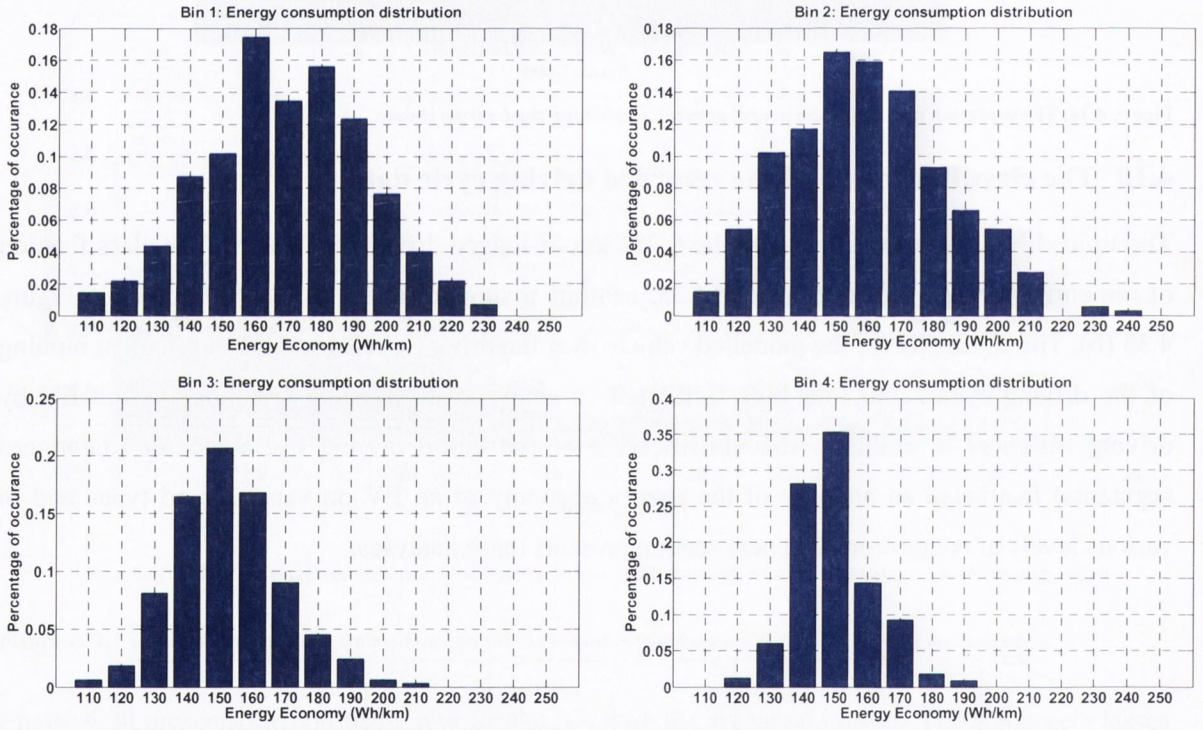

Figure 4.36. Energy economy distribution for each bin.

A box plot of the energy economy values of the micro segments in the six different driving environments is presented in Figure 4.37. On each box, the central mark is the median, the edges of the box are the 25th and 75th percentiles, the whiskers extend to the most extreme data points not considered outliers and outliers are plotted individually as red crosses. The average energy economy for each driving environment is overlaid on the plot. Overall, urban driving conditions have the highest energy economy followed by extra urban and motorway driving. Urban stop-start driving conditions have the largest average energy economy of 437 Wh/km and also display the largest spread of energy economy values. This is primarily due to the large spread of acceleration

rates and short distances travelled within the urban stop-start micro segments. The average energy economy in urban congested and urban free flowing conditions are 204 Wh/km and 137 Wh/km respectively. Motorway free-flowing conditions have the smallest spread of energy economy values as acceleration rates are low under these conditions. The average energy economy of motorway congested and motorway free-flowing conditions are 152 Wh/km and 171 Wh/km respectively.

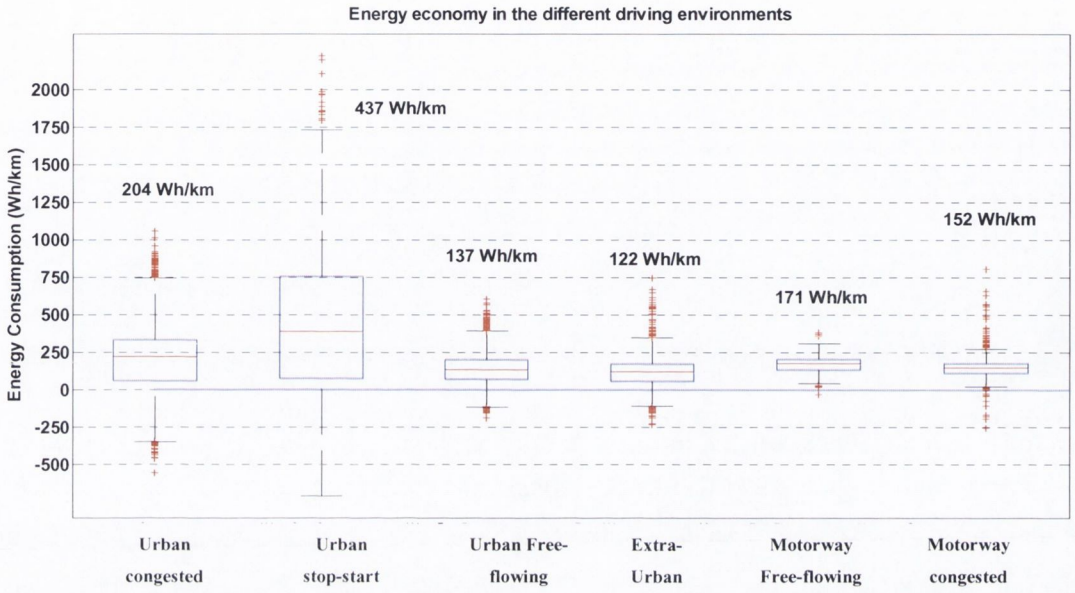

Figure 4.37. Energy economy in different driving environments.

The negative energy economy values in the box plot are as a result of the vehicle decelerating to a stop at the beginning of a micro segment and remaining idle for the remainder of the micro segment. Figure 4.38 illustrates a 90 second snippet (3 micro segments) of a typical driving cycle. In the micro segment in the 30-60 seconds time period the vehicle decelerated to a stop and remained idle for the remainder of the micro segment. During a deceleration event the energy consumption is negative due to regenerative braking which results in a negative energy economy value for the micro segment.

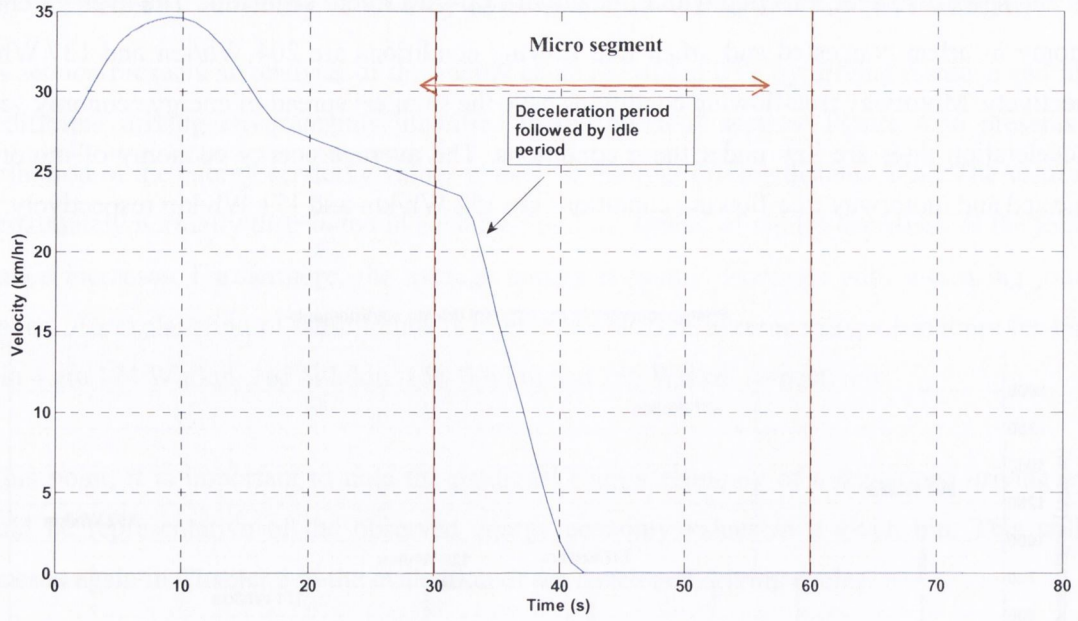

Figure 4.38. Illustration of a negative energy economy value.

The outliers (indicated by the red crosses) are primarily due to the vehicle being idle for the majority of a micro segment and then accelerating towards the end of the micro segment. Figure 4.39 illustrates a 120 second (4 micro segments) snippet of a typical driving cycle. In the micro segment in the 0-30 seconds time period the vehicle was idle for approximately the first 27 seconds before accelerating at the end of the micro segment. A very short distance was travelled in this micro segment. Dividing the energy consumption of the micro segment by a small distance value results in a large energy economy value for the micro segment.

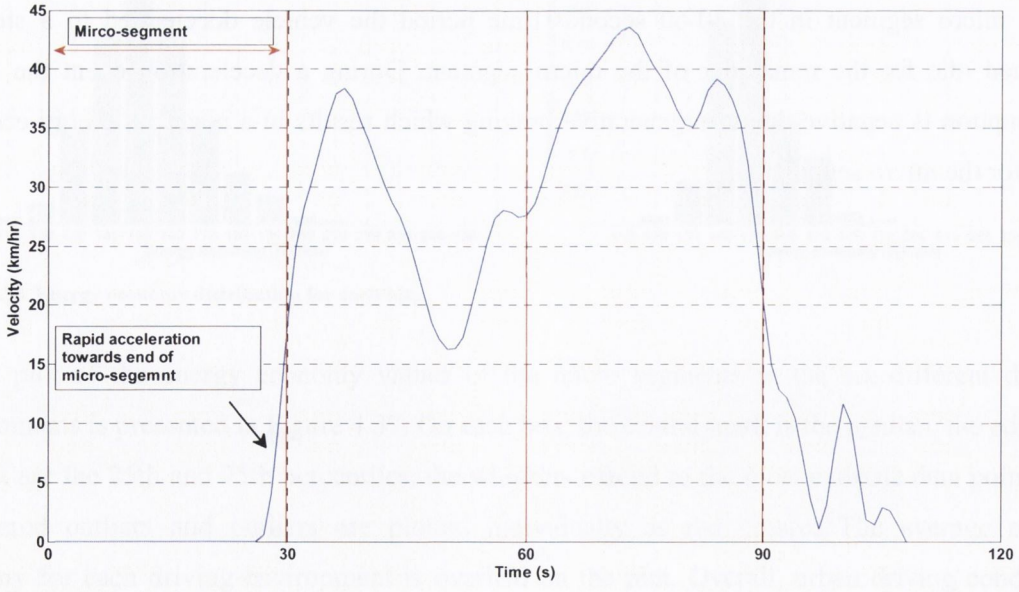

Figure 4.39. Illustration of an outlier in the box plot.

The classification of the micro segment data also facilitated an analysis of the proportion of time that the vehicles spent operating in each of the driving environments. The number of micro

segments in each category represents the amount of time that the vehicles were operating in each category. Figure 4.40 presents the proportion of time spent in each driving category for each driving distance bin. The vehicles operated in urban driving conditions predominately in each bin. In bin 4, for longer journeys a higher proportion of time (7%) was spent in motorway driving conditions.

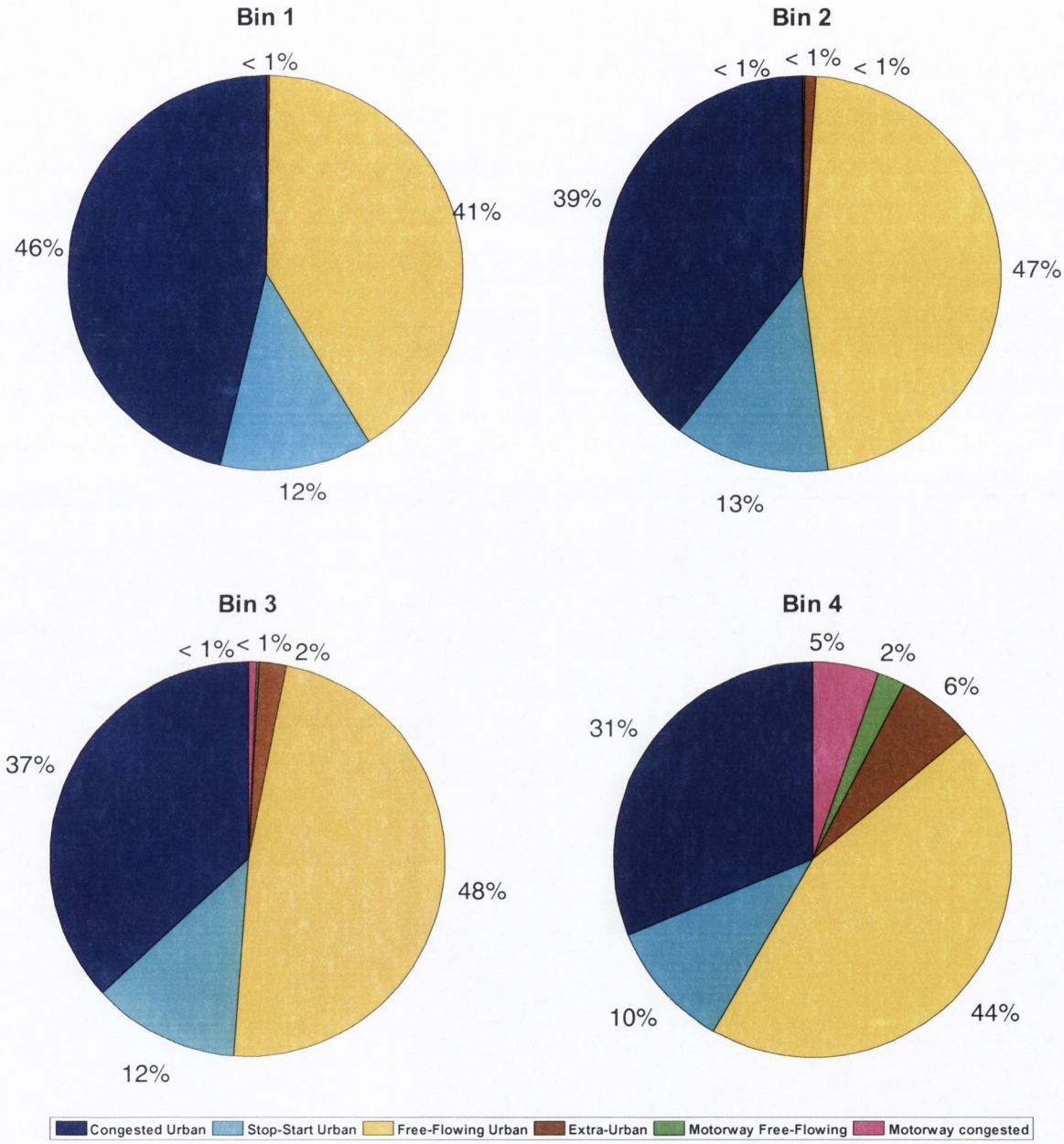

Figure 4.40. Percentage of time spent in each driving environment for each bin.

4.12 Summary and conclusions

This chapter reviewed existing driving cycles and driving cycle development methodologies for ICEVs and EVs. It was found that there are significant variations in real-world operating conditions compared to test procedures and that different test cycles are used in different regions of the world. It was determined that driving cycles play an important role in the design and evaluation of all vehicle propulsion systems and the energy economy of certain EV architectures are particularly sensitive to the driving cycles used in the design.

A four-step modelling approach for developing a set of real-world driving cycles for the GDA was proposed. The remainder of the chapter detailed the first step in the modelling approach. A methodology for conducting an analysis of real-world vehicle driving cycle data was presented in order to contribute to the knowledge regarding the real-world operating conditions and energy demands of EVs. A driving environment recognition tool, using a neural network technique was developed to identify the real-world operating conditions of EVs in terms of road types and levels of congestion. The analysis provided a more realistic picture of the operating conditions in which EVs predominantly operate in the real-world and the energy economy of EVs in those operating conditions. It was determined that EVs almost entirely operate in urban driving conditions and that the energy economy of an EV is highest on short journeys and in urban stop-start driving conditions. These results have implications for lifecycle and environmental impact analyses as the real-world energy economy and the driving environments in which EVs operate are critical inputs to these types of analyses and generally cannot be found in scientific literature. Furthermore, this analysis provided an insight into real-world driving conditions that a developed driving cycle should be representative of and hence set a benchmark for the development of the driving cycles presented in the next chapter.

5 Real-world drive cycle development for electric vehicles in the Greater Dublin Area

The processing and analysis of the logged driving cycle data presented in Chapter 4 provided an insight into the energy economy and operating conditions of EVs in the real-world. In this chapter, steps two to four of the proposed modelling approach for developing a set of real-world driving cycles are presented. In the second step, a discrete time Markov-chain model with states velocity and acceleration is developed. The transition probability matrices (TPM) for the model are extracted from each driving distance bin. The model generates candidate driving cycles for a given bin. In the third step, a statistical methodology, a regression analysis is performed to identify driving cycle parameters that are statistically significant in terms of influencing the energy economy of an EV over a driving cycle. When synthesising driving cycles with the Markov-chain model multiple iterations of the process are performed until the statistical parameters of the candidate cycles, identified by the regression analysis, match the mean of the statistical parameters of the real-world driving cycles within certain error bounds. This ensures that a developed driving cycle is representative of the real-world driving cycles in a given bin.

Four driving cycles of varying distances are developed for the Greater Dublin Area (GDA). In the final step, two methodologies are used to assess the representativeness of the developed driving cycles and a selection of well-established worldwide driving cycles of the real-world driving cycles in a given bin. An additional methodology is used to compare the developed driving cycles to the selection of worldwide driving cycles. Each of the developed driving cycles were shown to better match the mean of the parameters, identified by the regression analysis, of the real-world driving cycles in the original dataset. However, the two shortest developed driving cycles were outperformed by a number of the well-established worldwide driving cycles in terms of matching the speed and acceleration distribution (SAFD) of the real-world driving cycles in their respective bins.

This chapter is organised as follows: The Markov-chain driving cycle model is outlined in Section 5.1. This is followed by the regression analysis which is presented and validated in Section 5.2. The four developed driving cycles for the GDA are presented in Section 5.3. Further validation of the developed cycles, in relation to the predicted energy economy of the developed cycles, is conducted in Section 5.4. The properties of the cycles in terms of their road-types and traffic conditions composition and their SAFDs are presented in Section 5.5. A comparative assessment of the trends of the statistical parameters of the developed driving cycles to the real-world driving cycles with respect to distance travelled is also presented in Section 5.5. An assessment of the representativeness of the developed driving cycles and a selection of well-established worldwide driving cycles of the real-world driving cycles in a given bin is presented in Section 5.6. Sections 5.7 and 5.8 conclude the chapter and discuss areas for further research respectively.

5.1 The Markov-chain driving cycle model

This section presents the second step in the driving cycle development process, the Markov-chain driving cycle model. The methodology for synthesising driving cycles is based on Markov process theory, which defines a particular type of stochastic process (Norris, 1998). When the future probabilistic behaviour of a process depends only on the present state regardless of when the present state is measured, the resultant model is called a discrete time Markov-chain (Jensen and Bard, 2002). A Markov-chain model is used because it reflects the nature of the data, that is, the driving cycle data possesses the basic Markov property that velocity and acceleration at time t is conditioned on the velocity and acceleration at time t-1.

Markov processes have been widely applied in areas such as engineering, economics, psychology and sociology (Sheskin, 2010). For any Markov process, there are two major components: the state space and the transition probability matrix (TPM). The state space denoted by S, is defined as the distinct values a stochastic process can possibly take on. There exists the probability that state j will occur given the current state i. This probability, known as the transitional probability, is conditioned on the current state. If there are K states in the state space S, there will be K^2 transition probabilities forming the TPM. Each row of the matrix represents the current state and each column represents the future state. The next section discusses the TPMs for the model and how they are extracted from the dataset. This is followed by the third step, a regression analysis, to assess the representativeness of developed driving cycles of the original dataset.

5.1.1 The transition probability matrix

The state space of a discrete time Markov-chain is referenced by the index set (Jensen and Bard, 2002):

$$S = \{1, 2, 3,\ldots,K\} \tag{5.1}$$

This set identifies all possible states in which the system may be observed. The notation X_n is used to represent the state of the system at time n. X_n is a random variable restricted to the discrete values in the set S. The subscript n is the step index and takes the values in the set $N = \{0, 1, 2\ldots\}$, which can be measured in any appropriate unit such as seconds.

The system begins in state X_0, and over successive time periods transitions to states X_1, X_2, and so on. These transitions are governed entirely by transition probabilities that are assumed to be time invariant. The transitional probability of going from i to j is denoted as p_{ij} and the assumption is that the process possesses the Markovian property. This implies that each p_{ij} depends only on the current state i and not on the particular path that the process takes to reach state i.

The stochastic process is entirely defined by the m x m transition probability matrix P = (p_{ij}). An element of the matrix p_{ij}, is the probability that, given that the system is in state i at some time n, it will be in state j at time n+1 (Jensen and Bard, 2002).

$$P = \begin{bmatrix} p_{00} & p_{01} & p_{02} & \cdots & p_{0,m-1} \\ p_{10} & p_{11} & p_{12} & \cdots & p_{1,m-1} \\ \vdots & \vdots & \vdots & \cdots & \vdots \\ p_{m-1,0} & p_{m-1,1} & p_{m-1,2} & \cdots & p_{m-1,m-1} \end{bmatrix} \tag{5.2}$$

Since the system must always be in one of the m states, every row of the transition matrix must sum to 1.

$$\sum_{j=0}^{m-1} p_{ij} = 1, \qquad i = 0,1,\ldots,m-1 \tag{5.3}$$

Also, as the elements of P are probabilities, the following must be true

$$0 \leq p_{ij} \leq 1, \qquad i,j = 0,1,\ldots,m-1 \tag{5.4}$$

Lee and Filipi (2011) determined that the simplified vehicle dynamics equation (Equation 5.5) can be expressed using the two states of velocity and acceleration and hence they are suitable for the states of the Markov-chain.

$$F_{net} = F_{prop} - F_{rr} - F_{wr} - F_{gr} = m_e a_v = m_e v_v \tag{5.5}$$

Where F_{net} is the net force acting on the vehicle, F_{prop} is the propulsion force provided by the powertrain, F_{rr} is the rolling resistance force, F_{wr} is the wind resistance force and F_{gr} is the grade resistance force. The vehicle's mass, acceleration and velocity are m_e, a_v and v_v respectively.

As discussed previously in Chapter 4 and illustrated again in Figure 5.1, the real-world driving cycles were divided into four bins each having the same probability on the cdf. A TPM was then generated for each bin in the form of a two dimensional matrix with velocity and acceleration at current time t_k. The conditional probability is expressed as

$$P_{i,j,k+1|p,q,k} = P(v_{k+1} = v_i, a_{k+1} = a_j | v_k = v_p, a_k = a_q) \tag{5.6}$$

where i and p =1,2,…,M and j and q=1,2,…,N.

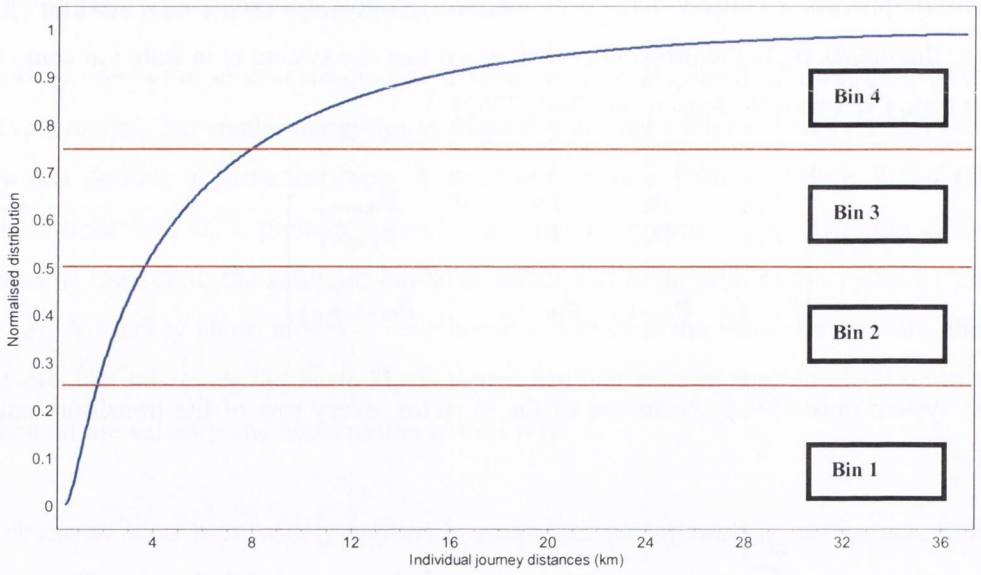

Figure 5.1. Cumulative distribution function of the individual journey distances and an illustration of the bin boundaries.

As the objective was to develop a representative driving cycle for each bin, the driving cycle model synthesises candidate driving cycles for each bin. However, since a Markov-chain is a stochastic process, there are no prior guarantees that a synthesised driving cycle will be representative of the real-world driving cycles in a particular bin. To address this issue, in the next section, a regression analysis is performed in order to determine significant statistical criteria that must be satisfied in order to confirm the representativeness of a synthesised driving cycle of the real-world driving cycles in a particular bin. This is the third step in the driving cycle development process.

5.2 The regression analysis

5.2.1 Overview of the regression analysis

As discussed in the previous section, Markov chains are a stochastic process, hence there are no prior guarantees that a synthesised cycle will be representative of the real-world driving cycles in a particular bin. This section provides an overview of a regression analysis that was performed to determine significant statistical criteria that must be satisfied in order to confirm the representativeness of a synthesised cycle of the real-world driving cycles in a particular bin. The explanatory variables in the regression equation will be chosen as statistical parameters for the assessment of the representativeness of a synthesised driving cycle. The selected parameters must be satisfied within certain error bounds to guarantee that a particular synthesised cycle satisfactorily represents the recorded real-world driving cycles in a particular bin. A similar regression analysis procedure was used by Lee et al (2009) for a virtual sensing study and by Lee and Filipi (2011) for assessing the representativeness of developed driving cycles for PHEVs.

The response variable in the regression analysis is the energy economy of the vehicle over a driving cycle. It is defined as the total energy used by the vehicle divided by the distance travelled

(Wh/km). This parameter has been used as a representative response variable in previous driving cycle studies (Carlson and Austin, 1997, Fellah et al, 2009, Lee and Filipi, 2011). After an investigation of the relationships between twenty-seven explanatory variables, eleven variables were nominated to be included in the model.

A detailed presentation of the regression analysis is outlined in the succeeding sections, however an overview of the process is presented in this section. A regression technique known as 'stepwise' regression, which is a semi-automated process of building a model by successively adding or removing variables based solely on the t-statistics of the estimated coefficients was used to choose the explanatory variables to be included in the model. Stepwise regression is an appropriate technique for identifying a useful subset of predictor variables from a large selection of variables (Barry, 2012). This method ensures that the model contains the smallest possible set of predictor variables. The final regression equation was determined by performing a multiple regression analysis, with the variables entered into the model in order of significance that was determined by the stepwise procedure that preceded this step.

In a regression analysis, a residual is the difference between the measured value and the predicted value of the regression model (Jiju, 2003). When the residuals (random errors) of the response variable approximate a straight line in a normal probability plot, the histogram of the residuals is normally distributed and there are no discernable patterns in the residuals plot, then the assumptions of linear regression are valid (Jiju, 2003). Based on the regression analysis, the explanatory variables in the final regression equation were chosen as statistical parameters for the assessment of the representativeness of a synthesised driving cycle. A flow chart of the driving cycle development procedure is presented in Figure 5.2. The next section provides an overview of the selection process of the final eleven explanatory variables to be included in the 'stepwise' regression analysis.

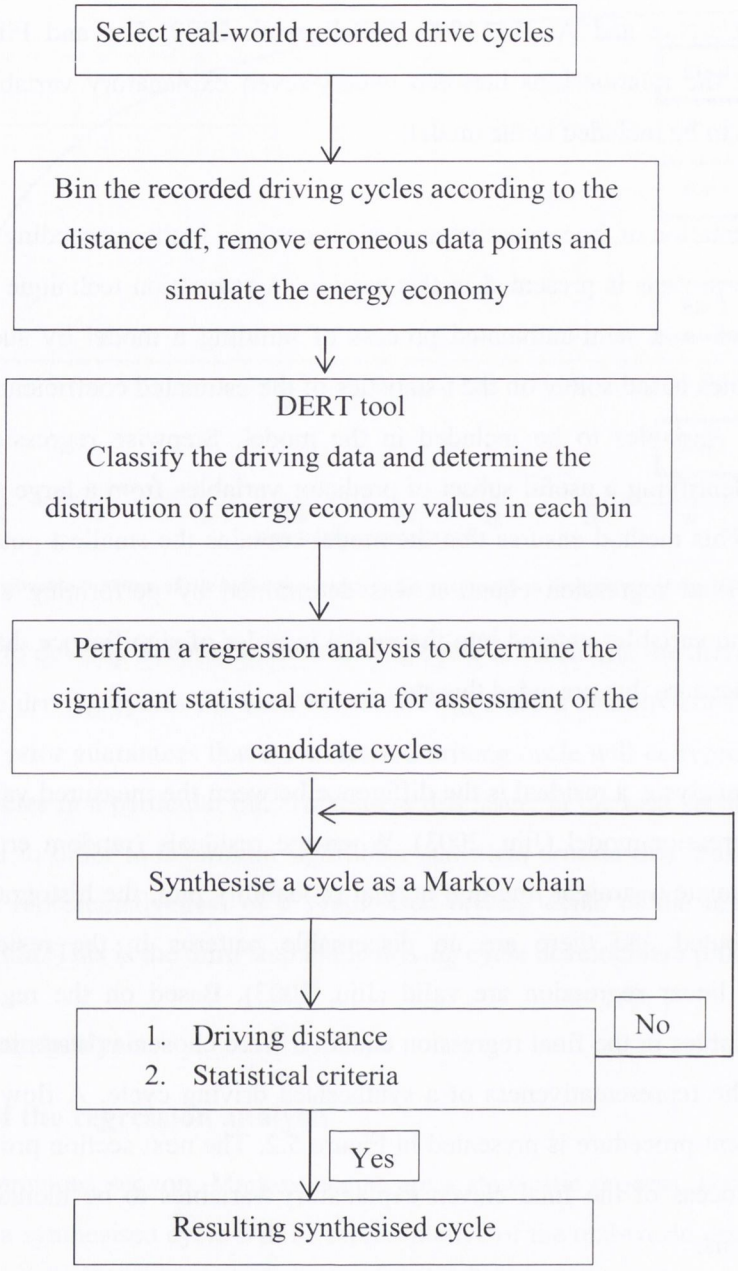

Figure 5.2. Flow chart of the driving cycle development procedure.

5.2.2 Nominated explanatory variables for the regression model

Initially twenty-seven explanatory variables were selected and categorised into velocity related, acceleration related, driving time and distance related, and driving characteristics related groups as shown in Table 5.1. Firstly, the Pearson product-moment correlations between the variables within the four categories were investigated. When two variables demonstrated a high correlation, the variable which was least correlated with the response variable was excluded as an explanatory variable. In Figure 5.3, two examples of within group correlations are presented; (a) the standard deviation of velocity is highly correlated with the maximum velocity. Thus, one of these variables could be excluded from the analysis. In Figure 5.3 (b), the same reasoning can be applied. This process resulted in fifteen initial nominated explanatory variables as shown in Table 5.1. Secondly, the correlations between the fifteen variables (i.e. between the groups) were investigated. Similarly,

when two variables demonstrated a high correlation, one of them was excluded from the initial set of fifteen nominated variables. In Figure 5.3, two examples of between group correlations are presented; (a) positive acceleration time is highly correlated with distance. Thus, one of these variables could be removed. In Figure 5.3 (b), the same reasoning can be applied. This process reduced the fifteen initial nominated variables to the final eleven nominated variables to be included in the regression analysis.

The succeeding sections firstly detail the analysis of the correlations between the explanatory variables within each of the four categories. Following that an analysis of the correlations between the fifteen initial nominated explanatory variables (i.e. between the groups) is presented. The abbreviations and the units of the variables are listed in Table 5.2.

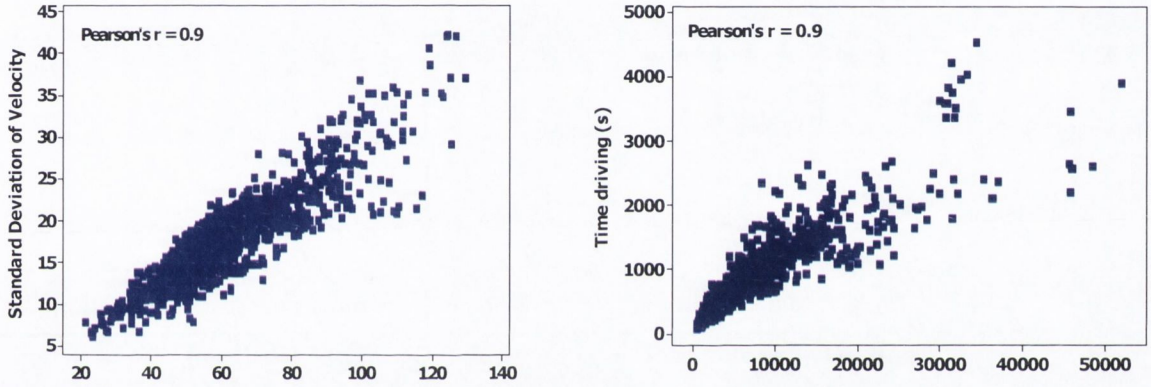

Figure 5.3. The correlation between two within group explanatory variables: (a) between the standard deviation of velocity and maximum velocity; (b) between time driving and distance.

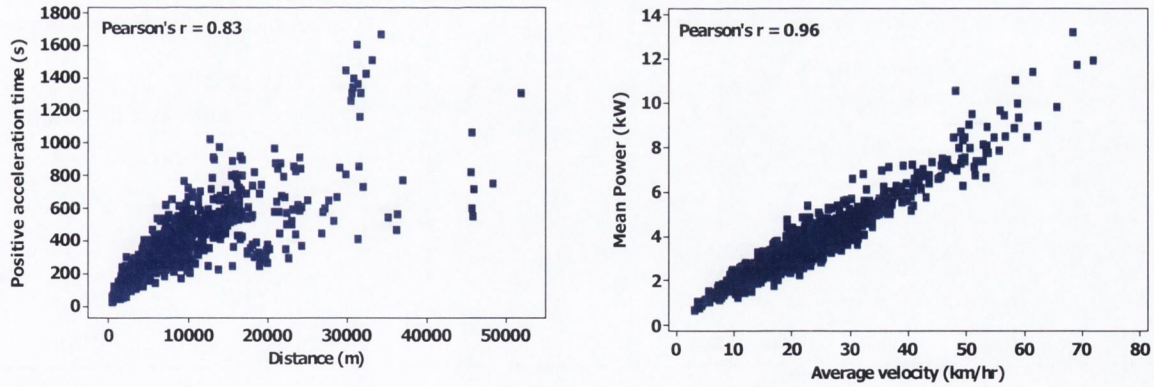

Figure 5.4. The correlation between two between group nominated explanatory variables: (a) between the positive acceleration time and distance; (b) between mean specific power and average velocity.

Table 5.1. The twenty-seven initial explanatory variables and the fifteen initial nominated variables from the four categories.

Category	Initial possible explanatory variables	Initial nominated explanatory variables
1.Velocity related variables	1. Mean velocity	1. Mean velocity
	2. Maximum velocity	
	3. Standard deviation of velocity	2. Standard deviation of velocity
	4. Mean cruising velocity	
2. Acceleration related variables	5. Mean positive acceleration	3. Mean positive acceleration
	6. Mean negative acceleration	
	7. Positive acceleration time	4. Positive acceleration time
	8. Negative acceleration time	
	9. Maximum acceleration	5. Maximum acceleration
	10. Minimum acceleration	6. Minimum acceleration
	11. Standard deviation of acceleration	
	12. Standard deviation of positive acceleration	
	13. Standard deviation of negative acceleration	
	14. Percentage of driving time under positive acceleration	
	15. Percentage of driving time under negative acceleration	7. Percentage of driving time under negative acceleration
3. Driving distance and time	16. Driving distance	8. Driving distance
	17. Driving time	
	18. Total time	
4. Driving characteristics	19. Idle time	
	20. Percentage of idle time	9. Percentage of idle time
	21. Number of stops	10. Number of stops
	22. Number of stops per kilometre	11. Number of stops per kilometre
	23. Mean specific power	12. Mean specific power
	24. Maximum specific power	13. Maximum specific power
	25. Minimum specific power	
	26. Cruising time	14.Cruising time
	27. Percentage of cruising time	15. Percentage of cruising time

Table 5.2. The abbreviations and units of the driving cycle variables.

Variable	Abbreviation	Unit
1. Mean velocity	Vel_avg	km/hr
2. Maximum velocity	Vel_max	km/hr
3. Standard deviation of velocity	SD_vel	
4. Mean cruising velocity	Vel_avg_cru	km/hr
5. Mean positive acceleration	Acc_pos	m/s^2
6. Mean negative acceleration	Acc_neg	m/s^2
7. Positive acceleration time	T_acc	s
8. Negative acceleration time	T_deacc	s
9. Maximum acceleration	Acc_max	m/s^2
10. Minimum acceleration	Acc_min	m/s^2
11. Standard deviation of acceleration	SD_acc	
12. Standard deviation of positive acceleration	SD_acc_pos	
13. Standard deviation of negative acceleration	SD_acc_neg	
14. Percentage of driving time under positive acceleration	Per_time_pos_acc	%
15. Percentage of driving time under negative acceleration	Per_time_neg_acc	%
16. Driving distance	Dis	m
17. Driving time	Drive_time	s
18. Total time	Total_time	s
19. Idle time	Idle_time	s
20. Percentage of idle time	P_idle	%
21. Number of stops	No. stops	
22. Number of stops per kilometre	Stops_per_km	
23. Mean specific power	Mean_p	W/km
24. Maximum specific power (Maximum power/distance travelled)	Max_p	W/km
25. Minimum specific power (Minimum power/distance travelled)	Min_p	W/km
26. Cruising Time	T_cru	s
27. Percentage of cruising time	Per_cruise	%
28. Energy economy (response variable)	Energy	Wh/km

5.2.2.1 Category one: velocity related variables

The Pearson product-moment correlation matrix for the variables in category one is presented in Table 5.3. The nominated variables from this category are listed in Table 5.1.

Table 5.3.The correlation coefficient matrix for the variables in category one.

	Vel_avg	Vel_max	SD_vel	Vel_avg_cru	Energy
Vel_avg	1				
Vel_max	0.73	1			
SD_vel	0.79	0.90	1		
Vel_avg_cru	0.91	0.78	0.88	1	
Energy	-0.40	-0.12	-0.19	-0.33	1

The variables' standard deviation of velocity and maximum velocity were highly correlated (0.9). The variable maximum velocity was excluded from the analysis because it was least correlated with the response variable (-0.12). The variables' mean velocity and mean cruising velocity were highly correlated (0.91). The variable mean cruising velocity was excluded from the analysis because it was least correlated with the response variable (-0.33). The variables' mean velocity and standard deviation of velocity were the initial nominated variables from this category.

5.2.2.2 Category two: acceleration related variables

The correlation matrix for the variables in category two is presented in Table 5.4. The nominated variables from this category are listed in Table 5.1. The variables' mean positive acceleration and mean negative acceleration were highly correlated (-0.77). The variable mean negative acceleration was excluded from the analysis because it was least correlated with the response variable (-0.58). The variables' standard deviation of positive acceleration, standard deviation of negative acceleration and the standard deviation of acceleration were all highly correlated with the variable mean positive acceleration (0.88, 0.62 and 0.83 respectively). These three variables were excluded from the analysis on the basis that the variable mean positive acceleration had the highest correlation with the response variable (0.64). The variables' percentage of driving time under positive acceleration and percentage of driving time under negative acceleration were highly correlated (0.7). The variable percentage of driving time under positive acceleration was excluded from the analysis because it was least correlated with the response variable (-0.54). The variables' positive acceleration time and negative acceleration time were also highly correlated (0.99). The variable negative acceleration time was excluded from the analysis because it was least correlated with the response variable (-0.13). The variables' mean positive acceleration, positive acceleration time, maximum acceleration, minimum acceleration and the percentage of driving time under negative acceleration were the initial nominated variables from this category.

Table 5.4. The correlation coefficient matrix for the variables in category two.

	Acc_pos	Acc_neg	T_acc	T_deacc	Acc_max	Acc_min	SD_acc
Acc_pos	1.00						
Acc_neg	-0.77	1.00					
T_acc	-0.09	0.01	1.00				
T_deacc	-0.05	0.03	0.99	1.00			
Acc_max	0.53	-0.45	0.42	0.44	1.00		
Acc_min	-0.38	0.53	-0.45	-0.44	-0.56	1.00	
SD_acc	0.83	-0.86	-0.08	-0.08	0.47	-0.44	1.00
SD_acc_pos	0.88	-0.68	0.03	0.06	0.75	-0.47	0.75
SD_acc_neg	0.62	-0.87	0.11	0.08	0.51	-0.77	0.74
Per_time_pos_acc	0.32	-0.53	-0.08	-0.10	0.02	-0.11	0.48
Per_time_neg_acc	0.60	-0.29	-0.13	-0.07	0.15	0.02	0.46
Energy	0.64	-0.58	-0.15	-0.13	0.23	-0.21	0.47

Table 5.4 Continued. The correlation coefficient matrix for the variables in category two.

	SD_acc_pos	SD_acc_neg	Per_time_pos_acc	Per_time_neg_acc	Energy
SD_acc_pos	1.00				
SD_acc_neg	0.64	1.00			
Per_time_pos_acc	0.14	0.33	1.00		
Per_time_neg_acc	0.40	0.09	0.70	1.00	
Energy	0.48	0.44	0.54	0.60	1.00

5.2.2.3 Category three: driving distance and time

The correlation matrix for the variables in category three is presented in Table 5.5. The nominated variable from this category is listed in Table 5.1. The variable driving distance was found to be highly correlated with the variables driving time and total time (0.90 and 0.81 respectively). The variables' driving time and total time were excluded from the analysis because they were least correlated with the response variable (-0.20 and -0.10 respectively). The variable driving distance was the initial nominated variable from this category.

Table 5.5. The correlation coefficient matrix for the variables in category three.

	Drive_time	Dis	Total_time	Energy
Drive_time	1			
Dis	0.90	1		
Total_time	0.96	0.81	1	
Energy	-0.20	-0.21	-0.10	1

5.2.2.4 Category four: driving characteristics

The correlation matrix for the variables in category four is presented in Table 5.6. The nominated variables from this category are listed in Table 5.1. The variables' maximum specific power and minimum specific power were highly correlated (-0.86). The variable minimum specific power was excluded from the analysis because it was least correlated with the response variable (-0.55). The variables' idle time and percentage of idle time were found to be correlated (0.59). The variable idle time was excluded from the analysis because it was least correlated with the response variable (0.12). The variables' percentage of idle time, number of stops, number of stops per kilometre, mean specific power, maximum specific power, cruising time and percentage of cruising time were the initial nominated variables from this category.

This section concludes the analysis of the correlations between the explanatory variables within each of the four categories. Fifteen variables were nominated from the four categories. The next section presents the analysis of the correlations between the initial fifteen nominated variables (i.e. between the four categories).

Table 5.6. The correlation coefficient matrix for the variables in category four.

	Idle_time	P_idle	No. stops	Stops_per_km	Mean_p
Idle_time	1.00				
P_idle	0.59	1.00			
No. stops	0.81	0.41	1.00		
Stops_per_km	-0.12	-0.33	-0.17	1.00	
Mean_p	-0.21	-0.56	-0.16	0.63	1.00
Max_p	-0.34	0.07	-0.40	-0.25	-0.29
Min_p	0.34	-0.02	0.40	0.23	0.22
T_cru	0.50	-0.07	0.57	0.36	0.42
Per_cruise	-0.28	-0.64	-0.21	0.47	0.44
Energy	0.12	0.48	0.07	-0.19	-0.12

Table 5.6 Continued. The correlation coefficient matrix for the variables in category four.

	Max_p	Min_p	T_cru	Per_cruise	Energy
Max_p	1.00				
Min_p	-0.86	1.00			
T_cru	-0.57	0.56	1.00		
Per_cruise	-0.30	0.30	0.44	1.00	
Energy	0.56	-0.55	-0.28	-0.64	1.00

5.2.2.5 Initial nominated variables correlation analysis

After the correlations of the variables within the four groups were investigated, the next step was to investigate the correlations between the groups (i.e. between the fifteen initial nominated variables). The correlation matrix for the fifteen initial nominated variables is presented in Table 5.7. The variables' mean specific power and mean velocity were found to be highly correlated (0.96). The variable mean specific power was excluded from the analysis because it was least correlated with the response variable (-0.12). The variables' positive acceleration time and distance were both found to be highly correlated with the variable cruising time (0.83 and 0.93 respectively). The variables' positive acceleration time and distance were excluded from the analysis because they were least correlated with the response variable (-0.15 and -0.21 respectively). The variables' percentage of driving time under negative acceleration and percentage of cruising time were found to be highly correlated (-0.88). The variable percentage of driving time under negative acceleration was removed from the analysis because it was least correlated with the response variable (0.60). This process reduced the fifteen initial nominated variables to the final eleven nominated variables.

The twenty-seven initial possible explanatory variables, the fifteen initial nominated explanatory variables and the final eleven nominated variables to be included in the regression analysis are listed in Table 5.8. The next section describes the developed regression model.

Table 5.7. The correlation coefficient matrix for the fifteen initial nominated variables.

	V_avg	SD_vel	Acc_pos	T_acc	Acc_max	Acc_min	Per_time_neg_acc	Dis	P_idle
V_avg	1.00								
SD_vel	0.80	1.00							
Acc_pos	-0.12	0.05	1.00						
T_acc	0.26	0.46	-0.09	1.00					
Acc_max	0.22	0.41	0.53	0.42	1.00				
Acc_min	-0.25	-0.44	-0.38	-0.45	-0.56	1.00			
Per_time_neg_acc	-0.50	-0.32	0.60	-0.13	0.15	0.02	1.00		
Dis	0.63	0.73	-0.17	0.83	0.38	-0.41	-0.39	1.00	
P_idle	-0.62	-0.23	0.19	0.11	0.12	-0.09	0.40	-0.11	1.00
No. stops	-0.17	0.13	0.00	0.82	0.34	-0.34	0.11	0.49	0.41
Stops_per_km	-0.68	-0.53	0.05	-0.21	-0.14	0.19	0.37	-0.38	0.61
Mean_p	0.96	0.82	0.08	0.23	0.30	-0.34	-0.35	0.60	-0.56
Max_p	-0.41	-0.42	0.37	-0.60	-0.11	0.24	0.39	-0.57	0.07
T_cru	0.48	0.58	-0.24	0.83	0.32	-0.36	-0.49	0.93	-0.07
Per_cruise	0.60	0.31	-0.48	0.04	-0.13	0.08	-0.88	0.35	-0.64
Energy	-0.36	-0.14	0.64	-0.15	0.23	-0.21	0.60	-0.21	0.48

Table 5.7 Continued. The correlation coefficient matrix for the fifteen initial nominated variables.

	No. stops	Stops_per_km	Mean_p	Max_p	T_cru	Per_cruise	Energy
No. stops	1.00						
Stops_per_k	0.21	1.00					
Mean_p	-0.16	-0.62	1.00				
Max_p	-0.40	0.41	-0.29	1.00			
T_cru	0.57	-0.30	0.42	-0.57	1.00		
Per_cruise	-0.21	-0.44	0.44	-0.30	0.44	1.00	
Energy	0.07	0.56	-0.12	0.55	-0.28	-0.64	1.00

5.2.3 The regression model

The explanatory variables in the final regression equation were chosen as statistical parameters for the assessment of the representativeness of a synthesised candidate driving cycle of the real-world driving cycles in a particular bin. The objective of the regression analysis was to identify the smallest set of significant predictors of the energy economy of a vehicle over a driving cycle. This section presents the regression model.

Before presenting the regression model, it is necessary to define a number of terms. In a regression analysis, the null hypothesis states that the coefficient of an explanatory variable is not significantly different from zero. A p-value is the probability, assuming that the null hypothesis is true, of observing a more extreme test statistic than the one observed (Pardoe, 2012).

Stepwise regression analysis was performed with the final eleven explanatory variables. Stepwise regression begins with an 'empty' model with no explanatory variables. It begins by adding the most significant variable and then each time a new variable is added to the model, the significance of each of the variables already in the model is re-examined, i.e. at each step in the forward selection procedure, the significance of each of the variables currently in the model is tested, and the variable with the highest p-value (if the p -value is greater than 0.05) is removed. The model is then re-fitted without this variable, before going to the next step in the forward selection procedure. The stepwise regression procedure continues until no more variables can be added or removed. The procedure stops when all variables not included in the model have p-values that are greater than the specified significance level (0.05) to enter the model and when all variables that are in the model have p-values that are less than or equal to a specified significance level (0.05) to remove a variable. Thus, this method ensures that the model contains the smallest possible set of predictor variables. Table 5.9 illustrates the stepwise regression analysis. The variable percentage of cruising time was the first variable entered into the model, followed by the variable maximum specific power. Ten steps were performed resulting in all of the variables being entered into the model except the variable standard deviation of velocity as its p-value was greater than the significance

level to enter into the model. Therefore, ten of the final eleven nominated explanatory variables were included in the final model.

Table 5.8. The twenty-seven explanatory variables, the fifteen initial nominated variables and the eleven final nominated explanatory variables for the regression analysis.

Category	Initial possible explanatory variables	Initial nominated explanatory variables	Initial nominated explanatory variables
1.Velocity related variables	1. Mean velocity	1. Mean velocity	1. Mean velocity
	2. Maximum velocity		
	3. Standard deviation of velocity	2. Standard deviation of velocity	2. Standard deviation of velocity
	4. Mean cruising velocity		
2. Acceleration related variables	5. Mean positive acceleration	3. Mean positive acceleration	3. Mean positive acceleration
	6. Mean negative acceleration		
	7. Positive acceleration time	4. Positive acceleration time	
	8. Negative acceleration time		
	9. Maximum acceleration	5. Maximum acceleration	4. Maximum acceleration
	10. Minimum acceleration	6. Minimum acceleration	5. Minimum acceleration
	11. Standard deviation of acceleration		
	12. Standard deviation of positive acceleration		
	13. Standard deviation of negative acceleration		
	14. Percentage of driving time under positive acceleration		
	15. Percentage of driving time under negative acceleration	7. Percentage of driving time under negative acceleration	
3. Driving distance and time	16. Driving distance	8. Driving distance	
	17. Driving time		
	18. Total time		
4. Driving characteristics	19. Idle time		
	20. Percentage of idle time	9. Percentage of idle time	6. Percentage of idle time
	21. Number of stops	10. Number of stops	7. Number of stops
	22. Number of stops per kilometre	11. Number of stops per kilometre	8. Number of stops per kilometre
	23. Mean specific power	12. Mean specific power	
	24.Maximum specific power	13. Maximum specific power	9. Maximum specific power
	25. Minimum specific power		
	26. Cruising time	14.Cruising time	10.Cruising time
	27. Percentage of cruising time	15. Percentage of cruising time	11. Percentage of cruising time

Table 5.9. The stepwise regression output (steps 1-6).

Step	1	2	3	4	5	6
Constant	196.05	179.76	131.32	100.98	96.03	97.57
Percentage cruise time	-1.512	-1.234	-0.915	-0.498	-0.884	-0.991
T-Value	-29.96	-26.88	-19.95	-11.05	-19.01	-21.5
P-Value	0	0	0	0	0	0
Maximum specific power		0.0006	0.00048	0.00026	0.00036	0.00049
T-Value		20.48	17.09	9.75	14.42	17.9
P-Value		0	0	0	0	0
Mean positive acceleration			71.5	97.2	82.8	79.3
T-Value			16.56	24.44	22.46	22.21
P-Value			0	0	0	0
Number of stops per km				3.39	4.82	4.51
T-Value				20.16	27.82	26.52
P-Value				0	0	0
Mean velocity					0.765	0.671
T-Value					17.12	15.21
P-Value					0	0
Cruise Time						0.0164
T-Value						9.94
P-Value						0
S	16.8	14.6	13.3	11.6	10.4	10.1
R-Sq	41.06	55.55	63.36	72.16	77.34	78.96
R-Sq(adj)	41.02	55.48	63.28	72.08	77.25	78.86

Table 5.9. Continued. The stepwise regression output (steps 7-10).

Step	7	8	9	10
Constant	102.06	100.92	100.77	96.44
Percentage cruise time	-1.114	-1.087	-1.089	-1.044
T-Value	-22.94	-22.75	-22.95	-18.31
P-Value	0	0	0	0
Maximum specific power	0.00041	0.00044	0.00044	0.00046
T-Value	14.18	15.28	15.38	15.66
P-Value	0	0	0	0
Mean positive acceleration	83.0	71.1	79.7	79.7
T-Value	23.41	18.49	18.43	18.5
P-Value	0	0	0	0
Number of stops per km	4.83	4.85	4.84	4.59
T-Value	27.90	28.58	28.74	24.5
P-Value	0	0	0	0
Mean velocity	0.553	0.5	0.531	0.594
T-Value	11.88	10.83	11.43	11.73
P-Value	0	0	0	0
Cruise Time	0.0292	0.266	0.0279	0.0248
T-Value	11.95	11.01	11.52	9.53
P-Value	0	0	0	0
No. of stops	-347	-0.387	-0.353	-0.314
T-Value	-6.99	-7.89	-7.16	-6.19
P-Value	0	0	0	0
Minimum acceleration		-4.32	-4.82	-4.67
T-Value		-7.29	-8.02	-7.78
P-Value		0	0	0
Maximum acceleration			-3.63	-3.92
T-Value			-4.24	-4.57
P-Value			0	0
Percentage of idle time				0.112
T-Value				3.07
P-Value				0.002
S	9.87	9.68	9.62	9.58
R-Sq	79.73	80.54	80.81	80.95
R-Sq(adj)	79.62	80.42	80.67	80.8

To obtain the final regression equation a multiple regression analysis was performed. The variables were entered into the model in order of significance that was determined by the stepwise procedure. The resulting model was statistically significant and accounted for approximately 82% of the variance of the response variable, energy economy (R^2 = 82.7%, Adjusted R^2 = 82.5%). The F-test which is used to determine whether a significant relationship exists between the response variable and the set of all the explanatory variables was statistically significant ($p < 0.05$) as shown in Table 5.10. Table 5.11 contains the coefficients of the regression model. All of the explanatory variables

were statistically significant ($p < 0.05$). The variance inflation factors (VIF) for each of the independent variables were less than 5, indicating that significant multicollinearity was not present in the model. In the next section the regression model is validated and the final regression equation is presented.

Table 5.10. Analysis of variance table of the multiple regression analysis.

Source	DF	SS	MS	F	P
Regression	10	438325	43832	579.83	0.000
Residual Error	1190	89959	76		
Total	1200	528284			

Table 5.11. Coefficients of the multiple regression model.

Predictor	**Coef**	**SE Coef**	**T**	**P**	**VIF**
Constant	99.102	2.922	33.91	0.000	
Percentage cruise time	-1.04776	0.05379	-19.48	0.000	3.751
Maximum specific power	0.00048930	0.00002806	17.43	0.000	2.513
Mean positive acceleration	76.308	4.045	18.87	0.000	2.607
Number of stops per km	4.6462	0.1850	25.12	0.000	2.866
Mean velocity	0.60632	0.04815	12.59	0.000	3.903
Cruise time	0.023239	0.002530	9.19	0.000	5.128
Minimum acceleration	-4.2880	0.5642	-7.60	0.000	1.795
Number of stops	-0.26281	0.04807	-5.47	0.000	4.354
Maximum acceleration	-3.6123	0.8006	-4.51	0.000	2.183
Percentage of idle time	0.07833	0.03500	2.24	0.025	3.379

5.2.4 Regression analysis – model validation

In a typical ordinary least squares multiple regression analysis the following four assumptions are made (University of Southern Denmark, 2012):

(i) Independence: The response variables, Y_i, are independent.

(ii) Normality: The response variables, Y_i, are normally distributed.

(iii) Homoscedasticity: The response variables, Y_i, all have the same variance, σ^2.

(iv) Linearity: The true relationship between the mean of the response variable, $E[Y]$ and the explanatory variables is a straight line.

Rather than checking assumptions on the response variables directly, it is convenient to re-express the assumptions in terms of the residuals and validate the assumptions on the residuals instead (University of Southern Denmark, 2012). The following four assumptions on the residuals are equivalent to the assumptions on the response variables.

(i) The residuals are independent.

(ii) The residuals are normally distributed.

(iii) The residuals have constant variance.

(iv) The residuals have zero mean.

A normal probability plot of the standardised residuals gives an indication of whether or not the assumption of normality of the residuals is valid. The normal probability plot in Figure 5.5 (a) approximates a straight line therefore it is reasonable to assume that residuals are normally distributed (Jiju, 2003). A histogram plot of the standardised residuals exhibits an approximate normal shaped distribution (Figure 5.5 ()), further indicating that the normality assumption is valid (Jiju, 2003).

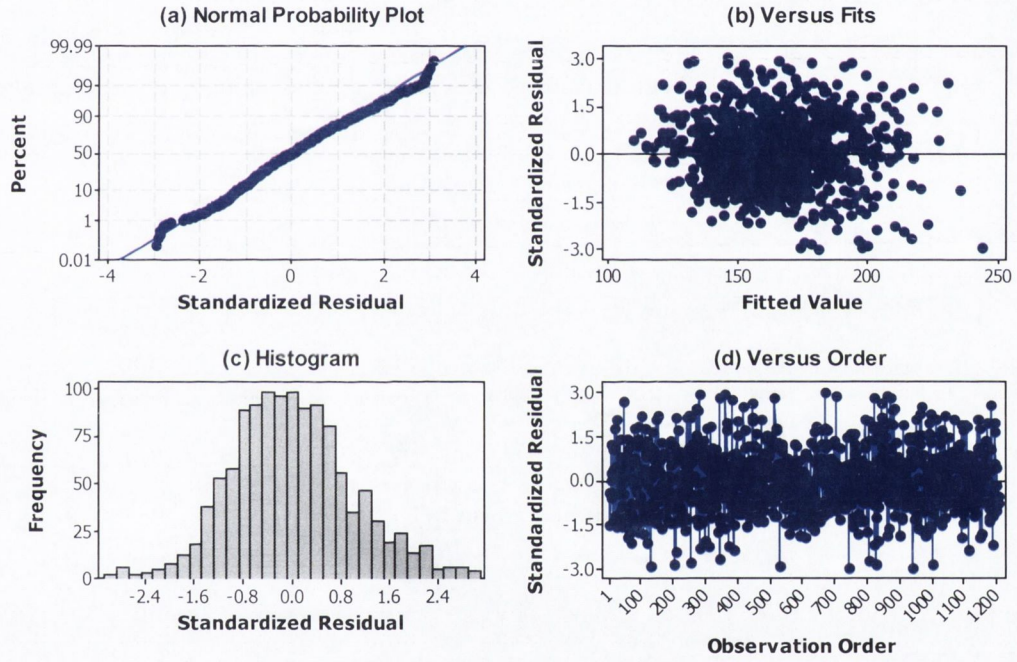

Figure 5.5. (a) Normal probability plot of standardised residuals, (b) standardised residuals against the fitted values, (c) histogram of the standardised residuals and (d) order of the standardised residuals.

The two assumptions, assumption (iii) the residuals have constant variance, and assumption (iv) the residuals have zero mean, can be validated at the same time. A residual plot is a scatterplot of the standardised residuals against the fitted values. If assumptions (iii) and (iv) are satisfied the residuals should vary randomly around zero and the spread of the residuals should be about the same throughout the plot (University of Southern Denmark, 2012). The data points in Figure 5.5 (d) fluctuate randomly around zero and no discernable patterns are present in Figure 5.5 (b). Thus, the plot does not suggest violation of the assumptions of zero mean and constant variance of the random errors (University of Southern Denmark, 2012). The final regression equation consisted of ten variables as shown in Table 5.12.

Table 5.12. The determined significant explanatory variables for a EV and the final regression equation.

Variables	Variables
1. Percentage cruising time (s)	6. Cruising time (s)
2. Maximum specific power (Wh/km)	7. Minimum acceleration (m/s^2)
3. Average acceleration (m/s^2)	8. Number of stops
4. Stops per kilometre	9. Maximum Acceleration (m/s^2)
5. Average velocity (km/hr)	10. Percentage of idle time (s)

Energy_Economy = 99.1 - 1.05 Percentage_crusing_time + 0.000489 Maximum_specific_power + 76.3 Average_acceleration + 4.65 stops_per_kilometre + 0.606 Average_velocity + 0.0232 Cruising_time - 4.29 Minimum_acceleration - 0.263 Number_of_stops - 3.61 Maximum_acceleration + 0.0783 Percentage_of_idle_time

Figure 5.6 illustrates the predicted energy economy using the developed regression equation versus the actual energy economy of the logged real-world driving cycles. The plot indicates that the predicted values are well correlated with the real-world values. Although the points are not perfectly aligned on the diagonal, the distribution is relatively tight, indicating that the regression equation captures the main characteristics of driving cycles that influence the energy economy of an EV. The next section presents the four developed driving cycles for the GDA.

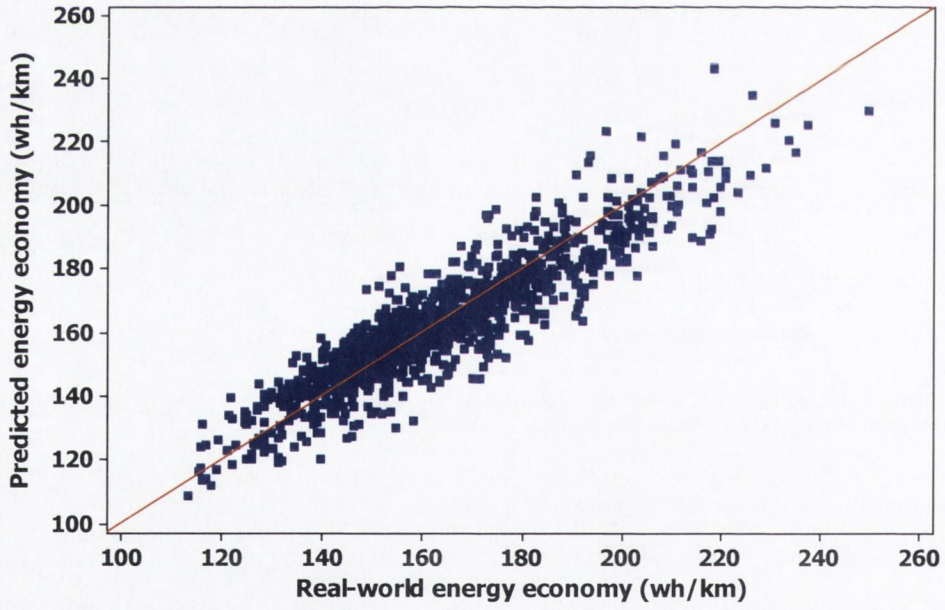

Figure 5.6. Scatter plot of the real-world energy economy values versus the predicted energy economy by the regression equation, of the driving cycles.

5.3 The developed driving cycles for the Greater Dublin Area

A representative driving cycle distance for each bin was selected as the median value of the bin range on the cdf, as shown in Figure 5.7 (green circle). The selected representative driving cycle distances were 1.2 km, 2.7 km, 5.9 km and 14.1 km. These are the distances of the developed driving cycles. This section presents the four developed driving cycles for the GDA, labelled DUB-01, DUB-02, DUB-03 and DUB-04 from hereafter.

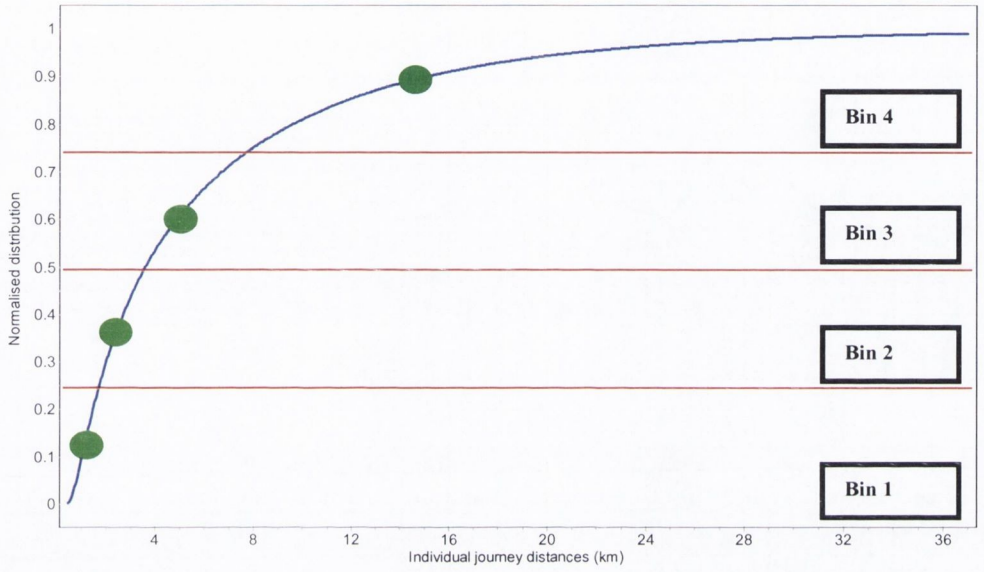

Figure 5.7. Cumulative distribution function of the individual journey distances and the selected driving cycle distance for each bin.

As discussed previously the Markov-chain driving cycle model synthesises candidate driving cycles. Several thousand iterations of the Markov-chain process were performed in order to satisfy the ten statistical variables determined by the regression analysis. The statistical parameters of the candidate cycles must match the mean value of the statistical parameters of real-world driving cycles in each bin within ±10%.

The final developed cycles are presented in Figures 5.8 – 5.11. The parameters of the four developed cycles are shown to represent well the mean values of the parameters of the real-world driving cycles in their respective bins, as shown in the comparison Tables 5.13–5.16. The next section presents further validation of the developed cycles by investigating the predicted energy economy of the developed cycles in relation to the real-world driving cycle energy economy values in their respective bins. Following that an assessment of the representativeness of the developed driving cycles and a selection of well-established worldwide driving cycles of the real-world driving cycles in a given bin is presented.

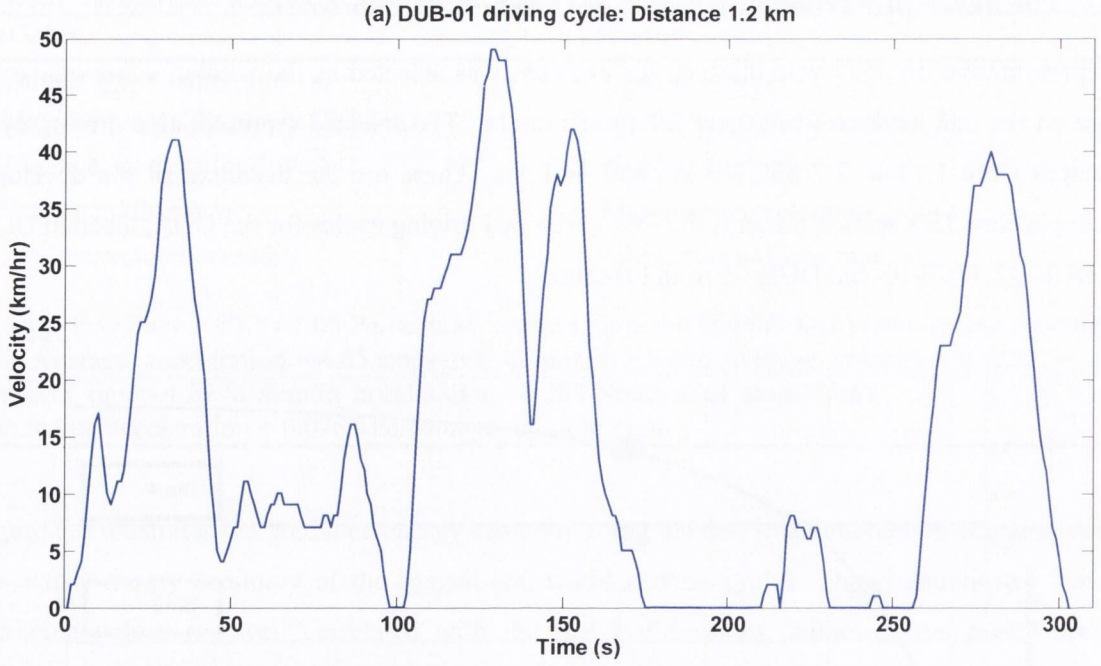

Figure 5.8. The DUB-01 cycle, the developed driving cycle for bin 1.

Table 5.13. Comparison of the statistical parameters of the DUB-01 cycle with the parameters of the driving cycles in bin 1.

Statistical parameters	Real-world driving cycles*	DUB-01 cycle
Average acceleration (m/s^2)	0.61	0.59
Number of stops per km	4.17	4.02
Percentage of cruising time (%)	19.17	18.54
Maximum specific power (W/km)	34,935	32,964
Number of stops	5	5
Minimum acceleration (m/s^2)	-1.79	-1.67
Percentage of idle time (%)	21.75	21.85
Average velocity (km/hr)	15.26	14.82
Max acceleration (m/s^2)	1.72	1.67
Cruising time (s)	54	56

*** Mean values are presented for the real-world driving cycles**

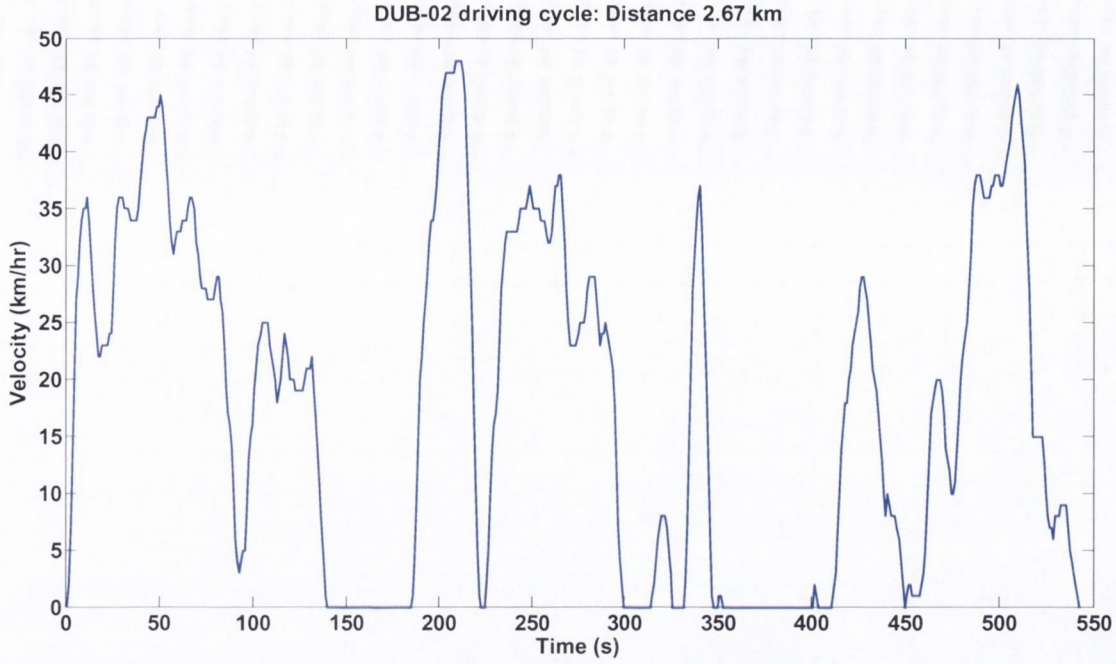

Figure 5.9. The DUB-02 cycle, the developed driving cycle for bin 2.

Table 5.14. Comparison of the statistical parameters of the DUB-02 cycle with the parameters of the driving cycles in bin 2.

Statistical parameters	Real-world driving cycles*	DUB-02 cycle
Average acceleration (m/s^2)	0.63	0.63
Number of stops per km	3.11	2.86
Percentage of cruising time (%)	21.36	19.49
Maximum specific power (W/km)	19,096	16,918
Number of stops	8	8
Minimum acceleration (m/s^2)	-2.07	-1.94
Percentage of idle time (%)	22.57	20.7
Average velocity (km/hr)	19.2	19.84
Max acceleration (m/s^2)	1.99	2.22
Cruising time (s)	108	99

*** Mean values are presented for the real-world driving cycles**

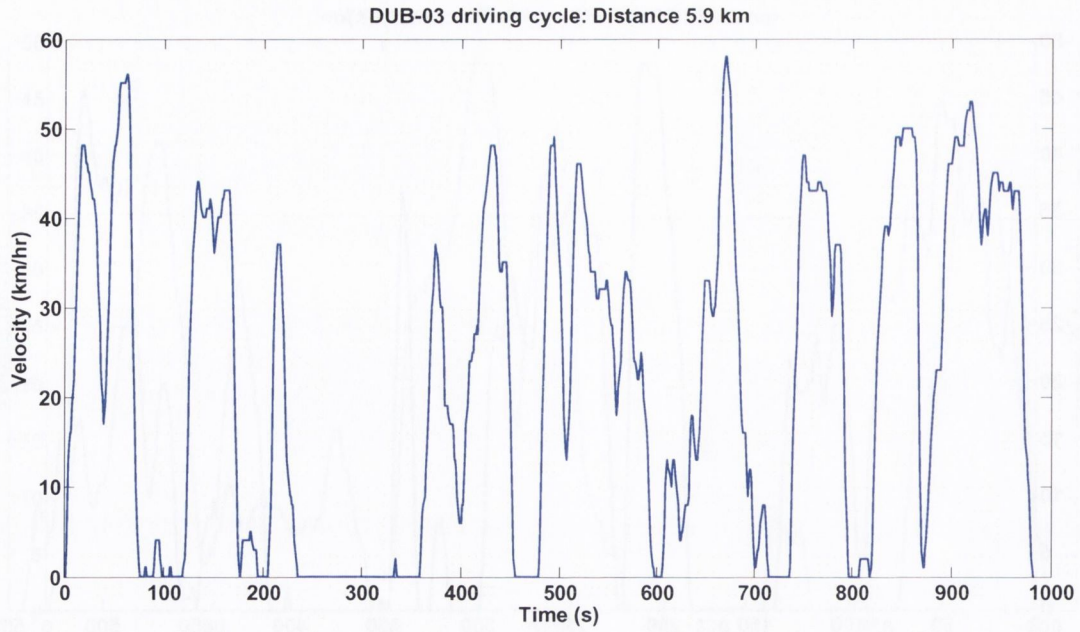

Figure 5.10. The DUB-03 cycle, the developed driving cycle for bin 3.

Table 5.15. Comparison of the statistical parameters of the DUB-03 cycle with the parameters of the driving cycles in bin 3.

Statistical parameters	Real-world driving cycles*	DUB-03 cycle
Average acceleration (m/s^2)	0.62	0.65
Number of stops per km	2.17	2.2
Percentage of cruising time (%)	21.38	21.4
Maximum specific power (W/km)	9,677	9,972
Number of stops	13	13
Minimum acceleration (m/s^2)	-2.39	-2.5
Percentage of idle time (%)	22.88	23.50
Average velocity (km/hr)	22.25	21.67
Max acceleration (m/s^2)	2.19	2.22
Cruising time (s)	226	210

*** Mean values are presented for the real-world driving cycles**

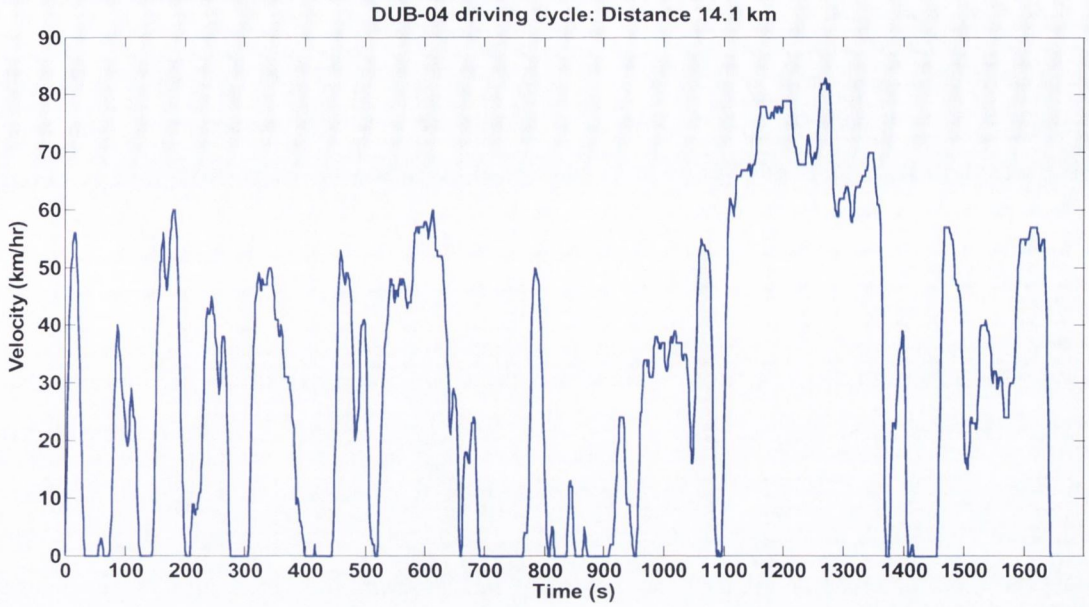

Figure 5.11. The DUB-04 cycle, the developed driving cycle for bin 4.

Table 5.16. Comparison of the statistical parameters of the DUB-04 cycle with the parameters of the driving cycles in bin 4.

Statistical parameters	Real-world driving cycles*	DUB-04 cycle
Average Acceleration (m/s^2)	0.59	0.62
Number of stops per km	1.4	1.42
Percentage of cruise time (%)	25.95	27.6
Maximum Specific Power (W/km)	4,540	4,805
Number of stops	20	20
Minimum acceleration (m/s^2)	-2.56	-2.5
Percentage of idle time (%)	19.64	20.67
Average velocity (km/hr)	30.60	30.87
Max Acceleration (m/s^2)	2.3	2.22
Cruising time (s)	495	454

*** Mean values are presented for the real-world driving cycles**

5.4 Further validation of the developed driving cycles

In addition to ensuring that the statistical parameters of a developed cycle are within ±10% of the mean values of the statistical parameters of the real-world driving cycles in a given bin, the predicted energy economy of a developed cycle must be representative of the energy economy values of the real-world cycles in a given bin. This section presents this aspect of the validation of the developed cycles.

As previously discussed in Section 4.11, the energy economy values of the real-world driving cycles are distributed broadly in each of the four bins. The distribution of the real-word driving cycle energy economy values (blue bars) for each of the bins are presented again in Figures 5.12-5.15 and are overlaid with a cdf (red line). The energy economy of the developed driving cycle for a given bin must be representative of the real-world energy economy values in that bin regardless of the density distribution. It is assumed that if the predicted energy economy of the developed cycle for a given bin is located around the median point of the observed real-world energy economy values in that bin, then the developed driving cycle is assumed to represent well the driving cycles in that bin. For example, in Figure 5.12, the predicted energy economy of the DUB-01 cycle is 171 Wh/km. This is located approximately at median point of the distribution (174.5 Wh/km) of the real-world energy economy values in bin 1.

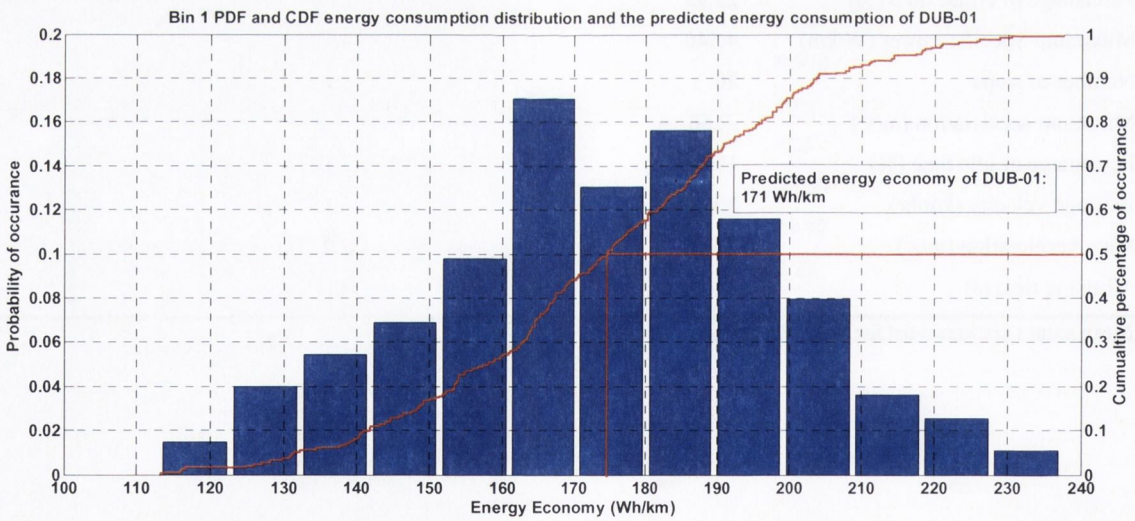

Figure 5.12. Probability distribution (blue bars) and cumulative distribution (red line) of the energy economy of the real-world driving cycles in bin 1 and the predicted energy economy of the developed driving cycle, DUB-01 for bin 1.

Similarly, as demonstrated in Figures 5.13-5.15, the predicted energy economy values of the DUB-02, DUB-03 and DUB-04 cycles (162 Wh/km, 156Wh/km and 154.5 Wh/km respectively), are approximately located at the median point of the distribution of the real-world energy economy values in their respective bins (162 Wh/km, 157 Wh/km and 153.5 Wh/km respectively). Thus, this indicates that the developed cycles represent well the distribution of energy economy values and

hence the real-world cycles in their respective bins. In the next section the properties of the developed cycles are investigated.

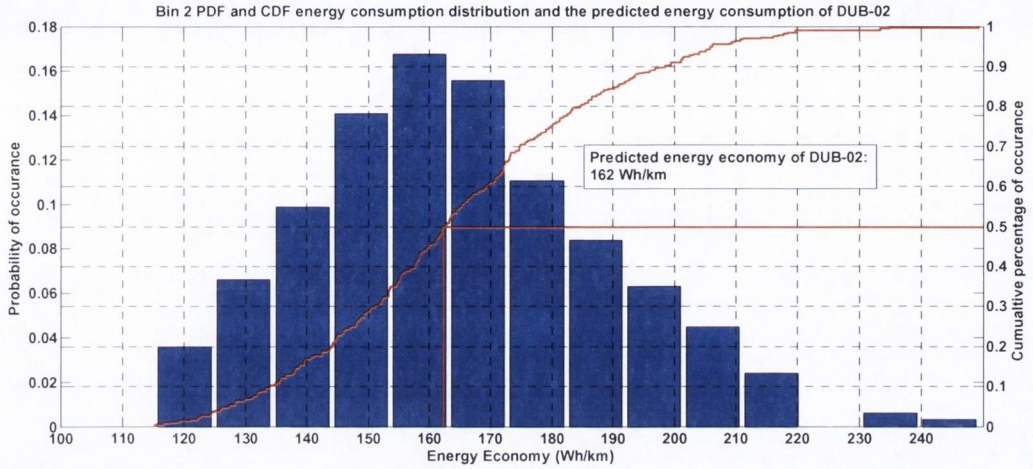

Figure 5.13. Probability distribution (blue bars) and cumulative distribution (red line) of the energy economy of the real-world driving cycles in bin 2 and the predicted energy economy of the developed driving cycle, DUB-02 for bin 2.

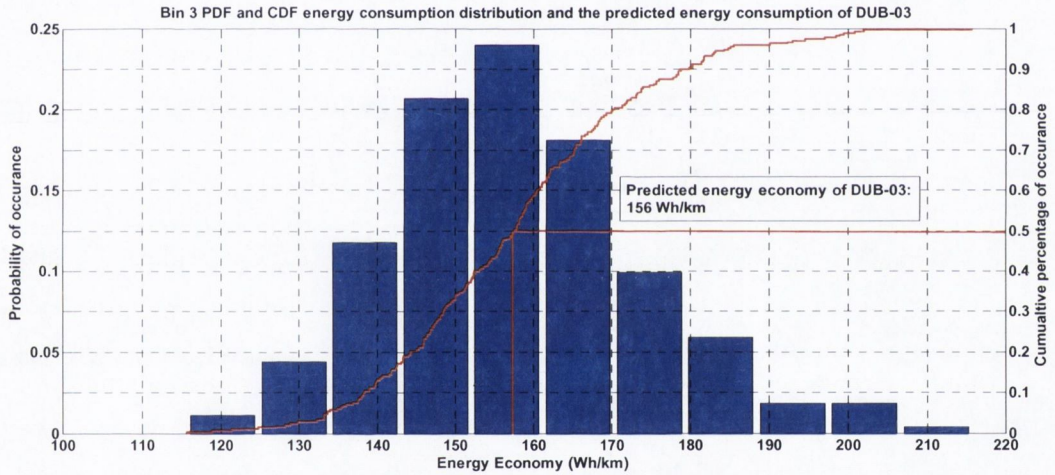

Figure 5.14. Probability distribution (blue bars) and cumulative distribution (red line) of the energy economy of the real-world driving cycles in bin 3 and the predicted energy economy of the developed driving cycle, DUB-03 for bin 3.

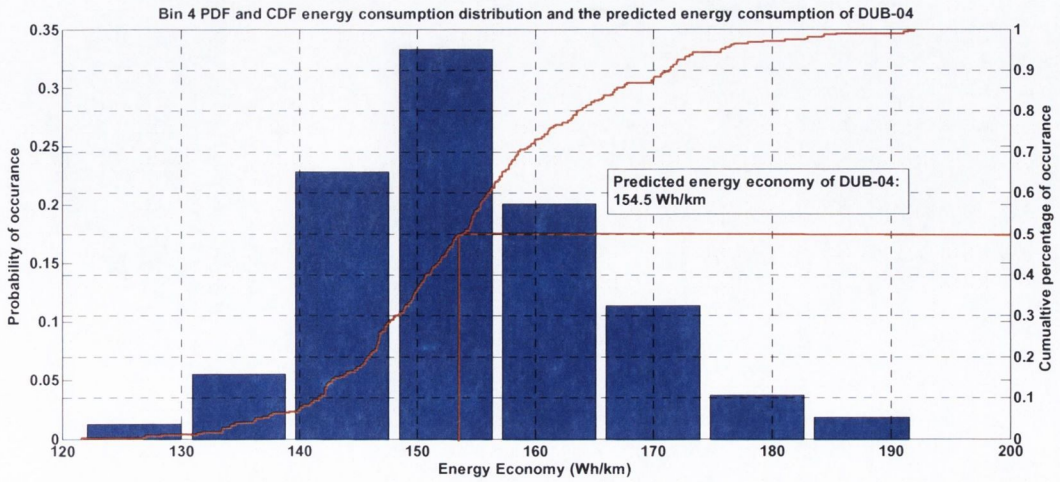

Figure 5.15. Probability distribution (blue bars) and cumulative distribution (red line) of the energy economy of the real-world driving cycles in bin 4 and the predicted energy economy of the developed driving cycle, DUB-04 for bin 4.

5.5 An analysis of the properties of the developed driving cycles

This section analyses the properties of the developed cycles. Firstly, the road-type and traffic condition composition of the developed driving cycles is presented. Secondly, the SAFD plots of the developed cycles are presented. Lastly, a comparative assessment of the trends of the statistical parameters of the developed cycles and real-world cycles with respect to distance travelled is presented.

5.5.1 The road/traffic conditions composition of the developed driving cycles

In this section the composition in terms of road-types and traffic conditions of the four developed cycles is presented. In Section 4.11 the composition in terms of road-types and traffic conditions of the real-world cycles in each of the four bins was determined. It was determined that EVs almost entirely operate in urban driving conditions.

The developed cycles were processed in the DERT tool developed in Chapter 4. This facilitated an analysis to determine if the developed cycles have a similar composition in terms of the road-types and traffic conditions compared to the real-world driving cycles in their respective bins. Figure 5.16 presents the proportion of time spent in each driving environment category for each of the developed cycles. The developed cycles consist of approximately the same proportions of driving conditions to those observed in real-world driving cycles. In each case the percentage difference in the proportions of driving environments is in the range of 2-3%. The DUB-01, DUB-02 and DUB-03 cycles represent solely urban driving conditions whereas the DUB-04 cycle consists of a small proportion of motorway driving (6%). The next section presents an analysis of the SAFDs of the four developed cycles.

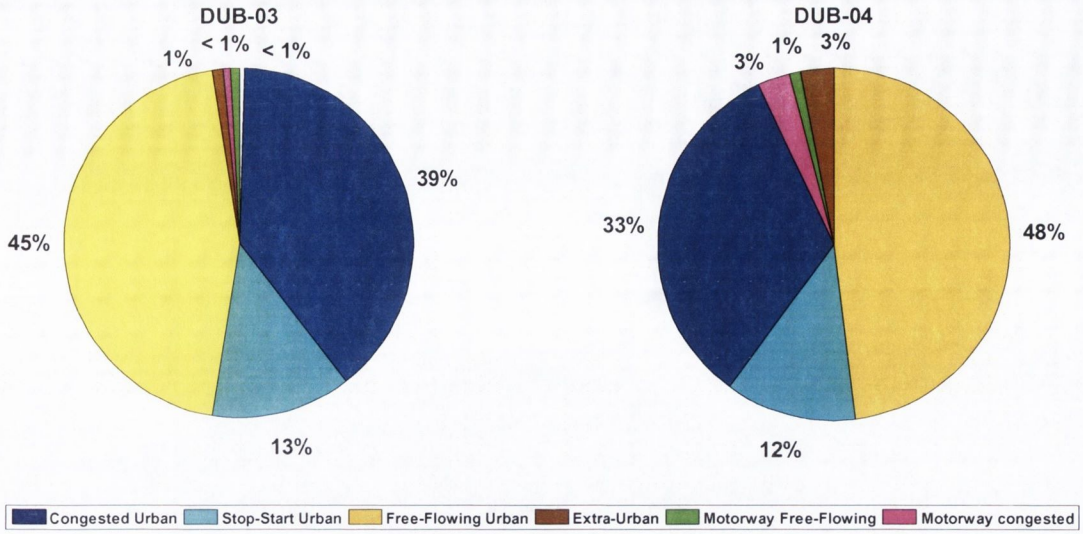

Figure 5.16. Percentage of time spent in each driving environment for each of the developed driving cycles.

5.5.2 Speed and acceleration distribution analysis of the developed driving cycles

The SAFD plots for the developed cycles are presented in Figures 5.17 – 5.20. The SAFDs express the amount of time spent in specific speed and acceleration bins. The velocity scale was partitioned into 120 bins from 0 to 120 km/hr (i.e. bins of 1 km/hr). The acceleration scale was partitioned into 80 bins from -4 to 4 m/s^2 (i.e. bins of 0.1 m/s^2). For each cycle the normalised frequency of the velocity-acceleration bin (0,0) was very large due the idle time in the cycles (i.e. velocity and acceleration are 0 km/hr and 0 m/s^2 during idle periods of the cycle). The normalised frequency of the velocity-acceleration bin (0,0) was assigned 0 in the displayed plots in order to emphasise all the other bins. An analysis of the SAFD plots of the developed cycles indicates that the driving cycles differ with respect to driving distance. For the DUB-01 cycle, the distribution pattern is concentrated in the low velocity region with a moderate acceleration range between ± 2 m/s^2. There is a dominant peak present at 7 km/hr and 0 m/s^2. The SAFD plot for the DUB-02 cycle exhibits a similar pattern to the SAFD plot of the DUB-01 cycle as the cycle distance is relatively short at 2.67 km and it has similar features to the DUB-01 cycle. It has one dominant peak present at a higher velocity of 41 km/hr and acceleration 0 m/s^2. As the cycle distance increases the distribution pattern shifts to higher velocities as illustrated in the SAFD plots for the DUB-03 and DUB-04 cycles. The DUB-04 cycle, the longest distance cycle, has dominant operating events at high velocities (between 70-80 km/hr) with a narrowed acceleration range (between -0.1 to 0.8 m/s^2), which corresponds to motorway driving. The medium cycle distance, DUB-03, has a number of dominant peaks at low and medium velocities. The next section presents a comparative assessment of the trends of the statistical parameters of the developed cycles compared to the real-world cycles with respect to the distance travelled.

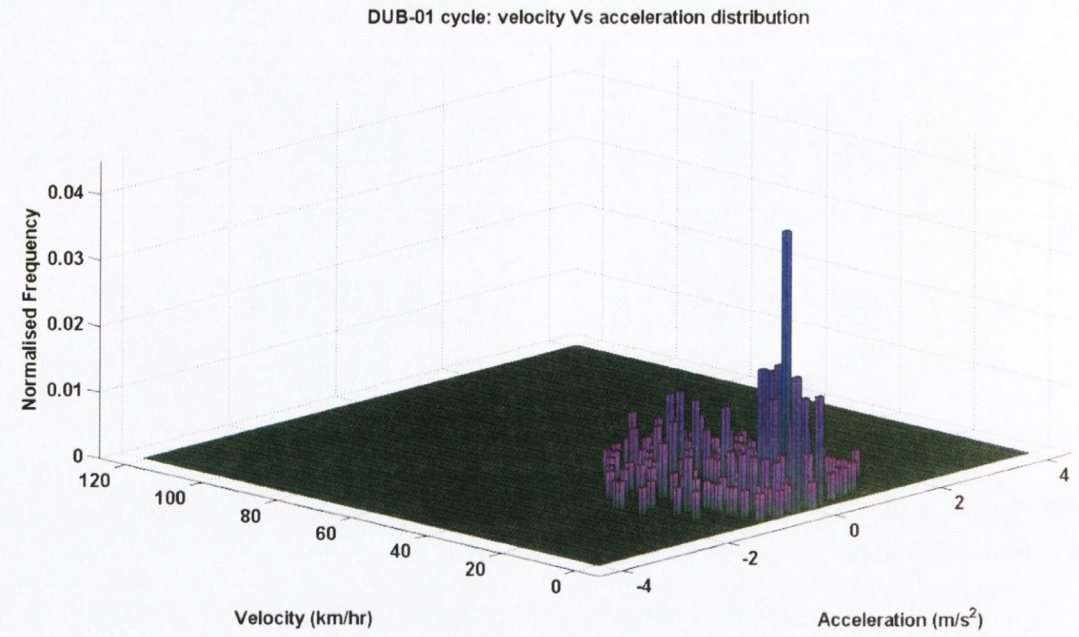

Figure 5.17. Speed vs acceleration distribution for the DUB-01 cycle.

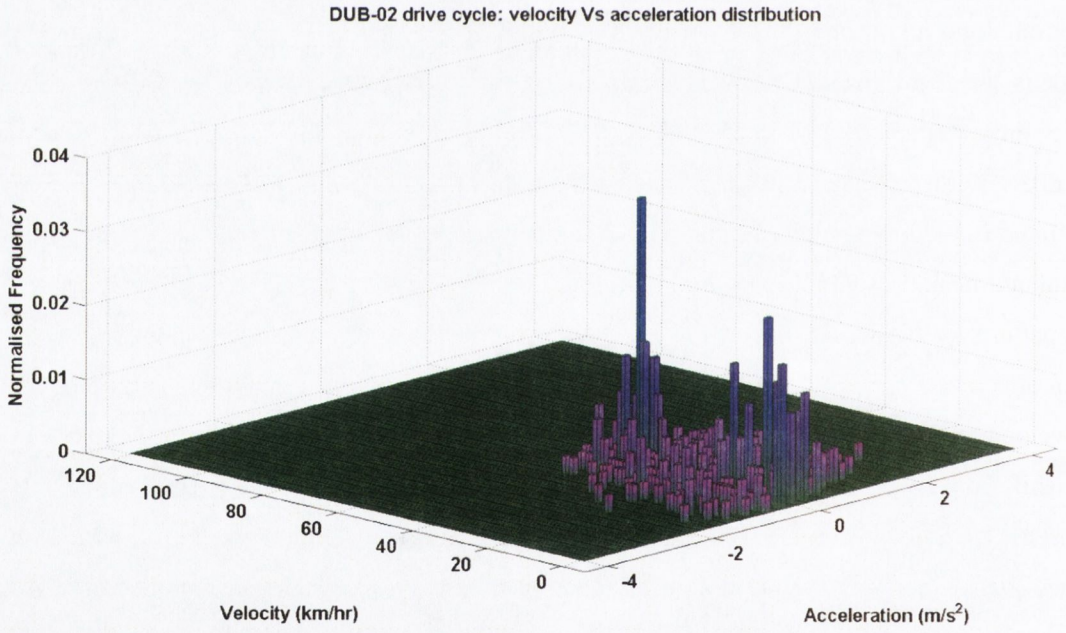

Figure 5.18. Speed vs acceleration distribution for the DUB-02 cycle.

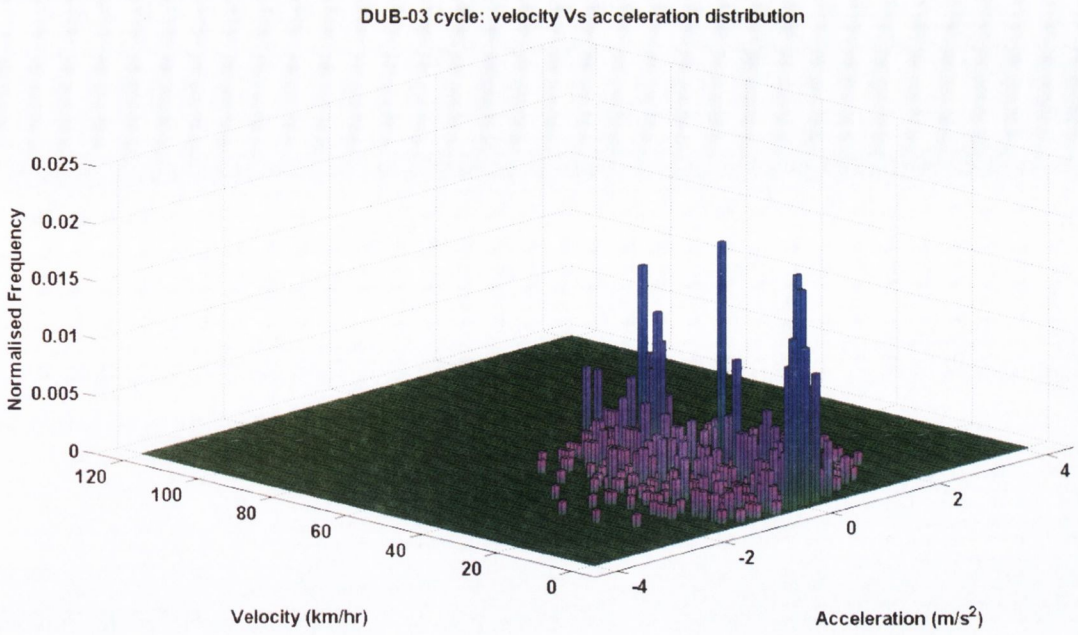

Figure 5.19. Speed vs acceleration distribution for the DUB-03 cycle.

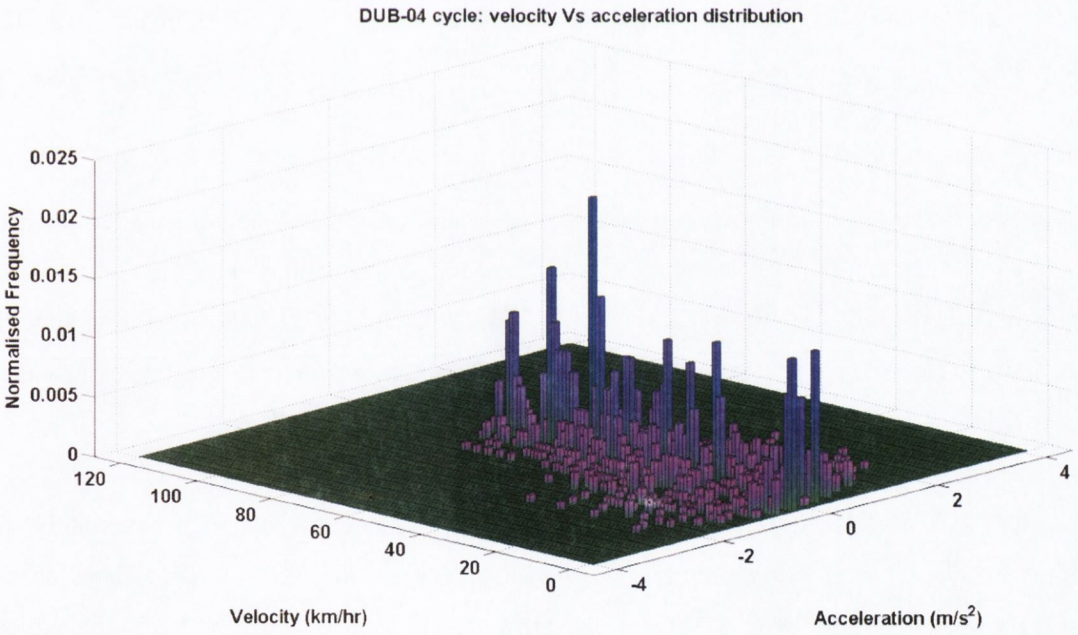

Figure 5.20. Speed vs acceleration distribution for the DUB-04 cycle.

5.5.3 A comparative assessment of the trends of the statistical parameters of the developed driving cycles to real-world driving cycles

A visual assessment and an analysis of the trends of the statistical parameters of the developed cycles compared to the real-world cycles are presented in this section. The objective was to investigate the similarity or otherwise of the trends of the statistical parameters of the developed cycles compared to real-world driving cycles with respect to driving distance. The trends of the statistical parameters of the developed cycles (right-hand side) and the real-world cycles (left-hand side) with respect to driving distance are presented in Figure 5.21. The presented parameters are 1) percentage of cruising time, 2) maximum specific power, 3) average acceleration, 4) stops per kilometre and 5) average velocity.

The trends of the developed cycles replicate well the trends of the real-world cycles. The average velocity and average acceleration for both the developed cycles and the real-world cycles have an opposite trend (Figure 5.21 (e) and (c)). The average velocity increases whereas the average acceleration decreases with respect to distance. These trends are related as acceleration is a result of a change in velocity. At shorter distances the number of stops per kilometre is higher (Figure 5.21 (d)) which indicates frequent stop-start events at low velocities. In contrast at longer distances, the number of stops per kilometre decreases which results in an increase in the average velocity and a decrease in the average acceleration. These trends are captured in the developed cycles. The average velocity and number of stops per kilometre of the DUB-01 and DUB-04 cycles are 15km/hr and 4.02 and 31 km/hr and 1.4 respectively.

As the number of stops per kilometre decreases, the percentage of cruising time of a cycle increases (Figure 5.21 (a)). The DUB-01 cycle, has the lowest percentage of cruising time,19%, whereas the DUB-04 cycle has the largest percentage of cruising time, 28%. In addition, the maximum specific power of a cycle decreases with respect to driving distance (Figure 5.21 (b)). For cycles less than 5 km the maximum specific power is large due to the short distances travelled.

The DUB-01 cycle, has the lowest maximum velocity of 49 km/hr, which is approximately the speed limit in built up areas (50 km/hr). The maximum velocity of the cycles increases as the distance increases. The maximum velocity of the DUB-04 cycle is 83 km/hr which is the typical velocity that an EV might travel at on a motorway.

The next section evaluates the representativeness of the developed cycles and a selection of existing well-established worldwide cycles of the real-world cycles in each bin and compares the developed cycles to the selection of cycles.

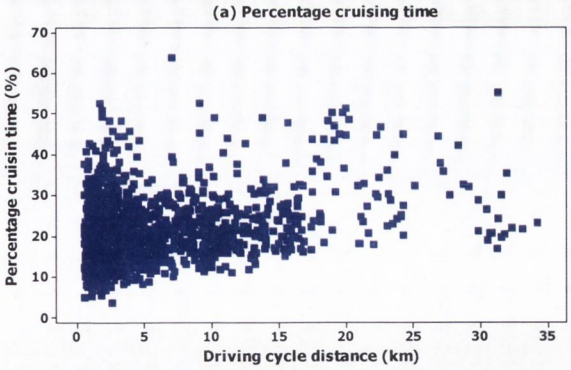
(a) Percentage cruising time
Percentage cruisin time (%)
Driving cycle distance (km)

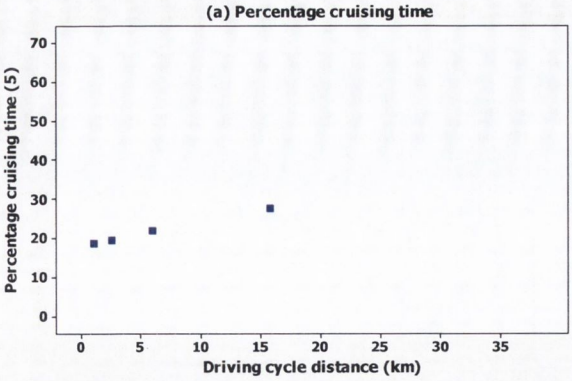
(a) Percentage cruising time
Percentage cruising time (5)
Driving cycle distance (km)

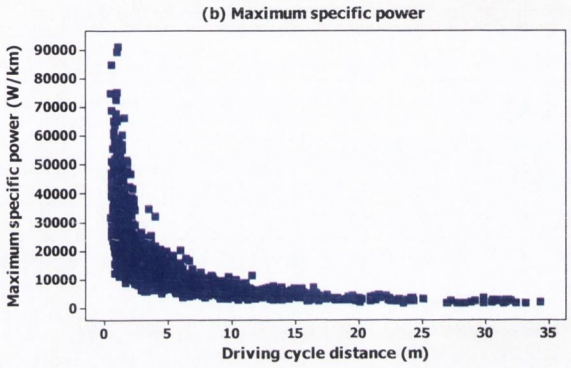
(b) Maximum specific power
Maximum specific power (W/km)
Driving cycle distance (m)

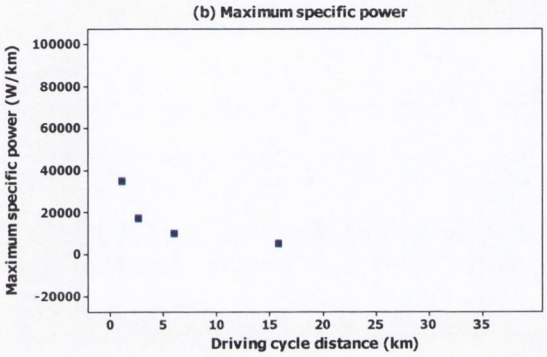
(b) Maximum specific power
Maximum specific power (W/km)
Driving cycle distance (km)

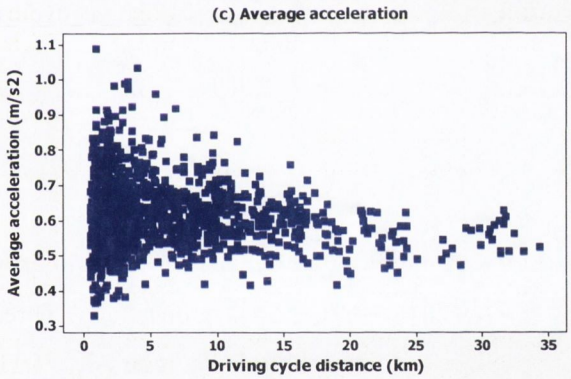
(c) Average acceleration
Average acceleration (m/s2)
Driving cycle distance (km)

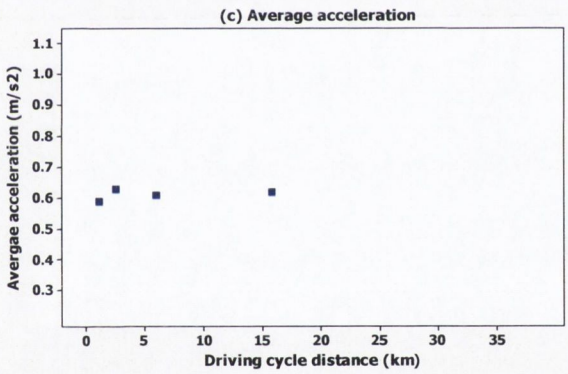
(c) Average acceleration
Avergae acceleration (m/s2)
Driving cycle distance (km)

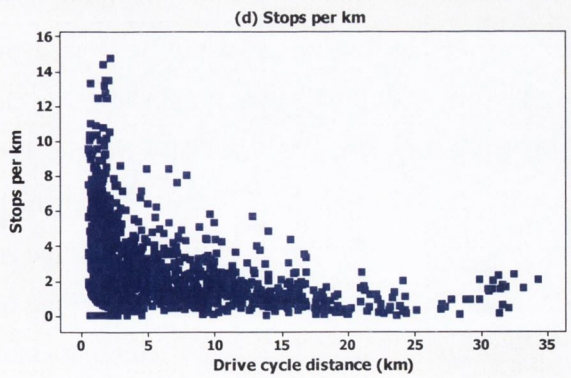
(d) Stops per km
Stops per km
Drive cycle distance (km)

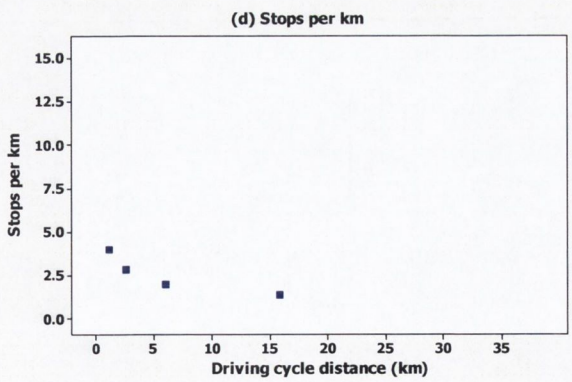
(d) Stops per km
Stops per km
Driving cycle distance (km)

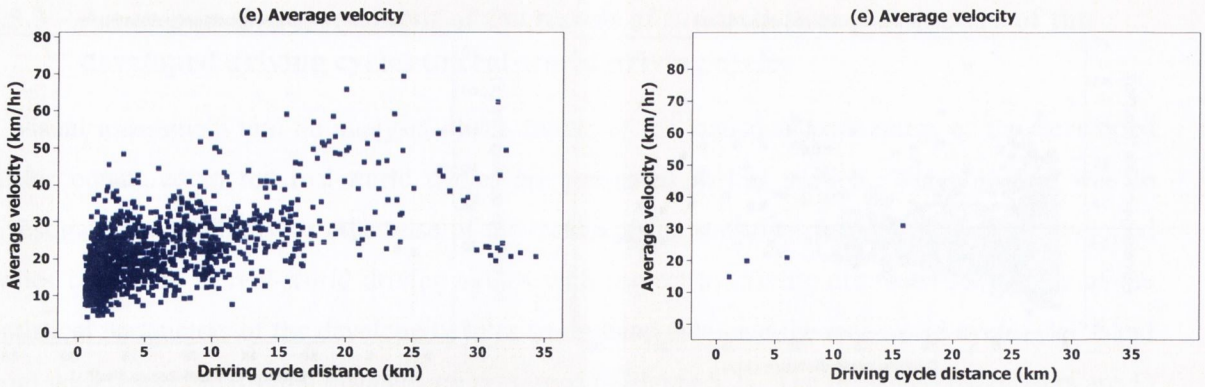

Figure 5.21. Comparison of the trends of the developed driving cycle's variables (right-hand side) to real-world driving cycles (left-hand side). Both are presented with respect to driving distance: (a) Percentage cruising time, (b) maximum specific power, (c) average acceleration, (d) stop per kilometre, and (e) average velocity.

5.6 An assessment of the representativeness of the developed driving cycles and existing worldwide driving cycles of real-world driving cycles

This section presents an assessment of the representativeness of the developed cycles and a selection of existing well-established worldwide cycles of the real-world cycles in each bin. The developed cycles are also compared to the selection of cycles. Considering the variety of cycles available, it was not straightforward to select the most relevant cycles to include in the analysis. Zaccardi and LeBerr (2012) selected eighteen worldwide legislative and non-legislative cycles, listed in Table 5.17, from Barlow et al (2009) to be used for the homologation and design of EVs. The selection was based on the assumption that an EV primarily operates in urban driving conditions.

This selection of cycles is a reasonable given that it has been determined that EVs are primarily used in urban driving conditions. Thus, thirteen of these cycles were adopted for this study. Three cycles were substituted with alternative cycles and two cycles were omitted. The class 3 WLTP cycle (dieselnet, 2013e) which was available at the time that this study was undertaken was substituted for the worldwide harmonised motorcycle emission test cycle, which was used by Zaccardi and Le Berr (2012). The FTP-75 cycle, which is an updated version of the FTP-72 cycle (United States Environmental Protection Agency, 1993), was substituted for the FTP-72 cycle. The JC08 cycle could not be sourced, therefore it was substituted with the JP 10-15 Mode cycle, which is the current legislative driving cycle in Japan (dieselnet, 2013b). The SCO3 cycle was omitted as it is used to represent the engine load and emissions associated with the use of air conditioning in ICEVs (dieselnet, 2013d). The Hyzem Rural cycle was omitted as it is used to represent rural driving conditions. An additional driving cycle, known as the Winnipeg cycle, developed by Ashtari et al (2012a) for EVs in the city of Winnipeg was included in the analysis. The 17 cycles are listed in Table 5.18. Detailed statistics relating to these cycles can be found in Barlow et al (2009). The velocity-time profiles of the cycles listed in Table 5.18 can be found in Appendix E. The velocity points of the cycles were converted to kilometres per hour if necessary and all velocity points were rounded to the nearest kilometre per hour.

Table 5.17. The driving cycles used in Zaccardi and LeBerr (2012).

Region	Driving cycles	Description
European cycles	NEDC	Composed of ECE & EUDC
	Artemis Traffic Jam	Congested urban traffic
	Artemis Urban	Urban traffic
	Artemis Road	Road conditions
French cycles	Hyzem Urban	Urban traffic
	Hyzem Rural	Rural conditions
	Eurev UL1	Congested urban traffic
	Eurev UF1	Urban traffic (moderate speed)
	Eurev UF3	Urban traffic (high speed)
	Eurev R1	Extra-urban traffic (moderate speed)
	Eurev R3	Extra-urban traffic (high speed)
	Eurev A1	Motorway traffic (moderate speed)
Japanese cycle	JC08	Urban traffic (high speed)
American cycles	UDDS	Urban traffic (high speed), aka FTP72
	SC03	Extra-urban traffic
	California Unified Cycle	Extra-urban traffic, aka UCDS & LA92
	New York City	Urban traffic (moderate speed)
Harmonised cycle	WMTC	Full version with reduced speed

Table 5.18. The driving cycles used for the comparative analysis.

Region	Driving cycles	Description	Type
European cycles	NEDC	Composed of ECE & EUDC	Modal
	Artemis Traffic Jam	Congested urban traffic	Transient
	Artemis Urban	Urban traffic	Transient
	Artemis Road	Rural road conditions	Transient
French cycles	Hyzem Urban	Urban traffic	Transient
	Eurev UL1	Congested urban traffic	Transient
	Eurev UF1	Urban traffic (moderate speed)	Transient
	Eurev UF3	Urban traffic (high speed)	Transient
	Eurev R1	Extra-urban traffic (moderate speed)	Transient
	Eurev R3	Extra-urban traffic (high speed)	Transient
	Eurev A1	Motorway traffic (moderate speed)	Transient
Japanese cycle	Japanese 10-15 Mode	Urban traffic (high speed)	Modal
U.S. cycles	FTP 75	Urban traffic (high speed)	Transient
	LA92	Extra-urban traffic	Transient
	New York City	Urban traffic	Transient
Harmonized cycle	WHTC	Class 3 cycle	Transient
Winnepeg, Canada	Winnepeg cycle	Real world EV cycle	Transient

The next section presents the methodologies used to (1) assess the representativeness of the developed cycles and the seventeen well-established worldwide cycles to the logged real-world cycles in each bin and (2) to compare the developed cycles to the seventeen worldwide cycles.

5.6.1 Methodology of the analysis

There is no consensus among researchers as to the best assessment procedure for developed cycles. Hence, two methodologies were used to compare a developed cycle and the seventeen existing cycles to the logged real-world cycles in a given bin. An additional methodology was used to compare the developed cycles to the seventeen existing worldwide cycles. However, the main objective was to identify which cycles are most representative of the logged real-world cycles in a given bin. The seventeen cycles selected for the analysis are referred to as the comparative cycles from hereafter.

The first method was based upon a comparison of the statistical parameters of the developed cycles and the comparative cycles to the mean of the statistical parameters of the real-world cycles in each bin. The comparative analysis was based upon the statistical parameters identified by the regression analysis as being statistically significant in terms of influencing the energy economy of a vehicle over a cycle. As the cycles are of varying distances, only the seven parameters that are independent

of driving distance were included in the comparative analysis. The parameters' maximum specific power, cruising time and the number of stops were excluded from the comparative analysis. A metric for comparing the overall difference between the cycles was created. The combined mean percentage difference, denoted $Diff$, between the seven parameters of a cycle and the mean of the statistical parameters of the real-world cycles in a given bin was computed according to Equation 5.7:

$$Diff = \sum_{i=1}^{N} (abs(x_i - \overline{x_i}))/N \tag{5.7}$$

where x_i is a parameter of a cycle, $\overline{x_i}$ is the mean value of that parameter in a particular bin and N is the number of parameters which is 7.

The second method analysed the difference between the SAFD of each of the cycles (both the developed and the comparative cycles) and all of the driving cycle data in a given bin. This technique has been used previously to evaluate developed cycles (Ashtari et al, 2012a, Bata R et al, 1994, Lin and Niemeier, 2002). The smaller the sum of differences between the SAFDs, the higher the commonality between the cycle in question and the logged data in a bin. $SAFD_{diff}$ represents the percentage difference between the SAFD of all the data in a particular bin and a selected cycle as defined by Equation 5.8.

$$SAFD_{diff} = \frac{\sum_i (SAFD_{cycle}(i) - SAFD_{data}(i))^2}{\sum_i SAFD_{data}(i)^2} \tag{5.8}$$

Where i is the i^{th} bin in the SAFD, $SAFD_{cycle}$ is the SAFD of a cycle, and $SAFD_{data}$ is the SAFD of all the cycles in a particular bin.

To illustrate, Figures 5.22 and 5.23 are the SAFD plots of the data in bin 4 and the DUB-04 cycle respectively. The $SAFD_{diff}$ between the DUB-04 cycle and the data in bin 4, computed according to Equation 5.7, is 4%. The significance of this $SAFD_{diff}$ value will discussed in the next section.

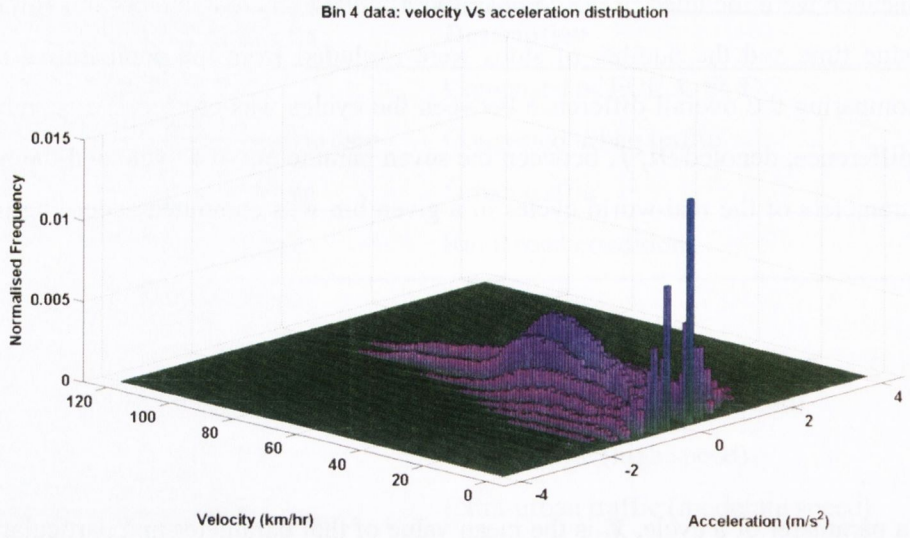

Figure 5.22. Speed vs acceleration distribution of the data in bin 4.

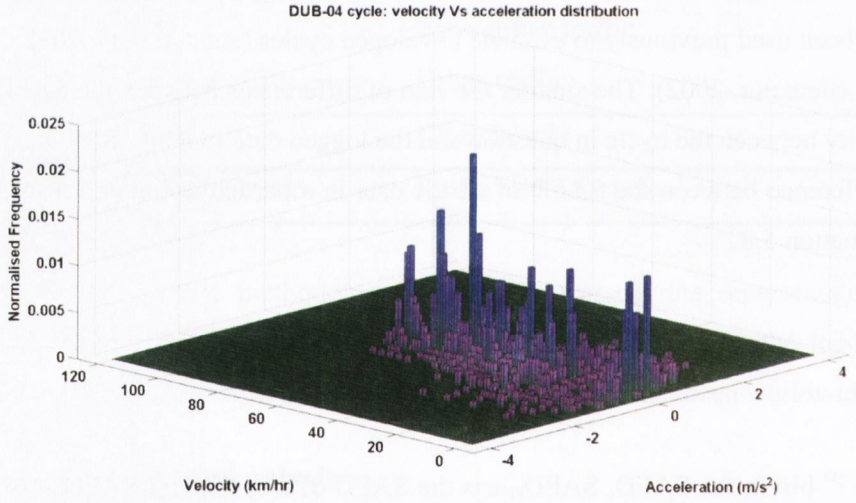

Figure 5.23. Speed vs acceleration distribution of the DUB-04 driving cycle.

When comparing the cycles (both the developed cycles and the comparative cycles) to the real-world cycles in each bin, the $Diff$ value is the primary method of assessment as it was ascertained in the regression analysis that these parameters are statistically significant in terms of influencing the energy economy of an EV over a driving cycle. Hence, it should be given more consideration than the $SAFD_{diff}$. The $SAFD_{diff}$ is a traditional method of comparing developed cycles to real-world driving cycles and as such is used to supplement the $Diff$ value. However, no direct link between the energy economy over a driving cycle and the SAFD of the cycle was established in this thesis.

A methodology, developed by Zaccardi and Le Berr (2012), was used to evaluate the similarities between the developed cycles and the comparative cycles by computing the differences between

their velocity profiles. This was a direct method, since the velocity profiles were considered in their entirety. The aim was not to quantify the links between different cycles, but simply to highlight the similarities that might be present between cycles. Since all cycles do not have the same duration, in order to apply this methodology, it was first necessary to scale the velocity profiles and to perform a linear interpolation (in steps of 0.1s) (Zaccardi and Le Berr, 2012). This was achieved by using the ECE part of the NEDC cycle as a reference. Consequently, once scaled, all the cycles had the same duration of 178 seconds. A full scale and scaled NEDC cycle are illustrated in Figure 5.24.

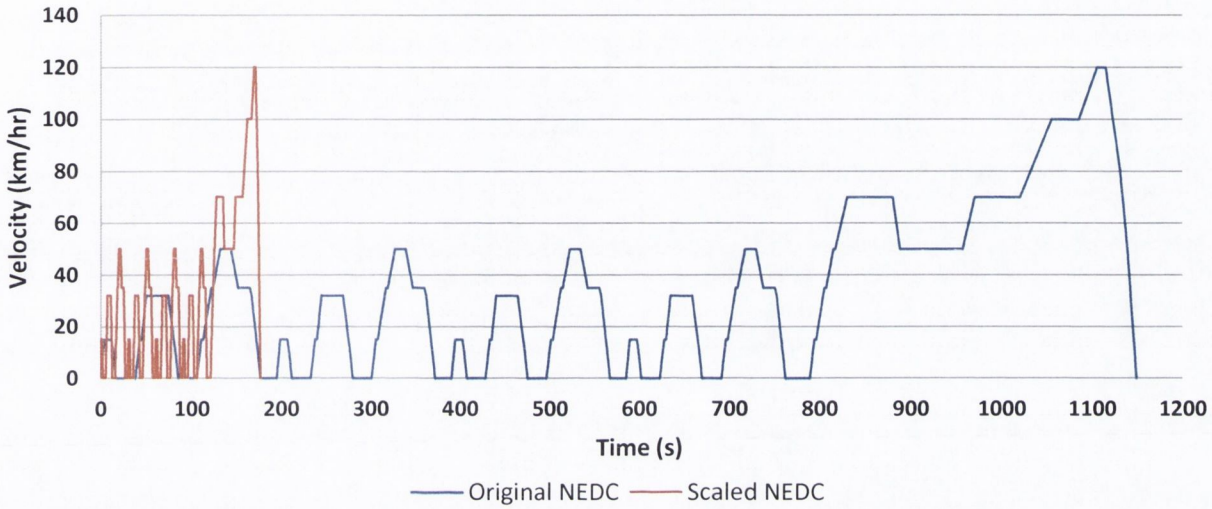

Figure 5.24. Illustration of a scaled NEDC cycle to the same length as an ECE cycle.

Subsequently, the similarity between the cycles was estimated by computing the quadratic distances (QD) between the cycles (Zaccardi and Le Berr, 2012). The distances were computed using Equation 5.9, where v_i and v_j correspond to the velocity values of cycles i and j at time t. N represents the number of samples and p the number of cycles.

$$QD_{i,j} = \sqrt{\frac{1}{N} \cdot \sum_{t=0}^{t=t_{final}} \left(v_i(t) - v_j(t)\right)^2} \quad \forall i,j \in [1,p] \tag{5.9}$$

As noted by Zaccardi and Le Berr (2012), it would not be appropriate to analyse the absolute QD values because high velocity cycles are associated with large QD values and low velocity cycles are associated with small QD values. However, this method allowed the closest neighbour of each of the developed cycles (i.e. the cycle with the smallest QD value) to be determined. Figures 5.25 and 5.26 schematically present as examples scaled DUB-04 and Artemis Road cycles, and scaled DUB-03 and NEDC cycles respectively. The yellow regions of the figures illustrate the differences between the two cycles that are being compared. The QD values for the two example comparisons presented are 11 m/s and 9.6 m/s respectively. The significance of these values is discussed in the next section.

The next section details the results of the analysis and this is followed by a discussion of the results.

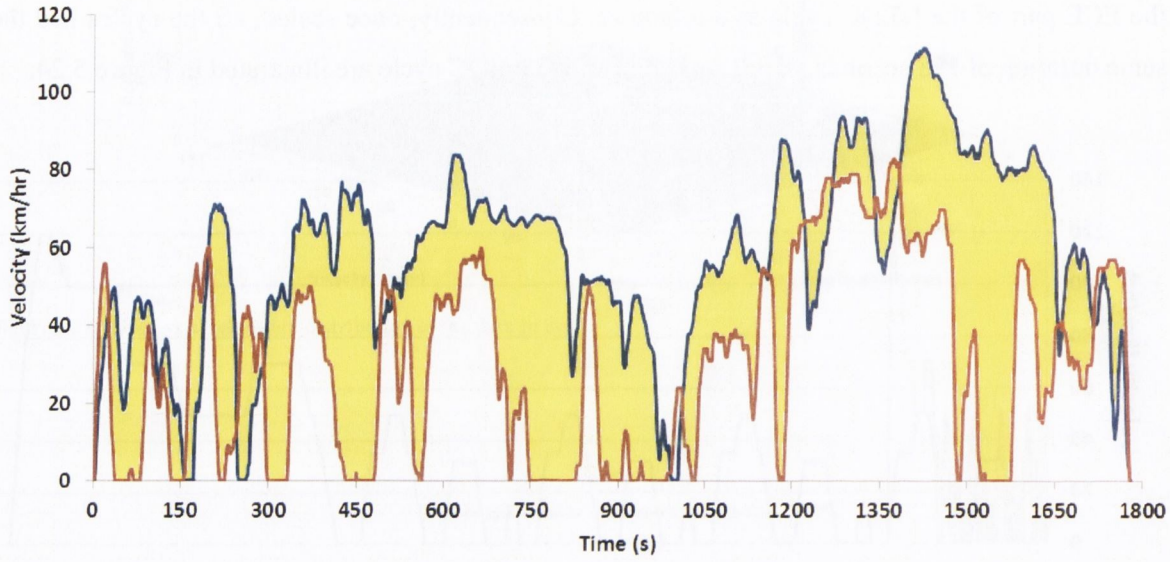

Figure 5.25. Comparison of the DUB-04 cycle and the Artemis Road cycle.

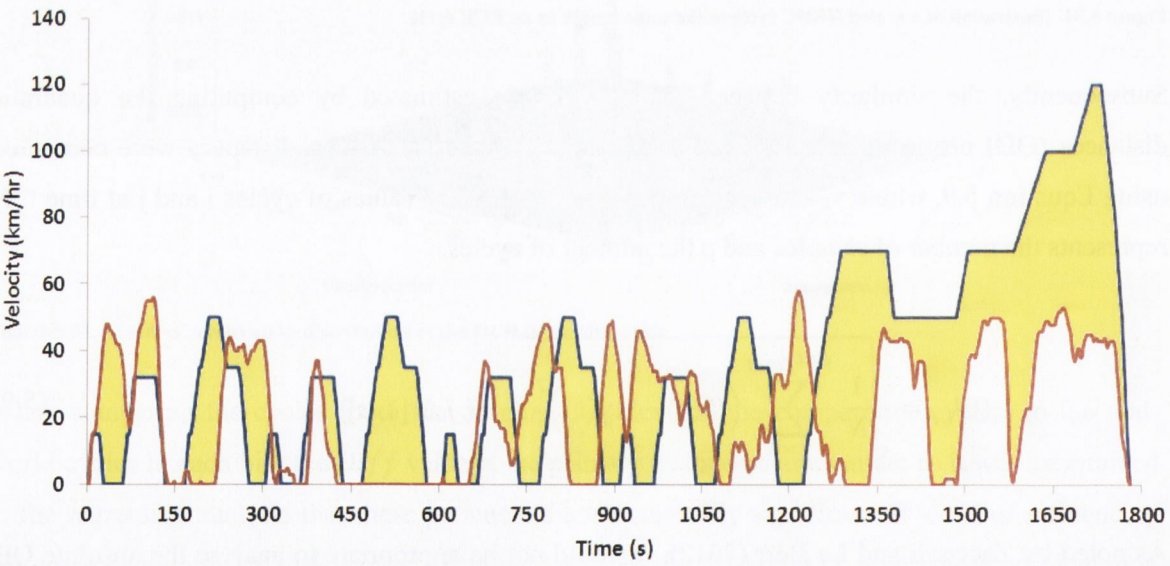

Figure 5.26. Comparison of the DUB-03 cycle and the NEDC cycle.

5.6.2 Results of the analysis

Table 5.19 compares the statistical parameters of the developed cycle DUB-01 and the seventeen comparative cycles to the mean of the statistical parameters of the real-world cycles in bin 1. The cycles are listed in order of their $Diff$ values. Table 5.20 presents the $SAFD_{diff}$ between the DUB-01 cycle and the comparative cycles to the real-world cycles in bin 1. The cycles are listed in

order of their $SAFD_{diff}$ values. In addition, Table 5.20 presents the QD values (in m/s) between the DUB-01 cycle and the comparative cycles.

Table 5.19. Statistical parameters of the cycles in bin 1, the DUB-01 cycle and the seventeen comparative cycles.

	Acc_pos	Stops_per_km	V_avg	Acc_min	Acc_max	P_idle	P_cru	Diff
Cycles in Bin 1*	0.61	4.17	15.3	-1.79	1.72	21.8	19.2	
DUB-01	0.59	4.02	14.8	-1.67	1.67	21.9	18.5	3
Hyzem Urban	0.71	1.15	23.0	-2.06	2.19	22.4	8.8	34
FTP-75	0.65	1.33	32.1	-1.67	1.67	17.7	25.3	35
Artemis Urban	0.78	4.31	18.1	-3.05	2.78	26.7	10.0	36
Eurev UF1	0.71	6.88	10.5	-2.22	2.5	30.1	11.0	38
New York City cycle	0.75	6.33	13.2	-2.78	2.78	30.0	11.4	41
Japanese 10-15	0.52	1.10	28.0	-0.83	0.81	26.4	22.8	45
Eurev UF3	0.73	1.52	25.1	-3.89	2.22	12.43	14.64	51
NEDC	0.60	1.09	34.5	-1.39	1.11	22.8	41.1	54
WHTC	0.54	0.3	46.8	-1.67	1.67	12.4	25.9	57
Artemis Traffic Jam	0.88	9.87	10.6	-2.5	2.22	40.7	7.3	61
Eurev R1	0.99	1.15	32.0	-4.17	2.78	16.6	9.5	73
LA92	0.74	0.95	40.7	-4.17	3.06	14.0	20.47	74
Winnepeg cycle	0.68	1.3	32.9	-6.39	2.78	20.3	22.1	77
Eurev R3	0.52	0.06	58.7	-2.50	2.22	7.3	29.0	83
Artemis Road	0.58	0.17	58.0	-4.17	2.5	2.24	29.45	100
Eurev A1	0.52	0.07	75.2	-3.06	3.06	1.4	36.1	119
Eurev UL1	0.64	42.12	3.9	-2.5	1.94	36.57	15.0	162

*Mean values are presented for the real-world driving cycles in bin 1

Table 5.20. The $SAFD_{diff}$ values and the QD values for the DUB-01 cycle.

	$SAFD_{diff}$	QD
Cycles in Bin 1	N/A	
DUB-01	11	N/A
Artemis Urban	5	5.3
Eurev UF1	5	5.0
New York City cycle	6	4.5
Eurev UL1	7	5.1
Hyzem Urban	9	7.1
Winnepeg cycle	13	10.8
FTP-75	17	9.1
Artemis Traffic Jam	18	6.4
Japanese 10-15 mode	21	7.3
Eurev R1	22	8.5
LA92	30	12.2
WHTC	33	13.2
Eurev UF3	36	6.6
NEDC	48	10.6
Eurev R3	59	15.0
Artemis Road	89	14.5
Eurev A1	105	18.9

The results in Table 5.19 show that the DUB-01 cycle better matches the mean of the statistical parameters of the real-world cycles in bin 1 than the comparative cycles. The combined mean percentage difference between the mean of the statistical parameters of the real-world cycles and the DUB-01 cycle is 3%. To illustrate, the mean velocity and the number of stops per kilometre of the DUB-01 cycle, 14.8 km/hr and 4.02 respectively, are close to the mean velocity and the mean number of stops per kilometre of the real-world cycles in bin 1, 15.3 km/hr and 4.17 respectively. After the DUB-01 cycle, the Hayzem Urban, the FTP-75, the Artemis Urban and the Eurev UF1 cycles are the most similar cycles in terms of matching the mean of the statistical parameters of the real-world cycles in bin 1. The combined mean percentage difference between the mean of the statistical parameters of the real-world cycles in bin 1 and these three cycles is in the range of 34-38%.

However, from Table 5.20, the $SAFD_{diff}$ between the real-world cycles in bin 1 and the DUB-01 cycle is 11%, compared to the Artemis Urban, the Eurev UF1, the New York City, the Eurev UL1 and the Hyzem Urban cycles which are all less than 11%.

According to the QD values in Table 5.20, the New York City cycle is the closest cycle in terms of its entire velocity profile to the DUB-01 cycle, with a QD value of 4.5 m/s. The small QD values in the range of 5.0-5.3 m/s for the Eurev UF1, the Eurev UL1 and the Artemis Urban cycles, indicate a similarity in terms of the entire velocity profiles of these cycles and the DUB-01 cycle. These cycles represent urban driving conditions of low to medium velocity which corresponds well with the traffic condition composition of DUB-01 cycle.

The least similar cycles in terms of matching the mean of the statistical parameters of the real-world cycles in bin 1 are the Artemis Road, the Eurev A1 and the Eurev UL1 cycles. To illustrate, the Artemis Road and the Eurev A1 cycles have large mean velocities, 58 km/hr and 75.2 km/hr respectively, compared to 15.3 km/hr, the mean velocity of the cycles in bin 1. Both cycles also have a small number of stops per kilometre, 0.17 and 0.07 respectively, compared to 4.17, the mean number of stops per kilometre of the cycles in bin 1. Correspondingly, the Artemis Road and the Eurev A1 cycles have the largest $SAFD_{diff}$ values of 89% and 105% respectively. Their QD values, 14.5 m/s and 18.9 m/s respectively, are also large, indicating that they are dissimilar in terms of their entire velocity profiles to the DUB-01 cycle. These cycles represent rural and highway driving conditions respectively.

The Eurev UL1 cycle, which represents highly congested urban driving conditions, has a low mean velocity and a large number of stops per kilometre, 3.9 km/hr and 42.12 respectively, compared to the mean velocity and the mean number of stops per kilometre, 15.3 km/hr and 4.17 respectively, of the cycles in bin 1. However, as discussed above the $SAFD_{diff}$ value for the Eurev UL1 cycle,

7%, is less than the $SAFD_{diff}$ for the DUB-01 cycle. In addition, its small QD value, 5.1 m/s, indicates that it is similar in terms of its entire velocity profile to the DUB-01 cycle.

Table 5.21 compares the statistical parameters of the developed cycle DUB-02 and the seventeen comparative cycles to the mean of the statistical parameters of the real-world cycles in bin 2. The cycles are listed in order of their $Diff$ values. Table 5.22 presents the $SAFD_{diff}$ between the DUB-02 cycle and the comparative cycles to the real-world cycles in bin 2. The cycles are listed in order of their $SAFD_{diff}$ values. In addition, Table 5.22 presents the QD values (in m/s) between the DUB-02 cycle and the comparative cycles.

Table 5.21. Statistical parameters of the cycles in bin 2, the DUB-02 cycle and the seventeen comparative cycles.

	Acc_pos	Stops_per_km	V_avg	Acc_min	Acc_max	P_idle	P_cru	Diff
Cycles in Bin 2*	0.63	3.11	19.2	-2.07	1.99	22.57	21.4	
DUB-02	0.63	2.86	19.8	-1.94	2.22	20.67	19.5	7
Hyzem Urban	0.71	1.15	23.0	-2.06	2.19	22.4	8.8	24
FTP-75	0.65	1.33	32.1	-1.67	1.67	17.7	25.3	29
Artemis Urban	0.78	4.31	18.1	-3.05	2.78	26.7	10.0	32
Japanese 10-15	0.52	1.10	28.0	-0.83	0.81	26.4	22.8	39
Eurev UF3	0.73	1.52	25.1	-3.89	2.22	12.43	14.64	39
Eurev UF1	0.71	6.88	10.5	-2.22	2.5	30.1	11.0	42
New York City	0.75	6.33	13.2	-2.78	2.78	30.0	11.4	44
NEDC	0.60	1.09	34.5	-1.39	1.11	22.8	41.1	46
WHTC	0.54	0.3	46.8	-1.67	1.67	12.4	25.9	50
Winnepeg cycle	0.68	1.3	32.9	-6.39	2.78	20.3	22.1	57
LA92	0.74	0.95	40.7	-4.17	3.06	14.0	20.47	57
Eurev R1	0.99	1.15	32.0	-4.17	2.78	16.6	9.5	59
Eurev R3	0.52	0.06	58.7	-2.50	2.22	7.3	29.0	65
Artemis Traffic	0.88	9.87	10.6	-2.5	2.22	40.7	7.3	69
Artemis Road	0.58	0.17	58.0	-4.17	2.5	2.24	29.45	80
Eurev A1	0.52	0.07	75.2	-3.06	3.06	1.4	36.1	96
Eurev UL1	0.64	42.12	3.9	-2.5	1.94	36.57	15.0	207

***Mean values are presented for the real-world driving cycles in bin 2.**

The results in Table 5.21 show that the DUB-02 cycle better matches the mean of the statistical parameters of the real-world cycles in bin 2 than the selection of worldwide cycles. The combined mean percentage difference between the mean of the statistical parameters of the real-world cycles and the DUB-02 cycle is 7%. To illustrate, the mean acceleration and the percentage of cruising time of the DUB-02 cycle, 0.63 m/s^2 and 19.5% respectively, are close to the mean acceleration and the mean percentage of cruising time of the cycles in bin 2, 0.63 m/s^2 and 21.4% respectively. Similar to that observed for the DUB-01 cycle, after the DUB-02 cycle, the Hayzem Urban, the FTP-75 and the Artemis Urban cycles are the most similar cycles in terms of matching the mean of the statistical parameters of the real-world cycles in bin 2. The combined mean percentage difference between the mean of the statistical parameters of the real-world cycles in bin 2 and these three cycles is in the range of 24-32%.

Table 5.22. The $SAFD_{diff}$ values and the QD values for the DUB-02 cycle.

	$SAFD_{diff}$	QD
Cycles in Bin 2	N/A	
DUB-02	11	N/A
Artemis Urban	4	7.1
Eurev UF1	5	6
New York City cycle	6	7.0
Hyzem Urban	8	6.5
Eurev UL1	8	6.6
Winnepeg cycle	12	9.3
FTP-75	16	10.2
Eurev R1	20	8.3
Artemis Traffic Jam	20	6.4
Japanese 10-15 mode	21	7.6
LA92	29	10.7
WHTC	32	12.3
Eurev UF3	35	7.2
NEDC	48	10.4
Eurev R3	58	13.9
Artemis Road	88	13.0
Eurev A1	105	18.4

However, similar to that observed for the DUB-01 cycle, from Table 5.22, the $SAFD_{diff}$ between the real-world cycles in bin 2 and the DUB-02 cycle is 11%, compared to the Artemis Urban, the Eurev UF1, the New York City, the Hayzem Urban and the Eurev UL1 cycles which are all less than 11%.

According to the QD values in Table 5.22, the Eurev UF1 is the closest cycle in terms of its entire velocity profile to the DUB-02 cycle, with a QD value of 6 m/s. The small QD values in the range of 6.4-6.6 m/s for the Artemis Traffic Jam, the Hyzem Urban and the Eurev UL1 cycle, indicate a similarity in terms of the entire velocity profiles of these cycles and the DUB-02 cycle. These cycles represent urban driving conditions of low to medium velocity which corresponds well with the traffic condition composition of DUB-02 cycle.

Similar to that observed for the DUB-01 cycle, the least similar cycles in terms of matching the mean of the statistical parameters of the real-world cycles in bin 2 are the Artemis Road, the Eurev A1 and the Eurev UL1 cycles. To illustrate, the Artemis Road and the Eurev A1 cycles have high mean velocities, 58 km/hr and 75.2 km/hr respectively, compared to 19.2 km/hr, the mean velocity of the cycles in bin 2. Both cycles also have a low percentage of idle time, 2.24% and 1.4% respectively, compared to 22.5%, the mean percentage of idle time of the cycles in bin 2. Correspondingly, the Artemis Road and the Eurev A1 cycles have the largest $SAFD_{diff}$ values of 88% and 105% respectively. Their QD values, 13 m/s and 18.4 m/s respectively, are also large, indicating that they are dissimilar in terms of their entire velocity profiles to the DUB-02 cycle.

The Eurev UL1 cycle has a low mean velocity of 3.9 km/hr and a large number of stops per kilometre of 42.12 compared to the mean velocity and the mean number of stops per kilometre, 15.3 km/hr and 4.17 respectively, of the cycles in bin 2. However, as discussed above the $SAFD_{diff}$ value for the Eurev UL1 cycle, 8%, is less than the $SAFD_{diff}$ for the DUB-02 cycle. In addition its small QD value, 6.6 m/s, indicates that it is similar in terms of its entire velocity profile to the DUB-02 cycle.

Table 5.23 compares the statistical parameters of the developed cycle DUB-03 and the seventeen comparative cycles to the mean of the statistical parameters of the real-world cycles in bin 3. The cycles are listed in order of their *Diff* values. Table 5.24 presents the $SAFD_{diff}$ between the DUB-03 cycle and the comparative cycles to the real-world cycles in bin 3. The cycles are listed in order of their $SAFD_{diff}$ values. In addition, Table 5.24 presents the QD values (in m/s) between the DUB-03 cycle and the comparative cycles.

Table 5.23. Statistical parameters of the cycles in bin 3, the DUB-03 cycle and the seventeen comparative cycles.

	Acc_pos	Stops_per_k	V_avg	Acc_min	Acc_max	P_idle	P_cru	Diff
Cycles in Bin 3*	0.62	2.17	22.6	-2.39	2.19	22.9	21.4	
DUB-03	0.65	2.2	21.7	-2.5	2.22	23.6	21.4	3
Hyzem Urban	0.71	1.15	23.0	-2.06	2.19	22.4	8.8	20
FTP-75	0.65	1.33	32.1	-1.67	1.67	17.7	25.3	26
Eurev UF3	0.73	1.52	25.1	-3.89	2.22	12.43	14.64	29
Japanese 10-15 mode	0.52	1.10	28.0	-0.83	0.81	26.4	22.8	34
Artemis Urban	0.78	4.31	18.1	-3.05	2.78	26.7	10.0	38
NEDC	0.60	1.09	34.5	-1.39	1.11	22.8	41.1	41
Winnepeg cycle	0.68	1.3	32.9	-6.39	2.78	20.3	22.1	44
LA92	0.74	0.95	40.7	-4.17	3.06	14.0	20.47	45
WHTC	0.54	0.3	46.8	-1.67	1.67	12.4	25.9	47
Eurev R1	0.99	1.15	32.0	-4.17	2.78	16.6	9.5	48
New York City cycle	0.75	6.33	13.2	-2.78	2.78	30.0	11.4	54
Eurev R3	0.52	0.06	58.7	-2.50	2.22	7.3	29.0	55
Eurev UF1	0.71	6.88	10.5	-2.22	2.5	30.1	11.0	55
Artemis Road	0.58	0.17	58.0	-4.17	2.5	2.24	29.45	67
Eurev A1	0.52	0.07	75.2	-3.06	3.06	1.4	36.1	82
Artemis Traffic Jam	0.88	9.87	10.6	-2.5	2.22	40.7	7.3	86
Eurev UL1	0.64	42.12	3.9	-2.5	1.94	36.57	15.0	290

***Mean values are presented for the real-world driving cycles in bin 3.**

The results in Table 5.23 show that the DUB-03 cycle better matches the mean of the statistical parameters of the real-world cycles in bin 3 than the selection of worldwide cycles. The combined mean percentage difference between the mean of statistical parameters of the real-world cycles in bin 3 and the DUB-03 cycle is 3%. To illustrate, the maximum acceleration and the mean velocity of the DUB-03 cycle, 2.22 m/s^2 and 21.7 km/hr respectively, are close to the maximum acceleration and the mean velocity of the cycles in bin 3, 2.19 m/s^2 and 22.6 km/hr respectively. After the DUB-03 cycle, the Hayzem Urban, the FTP-75 and the Eurev UF3 cycles are the most

similar cycles in terms of matching the mean of the statistical parameters of the real-world cycles in bin 3. The combined mean percentage difference between the mean of statistical parameters of the real-world cycles and these three cycles is in the range of 20-29%.

Table 5.24. The SAFDdiff values and the QD values for the DUB-03 cycle.

	SAFD	QD
Cycles in Bin 3	N/A	
DUB-03	4	N/A
Artemis Urban	4	7.6
Eurev UF1	6	6.9
Hyzem Urban	6	7.3
Winnepeg cycle	9	9.9
New York City cycle	9	7.3
Eurev UL1	12	7.2
FTP-75	13	8.8
Eurev R1	18	7.2
Japanese 10-15 mode	23	7.0
LA92	26	12.7
Artemis Traffic Jam	29	6.6
WHTC	29	11.8
Eurev UF3	32	8.0
NEDC	52	9.6
Eurev R3	56	14.6
Artemis Road	88	13.4
Eurev A1	107	18.2

In contrast to the DUB-01 and DUB-02 cycles, the $SAFD_{diff}$ between the real-world cycles in bin 3 and the DUB-03 cycle is 4%, which is the smallest value along with the Artemis Urban cycle. The Eurev UF1, the Hyzem Urban, the Winnepeg and the New York City cycles are the next closest cycles in terms of minimising the $SAFD_{diff}$, with values in the range of 6-9%.

According to the QD values in Table 5.24, the Artemis Traffic Jam cycle is the closest cycle in terms of its entire velocity profile to the DUB-03 cycle, with a QD value of 6.6 m/s. The small QD values in the range of 6.9-7.3 m/s for the Eurev UF1, the Japanese 10-15 mode, the Eurev R1, the Eurev UL1, the New York City and the Hyzem Urban, indicate a similarity in terms of the entire velocity profiles of these cycles and the DUB-03 cycle. These cycles represent congested urban traffic to moderate speed urban driving conditions which corresponds well with the traffic condition composition of DUB-03 cycle.

The least similar cycles in terms of matching the mean of the statistical parameters of the cycles in bin 3 are the Eurev A1, the Artemis Traffic Jam and the Eurev UL1 cycles. To illustrate, the Eurev A1 has a high mean velocity, 75.2 km/hr compared to 22.6 km/hr, the mean velocity of the cycles in bin 3. This cycle also has a small number of stops per kilometre, 0.07 compared to 2.17,

the mean number of stops per kilometre of the cycles in bin 3. Similarly, the mean velocity and number of stops per kilometre of the Artemis Traffic Jam and the Eurev UL1 cycles, 10.6 km/hr and 9.87 respectively and 3.9 km/hr and 42.12 respectively, are dissimilar to the mean velocity and number of stops per kilometre of the cycles in bin 3.

However, only the Eurev A1 cycle has a very large $SAFD_{diff}$ value of 107%. Its QD value, 18.2 m/s, is also large, indicating that it is also dissimilar in terms of its entire velocity profile to the DUB-03 cycle. The $SAFD_{diff}$ values of the Artemis Traffic Jam and the Eurev UL1 cycles are 29% and 12% respectively, which are only moderately large.

Table 5.25 compares the statistical parameters of the developed cycle DUB-04 and the seventeen comparative cycles to the mean of the statistical parameters of the real-world cycles in bin 4. The cycles are listed in order of their $Diff$ values. Table 5.26 presents the $SAFD_{diff}$ between the DUB-04 cycle and the comparative cycles to the real-world cycles in bin 4. The cycles are listed in order of their $SAFD_{diff}$ values. In addition, Table 5.26 presents the QD values (in m/s) between the DUB-04 cycle and the comparative cycles.

Table 5.25. Statistical parameters of the cycles in bin 4, the DUB-04 cycle and the seventeen comparative cycles.

	Acc_pos	Stops_per_km	V_avg	Acc_min	Acc_max	P_idle	P_cru	Diff
Cycles in Bin 4*	0.59	1.4	30.6	-2.56	2.3	19.64	26.0	
DUB-04	0.62	1.42	30.87	-2.5	2.22	20.67	27.6	4
FTP-75	0.65	1.33	32.1	-1.67	1.67	17.7	25.3	14
Hyzem Urban	0.71	1.15	23.0	-2.06	2.19	22.4	8.8	24
Eurev UF3	0.73	1.52	25.1	-3.89	2.22	12.43	14.64	27
NEDC	0.60	1.09	34.5	-1.39	1.11	22.8	41.1	30
Winnepeg cycle	0.68	1.3	32.9	-6.39	2.78	20.3	22.1	31
Japanese 10-15	0.52	1.10	28.0	-0.83	0.81	26.4	22.8	32
WHTC	0.54	0.3	46.8	-1.67	1.67	12.4	25.9	34
LA92	0.74	0.95	40.7	-4.17	3.06	14.0	20.47	34
Eurev R1	0.99	1.15	32.0	-4.17	2.78	16.6	9.5	36
Eurev R3	0.52	0.06	58.7	-2.50	2.22	7.3	29.0	40
Artemis Road	0.58	0.17	58.0	-4.17	2.5	2.24	29.45	50
Artemis Urban	0.78	4.31	18.1	-3.05	2.78	26.7	10.0	60
Eurev A1	0.52	0.07	75.2	-3.06	3.06	1.4	36.1	62
New York City	0.75	6.33	13.2	-2.78	2.78	30.0	11.4	82
Eurev UF1	0.71	6.88	10.5	-2.22	2.5	30.1	11.0	87
Artemis Traffic	0.88	9.87	10.6	-2.5	2.22	40.7	7.3	129
Eurev UL1	0.64	42.12	3.9	-2.5	1.94	36.57	15.0	450

***Mean values are presented for the real-world driving cycles in bin 4.**

The results in Table 5.25 show that the DUB-04 cycle better matches the mean of the statistical parameters of the real-world cycles in bin 4 than the selection of worldwide cycles. The combined mean percentage difference between the mean of statistical parameters of the real-world cycles and the DUB-04 cycle is 4%. To illustrate, the mean velocity and the number of stops per kilometre of

the DUB-04 cycle, 30.87 km/hr and 1.42 respectively, are close to the mean velocity and the mean number of stops per kilometre of the cycles in bin 4, 30.6 km/hr and 1.4 respectively. After the DUB-04 cycle, the FTP-75, the Hyzem Urban and the Eurev UF3 are the most similar cycles in terms of matching the mean of the statistical parameters of the real-world cycles in bin 4. The combined mean percentage difference between the mean of the statistical parameters of the real-world cycles and these three cycles is in the range of 14-27%.

Table 5.26. The SAFDdiff values and the QD values for the DUB-04 cycle.

	$SAFD_{dif}$	QD
Cycles in Bin 4	N/A	
DUB-04	4	N/A
Winnepeg cycle	4	8.5
Artemis Urban	6	9.0
Hyzem Urban	6	9.6
FTP-75	8	10.2
Eurev R1	12	10.1
Eurev UF1	16	9.5
LA92	19	11.5
New York City cycle	22	9.1
WHTC	22	11.9
Eurev UF3	26	8.6
Eurev UL1	28	10.4
Japanese 10-15 mode	33	10.8
Eurev R3	51	11.4
Artemis Traffic Jam	57	9.6
NEDC	66	9.4
Artemis Road	85	11.0
Eurev A1	110	16.0

Similar to that observed for the DUB-03 cycle, the $SAFD_{diff}$ between the real-world cycles in bin 4 and the DUB-04 cycle is 4%, which is the smallest value along with the Winnipeg cycle. The Artemis Urban, the Hyzem Urban and the FTP-75 cycles are the next closest cycles in terms of minimising the $SAFD_{diff}$, with values in the range of 6-8%.

According to the QD values in Table 5.26, the Winnipeg cycle is the closest cycle in terms of its entire velocity profile to the DUB-04 cycle, with a QD value of 8.5 m/s. The small QD values in the range of 8.6-9.1 m/s for the Eurev UF3, the Artemis Urban and the New York City cycles indicate a similarity in terms of the entire velocity profiles of these cycles and the DUB-04 cycle. These cycles represent low speed urban to high speed urban driving conditions which corresponds well with the traffic condition composition of DUB-04 cycle.

The least similar cycles in terms of matching the mean of the statistical parameters of the cycles in bin 4 are the Eurev UF1, the Artemis Traffic Jam, and the Eurev UL1 cycles. To illustrate, the Eurev UF1 cycle has a mean velocity of 10.5 km/hr compared to 30.6 km/hr, the mean velocity of the cycles in bin 4. The cycle also has a large number of stops per kilometre, 6.88 compared to 1.4, the mean number of stops per kilometre of the cycles in bin 4. Similarly, the mean velocity and number of stops per kilometre of the Eurev UL1 and the Artemis Traffic Jam cycles, 3.9 km/hr and 42.12 respectively and 10.6 km/hr and 9.87 respectively, are dissimilar to the mean velocity and mean number of stops per kilometre of the cycles in bin 4.

However, only the Artemis Traffic Jam cycle has a large $SAFD_{diff}$ value of 57%. Its QD value, 18.2 m/s, is also large, indicating that it is also dissimilar in terms of its entire velocity profile to the DUB-04 cycle. The $SAFD_{diff}$ values of the Eurev UF1 and the Eurev UL1 cycles are 16% and 28% respectively, which are only moderately large.

5.6.3 Comparative analysis discussion

The analysis used two comparative metrics to compare the developed cycles and the seventeen cycles selected for the comparative analysis to the logged real-world cycles in each bin. The metrics were (1) the combined mean percentage difference between seven parameters of each cycle and the mean of the seven parameters of the real-world cycles in each bin and (2) the percentage difference between the SAFD of the cycles (both the developed cycles and the comparative cycles) and the data in each bin.

The DUB-03 and DUB-04 cycles were shown to outperform the comparative cycles, with respect to both of the comparative metrics, in terms of representing the real-world cycles in their respective bins. However, the DUB-01 and the DUB-02 cycles were only shown to outperform the comparative cycles with respective to the mean percentage difference between the seven parameters of the cycles and the real-world cycles in their respective bins. The five cycles, the Artemis Urban, the Eurev UF1, the New York City, the Hyzem Urban and the Eurev UL1 cycles performed better than the DUB-01 and the DUB-02 cycles in terms of minimising the $SAFD_{diff}$ between the data in the respective bins. The QD values of these five cycles indicate that they are the closest cycles in terms of their entire velocity profiles to the DUB-01 and the DUB-02 cycles. As an SAFD is a probability distribution of the velocity and acceleration points of a cycle, the DUB-01 and the DUB-02 cycles could be too short, 1.2 km and 2.67 km respectively, to adequately compare the SAFDs of the these cycles to the SAFD of the data in their respective bins.

The legislative driving cycles are undoubtedly the most important point of reference for the comparison of the results. In this section the comparisons between the developed cycles and the legislative cycles, the NEDC, the FTP-75, the Japanese 10-15 Mode cycle and the WHTC cycle are

discussed. The velocity-time profiles of the cycles are shown in Figure 5.27. The statistical parameters discussed in this section were identified by the regression analysis as being statistically significant in terms of influencing the energy economy of a vehicle over a cycle.

The mean acceleration of the developed driving cycles DUB-01, DUB-02, DUB-03 and DUB-04 are 0.59 m/s^2, 0.63 m/s^2, 0.65 m/s^2 and 0.62 m/s^2 respectively. The average acceleration of the NEDC cycle, 0.60 m/s^2, is less than the average acceleration of the developed cycles with the exception of the DUB-01 cycle. The average acceleration of the Japanese 10-15 Mode and the WHTC cycles, 0.52 m/s^2 and 0.54 m/s^2 respectively, are lower than the mean acceleration of the NEDC cycle. The average acceleration of the FTP-75 cycle, 0.65 m/s^2, is similar to the mean acceleration of the DUB-02, DUB-03 and DUB-04 cycles. The average acceleration of a cycle was shown to be correlated to the degree of 0.64 with energy economy in the regression analysis.

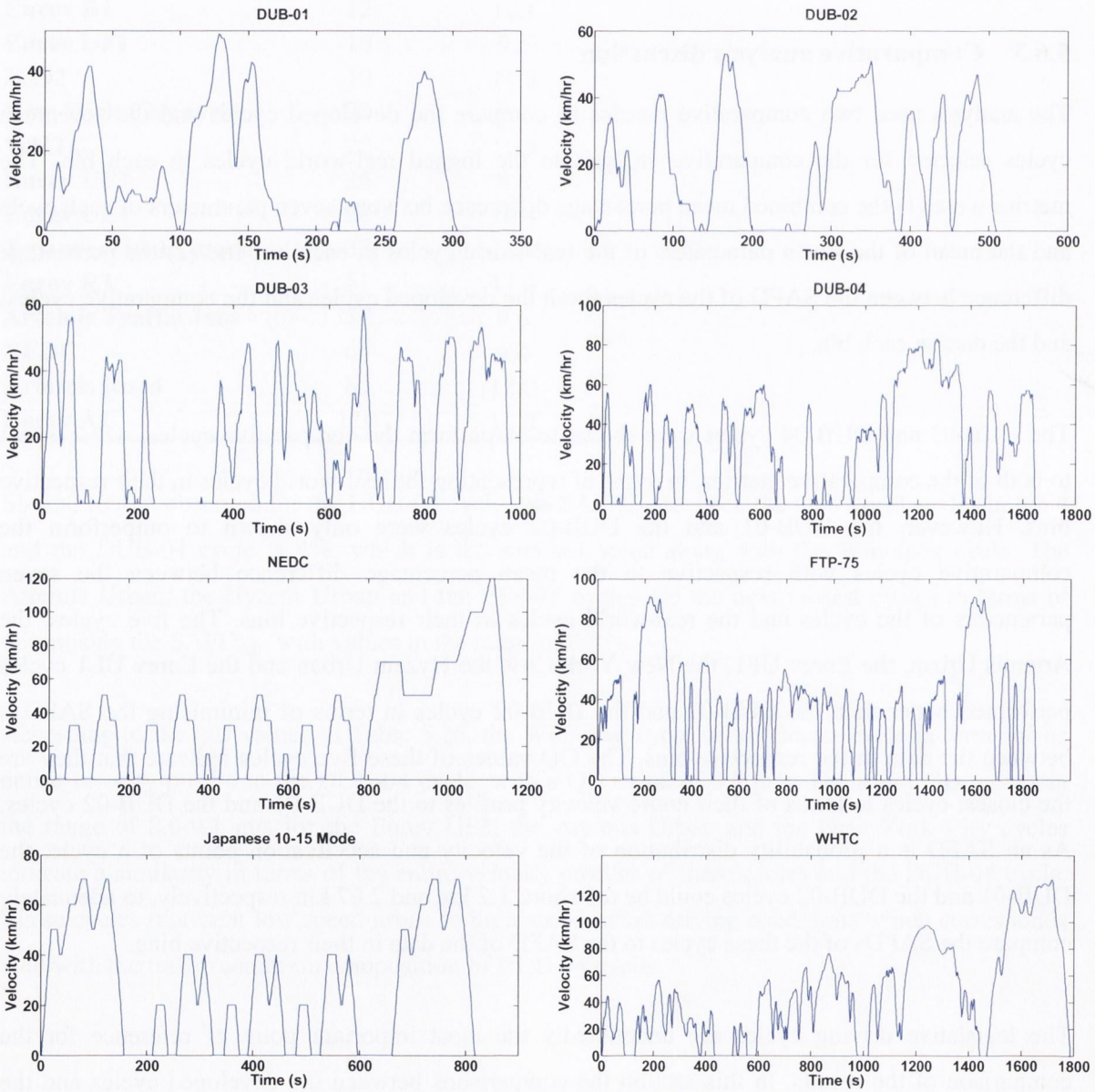

Figure 5.27. Driving cycles: DUB-01, DUB-02, DUB-03, DUB-04, NEDC, FTP-75 , Japanese 10-15 Mode cycle and the WHTC.

The number of stops per kilometre of the developed cycles DUB-01, DUB-02, DUB-03 and DUB-04 are 4.02, 2.86, 2.03 and 1.42 respectively. The number of stops per kilometre of the NEDC cycle, 1.09, is less than the number of stops per kilometre of all the developed cycles. The number of stops per kilometre of the FTP-75, the Japanese 10-15 Mode and the WHTC cycles, 1.33, 1.1 and 0.3 respectively, are also less than the number of stops per kilometre observed in the developed cycles. The number of stops per kilometre of a cycle was shown to be correlated to the degree of 0.56 with energy economy in the regression analysis.

The average velocity of the developed cycles DUB-01, DUB-02, DUB-03 and DUB-04 are 14.8 km/hr, 19.8 km/hr, 21.7 km/hr and 30.8 km/hr respectively. The average velocity of the NEDC cycle, 34.5 km/hr, is greater than the average velocity of all the developed cycles. The average velocity of the FTP-75 and the WHTC cycles, 32.1 km/hr and 46.8 km/hr respectively are also greater than the average velocity of the developed cycles. The average velocity of the Japanese 10-15 Mode cycle is smaller at 28 km/hr. The average velocity of a cycle was shown to be correlated to the degree of 0.36 with energy economy in the regression analysis.

The percentage of cruising time of the developed cycles DUB-01, DUB-02, DUB-03 and DUB-04 are 18.5 %, 19.5 %, 21.4 % and 27.6 % respectively. The percentage of cruising time of the NEDC cycle, 41.1 %, is significantly greater than percentage of cruising time of all of the developed cycles. The percentage of cruising time of the FTP-75 and the WHTC cycles, 25.3 % and 25.9%, respectively are greater than the percentage of cruising time of the shorter cycles, DUB-01 and DUB-02, but relatively similar to the longer cycles, DUB-03 and DUB-04. The percentage of cruising time of the Japanese 10-15 Mode cycle is 22.8 %, which is similar to the percentage of cruising time of the DUB-03 cycle. The percentage cruising time of a cycle was shown to be correlated to the degree of 0.64 with energy economy in the regression analysis.

The percentage of idle time of the developed cycles DUB-01, DUB-02, DUB-03 and DUB-04 are 21.8 %, 20.7 %, 23.5 % and 20.67 % respectively. The percentage of idle time of the developed cycles are similar to the percentage of idle time of the NEDC cycle, 22.8%, within ±2%. The percentage of idle time of the FTP-75 and the Japanese 10-15 Mode cycles are slightly lower and higher respectively, at 17.7% and 26.4% respectively. The percentage of idle time of the WHTC cycle is considerably less at 12.4%. The percentage of idle time of a cycle was shown to be correlated to the degree of 0.48 with energy economy in the regression analysis.

The maximum and minimum acceleration of the developed cycles are greater than the maximum and minimum acceleration of the NEDC and the Japanese 10-15 mode cycles in almost all cases. The maximum and minimum acceleration of the NEDC cycle are 1.11 m/s^2 and -1.39 m/s^2 respectively, whereas the maximum and minimum acceleration of the developed cycles are greater

than 2 m/s^2 and -2 m/s^2 with the exception of the DUB-01 cycle which has a maximum and minimum acceleration of 1.67 m/s^2 and -1.67 m/s^2 respectively. The maximum and minimum acceleration of the WHTC cycle, 1.67 m/s^2 and -1.67 m/s^2 respectively, matches the statistics of the DUB-01 cycle but are less than the maximum and minimum acceleration values of the DUB-02, DUB-03 and DUB-04 cycles. The maximum and minimum acceleration of a cycle are less correlated than other variables with energy economy, to the degree of 0.23 and 0.21 respectively.

The differences between the developed cycles and the existing legislative cycles could be attributed to the fact that the data were collected by an EV. An electric motor can provide maximum torque to the wheels immediately and can preserve this until the vehicle reaches the speed of maximum power. In contrast an ICEV must work up to the maximum torque through gear shifts. In addition, it was shown in Section 4.11 that EVs primarily operate in urban areas where the speed limits are typically in the range of 50 km/hr to 80 km/hr. The two characteristics of large average accelerations and low average velocities which are present in the data could be attributed to these facts.

In conclusion, the developed cycles better emulate real-world driving conditions in the GDA than the legislative cycles considered in this analysis. This implies that these cycles may be more suitable for the homologation of EVs or for design purposes for real-world applications in the GDA.

5.7 Summary and conclusions

This chapter extended the content presented in Chapter 4 and developed four driving cycles for the Greater Dublin Area (GDA). In Chapter 4, the real-world driving cycles were binned into 4 categories, each having an equal probability on the journey distance cumulative distribution function (cdf) curve. In this chapter a single driving cycle was developed to represent the real-world driving cycles in each bin. The median point in each bin on the journey distance cdf curve was selected as a representative driving cycle distance for that bin. A Markov chain model for generating driving cycles and that ensures that a generated cycle sufficiently represents the real-world cycles in a given bin was developed. Firstly, transition probability matrices (TPM) were extracted from each bin for a discrete time Markov chain with states of velocity and acceleration. The Markov chain was used to synthesise candidate driving cycles for a given bin. As Markov chains are a stochastic process, there are no prior guarantees that a synthesised driving cycle would be representative of the real-world driving cycles in a particular bin. Therefore, secondly, a multiple regression analysis was performed to identify driving cycle parameters that are statistically significant in terms of influencing the energy economy of an EV over a driving cycle. When generating driving cycles with the Markov chain model, multiple iterations of the process were performed until the statistical parameters, identified by the regression analysis, matched the mean

of the statistical parameters of the real-world driving cycles in a given bin within ±10%. This ensured that a generated driving cycle was representative of the real-world driving cycles in the given bin. In addition to ensuring that the statistical parameters of the developed cycles were within ±10% of the mean of the statistical parameters of the real-world driving cycles, the predicted energy economy of the developed driving cycles were shown to be representative of the real-world energy economy values in their respective bins. This was established by demonstrating that the predicted energy economy of the developed driving cycle for a given bin was located around the median point of the distribution of the observed real-world energy economy values in that bin.

The developed driving cycles were also shown to consist of the same proportions of driving conditions in terms of road types and traffic conditions to those observed in real-world operating conditions. Furthermore, the statistical parameters of the developed driving cycles demonstrated clear trends with respect to driving di stance, similar to the trends observed in real-world driving cycles.

An assessment of the representativeness of the developed driving cycles and a selection of seventeen well-established worldwide driving cycles of the real-world driving cycles in each bin was conducted. In each case the developed driving cycle outperformed the selection of worldwide driving cycles with respect to matching the mean statistical parameters of the real-world driving cycles in its respective bin.

Finally it was established that real-world driving conditions differ from the certification cycles developed for emissions testing in the U.S., Europe, and Japan. They generally consist of lower velocity driving and higher acceleration rates. Real-world driving cycles are essential for EV powertrain design and battery management systems. The developed driving cycles would aid in the design of EVs that are operating in the GDA. In addition, the developed driving cycles would allow electricity grid analysis, economic and lifecycle studies to be conducted with a higher degree of confidence.

5.8 Areas for further research

The contribution of road gradient to energy economy was not included in this analysis. An analysis of the potential for energy recovery from regenerative braking whilst travelling down slopes would be beneficial. This could be achieved by retrieving elevation data from Google maps from the corresponding GPS data and computing the slope of the road. Other factors which were not included in the model are road surfaces and tire pressure.

In more extreme climates, the additional loads due to climate control could significantly contribute to the energy consumption. An analysis of the usage patterns and energy consumption of climate

control systems requires further study. Predicting accessory loads is quite complex and is controlled by several factors such as ambient temperature, humidity and sun load.

6 Stochastic modelling of electric vehicle travel patterns

EVs are predicted to play a crucial part in achieving climate change goals and incorporating renewable energy into the energy sector. They are also a promising source of power system services. However, there are possible disadvantages of EVs if they are integrated without prior planning in terms of their potential impact on the grid. They may exacerbate peak demand and infrastructure upgrades may be required to increase transmission capacity whilst GHG emissions may not be reduced. The optimisation of the charging of EVs is paramount in order to maximise their benefits and for their successful integration. In this chapter a stochastic simulation methodology capable of generating a schedule of daily journeys for a population of EVs that correlate well with observed real-world travel patterns is presented. The driving cycles developed in Chapters 5 and 6 are used to determine the energy economy of vehicles. In Chapter 7 the travel pattern model is used to translate the travel patterns of a population of EVs into the respective power demand of the EVs. Such travel patterns and charging profiles would be the primary inputs into EV grid integration studies such as aggregated power demand, power systems services and charging optimisation analyses.

GPS travel data collected during the EV trial are used to derive distributions of travel pattern related variables. The dependence structure between six core variables is modelled using a non-parametric copula function. An iterative method of conditional distributions with a Bayesian inference is used to generate travel patterns that comply with the uncertainty of the inputs. The developed stochastic method is shown to closely adhere to the deterministic (i.e. the real-world data) results. These synthetic datasets capture the degree of uncertainty of the travel behaviour of EVs (contrary to single realisations) and are scalable to different EV populations (allowing uncertainty reduction effects in large populations). Moreover, such stochastic setups can be used for the design of systems where data from a sample of vehicles are not readily available.

This chapter is organised as follows: Section 6.1 introduces the role of EV travel pattern models in electricity grid modelling and Section 6.2 reviews existing EV travel pattern models. Section 6.3 provides an overview of the developed stochastic model and Section 6.4 describes the dataset used in the development of the model. Section 6.5 analyses the distributions and the dependence structure between travel pattern related variables. Section 6.6 opens with an overview of copula functions and then the dependence structure between the travel pattern related variables is modelled with a non-parametric copula function. The developed travel pattern model generates a journey schedule by synthesising journey distances, journey times and parking times. The distributions of journey distances, journey times and parking times are analysed in Section 6.7. An introduction to Bayesian probability and its application to the developed model are discussed in Section 6.8. In Section 6.9 the methodology of the developed travel pattern model and an example of the syntheses

of a journey schedule for a single EV are presented. The model is validated in Section 6.10. Section 6.11 concludes the chapter and Section 6.12 discusses areas for further research.

6.1 An introduction to the role of EV travel pattern models in electricity grid modelling

EVs, coupled with low carbon electricity, have the potential to contribute to climate change. In Chapter 2 a review of the literature demonstrated that EVs have the potential to reduce GHG emissions in several countries. They produce less effective CO_2 per kilometre (i.e. including CO_2 emitted from electricity generation) travelled and produce no local pollution such as PM_{10} and NO_2.

EVs are a sustainable alternative to ICEVs, provided that the energy used for charging is generated by renewable sources. However, electricity generation from renewable sources is dependent on weather conditions in the case of wind energy and as a consequence there is a high degree of variability in power generation. Given the absence of large-scale energy storage technology, electricity must be consumed at the time of generation. If weather conditions do not permit, there is no flexibility to produce additional power if required from renewable sources. In addition, in times of low demand and high availability of renewable electricity the full economic benefits of renewable energy may not be achieved. In the future, it is likely that the batteries in EVs will be used as energy storage devices, by supplying electricity to the grid during peak demand (vehicle to grid (V2G)) and by being charged at times where renewable sources are abundant. In addition, buildings constitute a significant part of the load in energy networks but are typically passive consumers. Therefore, going forward buildings are expected to be integrated into smart grids to utilise their currently unused flexibility of operations (i.e. shiftable loads, load shedding, duty-cycling), supported by building automation and information technology (Austrian Institute of Technology, 2013).

As previously discussed in Chapter 1, system operators are responsible for managing power system services and are constantly matching supply with demand. It is generally accepted that the charging of a large population of EVs will have two major effects on the grid; it will increase the overall power load needed and it will increase the load on local distribution networks. Either of these could become the limiting factor but it is believed that the local load distribution problems will become prevalent sooner than the more general overall power supply issue (Hill et al, 2012). However, the uncontrolled charging of a large population of EVs could increase peak demand substantially. System operators must largely rely on conventional generators (fossil fuels) to meet this demand. This would reduce the potential GHG reduction benefits. Moreover, increases in the peak demand could require transmission capacity expansion. To mitigate these concerns, controlled charging of EVs needs to be implemented.

In order to support policy decisions, the impacts of EVs on the power system needs to be evaluated. In order to achieve this, reliable models capable of translating the travel patterns of a large population of EVs into the respective power demand are needed. The complexity and stochastic nature of travel patterns point to a stochastic model to satisfactorily model travel patterns. In the past couple of years, the scientific community has been more focused on the analysis of the potential impact of charging EVs. The effect of the large-scale integration of EVs into the power grid has been studied in several papers (Dallinger et al, 2011, Di et al, 2011, Kristoffersen et al, 2011, Lojowska et al, 2012). Issues such as peak load, network losses and cost minimisation have been analysed. However, the majority of the early studies have used a deterministic approach to model travel patterns, using collected data directly or expected values and averages (Di et al, 2011, Mullan et al, 2011, Weiller, 2011). This approach fails to capture the stochastic nature of travel behaviour. Observed vehicle travel patterns have been reported in many studies (Golob and Gould, 1998) but the stochastic modelling of driving patterns has received little attention until recently (Green et al, 2010). The next section reviews existing EV travel pattern models.

6.2 A review of existing travel pattern models for EV grid integration studies

There are generally two ways in which to investigate the travel patterns and charging behaviour of a large population of EVs. One method would be to conduct a large scale EV trial and to use the results from that trial to inform and deduce charging patterns and power demand predictions. The second method would be to model a fleet of EVs and to use the results of the model as an indication of the power demands of the EVs.

For the second method, ideally a micro-simulation package combined with a charging decision algorithm would be used to achieve this. However, given the number of vehicles (e.g. 200,000) and the size of the area of interest it would be computationally intensive to model and predict charging patterns through direct simulation on an individual basis (Hill et al, 2012). In addition, currently no charging decision algorithm exists in literature, although research is being conducted in the area (Axsen and Kurani, 2010). As part of the work of this thesis, a charging decision model is proposed later in Chapter 7. Another option would be to scale the data collected in a large scale trial of EVs. However, these data could only be used to model the circumstances in which the data was collected and the explanatory power of the data would be limited to the fleet composition for which the data exists.

A stochastic model would be computationally less intensive than micro-simulation and would have more predictive power than just the use of historic data. In addition, as outlined in the introduction, driving patterns are stochastic in nature and as a consequence, the power demand of EVs should inherit this randomness. Recently several studies have examined the effect of EVs on power system demand and their ability to provide power system services. These studies have relied on fixed

travel survey data and/or broad assumptions about travel patterns, charging decision behaviour, fuel efficiency and access to charging facilities, which do not emulate real-world circumstances. (Dallinger et al, 2011, Di et al, 2011, Mullan et al, 2011). However, in 2012, a number of studies have been conducted using a stochastic approach. These stochastic models generally use data pertaining to travel surveys or data collected by ICEVs, they only model journeys to and from the home and make broad assumptions regarding charging decision behaviour(Keane and Flynn, 2012, Lojowska et al, 2012).

Studies using a deterministic approach are the most common. Kristoffersen et al (2011) derived the power demands of EVs and PHEVs by the clustering of data from a Danish national travel survey. They assumed that weekly travel patterns recorded in the dataset remained constant across the year and the EVs and PHEVs were assumed to have all-electric ranges of 150 km and 65 km respectively. The results showed that the vehicles provided power system flexibility within the day but only limited flexibility from day to day when driving patterns are fixed. Sioshansi and Denholm (2010) used vehicle travel data from 227 vehicles in Missouri to investigate the provision by PHEVs of V2G. The driving patterns of 227 vehicles over the course of a number of weekdays were logged. It was assumed that the PHEV fleet was evenly divided into the 227 driving profiles corresponding to the driving pattern data. The hours, in which the PHEVs are driven, the total distance travelled per hour and the vehicles that were grid-connected and could be dispatched to charge or discharge their batteries or provide ancillary services were analysed. It was assumed that the vehicles always had access to charging facilities whenever parked. The study found that a PHEV fleet can provide benefits to the electricity system, mainly through the provision of ancillary services, reducing the need to reserve conventional generator capacity. Dallinger et al (2011) investigated the provision of V2G by EVs. The vehicle travel patterns were drawn at random from a 2002 German transport survey. A dynamic approach was compared to a static approach. The author highlighted that 10,000 travel patterns were required to ensure consistent charging patterns.

A number of stochastic models have been published in 2012. Sundstrom and Binding (2012) developed a trip prediction model for a charging service provider. The model is a semi Markov chain model that predicts the next arrival location and the parking time at the current location of an EV. This was combined with the predicted time and energy consumption required to reach the next destination to determine the power demands for an EV throughout the day. The author compared the model with a simplistic model that predicted the current day's trips based on the previous day's trips. The model was shown to predict the next trip location with 84% accuracy.

Hill et al (2012) simulated the driving and charging behaviour of a fleet of EVs using a discrete time Markov chain approach. Data collected in an EV trial in the UK was used in the analysis. A TPM containing nine states, three states for the battery's State of Charge (SOC), high, medium and

low and three states for the vehicle's status, drive, park and charge, was created from the frequency of transitioning between each state over a specified time period. The model produced charging regimes that correlated well with the real world results. The author reported that the actual charging distribution was within the 95% confidence interval for the simulated charging events.

Lojowska et al (2012) used a travel survey dataset relating to ICEs to model the power demands on EVs in the Netherlands under the scenario of uncontrolled domestic charging. The travel patterns of the EVs were modelled using three variables: the time a vehicle departs home, the time a vehicle arrives home and the overall distance travelled during the day. The dependence structure between the variables was modelled using a normal copula function. The load due to EVs was computed based on the combination of simulated commuting patterns with the charging profile of a typical EV battery. The model only modelled journeys to and from the home (i.e. it excluded intermediate journeys) and assumed that the vehicles began charging immediately upon arrival home. The author did not discuss the accuracy of the model.

Pashajavid and Golkar (2012) proposed a stochastic approach using non-Gaussian pdfs fitted to travel survey data logged from ICEV commuter vehicles. The three variables were home departure time, distance travelled and home arrival time. The author did not model the correlation structure between the variables. A charging profile was determined for each individual EV and then an hourly aggregated load profile of the fleet was calculated. From this, a pdf of the aggregated load of the EVs within each hour was estimated. The author did not discuss the accuracy of the model.

Ashtari et al (2012b) used GPS data from 76 ICEVs in Winnipeg, Canada to predict the power demand of EVs. A deterministic simulation was compared to two existing stochastic methods and a new stochastic model developed by the author. The two existing models were quite simplistic and used independent pdfs of variables such as departure times, arrival times and distances travelled. In the proposed method iterative and conditional pdfs were used to generate departure times, arrival times and distances travelled. The model only modelled journeys to and from the home and it assumed that the vehicles began charging immediately upon arrival at home. The new method outperformed the two previous stochastic methods, with the lowest error of 3.4% when compared to the deterministic method.

6.3 An overview of the proposed stochastic travel pattern model

The model to be developed here is a Monte Carlo simulation. The simulation operates over two consecutive days in order to diminish the influence of initial assumptions. There were 1,955 occurrences on which an EV was used on two consecutive days in the dataset. The dataset is described in detail in the next section. A flow chart of the simulation process is presented in Figure 6.2. The departure time from home of the first journey of the day, the number of journeys

undertaken in the day and the total distance travelled in the day for the consecutive days were analysed and found to be correlated. The correlation analysis will be presented in Section 6.5.1. The dependence structure between these six variables (3 x 2 days), referred to as the core variables hereafter, was modelled with a non-parametric copula function. The simulation begins with step 1, simulating six values from the multivariate distribution created by the copula function. In step 2, the individual journeys distances are simulated using an iterative method of conditional distributions. In steps 3-5, a journey schedule for a two day period is synthesised. The synthesis procedure begins with the departure time from home and the distance of the first journey. A Bayesian inference approach is used to create a distribution and sample a journey time for the first journey (step 3), conditioned on the start time of the journey and the distance of the journey. The sampled journey time is added to the start time of the journey, resulting in the end time of the journey. A Bayesian approach is then used to create a distribution and sample a parking time (step 4) between the end of the first journey and start time of the second journey. The parking time distribution is conditioned on the end time of the journey, the time taken to complete the journey, the journey number and the time already parked that day. The sampled parking time is added to the end time of the first journey, resulting in the starting time of the second journey. The process is repeated for the simulated number of journeys for day 1 (step 5) resulting in a journey schedule for day 1 (Figure 6.1). The process is repeated for day 2.

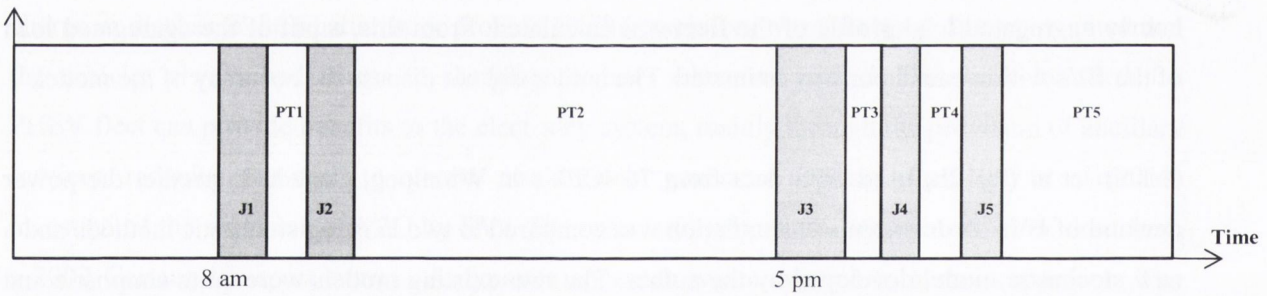

Figure 6.1. An example journey schedule for day 1. Journeys (J) are represented by the grey regions and white regions represent parking durations (PT), in which a vehicle would be available for charging.

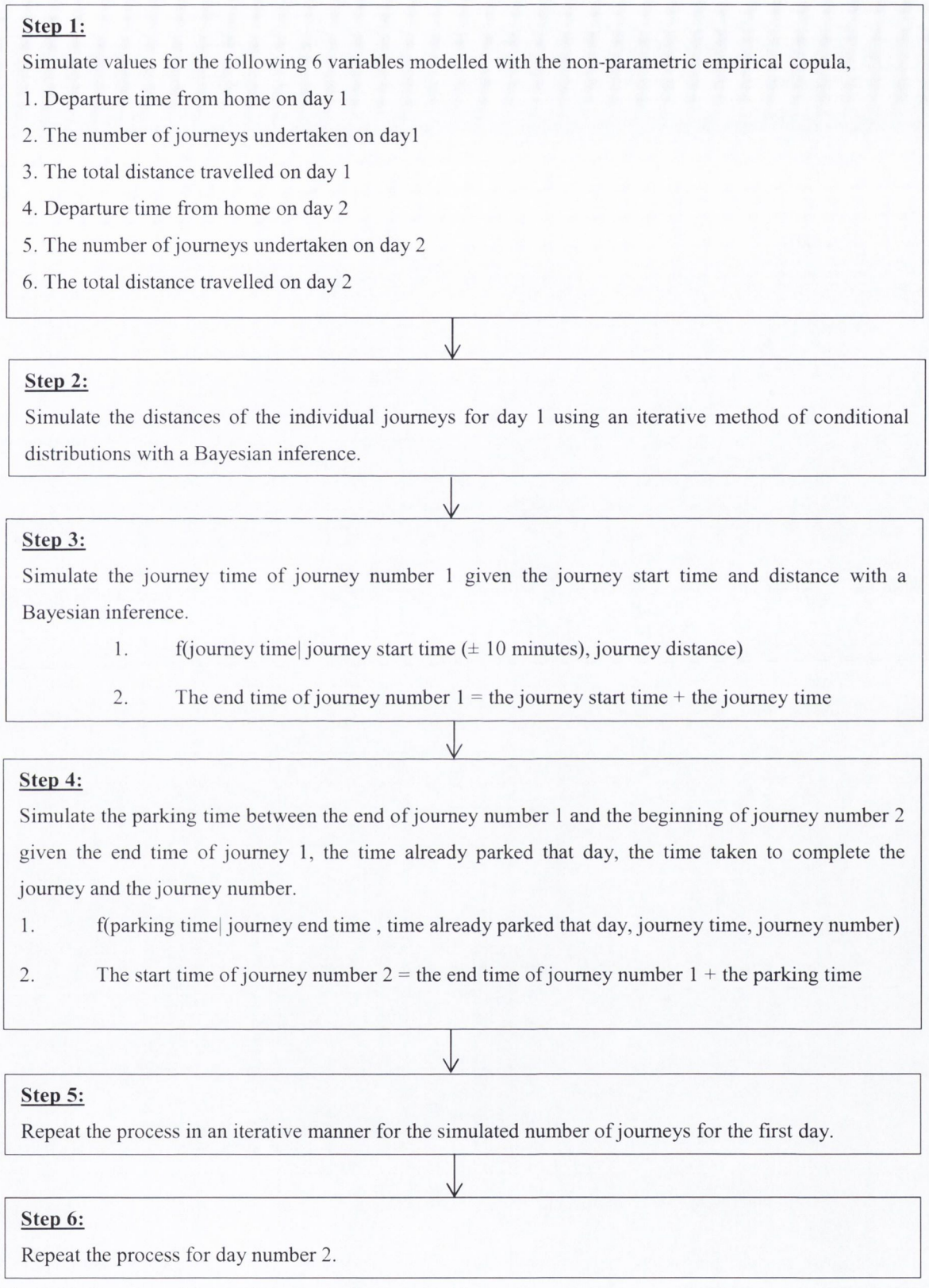

Figure 6.2. Flow chart of the travel pattern simulation methodology.

6.4 The dataset

The travel pattern model was developed using GPS data collected from 15 EVs operating nationwide in Ireland from January 2011 to October 2012. The EVs were trialled in households of ESB employees and members of the public. Throughout the trial, a number of vehicles were

stationed at the head office of the ESB and were available for use by employees for work related trips and could be brought home on an intermittent basis. This resulted in irregular travel patterns for those vehicles. The model is intended to model the travel patterns of the general public, hence all trips that originated or terminated at the ESB head offices were removed from the database. The database contained data pertaining to 18,300 journeys undertaken on weekdays. Due to the small population of vehicles in the trial, each day of data was treated as independent of all other days from that vehicle. In effect this resulted in a database of 4,021 days of EV data rather than a 666 day trial of 15 vehicles. The aggregation of the data means that care must be taken when interpreting any results. Despite the limitations of the dataset the intention is to use the approach as a test bed for a proof of concept.

In the next section the distributions of the core variables are presented and dependence between the variables is investigated.

6.5 Distributions of the core variables

This section presents and discusses the distributions of the core variables for the first day of the two modelled consecutive days in the database. The distributions for the second day are almost identical. The distribution of the departure times (i.e the first journey of the day) is shown in Figure 6.3. The departure time distribution peaks between 8-10 am, which corresponds well with general commuting times. After 10 am the probability gradually decreases and is very small after 9 pm.

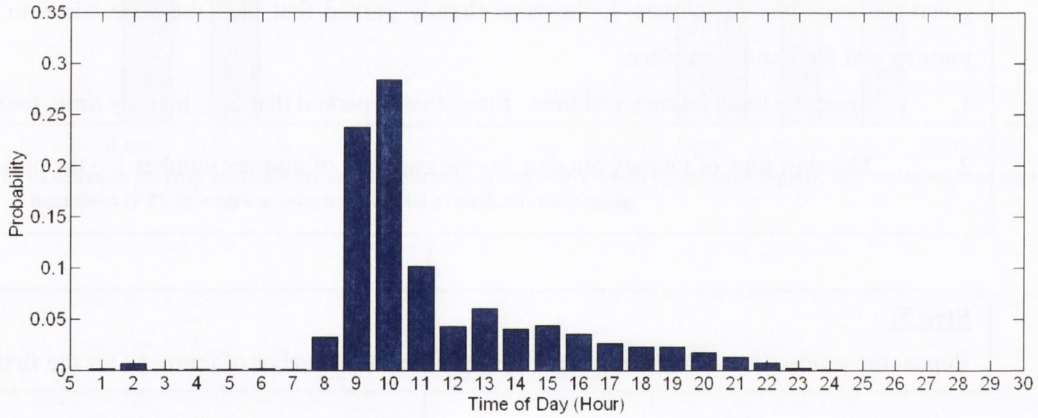

Figure 6.3. Distribution of the departure time from home.

Figure 6.4 presents the distribution of the number of journeys made per day. Two journeys per day have the highest probability density and the probabilities gradually decrease between 3 journeys and a maximum observed number of 11 journeys.

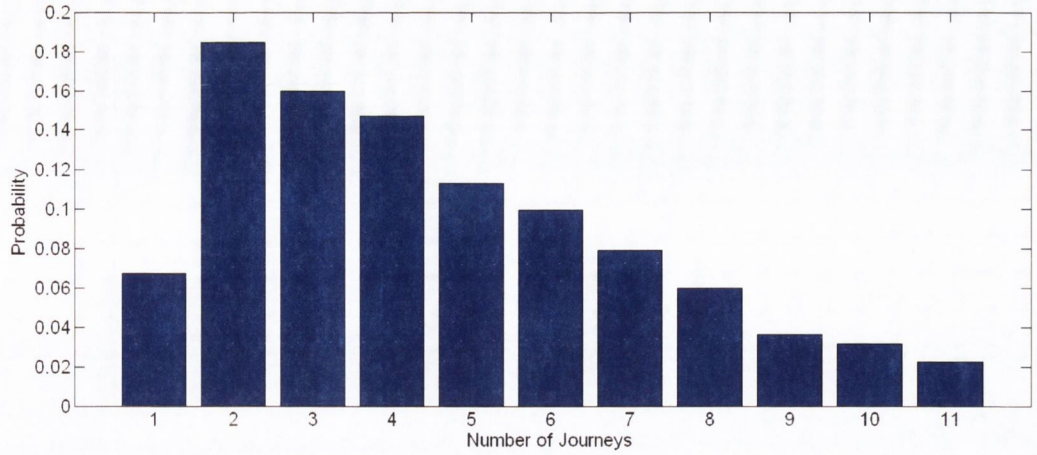

Figure 6.4. Distribution of the number of journeys per day.

The pdf of the total distance travelled in a day in presented in Figure 6.5. A total daily travel distance of between 1 km and 40 km is the most frequent and the probability decreases steadily for daily travel distances greater than 40 km. The figures indicates that the three variables have nonstandard pdfs.

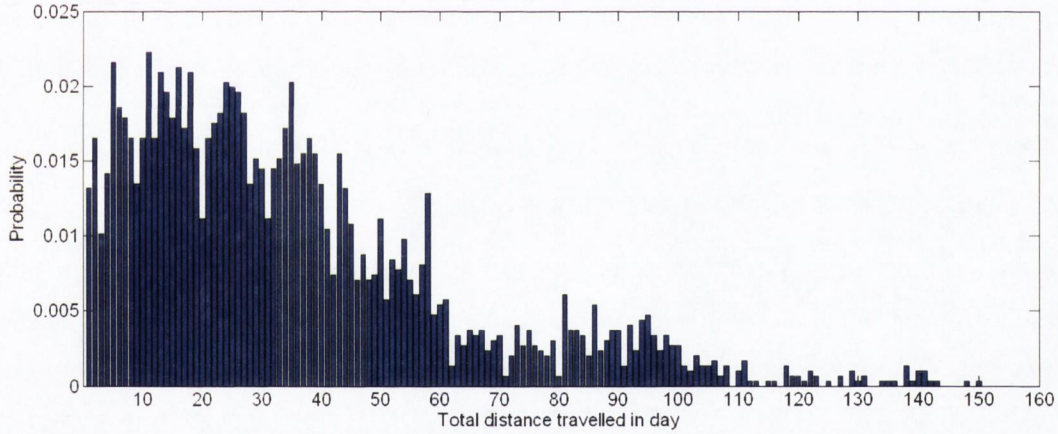

Figure 6.5. Distribution of the daily travel distance.

6.5.1 Modelling the dependence structure between the core variables

In order to verify if there is dependence among the variables (departure time (DT), daily travel distance (Dis) and the number of journeys per day (NJ)), the Pearson's linear correlation between the variables is estimated and placed in the matrix, R. The abbreviations DT1 and DT2 refer to the departure time on day 1 and day 2 respectively. The same abbreviation format applies to the other variables.

$$R = \begin{bmatrix} & DT1 & NJ1 & Dis1 & DT2 & NJ2 & Dis2 \\ DT1 & 1 & -0.31 & -0.37 & 0.31 & -0.12 & -0.19 \\ NJ1 & -0.31 & 1 & 0.34 & -0.19 & 0.38 & 0.02 \\ Dis1 & -0.37 & 0.34 & 1 & -0.25 & 0.02 & 0.51 \\ DT2 & 0.31 & -0.19 & -0.25 & 1 & -0.26 & -0.33 \\ NJ2 & -0.12 & 0.38 & 0.02 & -0.26 & 1 & 0.36 \\ Dis2 & -0.19 & 0.02 & 0.51 & -0.33 & 0.36 & 1 \end{bmatrix}$$

Testing the hypothesis of no correlation against the alternative that there is a nonzero correlation was applied to the elements in R. All coefficients in the matrix were found to be statistically significant at the 95% confidence level except for R(2,6) and R(3,5), which suggests no dependence exists between the number of journeys undertaken on day 1 and the totalled distance travelled on day 2 and vice versa. Therefore, there is strong evidence that the variables are correlated and it is important to model the dependence structure between the variables. As an example, from the correlation matrix R, the daily travel distance is negatively correlated with the departure time (R(1,3) and R(3,1)), which implies that the later an individual departs the home the shorter the daily travel distance.

It has been demonstrated that the core variables have nonstandard pdfs and that they are correlated. Therefore, in order to model the dependence structure between the variables it is necessary to construct a joint pdf using their respective marginal distributions and a copula function. This is discussed in the next section.

6.6 Modelling the core variables using a copula function

This section opens with an overview of copula function theory and the application of copula functions. Then a copula function is applied to the core variables and the section concludes with the verification of the copula function.

6.6.1 An overview of copula functions

Stochastic dependence refers to the behaviour of a random variable relative to another. Two random variables are said to be independent if the occurrence of a specific value of one variable has no impact on the probability of an occurrence of any value of the other variable.

Copula functions are useful tools for examining the dependence structure of random variables since they neither require normality in marginal or joint distributions (Papaefthymiou and Kurowicka, 2009). A copula function joins together univariate distribution functions to form a multivariate distribution function. This allows the joint distribution of variables with different marginal distributions to be constructed (Papaefthymiou and Kurowicka, 2009).

According to Sklar's theorem the random variables X, Y and Z with cumulative distribution functions (cdf), F_X, F_Y and F_Z respectively, can be joined by copula C if their joint distribution can be defined as

$$F_{XYZ}(x, y, z) = C(F_X(x), F_Y(y), F_Z(z)) \tag{6.1}$$

If F_X, F_Y and F_Z are continuous then C is unique.

From Equation 6.1, denoting F_X = u, $F_Y(y)$ = v, and $F_Z(z)$ =q, where u, v and q are realisations of uniform variables U, V and Q respectively, then the equation can be reformulated as

$$C(x, y, z) = F_{XYZ}(F_x^{-1}(u), F_Y^{-1}(v), F_Z^{-1}(z)) \tag{6.2}$$

This equation can be used for the construction of the copula function from the respective multivariate distribution function.

6.6.2 The application of copula functions

A continuous random variable can be transformed to uniform by the application of a cdf transformation. This uniform variable corresponds to the respective ranks of the distribution. Accordingly, the inverse cdf transformation can be used for transforming the uniform random variable back into its actual domain (Papaefthymiou and Kurowicka, 2009).

By definition, for a random variable with an invertible cdf, $F_x(x) = P(X \leq x)$, the random variable $F_x(x)$, follows a uniform distribution on the interval [0,1]. Thus, if it is invertible the following relationship holds:

$$X = F_x^{-1}(U) \leftrightarrow U = F_x(X) \tag{6.3}$$

where U is a random variable that is uniformly distributed on [0, 1]. In Figure 6.6, the relation (6.3) is presented schematically. This relationship forms the basis for the sampling of a random variable in Monte Carlo simulation.

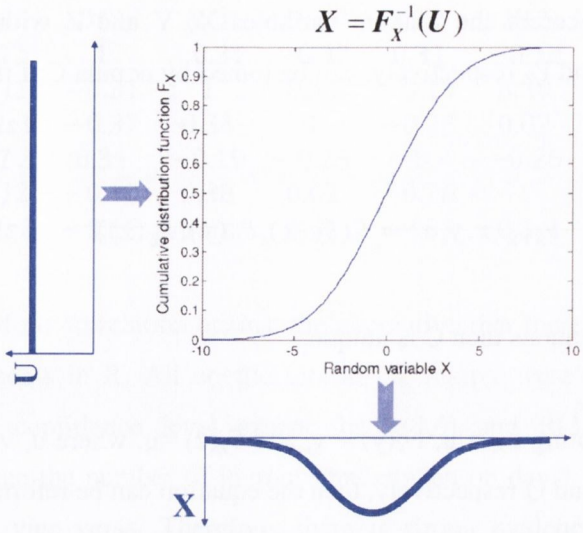

Figure 6.6. Sampling of an arbitrary random variable (Papaefthymiou and Kurowicka, 2009).

The significance of the cdf transformation lies in the property that its application does not affect the dependence structure. In particular, the ranking (and consequently the stochastic dependence) of a sample population remains the same under increasing transformations.

To measure the strength of dependence between random variables, the product moment correlation can be used. It measures the degree of linear relationship between the random variables and is invariant to linear transformations (Papaefthymiou and Kurowicka, 2009). However, since it is applied in the actual domain of the random variables, it is affected by the marginal distributions. To avoid this shortcoming, one should apply this measure to the respective ranks of the random variables (Papaefthymiou and Kurowicka, 2009).

As a result of applying a cdf transformation to all random variables in the model, the transition to a common uniform domain is achieved. The dependence modelling takes place in this common domain (Figure 6.7) and the random variables can be further transformed back to their original distributions by an inverse-cdf transformation. Figure 6.8 provides an illustration of this procedure when modelling dependent random variables using a normal copula function.

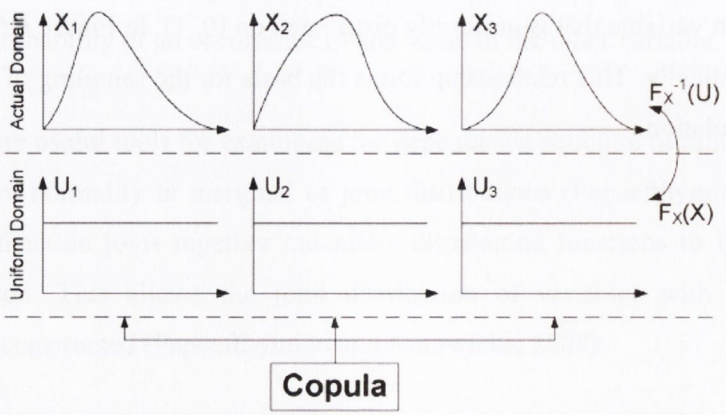

Figure 6.7. An illustration of the copula modelling mechanism (Papaefthymiou and Kurowicka, 2009).

As an example when modelling dependent random variables with a normal copula function, the following steps would be followed:

1. Transform the random variables to a uniform domain using their cdfs.
2. Transform the uniform variables to normal variables using the inverse of a standard normal distribution.
3. Estimate the product moment correlation, ρ, between the normal variables.
4. Simulate the modelled variables from the multivariate standard normal distribution with correlation ρ.
5. Apply a standard normal cdf and the inverse of the respective cdfs to transform the simulated values back into the original domain.

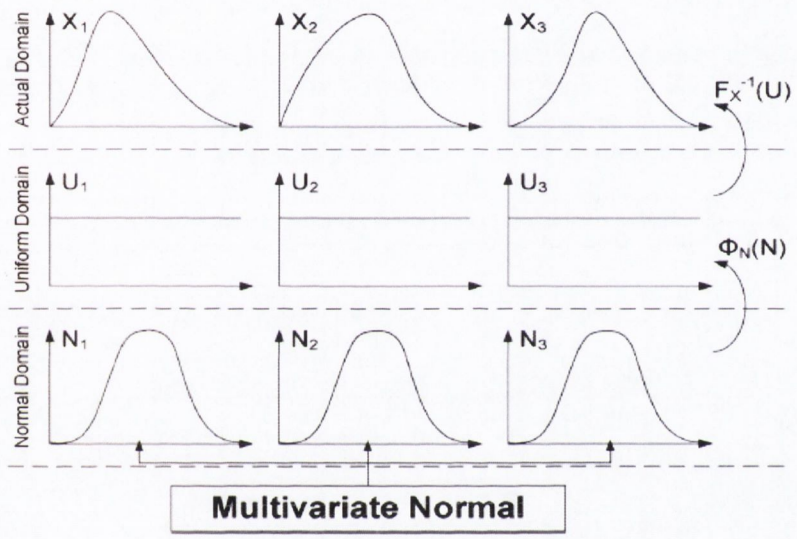

Figure 6.8. An illustration of modelling dependent random variables using a normal copula function (Papaefthymiou and Kurowicka, 2009).

6.6.3 Modelling the core variables using a copula function

Parametric copulas, Normal and T, were initially fitted to the data but were found not to model the correlation structure between the variables well. Figures 6.9 and 6.10 present the modelled correlation structure between the variables distance travelled and the number of journeys for a Normal copula and a T copula respectively. The observed values are in red in a uniform domain and 10,000 fitted data points by the copula function are in blue. Notice that the correlation structure is not well modelled in the range 0.6-1.0 of the variable total distance travelled and range 0.0-0.2 of the variable number of journeys. Parametric copulas rely on a symmetrical relationship between the variables, hence when fitting a parametric copula, the parameter of the copula that makes for a best fit to the data is determined, but the copula's functional form is retained. In order to better model the correlation structure an empirical copula was fitted to the data. With an empirical copula, the functional form itself (not just the parameter) is based on the data, which allows the correlation pattern, however unusual to be captured. Modelling with an empirical copula is achieved by

Bootstraping the ranks of the data to construct an approximation to an empirical copula (Vose, 2008).

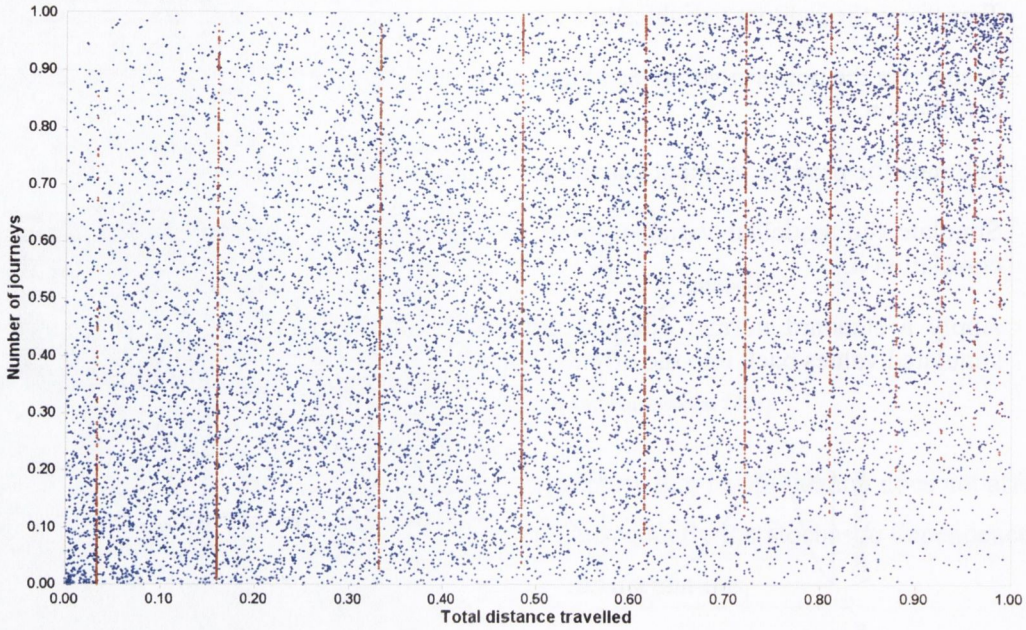

Figure 6.9. The modelled correlation structure by a Normal copula function between the variables number of journeys and total distance travelled. The actual observations are in red and the data fitted by the copula are in blue.

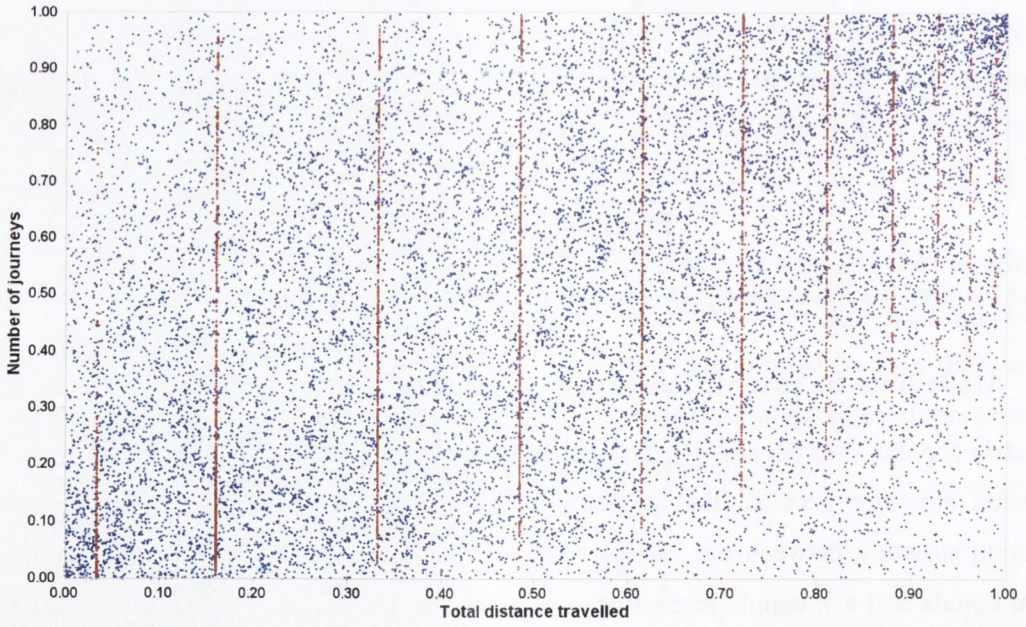

Figure 6.10. The modelled correlation structure by a T copula function between the variables number of journeys and total distance travelled. The actual observations are in red and the data fitted by the copula are in blue.

Figure 6.11 illustrates the modelled correlation structure by the empirical copula for the variables total distance travelled and the number of journeys. Notice a higher density of fitted points in areas where there is a high density of actual observations (in the bottom-left and top-right). Furthermore, the dependence structure (bottom right) in the region of the range 0.6-1.0 of the variable number of journeys and the range 0.0-0.2 of the variable distance travelled is modelled more accurately than was achieved using the parametric copulas, Normal and T, in Figures 6.9 and 6.10 respectively.

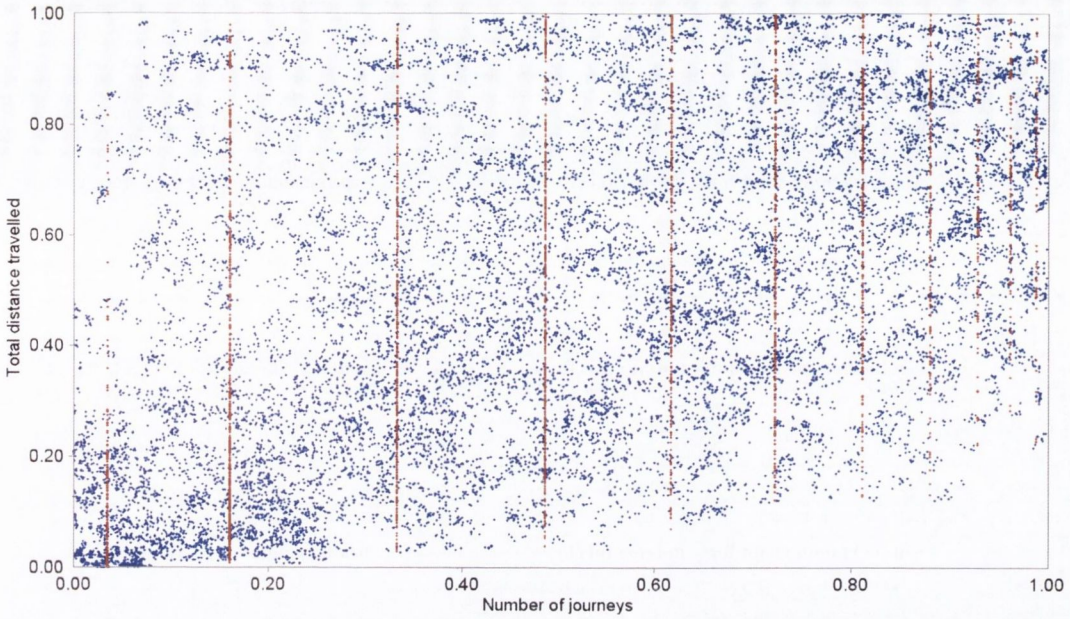

Figure 6.11. The modelled correlation structure by an empirical copula function between the variables total distance travelled and number of journeys. The actual observations are in red and the data fitted by the copula are in blue.

Figure 6.12 illustrates the modelled correlation structure by the empirical copula for the variables departure time and the number of journeys. Notice a slightly higher density of fitted points in areas where there is a high density of raw observations compared with the previous Figures 6.9 and 6.10.

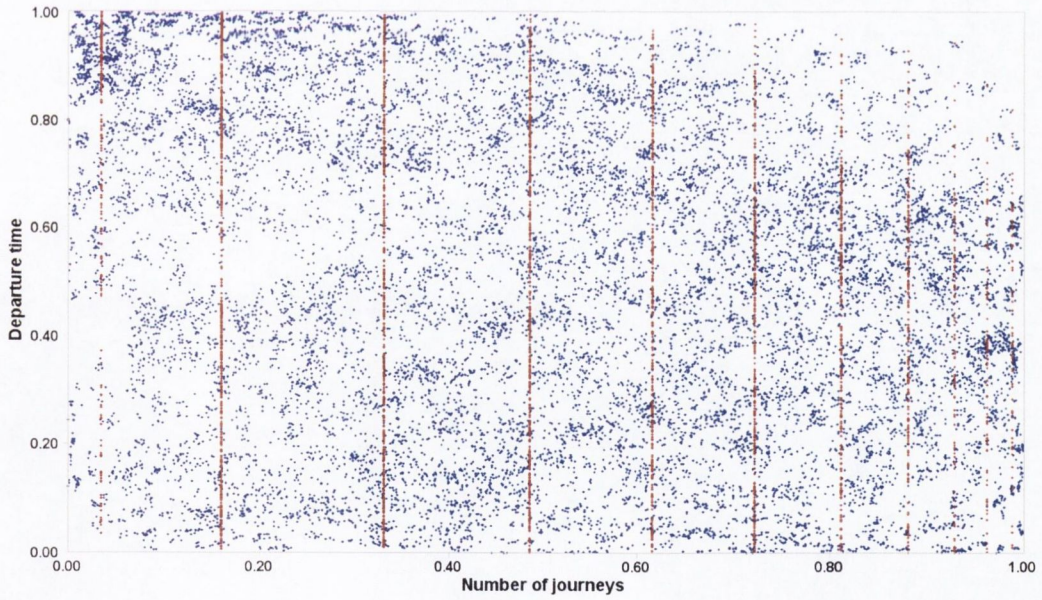

Figure 6.12. The modelled correlation structure by an empirical copula between the variables number of journeys and departure time. The actual observations are in red and the data fitted by the copula are in blue.

Figure 6.13 illustrates 2,000 observations in their uniform domain for the variables, total distance travelled and the departure time. Notice a slightly higher density but not that definable on the diagonal from left to right.

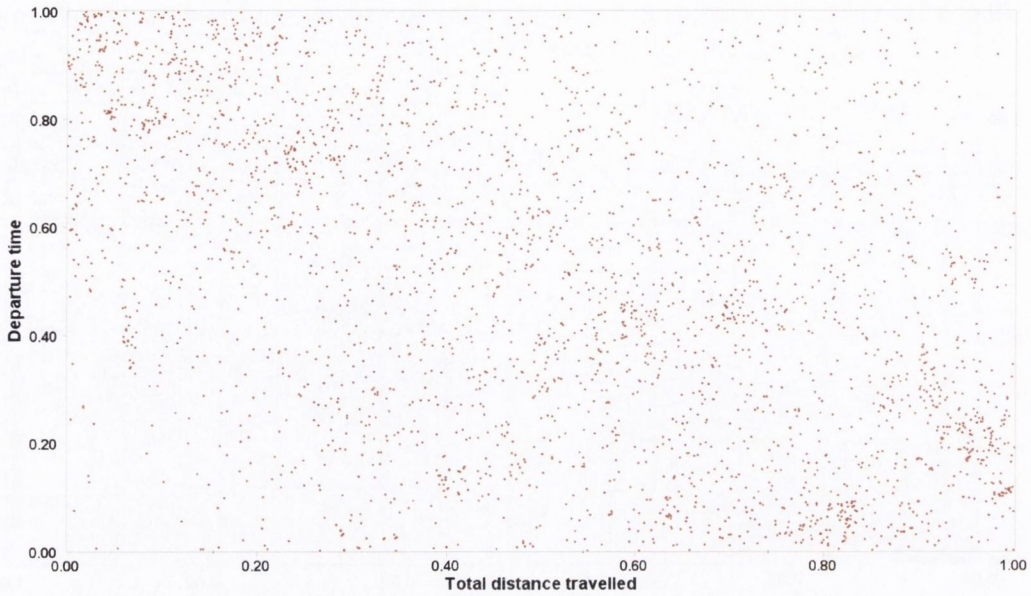

Figure 6.13. Plot of the raw observations for variables total distance travelled and departure time.

Figure 6.14 illustrates the 2,000 observations (in red) and 10,000 data points fitted by the copula (in blue). Notice a there is a higher density of fitted points in areas where there is a higher density of actual observations, especially on the diagonal from the top-left to the bottom-right.

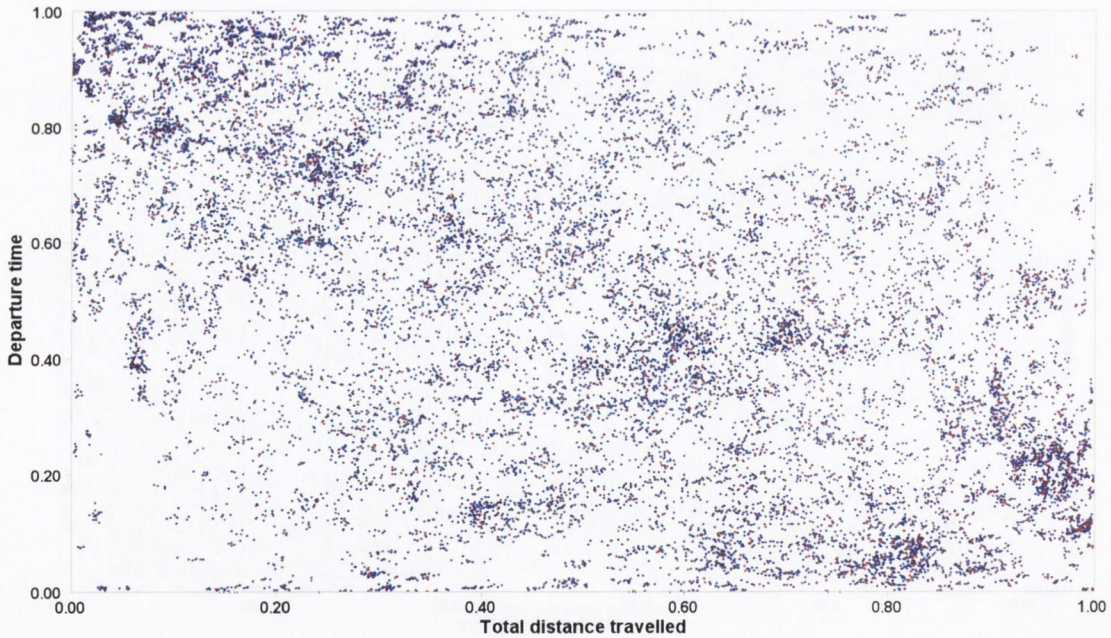

Figure 6.14. The modelled correlation structure by an empirical copula between the variables total distance travelled and departure time. The actual observations are in red and the data fitted by the copula are in blue.

6.6.4 Copula model validation

In this section an attempt to verify the modelled dependence structure between the core variables by copula function is made. If the structure is modelled correctly, the original and simulated values of the variables should have the same distribution. Quantile–Quantile (Q-Q) plots of the simulated and original data are used to investigate this. A Q-Q plot is a graphical method for comparing two

continuous distributions by comparing their quantiles against each other. If the two distributions being compared are similar, the points in the Q–Q plot will approximate a straight line. Figures 6.15 and 6.16 present the Q-Q plot for the original and simulated variables of departure time and total distance travelled respectively. In both cases, the plots approximate a straight line indicating that the simulated and original data are from the same distributions. In Figure 6.15, the range 0.03-0.25 corresponds to the time period 12:45 am to 06:00 am. The deviation from the straight line in this range is due to the fact that there were only 15 observations in the database for this time period. As the variable number of journeys per day is a discrete variable, a Q-Q plot is not a suitable method for validating this variable. Instead, a Chi-Squared goodness of fit test was used to test the hypothesis that the simulated and original data are from the same distribution. The test accepted the null hypothesis at the 95% confidence interval that the simulated and original data are from the same distribution. Figure 6.17 illustrates that the frequency of the expected and simulated number of journeys per day are very close.

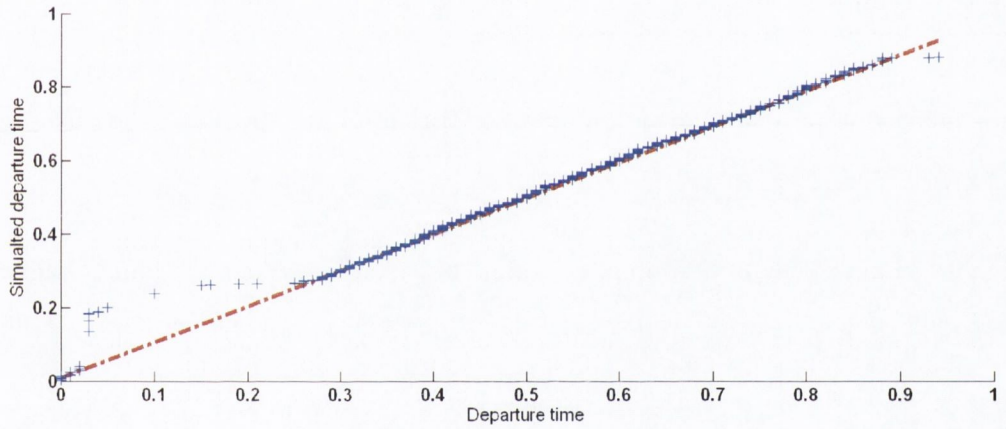

Figure 6.15. Q-Q plot of simulated and original variable departure time.

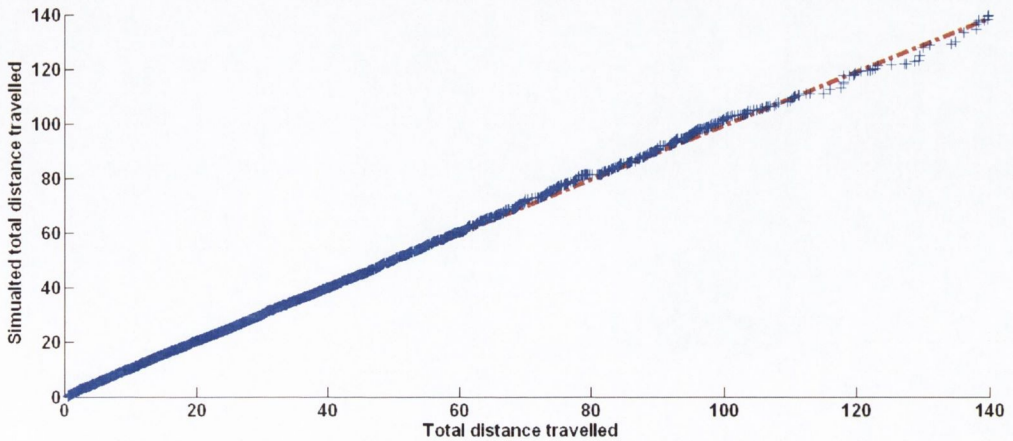

Figure 6.16. Q-Q plot of simulated and original variable total distance travelled.

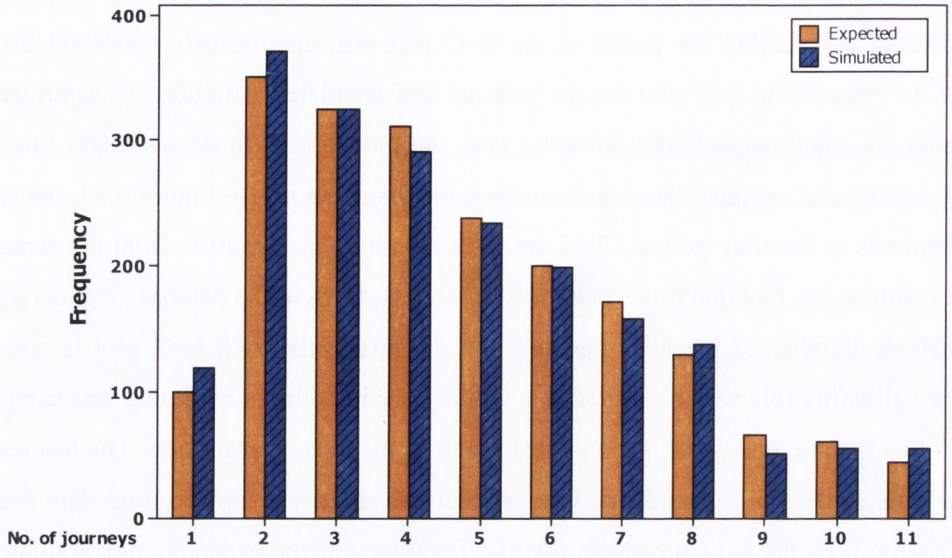

Figure 6.17. Frequencies of the simulated and expected number of journeys per day.

6.7 An overview of the journey distances, journey time and parking times distributions

As the model synthesises journey distances, journey times and the parking times between journeys in order to simulate a schedule of journeys for the day it is appropriate to investigate the distributions of these three variables.

The distribution of journey times from the logged data is presented in Figure 6.18. Journey times of 5 and 10 minutes are the most frequent journey times and 50% of all journeys take 15 minutes or less.

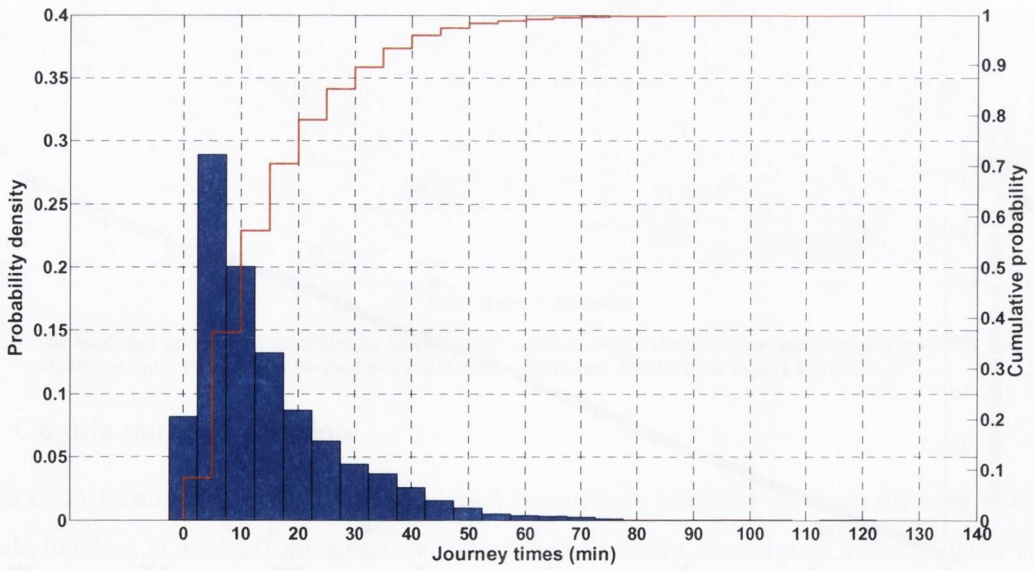

Figure 6.18. The probability density function and cumulative density function of journey time.

The distribution of parking times between journeys (i.e. no overnight parking times) from the logged data is presented in Figure 6.19. Parking times of 0 and 5 minutes are the most frequent parking times. In terms of interpreting the data in the figure, a parking time of 0 minutes represents a parking time less than 2.5 minutes (i.e. a drop-off). The distribution of journey distances from the logged data is presented in Figure 6.20. Journey distances of 1 km and 2 km have the highest frequency and 75% of all journeys are less than 10 km.

In the next section an overview of Bayesian probability and its application to the model is presented and discussed.

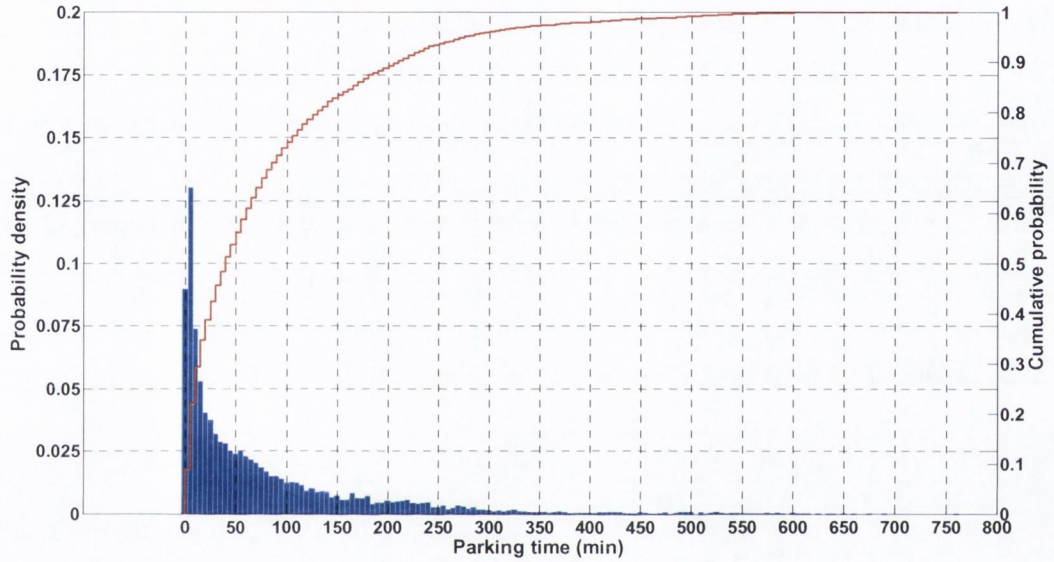

Figure 6.19. The probability density function and cumulative density function of parking time.

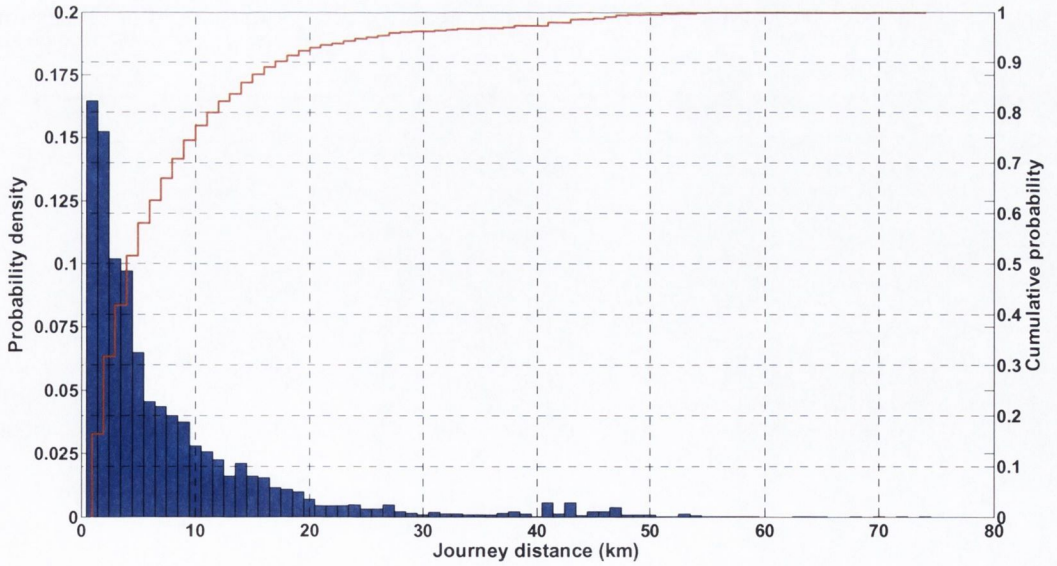

Figure 6.20. The probability density function and cumulative density function of journey distance.

6.8 An introduction to Bayesian probability and its application to the model

Bayesian probability theory provides a mathematical framework for performing inference, or reasoning, using probability. It represents a level of certainty relating to a potential outcome. This is in contrast to a frequentist probability that represents the frequency with which a particular outcome will occur over any number of trials.

In developing this work, it is understood that a model is only an approximation of the real-world and will ultimately be influenced by subjectivism. Decisions about the structure and acceptable accuracy of a model are very subjective. In addition the modeller often relies on subjective estimates for many inputs, frequently without data to support them.

Bayesian inference, based on Bayes' theorem (Equation 6.4), models the process of learning by using data to improve one's estimate of a parameter. There are essentially three steps involved: (1) determining a prior estimate of the parameter in the form of a confidence distribution; (2) finding an appropriate likelihood function for the observed data; (3) calculating the posterior estimate of the parameter by multiplying the prior distribution by the likelihood function and then normalising so that the result is a true distribution of confidence (Vose, 2008).

The travel pattern model operates on a five minute scale hence the time observations (i.e. start/end times of journeys, journey times and parking time) are binned into five minute intervals. Journey distances are rounded to the nearest kilometre. Inevitably, situations could arise live in the simulation in which an inference would be made regarding a bin in which there are no observations. This would cause the simulation to stop because a distribution could not be estimated. To address this issue, a Bayesian approach was implemented.

The notation for Bayesian inference for a discrete variable is:

$$f(\theta|x) = \frac{\pi(\theta).l(X|\theta)}{\sum \pi(\theta).l(X|\theta)} \tag{6.4}$$

Where, $\pi(\theta)$ is the prior distribution, $l(X|\theta)$ is the likelihood function and $f(\theta|X)$ is the posterior distribution.

$\pi(\theta)$ is the density function of one's prior belief about the parameter value θ before the data X is observed. It is a representation of one's state of knowledge about θ before the data X has been observed. $l(X|\theta)$ is the probability of observing the data X for a given value of θ. $f(\theta|X)$ is the

description of one's state of knowledge of θ that combines what one have learned from the data X together with what one knew about θ beforehand.

The shape of the prior distribution embodies the amount of knowledge that one has about the parameter to begin with. The more informed one is, the more focused the prior distribution would be. Figure 6.21 illustrates an example of a less informed prior and a more informed prior distribution.

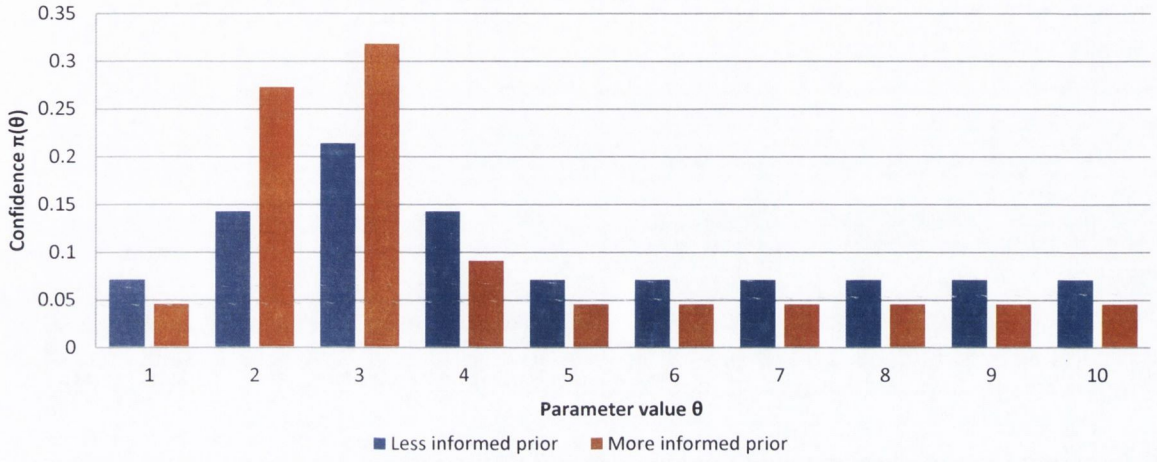

Figure 6.21. A comparison of the shape of a more informed and less informed prior distribution.

The shape of the likelihood function embodies the amount of information contained in the data. If the information contained in the data is small, the likelihood function will be broadly distributed, whereas if the information it contains is large, the likelihood function will be tightly focused around some particular value of the parameter. Figure 6.22 illustrates two likelihood functions, one that contains a lot of information and one that does not contain as much information.

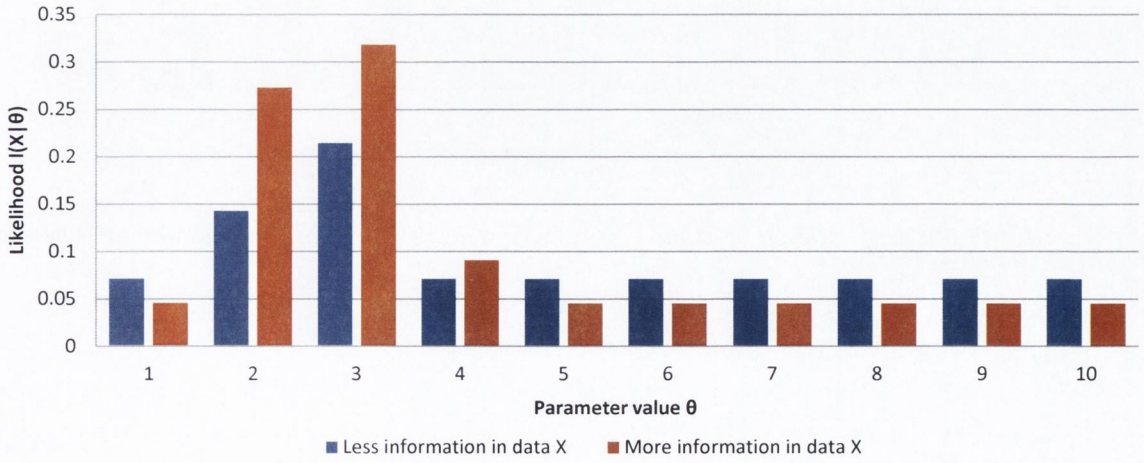

Figure 6.22. A comparison of the shape of likelihood functions for two data sets. The data set with the greatest information has a greater focus.

The amount of information contained in the data can only be measured by how much it changes one's prior belief about the variable. In Figure 6.23, the more flat the likelihood function relative to the prior distribution, the smaller the amount of information the data contains. The likelihood is flat relative to the prior distribution so it has little effect on the level of knowledge. In this case, the prior and posterior distributions will be very similar. In contrast, in Figure 6.24, the prior distribution and likelihood have similar shapes so the posterior distribution is not greatly influenced by the prior distribution. In the next section different types of prior distributions are discussed.

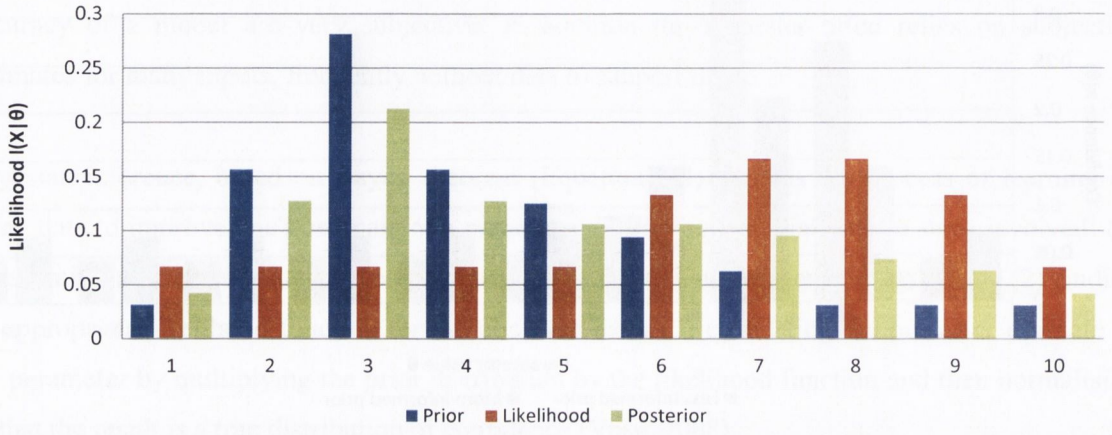

Figure 6.23. The likelihood is flat relative to the prior distribution so has little effect on the level of knowledge (the prior and posterior distribution are very similar).

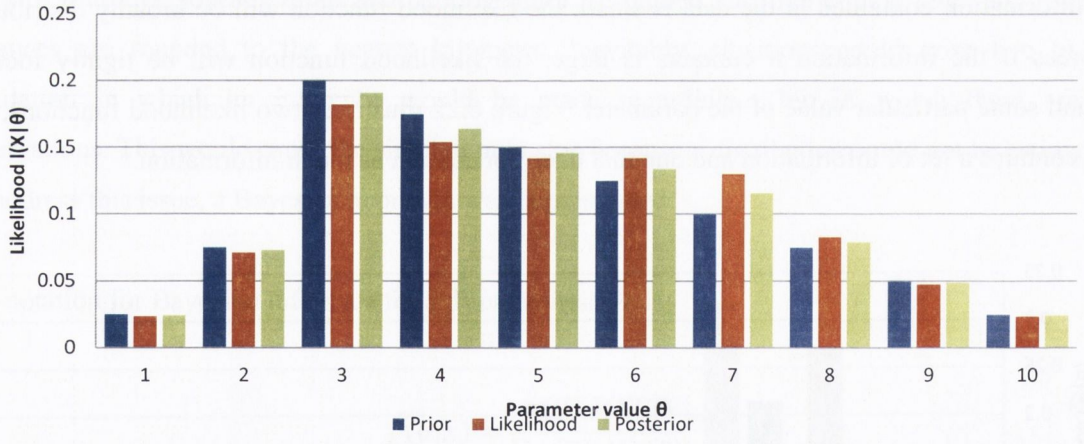

Figure 6.24. The prior distribution and likelihood have similar shapes hence the posterior distribution is not greatly influenced by the prior distribution.

6.8.1 Prior distributions

A prior distribution is a reflection of one's beliefs about a variable prior to observing any relevant data. The determination of the prior distribution is a primary area for criticism of Bayesian inference. This section describes three different types of prior distributions.

An uninformed prior has a distribution that would be considered to add no information to the Bayesian inference. For example, a uniform distribution (Figure 6.25) would be considered an

uninformed prior distribution because it states that prior to the collection of any data, it is believed that every possible value has an equal probability. An uninformed prior distribution reflects the fact that no prior knowledge about the variable is known.

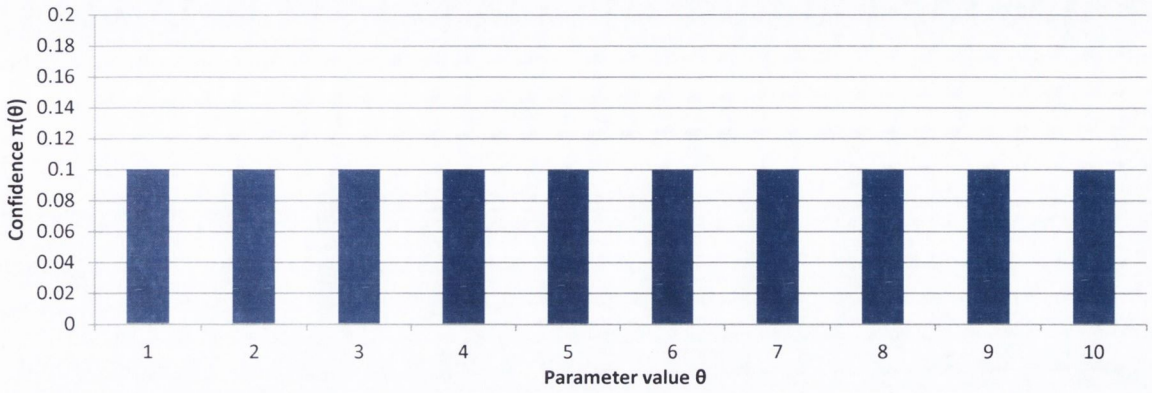

Figure 6.25. Uniformed prior for a discrete parameter.

An informed prior distribution is a distribution that adds information to the Bayesian inference. It is either the result of a previous analysis of other data or it is constructed from an expert's opinion on the parameter. An informed prior distribution reflects some knowledge about the variable. An informed prior distribution can be modelled in various ways. Informed prior distributions can be constructed graphically to describe an expert's estimate or can also be as a result of a logical argument. Figure 6.26 shows an example of an informed prior distribution - its shape is different from that of a uniformed prior distribution.

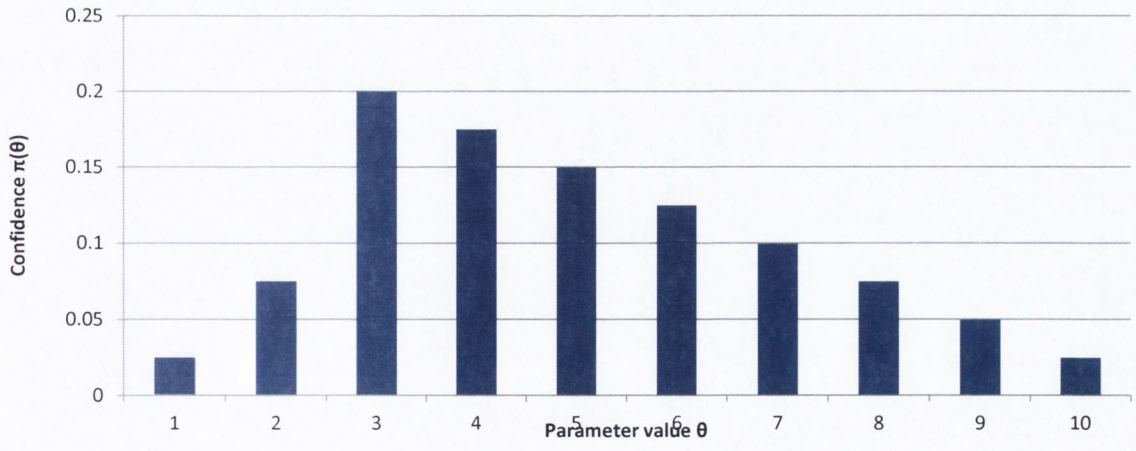

Figure 6.26. Example of an informed prior.

From Bayes theorem, which was presented in Section 6.8, the posterior distribution is equal to the product of the likelihood function $p(X|\theta)$ and the prior $p(\theta)$, normalised by the probability of the data:

$$f(\theta|x) = \frac{\pi(\theta).l(X|\theta)}{\int \pi(\theta).l(X|\theta)d\theta} \tag{6.5}$$

The likelihood function is fixed. Different choices of the prior distribution $p(\theta)$ may make the integral more or less difficult to calculate, and the product $p(x|\theta)p(\theta)$ may take many algebraic forms. For certain choices of the prior distribution, the posterior distribution has the same algebraic form as the prior distribution. In Bayesian probability, if the posterior distribution $p(\theta|x)$ is in the same family of distribution as the prior distribution $p(\theta)$, the prior and posterior are then called conjugate distributions, and the prior distribution is called a conjugate prior for the likelihood function. Conjugate priors are often called convenience priors because they result in a closed form expression for the posterior distribution. Otherwise difficult numerical integration would be required (Vose, 2008). In this model a prior distribution know as a Dirichlet distribution (Frigyik et al, 2010) is used and the theory behind it is presented in the next section.

6.8.1.1 The Dirichlet distribution

The Dirichlet distribution is commonly used as a prior on the parameters to a multinomial distribution and is used in this model. This is because the multinomial distribution is a member of the exponential family, and accordingly, has an associated conjugate prior.

The multinomial distribution is parameterised by an integer n and a pmf $q = [q_1, q_2, \dots, q_k]$, and can be thought of as follows. If there are n independent events, and for each event, the probability of outcome i is q_i, then the multinomial distribution specifies the probability that outcome i occurs x_i times, for $i = 1,2, \dots, k$. If $X \sim Multinomial_k(n, q)$, then its probability mass function is given by (Frigyik et al, 2010):

$$f(x_1, x_2, \dots, x_k|n, q, = (q_1, q_2, \dots, q_k)) = \frac{n!}{x_1! x_2! \dots x_k!} \prod_{i=1}^{k} q_i^{x_i} \tag{6.6}$$

where $n = \sum_{i=1}^{n} x_i$.

The Dirichlet distribution serves as a conjugate prior for the probability parameter q of the multinomial distribution. Let $\pi(\cdot)$ be the density of the prior distribution for Q and $\pi(\cdot\,|x)$ be the density of the posterior distribution. Then, using Bayes rule

$$\pi(q|x) = \gamma f(x|q)\pi(q) \tag{6.7}$$

$$= \gamma \left(\frac{n!}{x_1! x_2! \dots x_{k!}} \prod_{i=1}^{k} q_i^{x_1} \right) \left(\frac{\Gamma(\alpha_1 + \cdots + \alpha_k)}{\prod_{=1}^{k} \Gamma(\alpha_{1)}} \prod_{i=1}^{k} q_i^{\alpha_{1-1}} \right)$$

$$= \gamma \prod_{i=1}^{k} q_i^{a_i + x_i - 1}$$

$$= Dir(\alpha + x)$$

Hence, $(Q|X = x) \sim Dir(\alpha + x)$

The next section describes the methodology for synthesising a schedule of journeys.

6.9 The developed travel pattern model - synthesising a journey schedule

As described in Section 6.3, in step 1 of the simulation the copula function generates a total distance to be travelled in a given day, the number of journeys to be undertaken in the day and the departure time from home (i.e. the start time of the first journey). The second step of the simulation is to iteratively generate values for the individual journey distances, the journey times and parking times between journeys in order to synthesise the daily travel schedule. This is achieved by using conditional distributions with a Bayesian inference. This section describes the methodology for each step in the process and illustrates an example of the procedure.

6.9.1 Individual journey distance distributions

This section presents the methodology for creating distributions and sampling journey distances. The journey distance observations in the database were analysed and four new variables, describing the conditions under which an individual journey distance was travelled, were computed. They are as follows:

1. *The total distance travelled on that day:*

   This variable represents the total distance travelled on the day in which the individual journey was undertaken.

2. *The remaining distance to travel on that day:*

   This variable represents the remaining distance to travel on the day prior to the individual journey being undertaken.

3. *The distance of the previous journey:*

   This variable represents the distance of the previous journey to the journey in question.

4. *Journey number:*

This variable represents the journey number in the day. Instead of labelling the journeys 1, 2,...n, the journeys were labelled as either 1 or 0. The number 1 represents "not the last journey in the day". For example if there were 4 journeys in the day, journeys 1, 2 and 3 would be labelled 1. The number 0 represents the last journey of the day. The reasoning behind this logic is explained in the following paragraphs.

An example of the data is presented in Table 6.1. Taking the first row as an example, a journey of 6 km was travelled on a day in which the total distance travelled was 12 km, the remaining distance to travel on the day prior to undertaking the journey was 8 km, the distance of the previous journey was 4 km and it was not the last journey of the day.

Table 6.1. Example data of the four variables created to describe the conditions in which a journey was undertaken.

Distance	Total distance travelled on the day	Remaining distance to travel in the day	Distance of previous journey	Journey number
6	12	8	4	1
2	12	2	6	0
8	40	40		1
2	40	32	8	1

A limit of using condition distributions for modelling is that the number of observations returned from a database is dependent on the number of conditions placed on a distribution. The more conditions that are placed on a distribution the less observations that are returned from the database. Therefore, throughout the modelling it was important to find the right balance between the number of conditions placed on a distribution and efficiently estimating a distribution.

The methodology for creating a distribution of journey distances is described hereafter and is demonstrated by way of an example. There are three possible sets of conditions, listed in Table 6.2, which can be placed on a distribution. The conditions implemented are determined by the journey number. In order to maximise the amount of data retuned from the database it was necessary to limit the number of conditions that were placed on a journey distance distribution to two. Journey number 1 is only conditioned on the total distance travelled in the day. Every second journey (i.e. journey numbers 2, 4, 6, 8, and 10) are conditioned on the distance of the previous journey and the remaining distance to travel. Odd numbered journeys (i.e. journey numbers 3, 5, 7, 9, and 11) are conditioned on the remaining distance to travel and the journey number. Every second journey was conditioned on the distance of the previous journey because the assumption was that the return leg of a journey should be conditioned on the outward journey. Table 6.2 also lists the type of prior distribution implemented for each journey number and the degree to which the distributions are truncated, which are discussed in the next section.

Table 6.2. The sets of conditions placed on a distribution of journey distances, determined by the journey number. The type of prior distribution used and the degree of distribution truncation.

Journey number	Condition on the distribution	Type of prior distribution	Degree of truncation
1	The total distance travelled	Uniformed distribution (i.e. uniform distribution)	Between 1 km and ½ the total distance to travel
2, 4, 6, 8, 10	The distance of the previous journey and the remaining distance to travel in the day	Informed distribution	Between 1 km and ¾ of the remaining distance to travel
3, 5, 7, 9, 11	The remaining distance to travel and the journey number	Uniformed distribution (i.e. uniform distribution)	Between 1 km and ¾ of the remaining distance to travel

6.9.1.1 Generating journey distance distributions

This section provides a demonstration of the methodology to generate individual journey distances, step 2 in the simulation. Assume that the copula function generated a total distance to travel of 40 km and 4 journeys for the day. Denote the distances of the journeys as x_1, x_2, x_3, and x_4.

Simulating journey number one

The distance of the first journey, x_1, is generated from the distribution of all journey distances given that the total distance travelled on the day was 40 km.

$$f(x_1 | \text{ The total distance travelled on the day } = 40 \text{ km}) \tag{6.8}$$

A uniform prior distribution is assumed (i.e. it is the prior belief that each journey distance is equally likely) (Figure 6.27). Next, the probability of observing a journey distance X, the likelihood function, is computed by observing the data in the dataset (Figure 6.28). The posterior distribution is computed by multiplying the prior distribution by the likelihood function and normalising the result (Figure 6.29). As the number of journeys is greater than two, a situation in which x_1 is very large (e.g. 35 km) has to be avoided. This would result in x_1 being very large and the remaining journey distances, x_1, x_2 and x_3 being very small, which could be unrealistic. Therefore, the distribution is truncated to only allow it to generate a distance in the range 1 to 20 km (half of the total distance for the day). Assume a distance of 9 km is sampled from the posterior distribution for x_1.

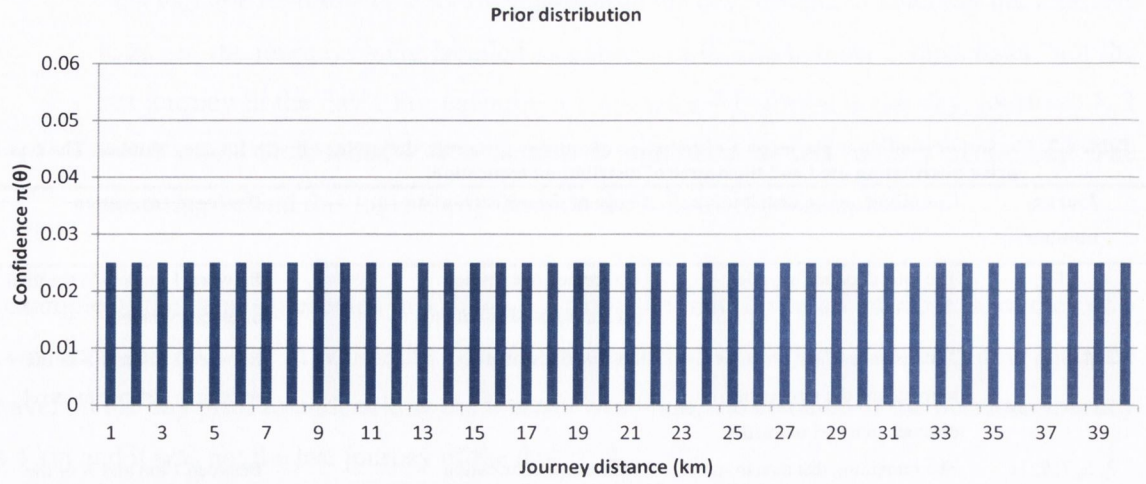

Figure 6.27. A uniform prior distribution is assumed for x1.

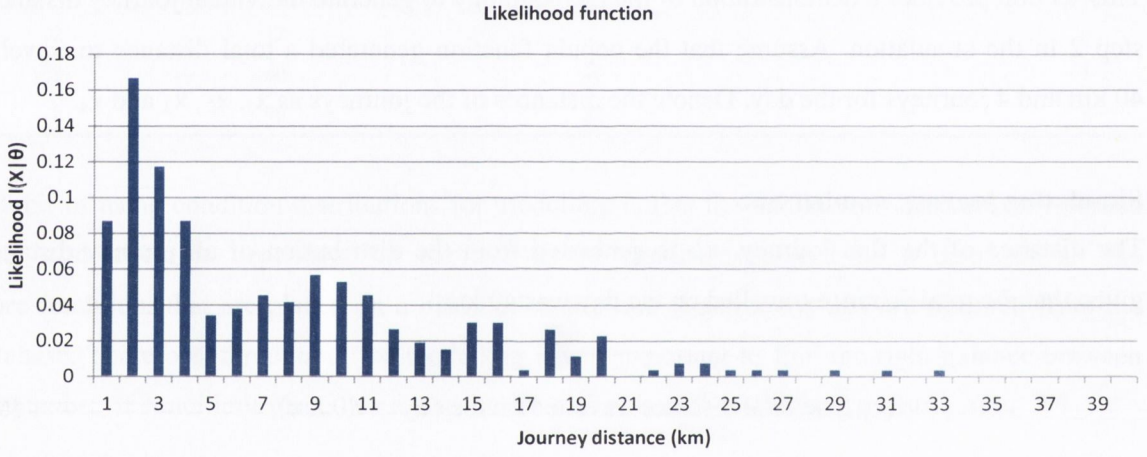

Figure 6.28. The likelihood function for the dataset.

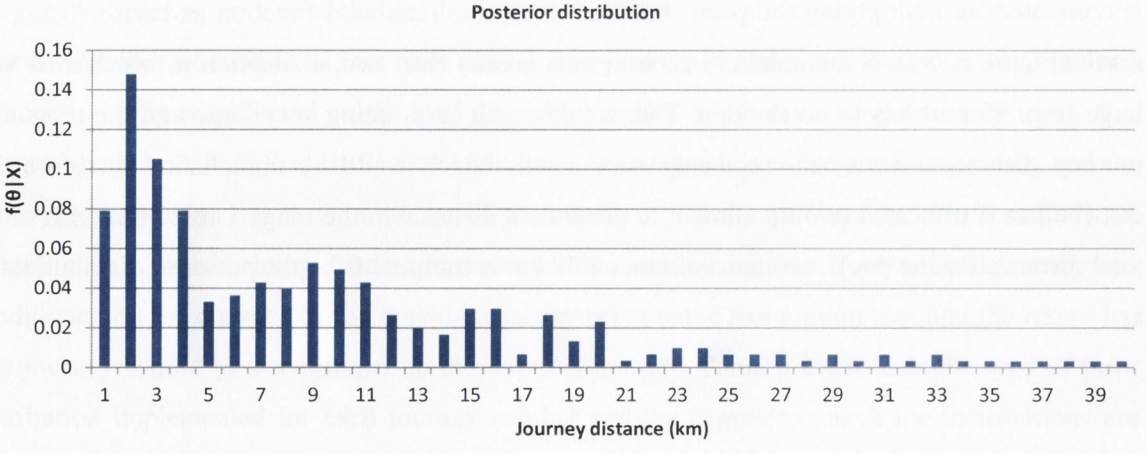

Figure 6.29. The posterior distribution for x1.

Simulating journey number two

The distance of the second journey, x_2, is generated from the distribution of all journey distances given that the previous journey was 9 km and that the remaining distance to travel is 31 km (i.e. 40 km – 9km).

$$f(x_2|\ x_1 = 9\text{km and the remaining distance to travel} = 31) \tag{6.9}$$

An informed prior distribution is assumed. As x_1 was 9km, a hyperparameter (a parameter of a prior distribution) value of 3 is assigned to the distance value of the previous journey and to the distances immediately either side of the previous journey distance (i.e. 8, 9 and 10 km). A hyperparameter value of 2 is assigned to the distance values immediately either side of the distance values which are assigned a hyperparameter value of 3 (i.e. 7 and 11 km) and a hyperparameter of 1 is assigned to the remaining distance values. The result is a triangular shaped prior distribution for x_2, indicating that the prior belief is that for example a journey distance of 8 km is three times more likely than a journey of for example of 15 km (Figure 6.30). This is a subjective opinion and the validity of the assumption is evaluated in Section 6.7.1.2. The probability of observing a journey distance X, the likelihood function, is computed by observing the data in the dataset (Figure 6.31). The posterior distribution is computed by multiplying the prior distribution by the likelihood function and normalising the result (Figure 6.32). Similar to journey number one, the distribution is truncated to only generate a distance in the range 1 to 23 km (three quarters of the remaining distance). Assume a distance of 10 km is sampled from the posterior distribution for x_2.

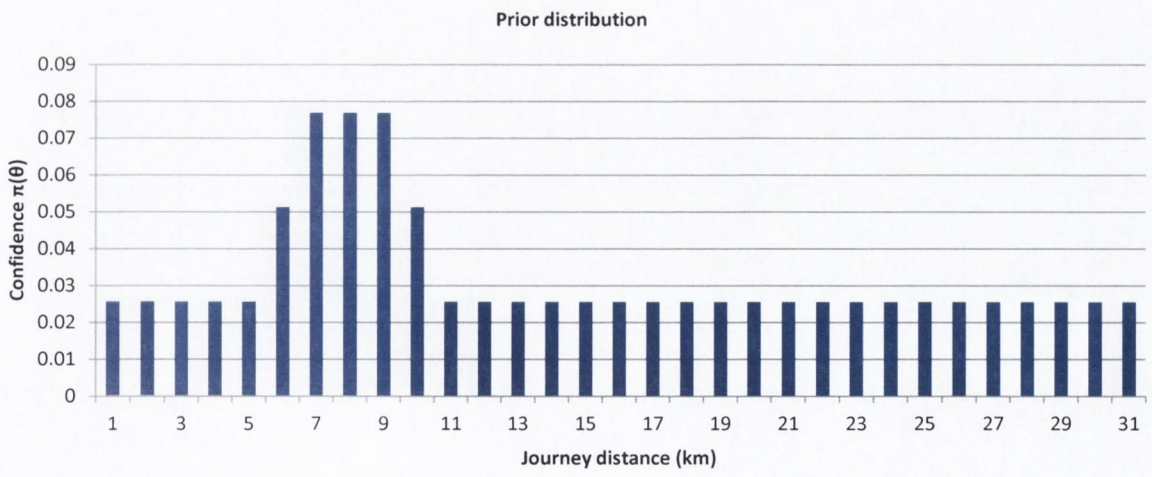

Figure 6.30. An informed prior distribution was assumed for x1.

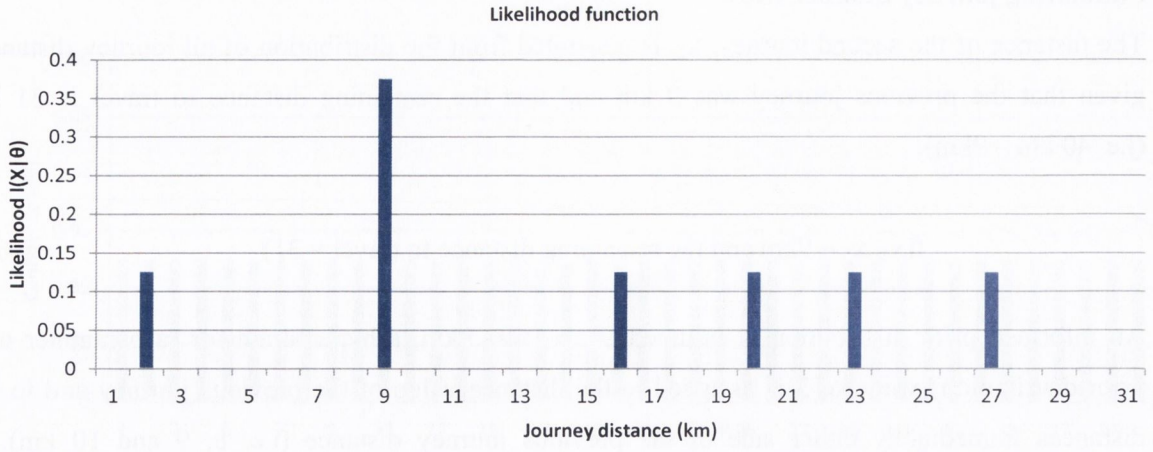

Figure 6.31. The likelihood function for the dataset.

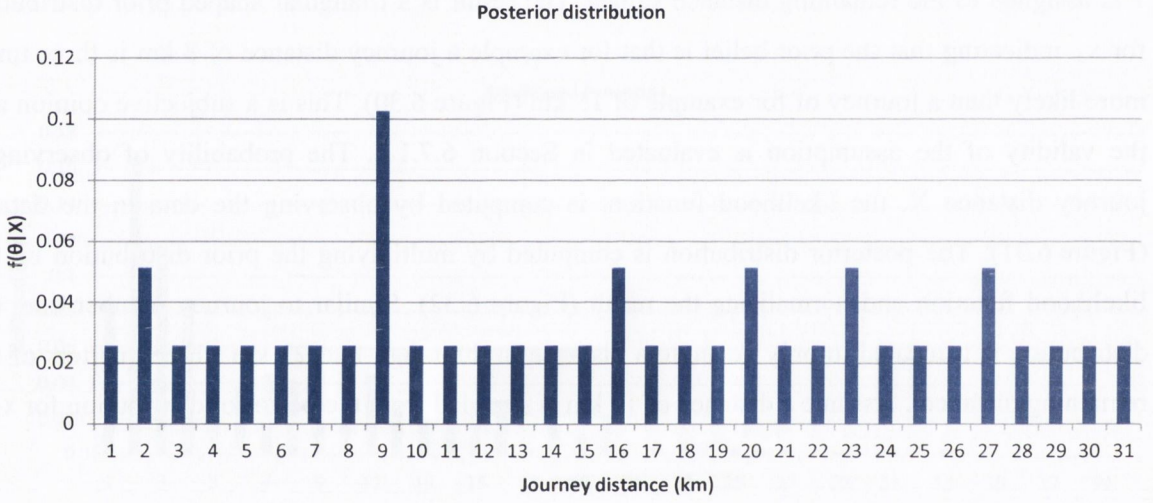

Figure 6.32. The posterior distribution for x2.

Simulating journey number three

The distance of the third journey, x_3, is generated from the distribution of all journey distances given that the remaining distance to travel is 21 km (i.e. 40 km – 9km – 10km) and that the journey is not the last journey in the day.

$$f(x_3|\text{ remaining distance to travel} = 21 \text{ km and the journey number} = 0) \quad (6.10)$$

Similar to journey number 1, a uniform prior distribution is assumed (Figure 6.33). The probability of observing a journey distance X, the likelihood function, is computed by observing the data in the dataset (Figure 6.34). The posterior distribution is computed by multiplying the prior distribution by the likelihood function and normalising the result (Figure 6.35). Similar to the previous journeys, the distribution is truncated to only generate a distance in the range 1 to 16 km (three quarters of the remaining distance). Assume a distance of 8 km is sampled from the posterior distribution for x_3.

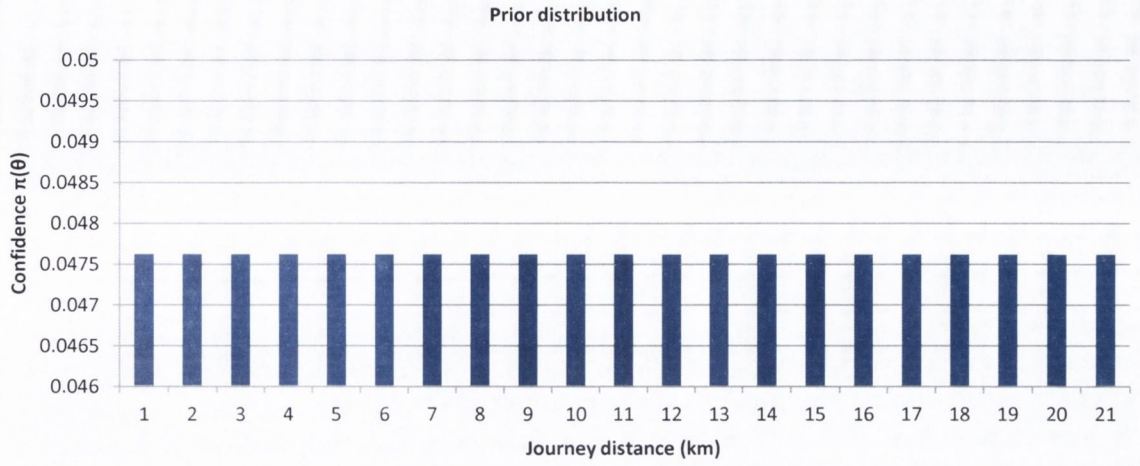

Figure 6.33. A uniform prior distribution was assumed for x3.

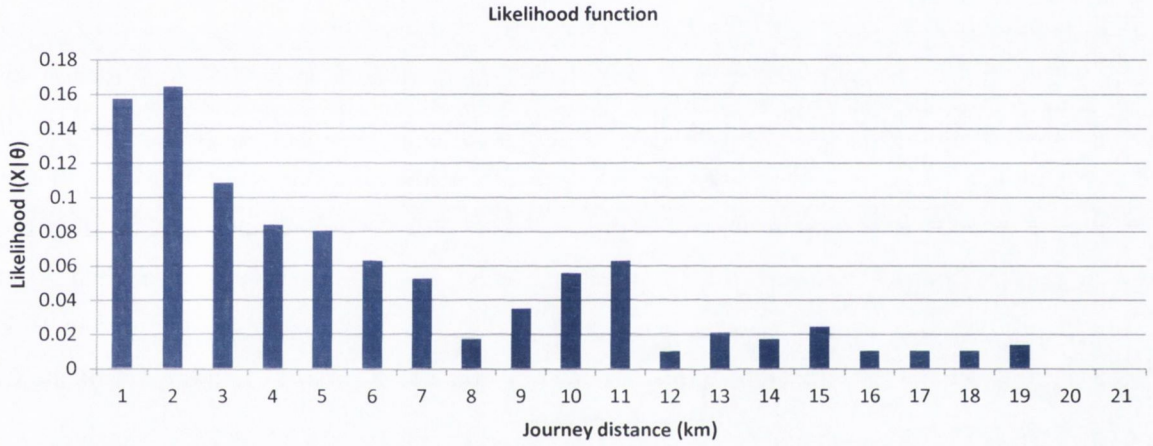

Figure 6.34. The likelihood function for the dataset.

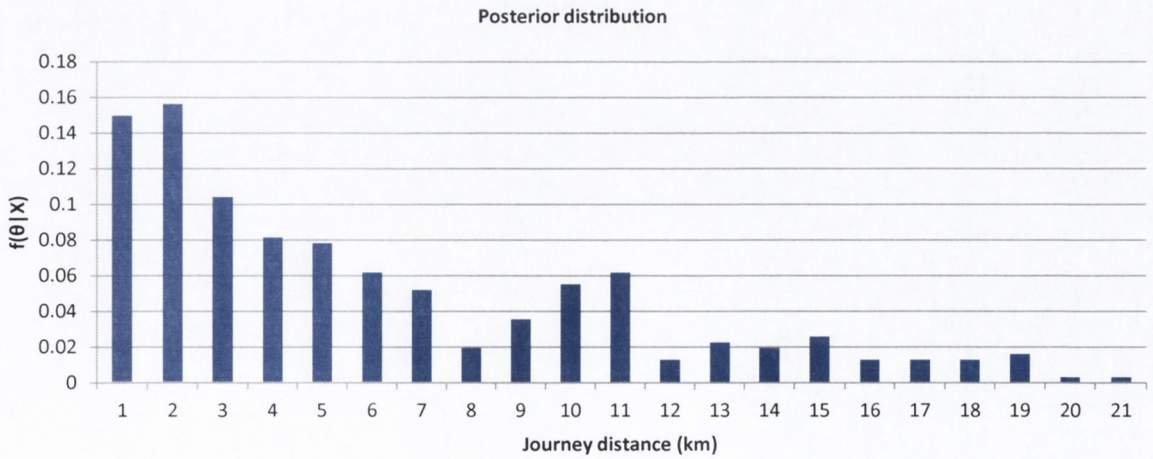

Figure 6.35. The posterior distribution for x3.

Simulating journey number four

The last journey of the day, in this example, the distance of the fourth journey, x_4, is calculated by subtracting the sum of the individual journey distances from the total distance to be travelled in the day.

$$x_4 = 40 - x_1 - x_2 - x_3 = 13 \text{ km} \tag{6.11}$$

6.9.1.2 Validation of the journey distances modelling

In order to verify the assumptions made regarding the conditional distributions from which the individual journey distances are generated, the distributions of the simulated and observed real-world journey distances were analysed. A Chi-Square goodness of fit test was performed on the simulated and observed journey distances. The test rejected the null hypothesis that the simulated and the observed journey distances were from the same distribution at the 95% confidence level. However, a graph of the expected and observed frequencies of each journey distance indicates that the distributions are sufficiently close for the purposes of the simulation (Figure 6.36). A graph indicating which journey distances statistically contribute the most to the significant difference can be found in Appendix F. The graph indicates that larger journey distances (greater than 30 km) contribute most to the significant difference, but significantly journey distances less than 10 km, which account for 90% of all journey distances, only contribute to approximately 5% of the Chi-Square value.

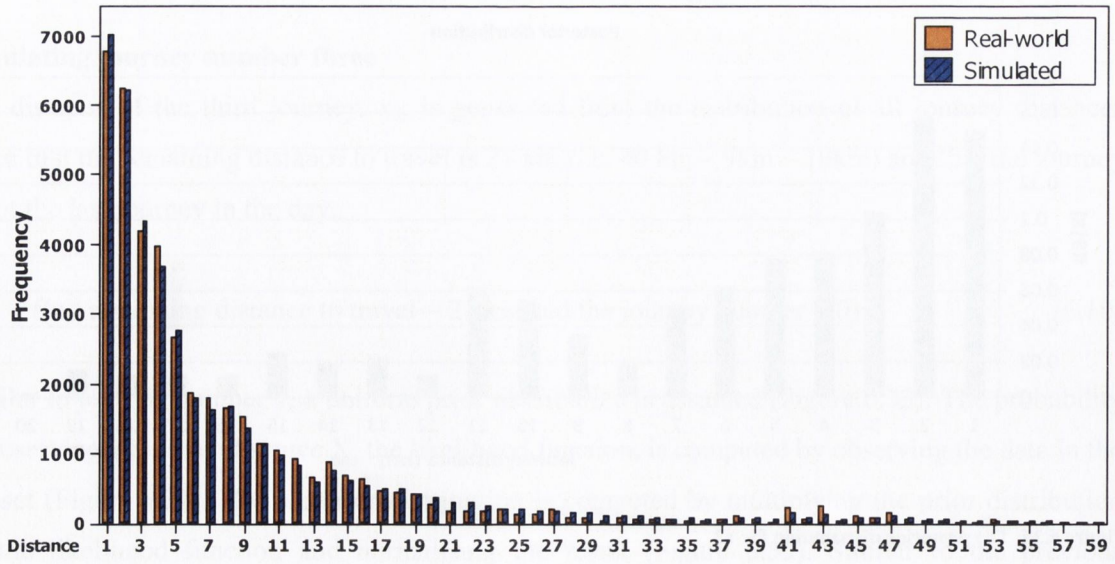

Figure 6.36. Frequencies of the simulated and the expected real-world journey distances.

6.9.2 Generating journey time distributions

This section demonstrates the methodology for creating the journey time distributions, step 3 in the simulation. The distribution for the time taken to complete a journey is conditioned on the starting time (± 10 minutes) and distance of the journey (Equation 6.12).

$$f(\text{Journey time}|\ \text{journey start time } (\pm\ 10 \text{ minutes}),\ \text{journey} \tag{6.12}$$

An informed prior distribution is assumed. The prior distribution is created by assigning a large hyperparameter to the expected journey time (given the start time and the distance of the journey) and hyperparameters decreasing in value to the journey times either side of the expected journey time. A demonstration of the methodology to create the distribution of journey times for journey number one from the example in the previous section is presented here.

The journey in question has a start time of 8 am and a distance of 9 km. The rule for creating the prior distribution is that if the journey start time is between 7-10 am or 4-7 pm an average speed of 30 km/hr (representing traffic congestion in peak periods) is assumed and at all other times an average speed of 45 km/hr is assumed. Therefore, in this example, the average speed for the journey would be 30 km/hr. From the relationship, $distance = speed\ x\ time,$ the expected journey time would be approximately 20 minutes (rounded to the nearest 5 minutes). Therefore, a hyperparamter value of 3 would be assigned to the expected journey time (i.e 20 minutes), a hyperparamter value of 2 would be assigned to the journey times immediately either side of the expected journey time and a hyperparamter value of 1 would be assigned to the journey times either side of the journey times that were assigned a hyperparamter value of 2. The result is a triangular shaped prior distribution for the journey time, indicating that the prior belief is that a journey time of 20 minutes is three times more likely than a journey time of for example of 30 minutes (Figure 6.37). Next, the probability of observing a journey time X, the likelihood function, is computed by observing the data in the dataset (Figure 6.38). The posterior distribution is computed by multiplying the prior distribution by the likelihood function and normalising the result (Figure 6.39). Assume a journey time of 15 minutes is sampled from the posterior distribution.

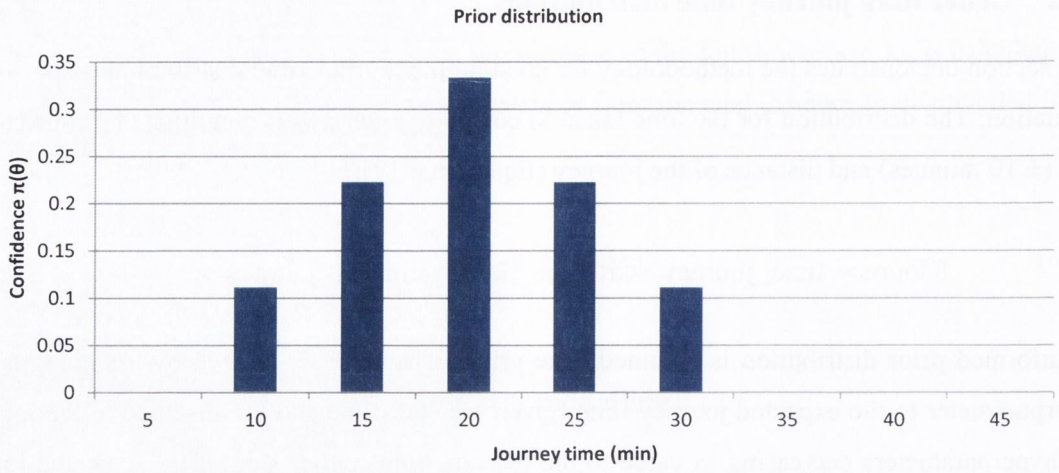

Figure 6.37. An informed prior distribution was assumed for the journey time.

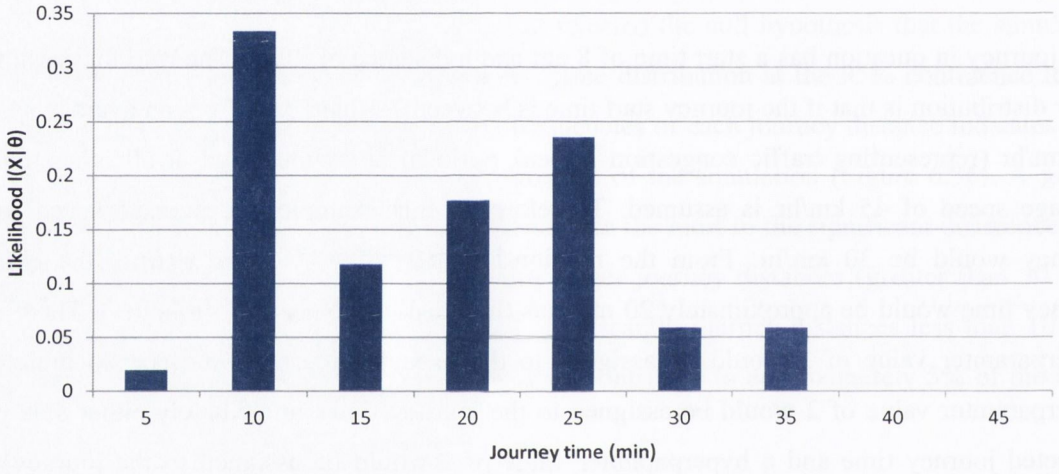

Figure 6.38. The likelihood function for the dataset.

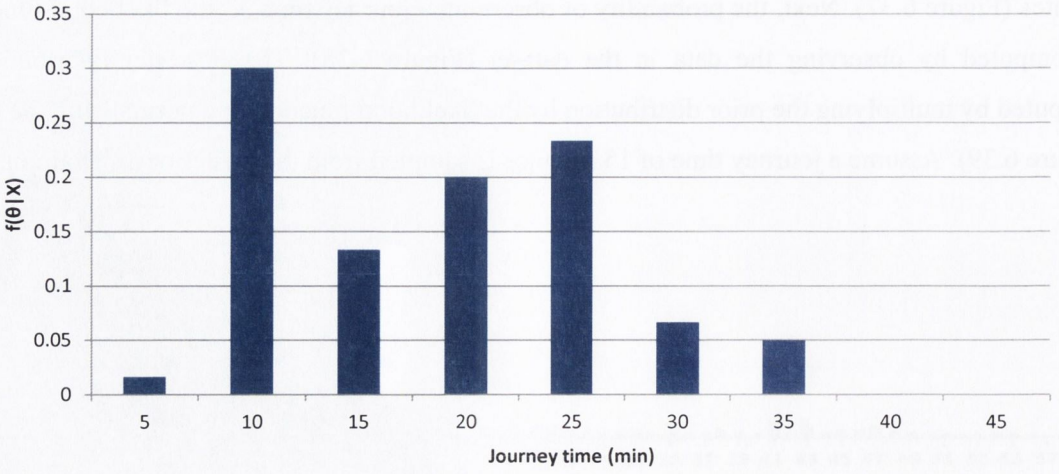

Figure 6.39. The posterior distribution for the journey time.

6.9.3 Parking time distributions

This section demonstrates the methodology for creating the parking time distributions, step 4 in the simulation. Given the complexity of the problem and the numerous possible variables that could influence parking time, creating the parking time distributions was the most challenging aspect in the development of the model. The distribution of parking times is conditioned on the end time of the journey (± 30 minutes), the time already parked that day (± 30 minutes), the journey time (± 10 minutes) of the previous journey and the journey number (Equation 6.13). The variable, the time already parked that day, was created and used as a condition on the distribution to try and ensure that the journey schedules generated remain in the 24 hour time period. This prevents for example a parking time of 8 hours being generated at 6 pm when there are still 1 or 2 journeys to be undertaken in the remainder of the day. It also accounts for the time a vehicle has already been parked that day, for example if a vehicle was parked for 8 hours during the day then it is reasonable to assume that the parking times between the reminder of the journeys in the day will be relatively short. In addition, a maximum cumulative parking time of 12 hours (720 minutes) was permitted over the course of a day, not including the overnight parking time.

$$f(\text{parking time}|\ \text{journey end time}\ ,\ \text{time already parked, journey time, journey} \tag{6.13}$$

An example of the data is presented in Table 6.3. Taking the first row as an example, a parking time of 560 minutes occurred when a journey ended at 08:25 am and took 20 minutes to complete. The time already parked that day was 0 minutes, indicating that it was the first journey of the day. The time already parked is only counted after a journey is completed. On the second row, a parking time of 220 minutes occurred when a journey ended at 18:15 pm and took 30 minutes to complete. The time already parked that day was 560 minutes, indicating that the vehicle was already parked for 9 hours and 20 minutes earlier during the day.

Table 6.3. Example data of the conditions on a parking time distribution.

Journey end time	Time already parked that day (min)	Journey time (min)	Parking time (min)	Journey number
08:25:00	0	20	560	1
18:15:00	560	30	220	2

Initially in keeping with the structure of the model, a Bayesian approach to modelling the parking times was implemented in the model. To illustrate this approach, a demonstration of the methodology to create the distribution of parking times for journey number one from the example in the previous section is presented here.

The journey in question had a journey end time of 8:15 am, the time already parked was 0 minutes (as it was the first journey of the day), the journey time was 15 minutes and it was journey number 1 of the day. A uniform prior distribution was assumed (Figure 6.40) because given the complexity of the problem it was not possible to formulate a rule for an informed prior distribution. Next, the probability of observing a parking time X, the likelihood function, was computed by observing the data in the dataset (Figure 6.41). The posterior distribution was then computed by multiplying the prior distribution by the likelihood function and normalising the result (Figure 6.42).

Figure 6.40. The prior distribution of the parking time.

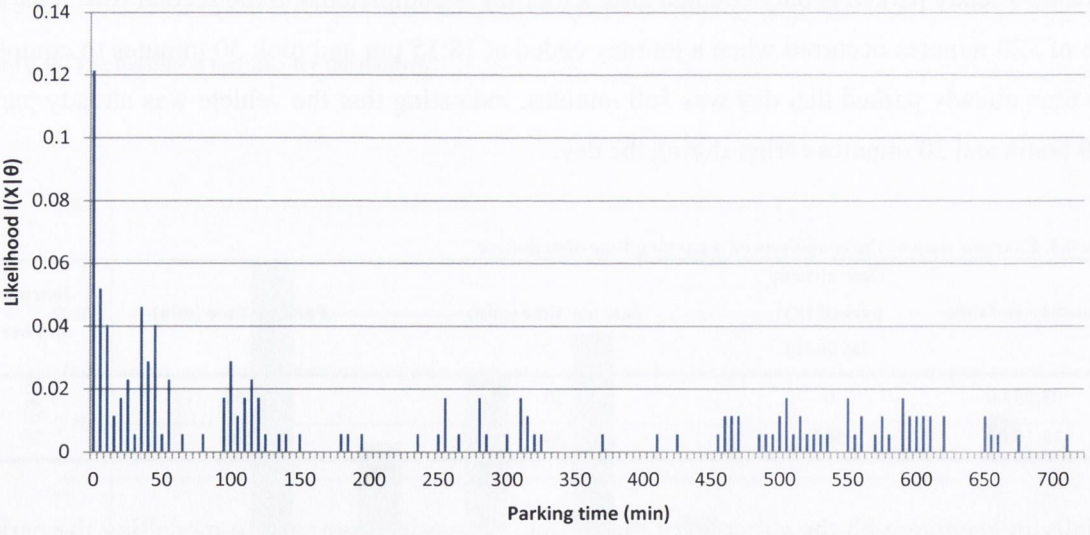

Figure 6.41. The likelihood function of the parking time.

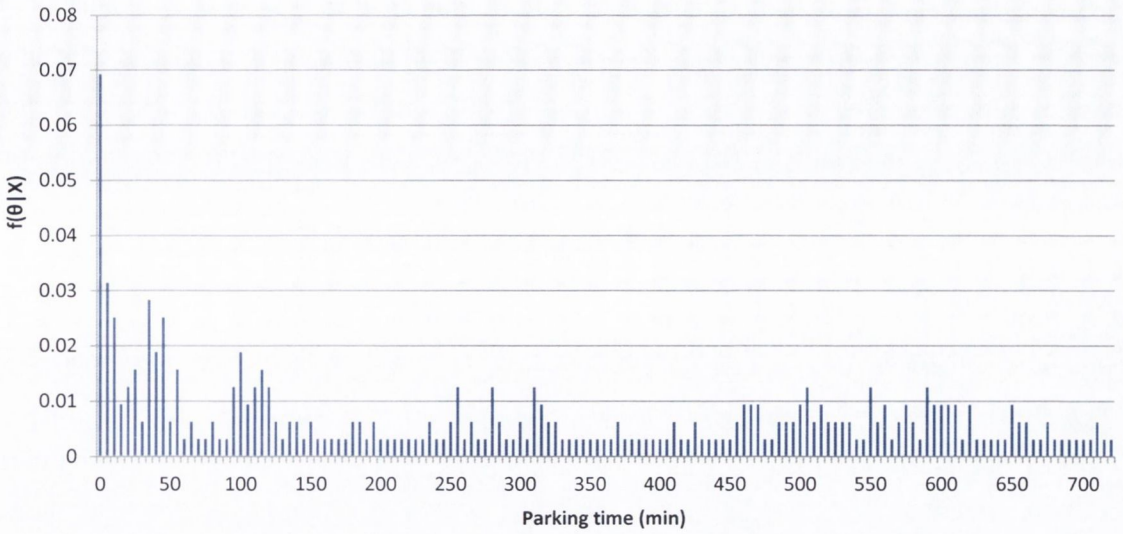

Figure 6.42. The posterior distribution of the parking time.

However, it was determined that the Bayesian approach to modelling the parking times did not produce satisfactory results. Given the number of conditions on the distribution (4), typically a small amount of data are returned from the database following a query. Combining this data (the likelihood function) with the uniform prior distribution resulted in a relatively flat posterior distribution from which a parking time would be sampled from.

To improve the performance of the model, if data are retuned from the database following a query, it was decided to just create an empirical distribution directly from the data and to sample a parking time from that distribution. Figure 6.43 illustrates the empirical parking time distribution from the example described above.

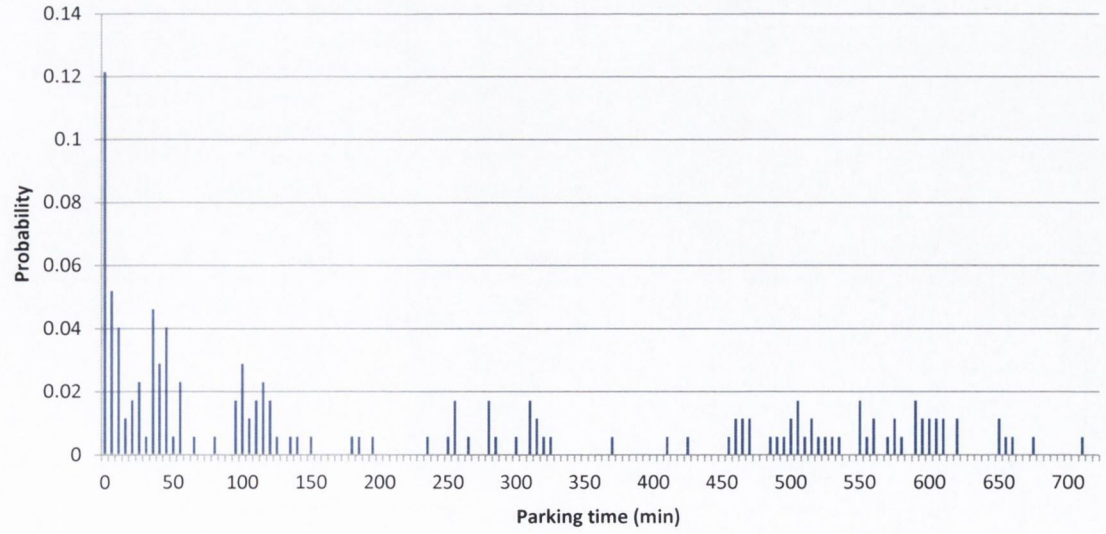

Figure 6.43. The empirical parking time distribution.

When data are not returned from the database, typically 13% of the time during a simulation, the Bayesian approach is implemented. The probability of observing a parking time X, the likelihood function would be zero (as no data would be returned from the database) hence the posterior distribution, from which a parking is sampled from, would be uniform, the same as the prior distribution.

6.10 Model validation

This section compares the developed stochastic simulation model to the deterministic model. The deterministic model uses all the data directly in the database, approximately 18,300 journeys, to create the weekly driving profile presented in Figure 6.45. There are two peaks in driving during weekdays, corresponding to morning and evening commutes. Considering the use of the vehicles, it is reasonable to assume that distributions of the variables on weekdays are similar, therefore the observations for weekdays are aggregated together (Figure 6.46). The arrival time home in the evening (i.e. the stop time of the last journey) is presented in Figure 6.48 (orange bar).

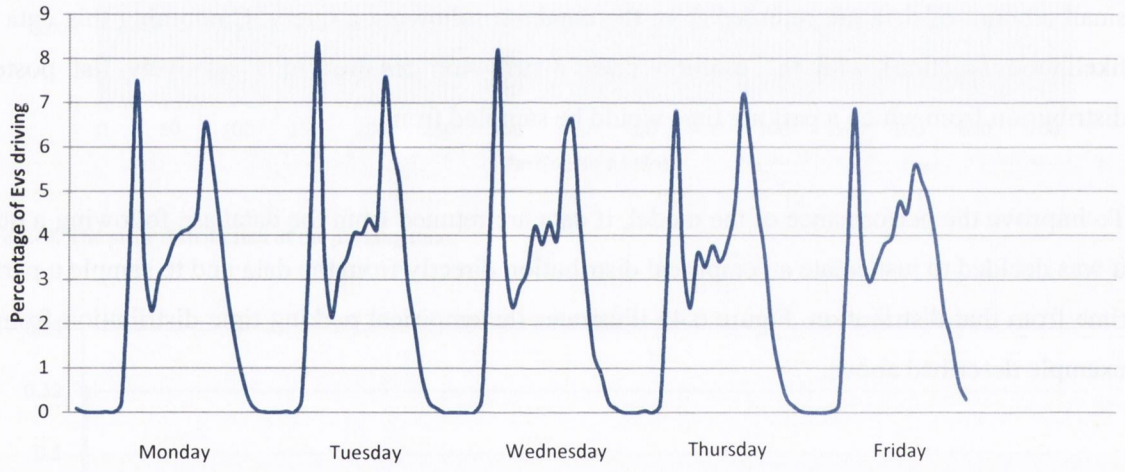

Figure 6.44. Percentage of EVs driving (hourly average).

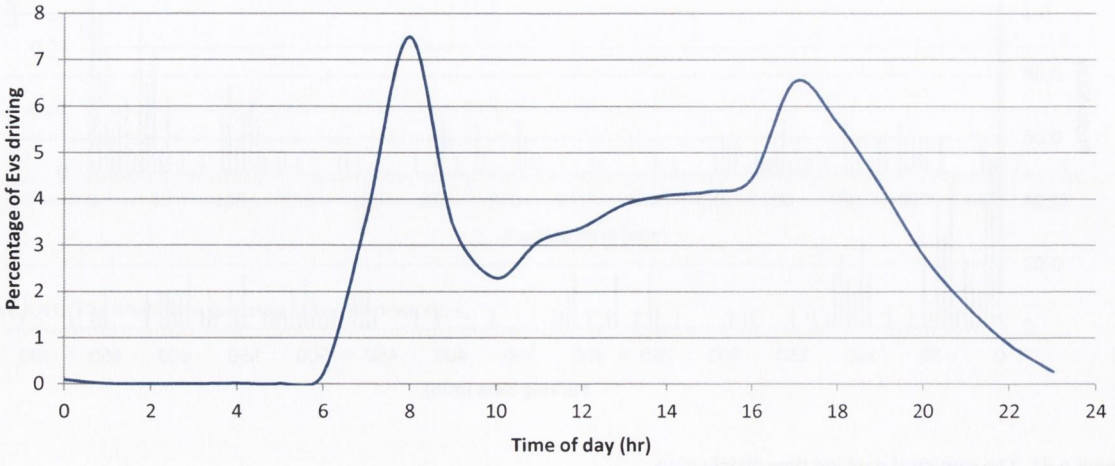

Figure 6.45. Percentage of EVs driving by hour of day (aggregated data).

In order to analyse the scenario of one hundred thousand EVs, the simulation is run for 1,800 EVs and the results scaled up accordingly. This is repeated twenty times to represent 20 days. Figure 6.47 illustrates the travel profiles for 20 days. The basic principle of a Monte Carlo simulation, uncertainty propagation, is evident in the resulting shapes of the travel profiles. The trend of a daily travel profile is reproduced for each day. However, compared to Figure 4.6, the evening peak in the number of vehicles travelling is not as prominent as observed in the real-world data.

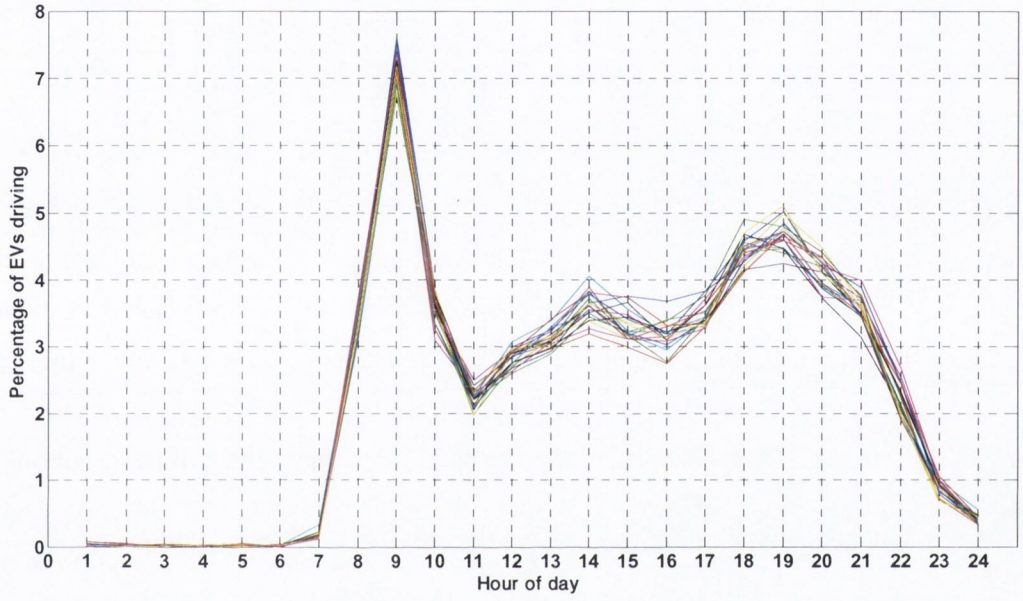

Figure 6.46. A 20 day simulation of the percentage of EVs driving per hour.

Figure 6.48 illustrates that the arrival time home distribution simulated by the model does not match the deterministic distribution exactly. A Chi-squared goodness of fit test confirms this by rejecting the null hypothesis at the 95% confidence interval that the two distributions match. There are a higher proportion of vehicles than expected arriving home between the hours of 9 am and 5 pm and correspondingly fewer vehicles than expected arriving home between 5 pm and 12 am. A number of vehicles are also simulated arriving home between 1 am and 7 am. This is due to large parking times (e.g. 10 hours) being generated in the evening (e.g. 6 pm) from the uniform parking time distribution when the Bayesian approach is implemented.

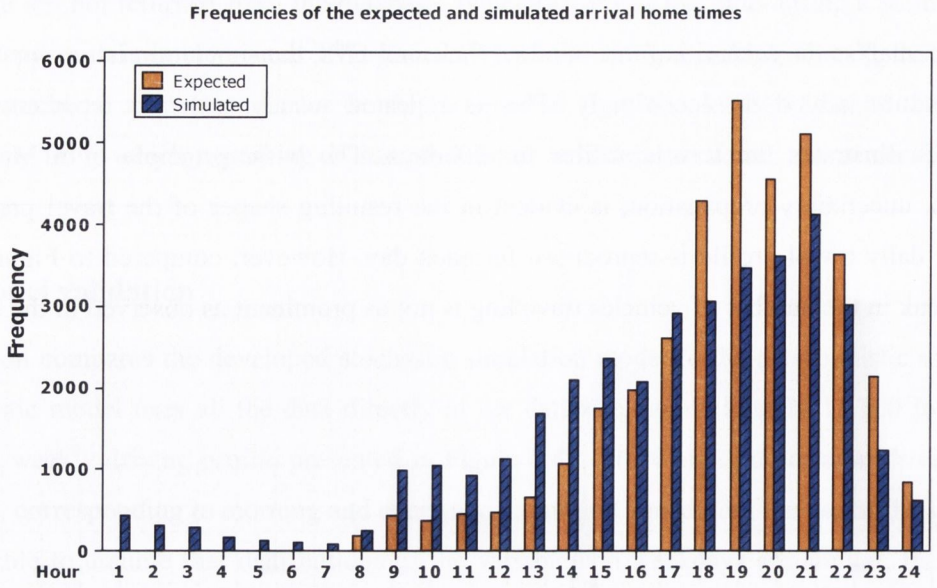

Figure 6.47. Frequency distribution of the simulated and expected arrival home times.

An investigation of the distribution of the simulated parking times between journeys reveals the source of the error in the model. Figure 6.49 illustrates the frequency distribution of the simulated parking times between journeys and the observed parking times between journeys for a 5 hour period. The distributions are well matched except for the frequency of 0 minute and 5 minute parking times. The model simulates more than expected 0 minute and 5 minute parking times between journeys. This explains why more vehicles arrive home earlier than expected. The existence of this property in the model can be attributed to the conditions placed on the parking time distributions. As demonstrated in Figure 6.19 in Section 6.7, 0 minute and 5 minute parking times are the most frequent parking times between journeys. Furthermore, as discussed in Section 1.7.3, the bounds on the conditions of the parking distributions are not set exact. As a reminder, the distribution of parking times is conditioned on the end time of the journey (± 30 minutes), the time already parked that day (± 30 minutes), the journey time (± 10 minutes) of the previous journey and the journey number. By allowing the conditions to return data within ± 30 minutes of the conditions on the distributions, the number of 0 and 5 minute parking time intervals returned are greater and thus they have a higher probability density. This results in a higher frequency of 0 and 5 minute parking time intervals between journeys being simulated in the model, which results in vehicles arriving home earlier than expected.

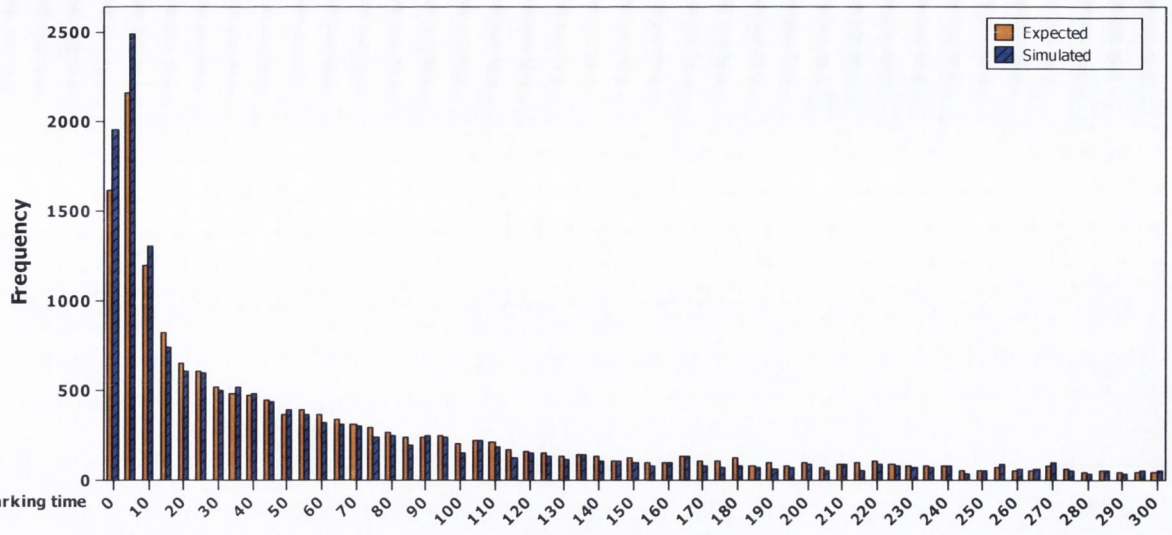

Figure 6.48. Frequency distribution of the simulated and expected parking time intervals.

6.11 Summary and conclusions

This chapter presented a Monte Carlo simulation approach to simulate the travel patterns of EVs. The results indicate that the proposed model is a step toward accurate travel pattern modelling for a population of EVs. The core variables of the model, departure time from home, the number of journeys undertaken and the total distance travelled on consecutive days are characterised by stochastic behaviour and are correlated. Therefore, a multivariate distribution function was built using an empirical copula function and the respective marginal empirical distributions. Using an iterative method of conditional pdfs with a Bayesian inference the journey schedules of individual vehicles were synthesised. The travel patterns simulated by the model were shown to adhere closely to the deterministic data.

The model is evaluated with the explanatory variable, arrival time home. The current structure of the model simulates in a higher proportion of vehicles than expected arriving home between the hours of 9 am and 5 pm and correspondingly fewer vehicles than expected arriving home between 5 pm and 12 am. Coupled by a shortage of data and the complexity of modelling parking times, the loss of accuracy in the model can be primarily attributed to the simulated parking times between journeys. The number of observations returned from the database is dependent on the number of conditions placed on a distribution. As there were only 18,300 journeys in the database the number of conditions placed on the distributions was limited to four, the journey end time, the journey number, the time already parked in the day and the journey time. Increasing the number of conditions on the parking time distributions and by narrowing the bounds around the conditions down from ±30 minutes would most likely improve the accuracy of the parking time distributions and hence the overall accuracy of the model. However, adding dependencies is done at the cost of increasing the number of dimensions, drastically increasing the amount of data needed for efficient

estimation of the pdfs. In addition, the Bayesian approach to generating the parking times, which is implemented approximately 13% of the time in a simulation relies on a uniform prior distribution. This assumes that all parking times are equally likely which could be an unrealistic assumption.

Compared to existing studies this model attempted to synthesise precise journey schedules on an individual basis, using travel data from EVs, as opposed to modelling journeys to and from the home or the workplace of a fleet of vehicles using data pertaining to travel surveys or data collected by ICEVs. However, whilst the travel patterns simulated by the model were shown to adhere relatively close to the deterministic data, the additional complexity of the model structure adversely affects the performance of the model. The developed methodology is flexible but future work is needed to fully investigate the usefulness of the current model structure. Refinement of the model could improve the model's usefulness as a tool to predict the large scale travel patterns and subsequently large scale fleet charging patterns.

6.12 Areas for further study

In relation to the current model structure, the implementation of an informed prior distribution as opposed to a uniform prior distribution for generating parking times is an aspect requiring further development.

In future work, when modelling individual travel patterns it would be beneficial to electricity utilities to incorporate vehicle location into such a model using GPS data as the location of charging has implications for local distribution networks. Furthermore, the parking time of a vehicle should ideally be conditioned on the current location. There are a number of approaches in literature for vehicle trip prediction, for example, Simmons et al (2006) developed a hidden Markov model to predict driver routes. Figure 6.50 illustrates journey end locations for a period of 3 months in Limerick city for a participant in the EV demonstration project refferred to earlier. If the GPS data from each stop location was used there would be a very high number of potential locations (red circles).

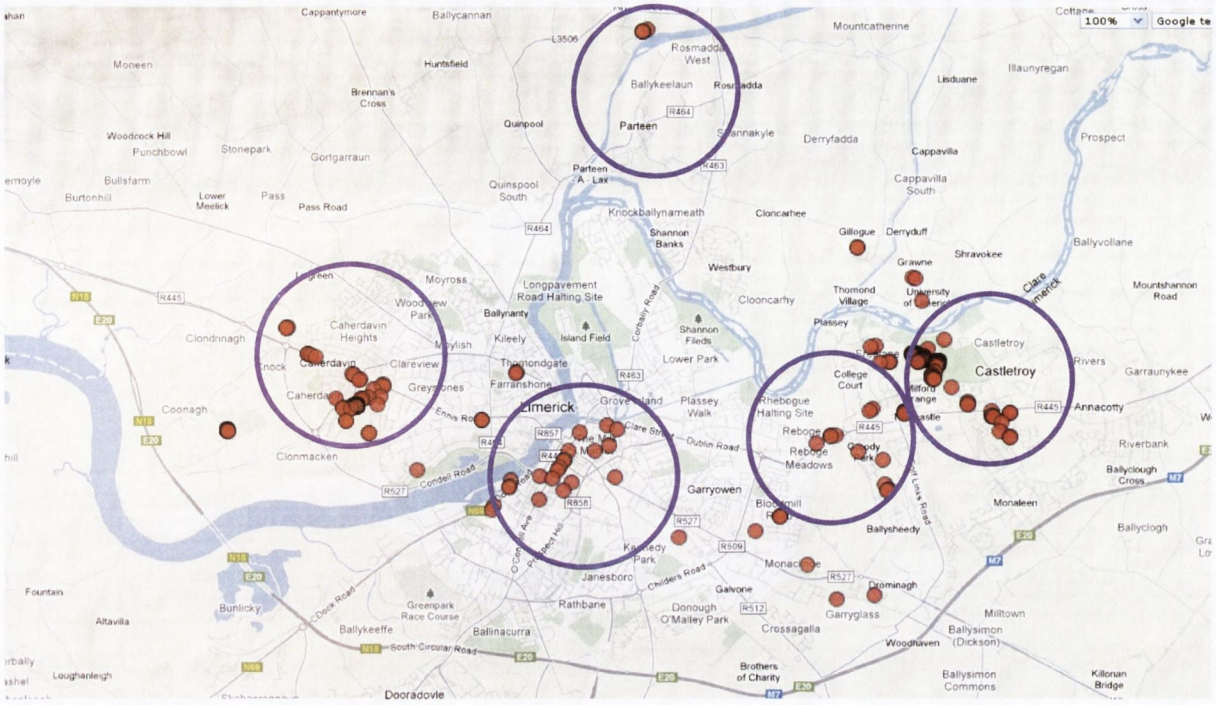

Figure 6.49. Illustration of the potential clustering of GPS locations for an EV driver in Limerick City.

A solution would be to cluster locations to identify geographical areas (e.g. a 1x1 kilometre area) in which an individual frequents regularly (purple circles). This would greatly reduce the number of potential locations (note the purple circles are for illustration purposes only and not the results of clustering). However, incorporating location into the model would prevent the aggregation of data as locations are unique to each individual. This would result in a large amount of data being required for each individual driver in order to implement an iterative condition distribution method, similar to the developed model. In order to include location into such a model then a Markov chain approach would be a better option as such a large amount of data for each individual would not be required. A transition probability matrix of locations could be created for an individual using logged data and used to simulate the travel patterns of the individual in terms of location. Then the parking time could be conditioned on each location.

Figures 6.51 and 6.52 illustrate the spatial distribution of journey end locations and the location of charging posts in the GDA respectively.

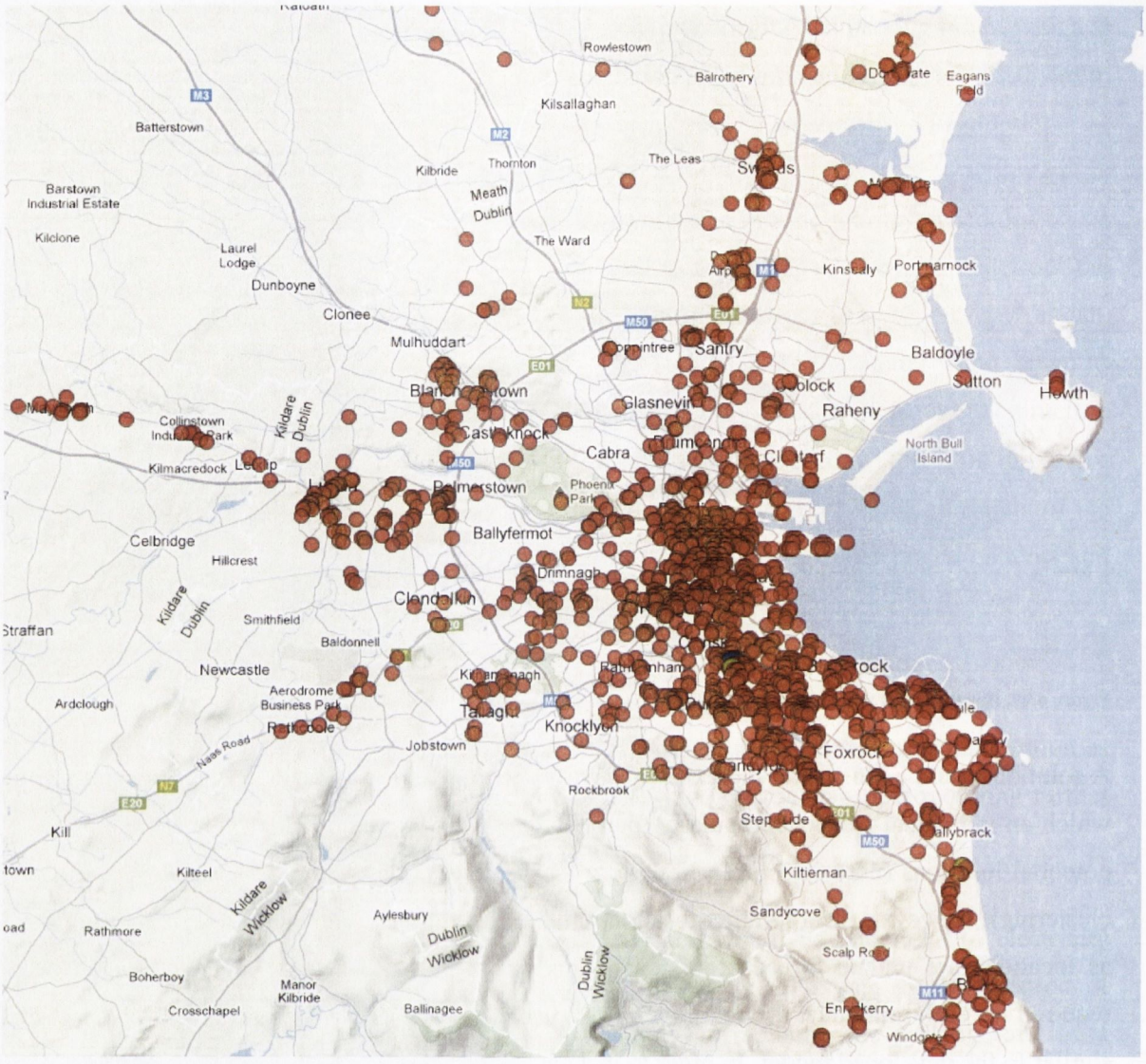

Figure 6.50. The spatial distribution of the starting locations of EV journeys in the Greater Dublin Area.

An avenue for future research would be to investigate methods in which electricity utilities could ensure that there are charging points available when required both in terms of location and time of day for a large population of EVs. In addition, large volumes of EVs charging simultaneously could cause problems for local transmission networks. Therefore it is important to manage charging infrastructure in order to minimise the demand placed on local distribution networks. Predicting the location and power demands of EVs is critical to managing charging infrastructure and minimising infrastructure costs and network distribution. This would require the state of charge of each vehicle and possible future destinations to be predicted. If a model could predict these variables then the utility could potentially direct EVs through an on-board interface to maximise the use of charging infrastructure. Furthermore, in order to minimise cost and street space reserved for charging posts, it is vital that the ratio of charging points to EVs is maximised. Adequately managing the infrastructure would contribute towards this.

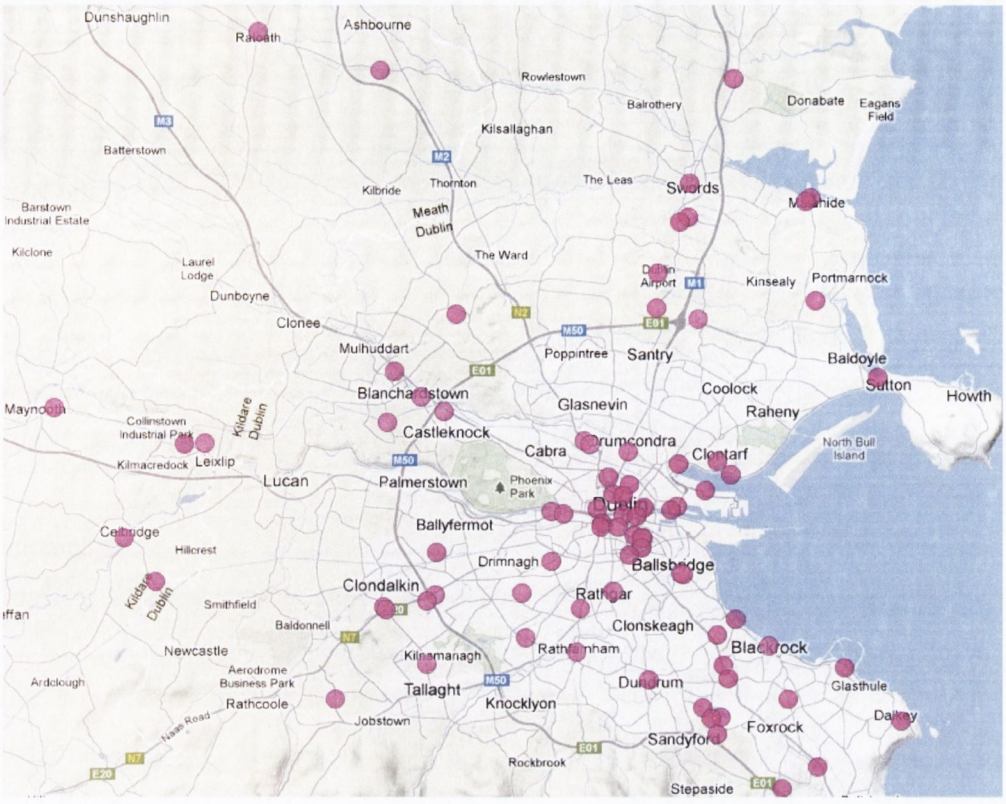

Figure 6.51. Current charging post locations in the Greater Dublin Area.

7 Translating travel patterns to power demand: Stochastic modelling of the uncontrolled charging of electric vehicles

In this chapter the travel pattern model developed in Chapter 6 is developed further to translate the transportation patterns of a population of EVs into the respective power demand of the EVs. At the end of each journey scheduled by the travel pattern model a decision is required as to whether or not to charge the battery. A number of different methods of modelling charging decision making behaviour are investigated and a probabilistic charging model is incorporated into the travel pattern model and evaluated. Additional factors such as battery characteristics, the probability of charging point availability at destinations and plugging in behaviour are included in the model.

The stochastic travel pattern model and the probabilistic charging decision model combined have the potential to be used as a tool to analyse the large scale charging patterns of a fleet of EVs. However, a number of aspects of the model require further development, specifically the modelling of parking time intervals between journeys. The implementation of an informed prior distribution in the Bayesian approach to generating parking times when data are not returned from the database would significantly improve the model. A larger dataset would be beneficial also as it would reduce the reliance on the Bayesian approach and hence the prior distribution of the parking times. The cumulative effect of the limitations in the parking time aspect of the travel pattern model has implications for the probabilistic charging decision model, as the probability of charging at a destination is conditioned on the parking time between two journeys. Logging the precise SOC of the batteries of a fleet of EVs would significantly contribute to a model of this nature as the probability of charging and travelling is conditioned on the SOC of the battery.

This chapter is organised as follows: Section 7.1 provides a review of charging decision rules and models in existing EV electricity grid integration studies. Section 7.2 describes the reduced dataset used in this chapter. Section 7.3 presents the model structure, key assumptions and calculations in the model. Section 7.4 provides an overview of the investigated charging decision models. Section 7.5 provides a theoretical background to fuzzy logic and developed fuzzy logic charging decision models are presented in Section 7.6. In the Section 7.7 a probabilistic charging decision model, which is the model that is ultimately integrated in to the travel pattern model is outlined. The model is validated in Section 7.8. Section 7.9 concludes the chapter and Section 7.10 discusses areas for further research.

7.1 A review of modelling charging decision making behaviour in electric vehicle electricity grid integration studies

There is little scientific literature available with regards to modelling charging decision making behaviour. In general EV electricity grid integration studies either assume definite charging upon arrival at a destination or the decision to charge is implemented based upon a set of rules. As discussed in Chapter 6, the majority of studies simulate vehicle travel to and from the home and workplace and correspondingly simulate charging profiles at the workplace and overnight. Keane and Flynn (2012) assumed that drivers will charge the battery during the day if the projected SOC upon arrival home is less than 30%. Lojowska et al (2011) assumed two charging scenarios (1) that EVs start charging immediately upon arrival home and (2) that EVs only charge when the SOC is below 50%. Ashtari et al (2012b) assumed that drivers charge immediately upon arrival at work or home. To this author's knowledge there are no existing stochastic models that can simulate a detailed journey schedule for a fleet of EVs that include a probabilistic charging model at each destination.

The decision making process regarding the charging of a battery is a complex problem which can be influenced by many factors and individuals exhibit different behaviour. Shahidinejad et al (2012) proposed an interesting approach using a simple Mamdani-type fuzzy logic model to emulate the decision making behaviour with respect to charging PHEVs in Manitoba, Canada. The state of charge of the battery and the estimated parking duration were the inputs to the model. Figure 1 demonstrates the membership functions used for the linguistic variables involved. Parking times less than 30 minutes were considered 'short'; parking times between 30 minutes and 3 hours were considered 'average' and parking times greater than 3 hours were considered 'long' (Figure 7.1 (b)). The same interpretation applies to the SOC membership functions (Figure 7.1 (a)). An output greater than 0.5 of the output membership function, charging probability (Figure 7.1 (c)), was considered as a decision to charge. Note that the authors hypothesised the shapes of the membership functions and that they are not derived from real-world data. Note that the author has misleading labelled the output membership function as 'charging probability' (Figure 7.1 (c)). It should be labelled as "the degree of membership of the output function, charging". This will become more apparent in a later section.

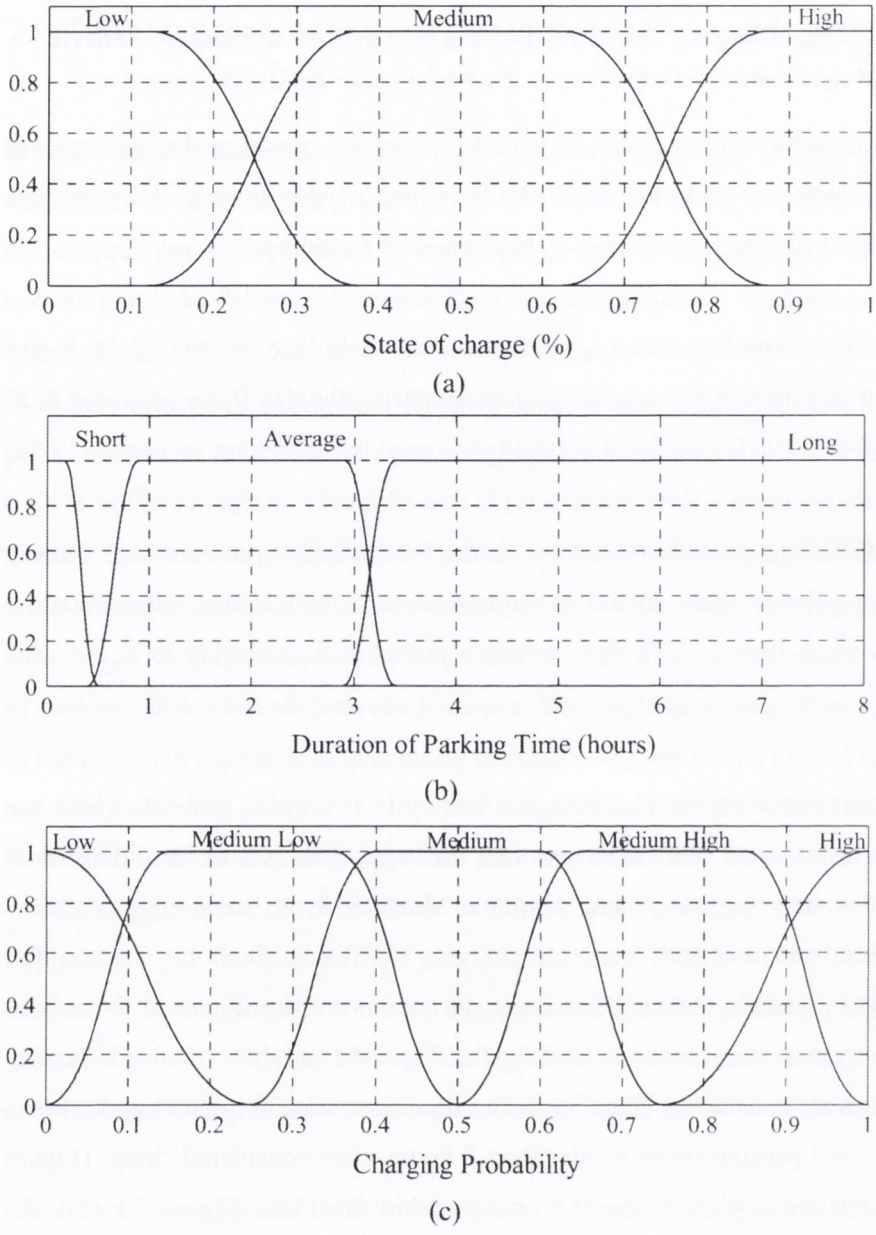

Figure 7.1. Membership functions. (a) Battery state-of-charge, (b) duration of parking time, (c) charging probability (Shahidinejad et al, 2012).

The travel pattern model, developed in Chapter 6, synthesises a two day journey schedule for each EV (Figure 7.2). At the end of each journey a decision is required as to whether or not to charge the battery. In this chapter four different methods of modelling charging decision making behaviour are investigated and a probabilistic charging model is incorporated into the travel pattern model and evaluated. The next section describes the dataset used in this chapter.

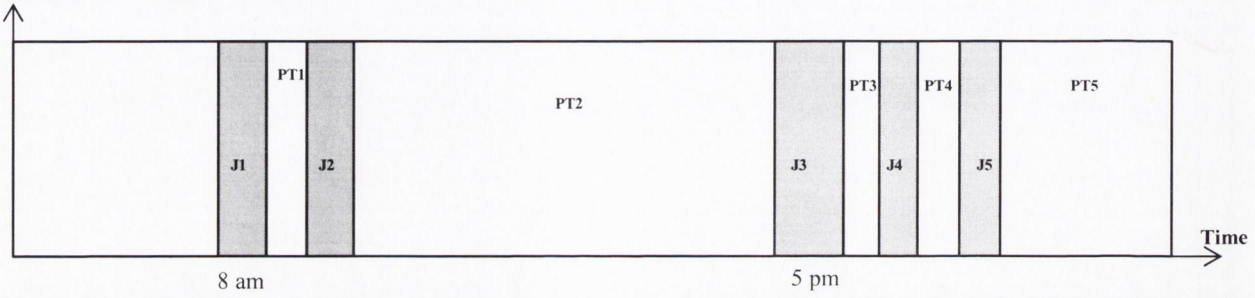

Figure 7.2. An example journey schedule for day 1. Journeys (J) are represented by the grey regions and white regions represent parking durations (PT), in which a vehicle would be available for charging.

7.2 The dataset

The travel pattern model developed in Chapter 6 was developed using GPS data collected from 15 EVs from January 2011 – October 2012 and this model is extended in this chapter. Only GPS data logged during periods in which data logging from the Can-bus was enabled in 12 of the vehicles were included in the model. This was necessary as charging events were logged on the Can-bus. In addition, data logged from vehicles stationed at the ESB head offices and weekend data were included in the database. This was necessary in order to maximise the amount of data in the database. This database contained 28% less journey data than the database used to develop the travel pattern model in Chapter 6. The database contained data pertaining to 13,200 journeys and 2,786 charging events from the period January 2012 – January 2013. Of the 2,786 charging events, 1,524 were overnight charging events and 1,262 were logged during the day. Due to the small population of vehicles in the trial, each day of data was treated as independent of all other days from that vehicle. In effect this resulted in a database of 2,850 days of EV data rather than a 365 day trial of 12 vehicles. The aggregation of the data means that care must be taken when interpreting any results. Despite the limitations of the dataset the intention is to use the approach as a test bed for a proof of concept.

As discussed in Section 4.6 of Chapter 4, readings from the battery such as voltage and current could not be detected on the Can-bus. The only measurement directly related to the battery that could be logged from the Can-bus was the number of 'bars' displayed on the battery gauge on the dashboard (Figure 7.3). There are 16 bars in total. Each bar was assigned an approximate energy value (kWh) sourced from Cenex, a UK company, who tested the vehicle in a laboratory (Carroll, 2011). The approximate kWh values assigned to each bar are listed in Table 7.1. The SOC of a vehicle before and after a trip and charge event was estimated by summing the kWh values of the bars displayed on the battery gauge and dividing by 14 kWh. If a bar was not expended during a journey then the energy consumption was calculated manually given the distance travelled and an assumed energy economy of 175 Wh/km. Note that the absence of precise SOC measurements and the reliance on the battery gauge display to estimate the SOC of the battery has implications for the accuracy of the model and will be discussed again. As an example, a vehicle could start a journey with a fully charged battery (16 bars) and complete the journey without expending a bar. In this case the estimated consumption could potentially be inaccurate up to 1.8 kWh (the 16^{th} bar represents approximately 1.8 kWh). Similarly a vehicle could start a journey with 16 bars and the 16^{th} bar could be expended immediately, falsely indicating that 1.8 kWh of energy had been consumed. However, the battery gauge indicator takes into account energy consumed by the air conditioning, terrain and driving styles which are important factors.

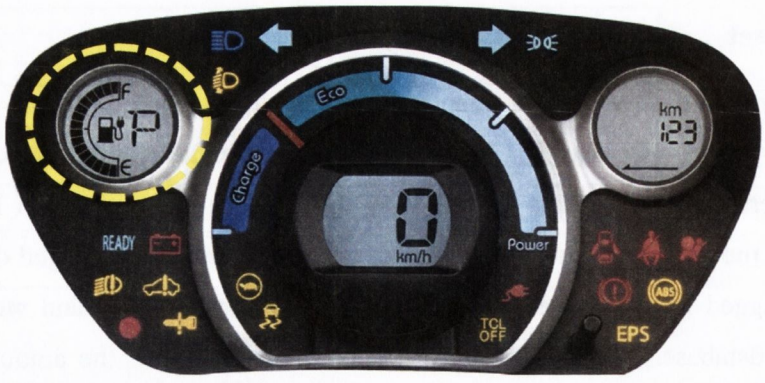

Figure 7.3. Image of a Mitsubishi iMiEV's dashboard (Cleanmpg, 2013).

Table 7.1. Energy values (kWh) assigned to each bar displayed on the battery gauge.

Bar number	kWh value	Bar number	kWh value
Bar 1	1.44	Bar 9	0.65
Bar 2	0.59	Bar 10	0.62
Bar 3	0.61	Bar 11	0.65
Bar 4	0.72	Bar 12	0.64
Bar 5	0.75	Bar 13	0.65
Bar 6	0.61	Bar 14	0.62
Bar 7	0.64	Bar 15	0.66
Bar 8	0.62	Bar 16	1.8

When modelling charging decision making behaviour it is important to only use data from destinations in which charging the vehicle was an option to the driver. If no charging post was available at the destination then naturally the driver would not have had the option to charge the vehicle. Therefore, at each destination (GPS coordinates) the availability of a charging point was ascertained by (1) cross referencing the coordinates against a national public charging point location map (ESB, 2013) and (2) by comparing the current location against previous locations in which charging events were logged for a given vehicle (this identified charging point locations not included on the map such as home charging points). A segment of summary data pertaining to charging events is presented in Table 7.2.

Table 7.2. An example of summary data relating charging events.

Time of arrival	**SOC (%) upon arriving at the destination**	**Parking time (min)**	**Remaining distance to travel (km)**	**Charger Availability/Decision**
09:00:00	60	170	24	Charger available, charged
15:10:00	55	120	37	Charger available, did not charge
16:50:00	60	150	5	No charger available

Taking the first row as an example, upon arriving at the destination the vehicle had a State of Charge (SOC) of 60%, the parking time was 170 minutes and the remaining distance to travel that

day was 24 km. A charging post was available at the location and a decision was made to charge the vehicle.

The nest section describes key aspects of the model in relation to its structure and calculations. This is followed by an overview of the investigated charging decision models.

7.3 Model description

This section describes (1) the simulation structure, (2) specific calculations in relation to determining the SOC of the battery upon arrival and departure from destinations and (3) the modelling of the availability of a charging point at a destination.

7.3.1 Simulation structure

The empirical distribution of the SOC of a battery (measurements from the vehicles) at the beginning of the first journey of each day in the database is presented in Figure 7.4. Approximately 50% of vehicles had a fully charged battery at the start of the first journey of the day and the SOC of the remaining 50% of vehicles was relatively evenly distributed between 40% and 99%.

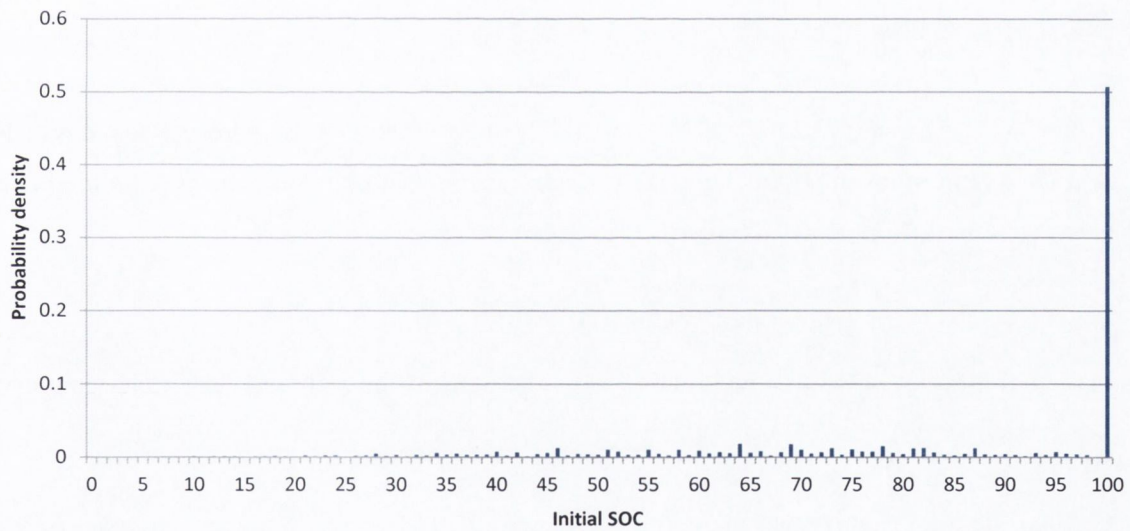

Figure 7.4. The empirical distribution of the SOC of the battery at the beginning of the first journey of each day in the database.

The simulations are performed for two consecutive days to diminish the influence of initial assumptions and to incorporate overnight charging. Figure 7.5 illustrates the simulation process.

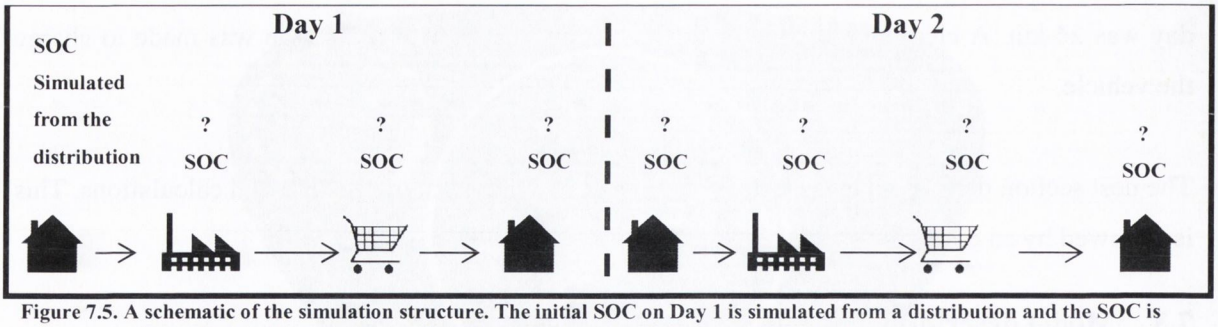

Figure 7.5. A schematic of the simulation structure. The initial SOC on Day 1 is simulated from a distribution and the SOC is then calculated iteratively at end of trip and charge events.

Instead of assuming that each vehicle has a 100% SOC upon departure from the home on the first day of the simulation, the initial SOC of a battery as the vehicle departs the home is simulated from this distribution (Figure 7.4). The SOC upon arrival and departure from each subsequent destination (i.e. after trip and charge events) over the day two-day period is calculated in an iterative manner as illustrated in Figure 7.5. These calculations are discussed in the next section. The charging profile of the EVs is computed for the second day to diminish the initial assumption. In addition, the profiles include overnight charging.

The simulation is run for 2,000 EVs. This is repeated ten times to represent ten days. The simulation assumes uncontrolled charging. The next section describes how the SOC of the battery is estimated upon arrival and departure from each destination.

The simulation is run for 2,000 EVs. This is repeated ten times to represent ten days. The simulation assumes uncontrolled charging. The next section describes how the SOC of the battery is estimated upon arrival and departure from each destination.

7.3.2 Electric vehicle state of charge simulation

This section describes how the model increments the SOC of the battery during a charging event and calculates the SOC of the battery upon arrival at a destination after a journey event.

Assuming that a decision is made to charge the battery, then during a charging cycle, the SOC of the battery is incremented by the rated power of the charger minus charging losses according to Equation 7.1.

$$SOC_{departure} = SOC_{arrival} + \frac{\eta_c . kW_{plug} . \Delta t}{kWh_{battery}} x \frac{100}{1} \tag{7.1}$$

where $SOC_{departure}$ and $SOC_{arrival}$ denote the percentage SOC of the battery upon departure and arrival at a destination respectively. A 95% inverter/transformer efficiency and a 97% battery input efficiency was assumed to give a charging efficiency of 92% (η_c) (Keane and Flynn, 2012). The

charging time and the battery capacity (14 kWh) are denoted by Δt and $kWh_{battery}$ respectively. The rated power of home and work chargers is assumed to be 3.7 kW (230 V, 16 A) and is denoted by kW_{plug}. Direct current 3-phase chargers (fast chargers) are not included in the study. Note that once a decision to charge is made, charging continues until the battery is fully charged, or the parking time elapses, whichever occurs first.

During a journey the battery is discharged according to Equation 7.2.

$$SOC_{arrival} = SOC_{departure} - \frac{km_{trip} \cdot \eta_{fuel}}{kWh_{battery}} x \frac{100}{1} \tag{7.2}$$

The journey distance is denoted by km_{trip}. The energy economy of the vehicle for a journey denoted η_{fuel}, is assumed to be fixed value of 0.265 kWh/km. This value is the average energy economy of the all the vehicles in the dataset, which was calculated by dividing the SOC of vehicles estimated from the battery gauge by the distance travelled. The next section describes how the model accounts for the observed real-world delay in plugging in a vehicle upon arrival at an overnight destination.

7.3.3 Modelling plugging-in behaviour

For charging events that occur during the day it is assumed that charging starts immediately at the end of a journey. Whilst the simulation assumes uncontrolled charging, in the real-world it was observed that when a vehicle arrives home after the last journey of the day and the battery is charged overnight, charging did not always begin immediately. This could be due to the fact that the individual used a timer-switch or that the vehicle was simply not plugged-in until later in the evening. Figure 7.6 illustrates the distribution of times between the end time of the last journey of the day and the start time of an overnight charging event. Approximately 70% of the time a vehicle is plugged-in immediately at the end of the last journey of the day but approximately 30% of the time there is a relatively evenly distributed delay in plugging-in between 15 minutes and 5 hours. This was accounted for in the model by simulating a value from this distribution and adding it to the end time of the last journey of the day to simulate the starting time of a charging event. The next section describes how the availability of a charging point at each location is accounted for in the model.

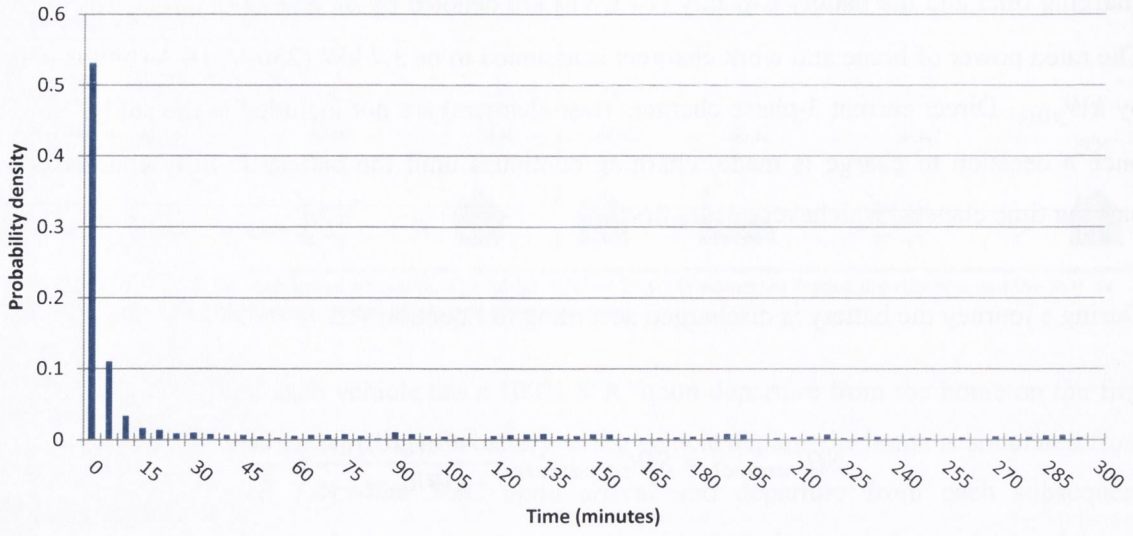

Figure 7.6. Distribution of time between the end time of the last journey of the day and the start time of an overnight charging event.

7.3.4 Modelling charging point availability

The availability of a charging point at a destination ultimately determines whether or not a vehicle can charge and as such this is critical in a model of this nature. In the real-world, the probability that a charging point is located at a journey's destination is wholly dependent on the location of the destination. As the location of a destination of a journey is not explicitly included in the model, modelling the availability of a charging point at a destination was a challenging aspect in the development of the model.

Initially the probability that a charging point is available at a destination was calculated to be 0.46 according to Equation 7.3.

$$P_{availability} = \frac{\sum_{i=0}^{i=N} Destinations\ in\ which\ a\ charging\ point\ is\ available}{\sum_{i=0}^{i=N} All\ destinations} \tag{7.3}$$

However, it was deemed too simplistic to assume that the probability of the availability of a charging point at each destination is 0.46. Therefore, it was proposed to condition the probability of the availability of a charging point on the time of day. The assumption was that there could be a higher probability that a charging point would be available at certain times of the day (i.e. between 8 am and 9 am as individuals arrive at the workplace or between 5 pm and 7 pm as individuals arrive home). However, as discussed in Section 6.10, the distribution of the simulated start-times and end-times of journeys do not match the real-world distributions exactly, hence this method could not implemented. Alternatively it was decided to condition the probability of the availability of a charging point at a destination on the journey number of the day according to Equation 7.4:

$$P_{availability}(x) = \frac{\sum_{i=0}^{i=N} Charging\ point\ available\ _{Journey\ number=x}}{\sum_{i=0}^{i=N} Number\ of\ journeys\ _{Journey\ number=x}} \quad (7.4)$$

$Charging\ point\ available\ _{Journey\ number=x}$ denotes the number of times that a charging post was available at the end of a journey number x. $Number\ of\ journeys\ _{Journey\ number=x}$ denotes the number of journeys of journey number x in the database. For example, $Charging\ point\ available\ _{Journey\ number=2}$ would denote the number of times that a charging post was available at the end of the second journey of a day and $Number\ of\ journeys\ _{Journey\ number=2}$ would denote the total number of journeys which were the second journey of the day in the database.

This approach facilitates to an extent the varying probability of the availability of a charging point by time of day to be accounted for in the model. The assumption was that for example the destination of journey number 1 or 2 could be at the workplace and that the destination of the last journey of the day could be at the home, hence at these destinations there could be a higher probability of the availability of a charging point. The probabilities calculated directly from the dataset of the availability of a charging point at a destination given the journey number are listed in Table 7.3.

Table 7.3. The probability of the availability of a charging point at a destination given the journey number of the day.

Journey number	Probability
1	0.38
2	0.50
3	0.47
4	0.47
5	0.44
6	0.47
7	0.45
8	0.45
9	0.51
10	0.46
11	0.51
Last journey of the day	0.83

This section described the simulation structure, key assumptions of the model, calculations in relation to determining the SOC of the battery and modelling the probability of the availability of a charging point at a destination. The next section provides an overview of the investigated charging decision models.

7.4 Overview of the investigated charging decision models

As discussed earlier, at the end of each journey a decision is required as to whether or not to charge the battery. Four different methods of modelling charging decision making behaviour are investigated and a probabilistic charging model is incorporated into the travel pattern model and evaluated. This section provides an overview of the four investigated methods.

The first method investigated is based on Shahidinejad et al's (2012) implementation of a simple Mamdani-type fuzzy logic charging decision model. An adaptive neuro-fuzzy inference system, which is based on a Takagi-Sugeno fuzzy logic model is developed. Data collected from the EV trial is used to train the model. It is postulated that a fuzzy inference of (1) the SOC of the battery, and (2) the estimated parking duration are the main factors that govern a driver's decision whether or not to charge the vehicle whilst parked during the day. A driver's decision making logic is expected to be based mainly on the concern about the possibility of completing the foreseen remaining journeys in the day given the current state of charge of the battery and the parking duration. At overnight destinations, it is postulated that a fuzzy inference of the SOC of the battery only is the main factor that governs a driver's decision whether or not to charge. This approach was not incorporated into the travel pattern model for reasons to be discussed later.

Secondly, the conditional probability of a vehicle undergoing a charge event was determined by deriving the proportion of charging events as a function of all events (trip and charge) given the SOC of the battery according to Equation 7.5:

$$P_{charge}(x) = \frac{\sum_{i=0}^{i=N} Charge\ events_{soc=x}}{\sum_{i=0}^{i=N} Charge\ and\ trip\ events\ _{soc=x}} \tag{7.5}$$

where x is the current SOC, $Charge\ events_{soc=x}$ and $trip\ events\ _{soc=x}$ is the number of charge and trip events at a given SOC respectively. Figure 7.7 demonstrates that the probability of a charge event increases as the SOC decreases. This provides an insight into charging behaviour given the SOC of the battery. However, it excludes factors such as available parking time, remaining distance to travel in the day (i.e. the required SOC to complete the remaining journeys of the day) and the destination of a journey (i.e. charging availability).

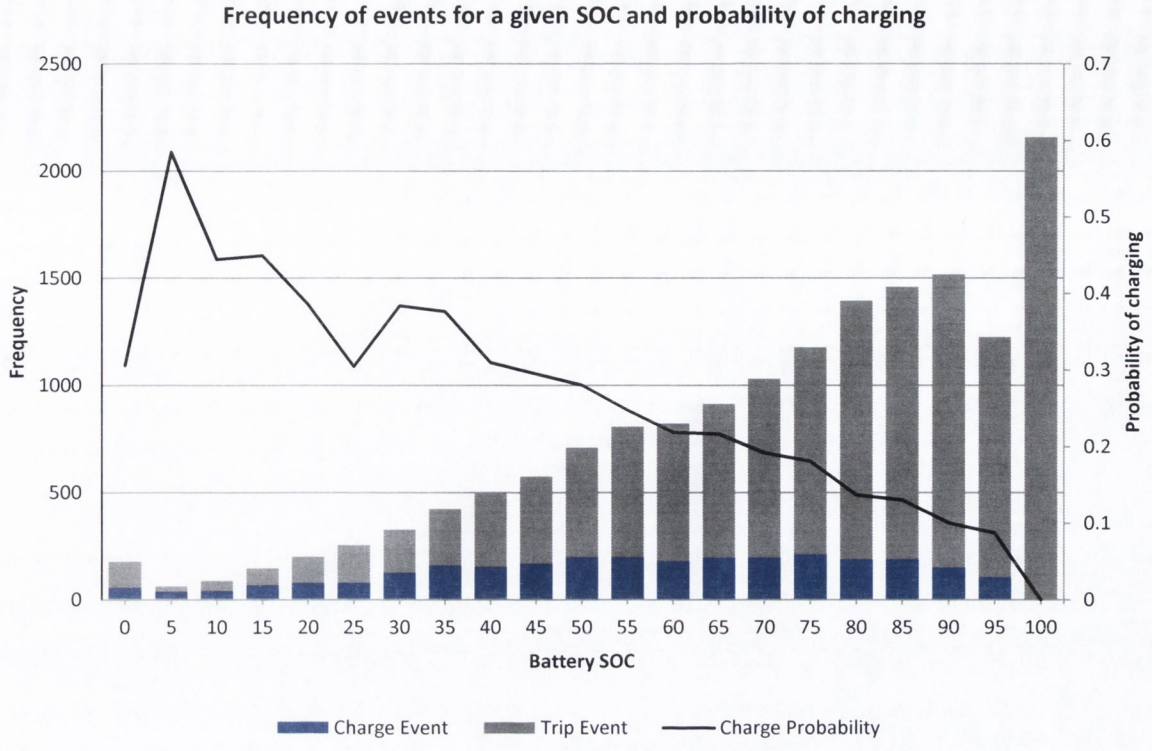

Figure 7.7. Frequency of trip and charge events and the probability of charging for a given SOC.

Thirdly, calculating the conditional probability of charging upon arrival at a destination given the current SOC of the battery, the available parking time and the remaining distance to travel in the day was considered (Equation 7.6). However, it was found not to be feasible due to the small number of charging event data. Given the number of dimensions, in many cases data would not be returned from the database and a probability of charging could not be estimated.

$$P(\text{Charging}|\ \text{Battery SOC, parking time, remaining distance to travel}) \tag{7.6}$$

Following on from this it was decided to calculate the conditional probability of charging upon arrival at a destination given the current SOC, the available parking time and the current journey number of the day (Equation 7.7).

$$P(\text{Charging}|\ \text{Battery SOC, parking time, journey number}) \tag{7.7}$$

If data are not returned from the database then the number of conditions is reduced by one and database is queried again. At overnight destinations, the probability of charging is conditioned on the SOC only. This approach is referred to as the probabilistic charging decision model hereinafter and is discussed in detail in Section 7.7. While other factors such as the price of electricity could also be considered, charging was free of charge during the trial and this was not taken into account here. However, in the future it could be included in the model by logging the price of electricity at the end of journey events and including the price of electricity as a condition on the distribution.

The next section provides an overview of fuzzy logic systems. This is followed by the developed fuzzy logic charging decision models in Section 7.6. The probabilistic charging decision model is described in Section 7.7.

7.5 Fuzzy logic systems

This section presents an overview of the theory of fuzzy logic. The theory of fuzzy logic was formulated by the mathematician Lotfi A. Zadeh in 1965 as response of to the insufficiency of Boolean Algebra in real-world problems (Ross, 2004). Most of the information in the real-world is imprecise, and one of humans' greatest abilities is to effectively process imprecise and 'fuzzy' information. Fuzzy logic was proposed on fuzzy set theory to capture the way humans represent and reason real-world knowledge to solve uncertain problems. A fuzzy set is represented mathematically by assigning each member in the set a value representing its grade of membership in the fuzzy set, where the grade corresponds to the degree to which the member is similar or compatible with the concept represented by the fuzzy set. In mathematical set theory an element exhibits the property of whether it belongs to the set or not and so they are called crisp sets. However, in fuzzy sets many degrees of freedom are allowed. A membership function is associated with a fuzzy set so that the function maps every element in the set on to a value between 0 and 1. Fuzzy logic is a powerful representation of uncertainty. It provides a meaningful representation of vague concepts which are expressed in any natural language. Symbolic logic formed from mathematical set theory and fuzzy logic formed from fuzzy set. Only two values 'true' and 'false' are allowed in symbolic logic but in fuzzy logic multi valued truth values such as 'true', 'absolutely true', 'fairly true', 'false', 'absolutely false', 'partly false' are allowed. Fuzzy inference rules are computational procedures used in evaluating linguistic descriptions and fuzzy rule based systems are a set of fuzzy if-then statements. Fuzzy logic is applicable in the areas of control systems, and pattern recognition applications. The definition of a fuzzy set, terms such as membership functions and fuzzy set operators and types of fuzzy logic models are presented and discussed in the following sections. To summarise, fuzzy inference is a method that interprets the values in an input vector and based on some set of rules, assigns a value(s) to the output vector. An in depth overview of the theory of fuzzy logic and a neuro-adaptive learning methodology is available in Appendix H.

7.6 Development and training of the fuzzy logic charging decision models

The neuro-adaptive learning method described in Appendix H provides a method for the fuzzy modelling procedure to learn information about a dataset. The charging decision models were implemented using the fuzzy logic toolbox in Matlab. The software computes the membership function parameters that best allow the fuzzy inference system to track the given input/output training data. The membership function parameters are adjusted using a combination of a backpropagation algorithm and a least squares type method and the parameters associated with the membership functions change through the learning process. The computation of the parameters is

facilitated by a gradient vector. The gradient vector provides a measure of how well the fuzzy inference system is modelling the input/output data for a given set of parameters (Mathworks, 2013). This error measure is defined by the sum of the squared difference between the actual and desired outputs. From Section 7.4, it is postulated that a fuzzy inference of (1) the SOC of the battery and (2) the estimated parking duration are the main factors that govern a driver's decision whether or not to charge when an EV is parked during the day. At overnight destinations, it is postulated that a fuzzy inference of the SOC of the battery only is the main factor that governs a driver's decision whether or not to charge. The inputs to each of the fuzzy logic models are graphically illustrated in Figures 7.8 and 7.9 respectively.

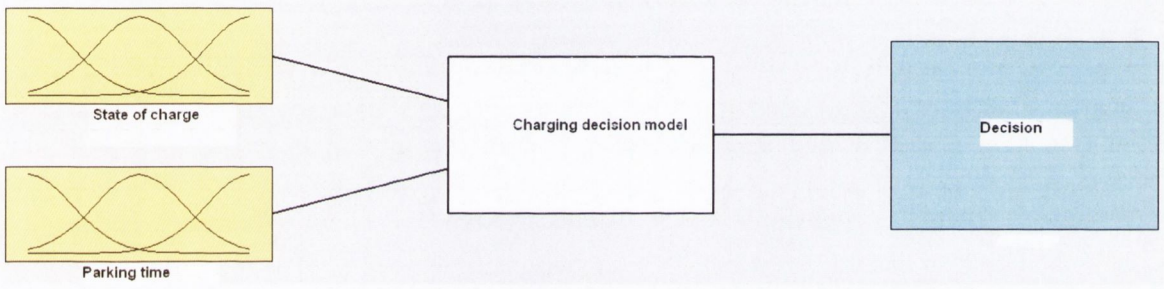

Figure 7.8. Structure of the fuzzy logic model at daytime destinations.

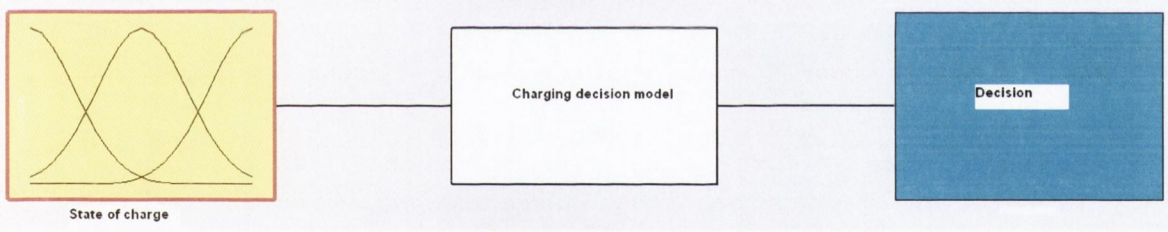

Figure 7.9. Structure of the fuzzy logic model at overnight destinations.

7.6.1 The training dataset for the fuzzy logic model

Data from 6,016 destinations in which a charging point was available to the driver were used to train the fuzzy logic models. An example of the training data in presented in Table 7.4. Taking the first row as an example, upon arriving at the destination the vehicle had a SOC of 60% and the parking time was 170 minutes. A charging post was available at the location and a decision was made to charge the vehicle.

Table 7.4. Example of training data for the fuzzy logic model.

SOC (%)	Parking time (min)	Charger Availability/Decision
60	170	Charger available, charge
53	120	Charger available, no charge

7.6.2 Membership functions and fuzzy rules

Figure 7.10 illustrates the membership functions use for the linguistic variables for each input variable prior to training for each model. Gaussian membership functions were used for each input variable because they facilitate smooth continuously differentiable hypersurfaces in the model. For example, for the input variable SOC, a 'low' SOC is considered less than 50%, a 'medium' SOC is considered between 20% and 80% and a high SOC is considered greater than 50%. These membership function change during the training process.

(a)

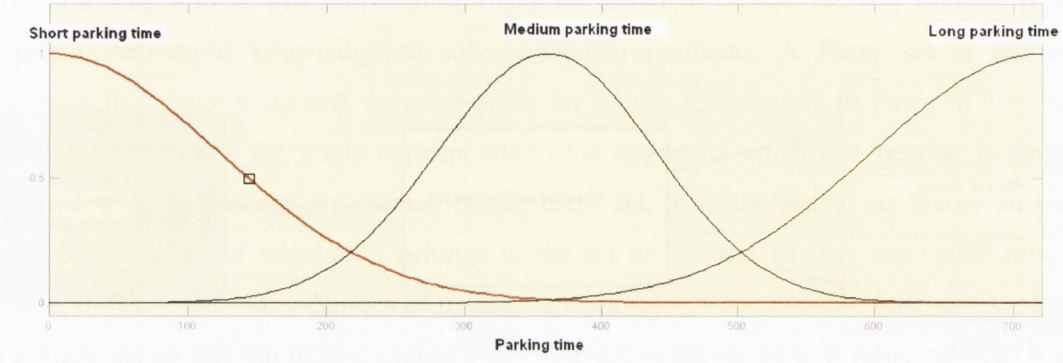

(b)

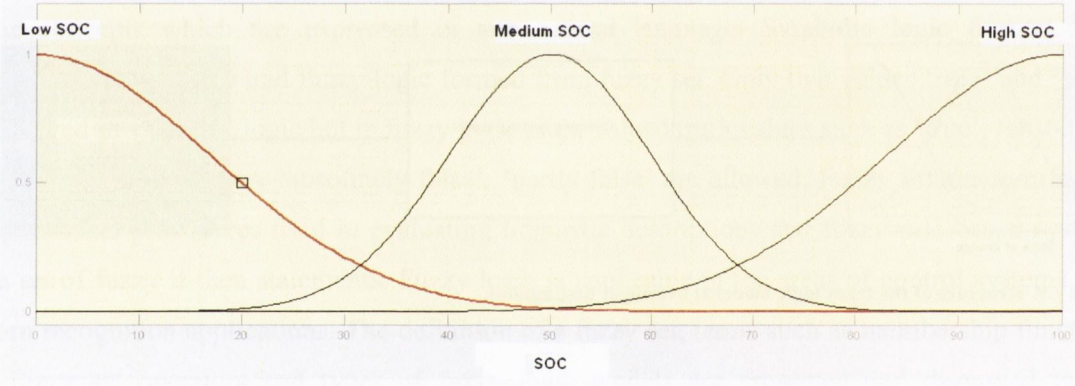

Figure 7.10. Membership functions prior to training for (a) duration of parking time (b) battery state-of-charge.

For a well-defined fuzzy system, rules need to be defined for every possible combination of input membership functions. For the daytime model, with two inputs, each with three membership functions, there are 3^2 (9) fuzzy rules. For the overnight model there are 3 rules. Tables 7.5 and 7.6 list the fuzzy rules for the daytime and overnight model respectively.

Table 7.5. Fuzzy rules of the daytime fuzzy logic charging decision model.

1. If (SOC is low) and (parking time is short) Then (Charge)
2. If (SOC is low) and (parking time is medium) Then (Charge)
3. If (SOC is low) and (parking time is long) Then (Charge)
4. If (SOC is medium) and (parking time is short) Then (No Charge)
5. If (SOC is medium) and (parking time is medium) Then (No Charge)
6. If (SOC is medium) and (parking time is long) Then (Charge)
7. If (SOC is high) and (parking time is short) Then (No Charge)
8. If (SOC is high) and (parking time is medium) Then (No Charge)
9. If (SOC is high) and (parking time is long) Then (No Charge)

Table 7.6. Fuzzy rules of the overnight fuzzy logic charging decision model.

1. If (SOC is low) Then (Charge)
2. If (SOC is medium) Then (Charge)
3. If (SOC is high) Then (No Charge)

A three-dimensional surface plot of the daytime model prior to training is illustrated in Figure 7.11. It represents the mapping from the inputs to the outputs. A two-dimensional surface plot of the overnight model prior to training is illustrated in Figure 7.12.

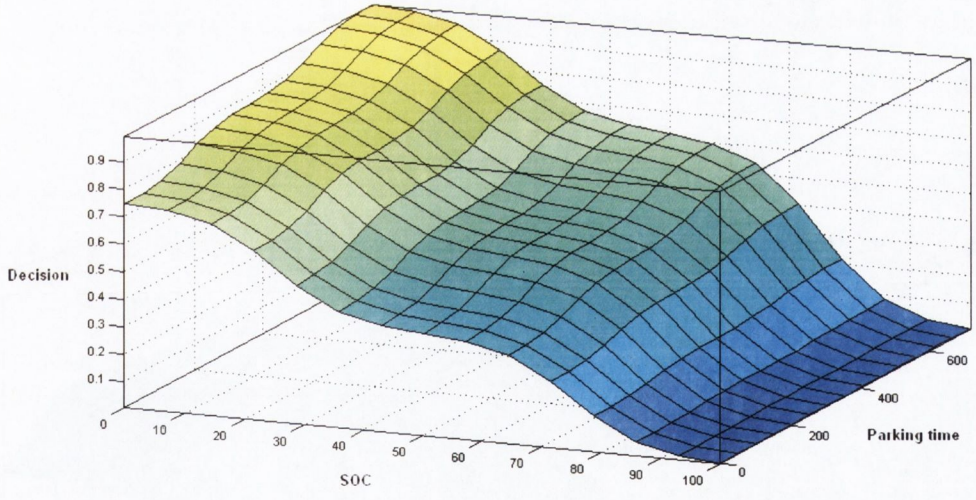

Figure 7.11. Surface plot of the fuzzy logic model for the input variables parking time and battery SOC.

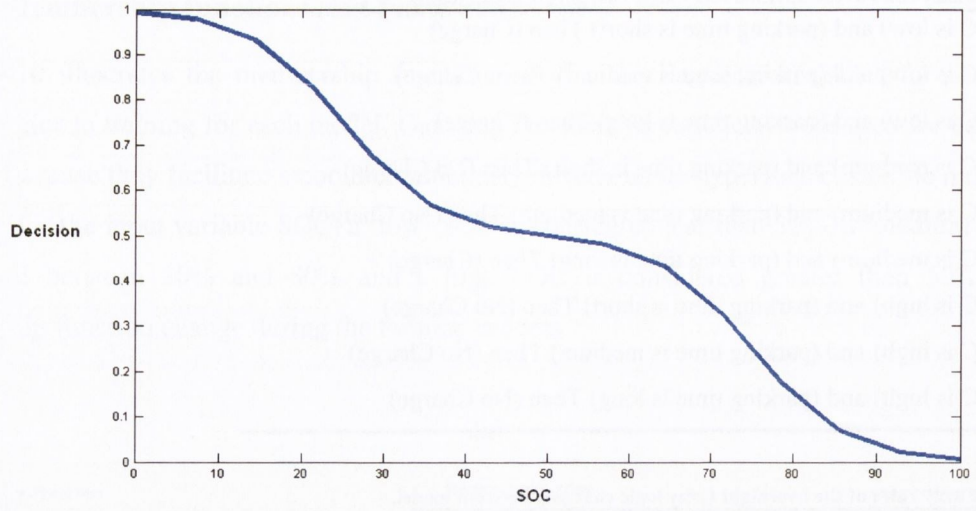

Figure 7.12. Surface plot of the fuzzy logic model for the input variable battery SOC.

7.6.3 Results and discussion

The surface plots after training for the daytime and overnight model are illustrated in Figures 7.13 and 7.14. The surface plot of the daytime model illustrates how the model has learned the information in the dataset. As expected, the general trend of the plot is that as the SOC decreases and the parking time increases, the degree of membership of the output function, decision, increases. Similarly for the overnight model, the plot indicates that as the SOC decreases the degree of membership of the output function, decision, increases.

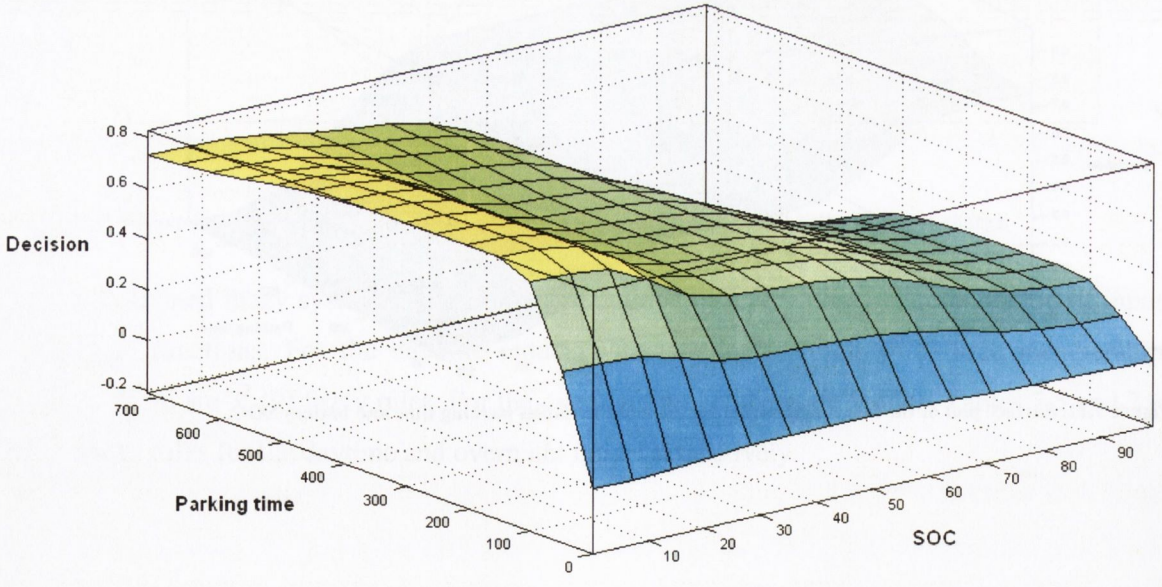

Figure 7.13. Surface plot of the daytime model after training.

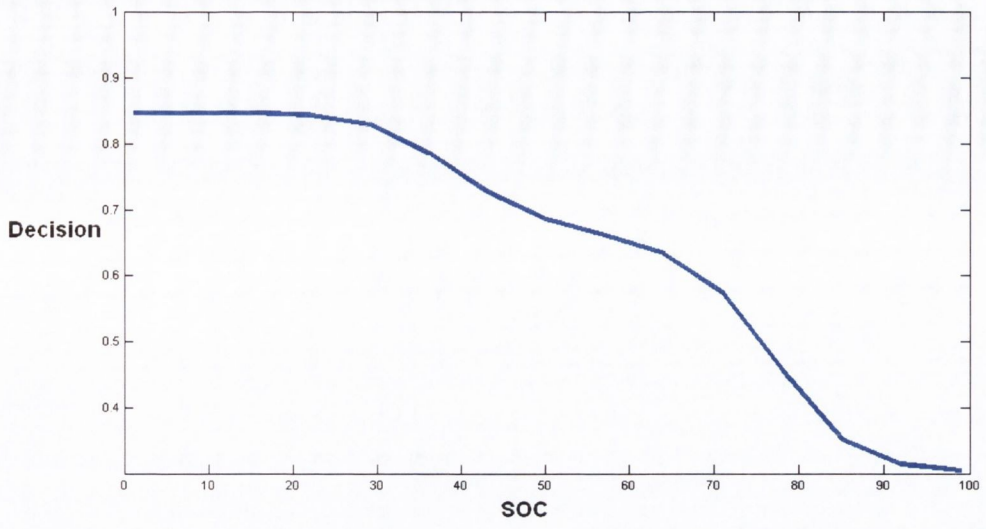

Figure 7.14. Surface plot of the overnight model after training.

The development of the ANFIS model is a novel approach to modelling charging decision making behaviour. However, its application is not suitable in a stochastic model. A fuzzy logic model only works well in systems which follow precise rules. With regards to charging a vehicle, individuals, including the same individual, exhibit random behaviour, given that in one instance they might charge a vehicle given a certain state of charge and parking time and in another instance they do not charge a vehicle even though the input variables are of the same or approximately the same value. During the training of the fuzzy logic model, the model adjusts the parameters of the membership functions such that training inputs produce the training targets. A conflict arises during the training of the model when two input vectors of the same values are presented to the model with different outputs (i.e. charge (1) and do not charge (0)). The least squares method that is used in the training process tries to minimise the error between the inputs and outputs and therefore the model tries to specify an output between the two presented training targets. Overall the random behaviour exhibited by individuals with respect to charging indicates that a probabilistic charging model would be a more suitable approach to be implemented into the stochastic travel pattern model.

7.7 The probabilistic charging decision model

As discussed in Section 7.4, the probabilistic charging decision model, calculates the conditional probability of charging upon arrival at a destination given the current SOC, the available parking time and the current journey number (Equation 7.8). The reason for conditioning the probability on the variable journey number is because in the absence of location and time as conditions, the variable journey number provides a vague indication as to the assumed location of the vehicle. The assumption being that an individual may be more likely to charge after journey number 1 or 2 as they arrive at work. In addition there is high probability that an individual would charge after the last journey of the day. As discussed in Section 7.2 the SOC of the vehicles operating in the real-

world is estimated using the battery gauge display whereas the SOC of the battery is estimated in the model according to Equations 7.1 and 7.2 in Section 7.3.2. In order to compensate for the different methods of estimating the SOC of the battery and to ensure that data is retuned from the database the bounds on the SOC condition are set to ± 2% and the bounds on the parking time condition are set to ± 5 minutes.

$$\text{P(Charging| Battery SOC , parking time, journey number)} \tag{7.8}$$

Typically 43% of the time during a simulation no data would be returned from the database given these three conditions. If this occurs the number of conditions on the probability is reduced by one, the database is queried again and the probability is calculated conditioned on the SOC and the parking time only.

$$\text{P(Charging| Battery SOC, parking time)} \tag{7.9}$$

Furthermore, typically less than 1% of the time during a simulation no data would be returned from the database given these two conditions. If this occurs the number of conditions on the probability is reduced by one, the database is queried again and the probability is conditioned on the SOC only.

$$\text{P(Charging| Battery SOC)} \tag{7.10}$$

After the last journey of the day (i.e. arrival home) the probability of charging is calculated given the SOC only as it is assumed that overnight parking time and the journey number do not influence the probability of charging overnight. However, typically less than 1% of the time during a simulation no data would be returned from the database given this single condition. If this occurs the probability of charging overnight is assumed to be 0.56. This probability was calculated directly from dataset according to Equation 7.11:

$$P_{overnight\ charge}(x) = \frac{\sum_{i=0}^{i=N} overnight\ charge\ events}{\sum_{i=0}^{i=N} nights} \tag{7.11}$$

where $overnight\ charge\ events$ and $nights$ are the logged number of overnight charge events and the total number of nights in the dataset respectively.

Two fixed rules are also built into the model to overwrite the charging decision model to force a charging event to occur if either of the situations below occur during a simulation. This prevents a negative SOC from occurring.

1. If the SOC required to complete the next journey is greater than the current SOC of the battery.
2. If the SOC of the battery is less than 10%.

In the next section the simulated travel profiles using the smaller dataset are presented. This is followed by an evaluation of the combined stochastic travel pattern model and the probabilistic charging model.

7.8 Simulated travel profiles from the reduced dataset

Given that a smaller database to that used to develop the travel pattern model in Chapter 6 is used in this chapter, it is appropriate to investigate the travel profiles simulated from the new database and to re-examine the performance of the travel pattern model. This section compares the simulated travel profiles to the deterministic travel profile of the reduced dataset. The deterministic model uses all the data directly in the database, 13,300 journeys, to create the driving profile in Figure 7.15. The profile is different to that observed in Figure 6.46 in Chapter 6. There are two peaks in the profile corresponding to morning an evening commutes. However, the evening peak is more prominent than that observed in Figure 6.46 in Chapter 6. This could be due to the fact that data from vehicles stationed at the ESB's head office and weekend data are included in the database. The distribution of the arrival time home in the evening (i.e. the stop time of the last journey) is illustrated in Figure 7.17 (orange bar).

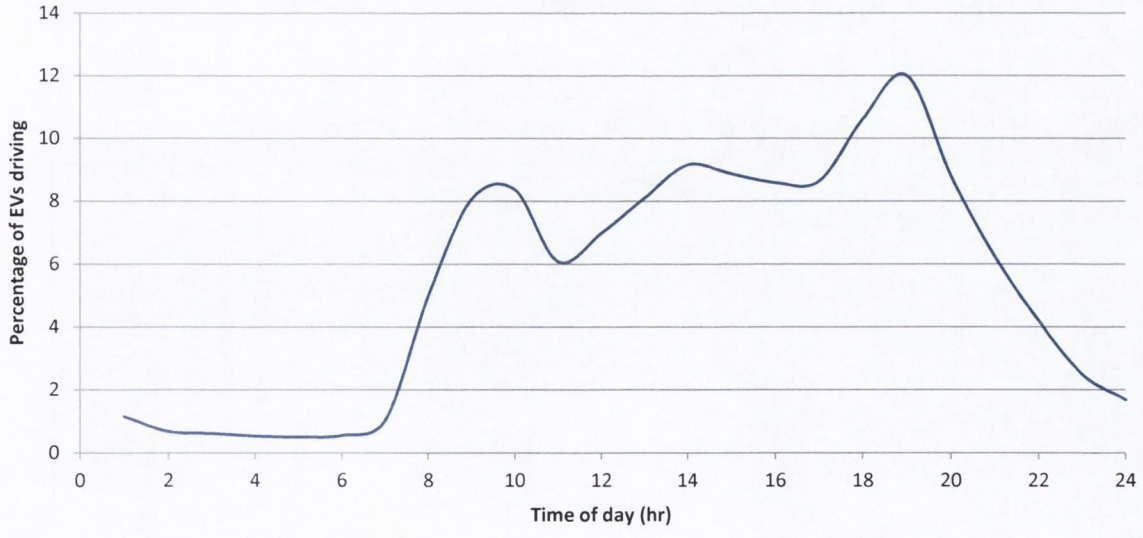

Figure 7.15. Percentage of EVs driving by hour of day (aggregated data).

Figure 7.16 illustrates the simulated 2-day travel profiles for 10 days. The trend of a daily travel profile is reproduced for each day but the observed evening peak in the number of vehicles travelling is not as prominent as observed in the real-world data in Figure 7.15.

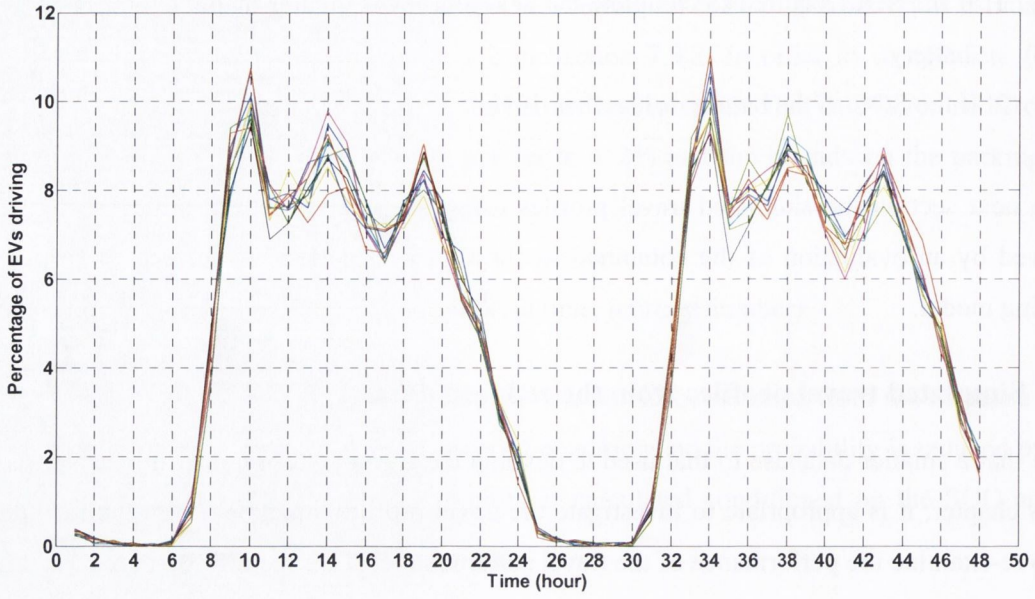

Figure 7.16. A 20 day simulation of the percentage of EVs driving per hour over the two-day time period.

Figure 7.17 illustrates that the arrival time home distribution simulated by the model does not match the deterministic distribution exactly. A Chi-squared goodness of fit test confirms this by rejecting the null hypothesis at the 95% confidence interval that the two distributions match. There are a higher proportion of vehicles than expected arriving home between the hours of 9 am and 5 pm and correspondingly fewer vehicles than expected arriving home between 5 pm and 12 am. This is illustrated by the blue bars in Figure 7.17. A small number of simulated vehicles arrive home between 1:00 am and 6:00 am. As discussed in Chapter 6, this as a result of large parking times generated from the uniform prior distribution.

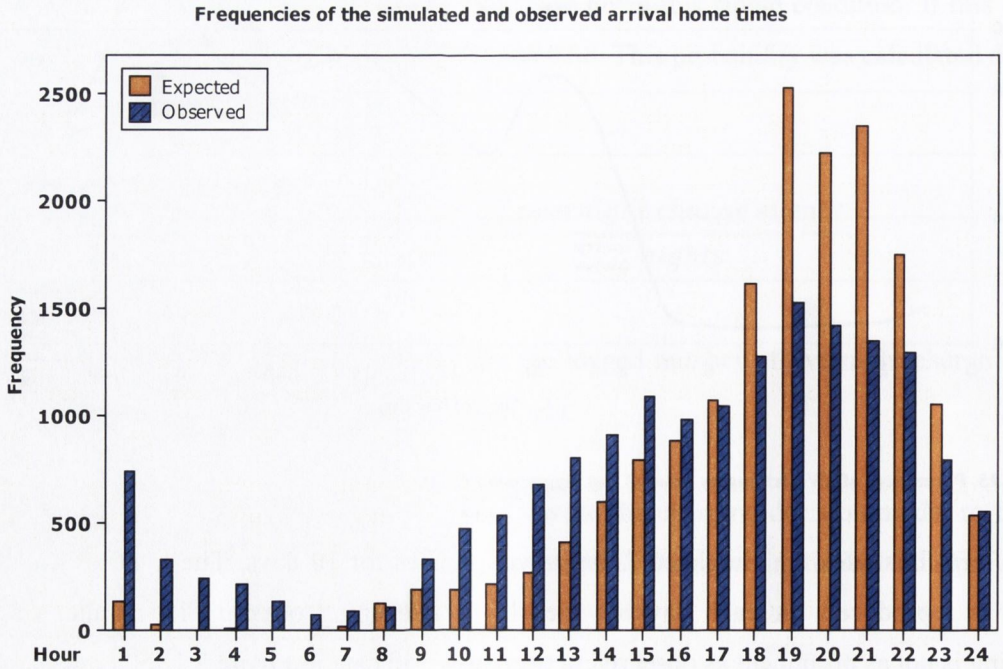

Figure 7.17. Frequencies of the simulated and expected arrival home times.

The source of the error, as discussed in Section 6.10 in Chapter 6, can be attributed to the fact that the model simulates more than expected 0 minute, 5 minute, 10 minute and 15 minute parking times between journeys (Figure 7.18). This is primarily due to fact that the bounds are not set exactly on the conditions of the parking time distributions. This results in a higher frequency of short parking time intervals being returned from the database and thus they have a higher probability density. The percentage difference in the number of each of these four simulated parking time intervals is listed in Table 7.3. A complete list of the expected frequency, simulated frequency and percentage difference for each parking time interval is available in Appendix G.

As a result of the 28% less journey data in the database used here (compared to the model presented in Chapter 6), the Bayesian approach to generating the parking times is required to be implemented approximately 23% of the time during a simulation, 11% more than was required by the model presented in Chapter 6.

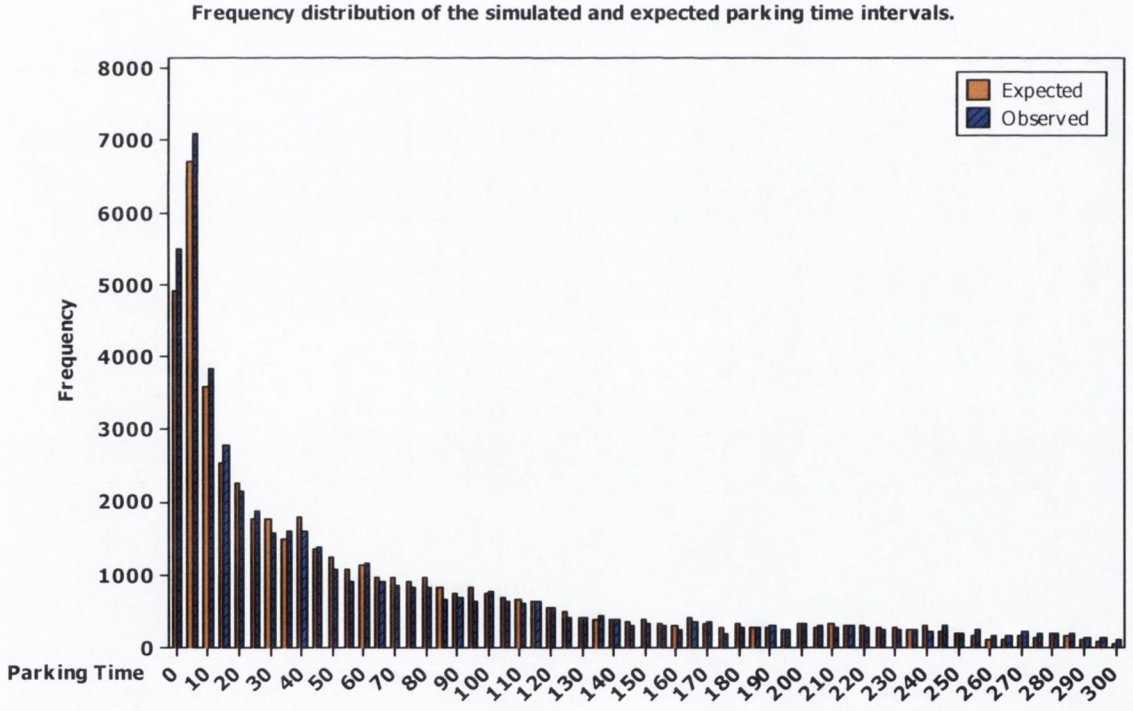

Figure 7.18. Frequency distribution of the simulated and expected parking time intervals.

Table 7.7. Expected and observed frequency of 0-15 minute parking time intervals.

Parking time interval	Simulated frequency	Expected frequency	Percentage difference
0	5493	4998	+10
5	7085	6825	+4
10	3835	3655	+5
15	2795	2573	+9

7.9 Model validation

This section compares the developed stochastic travel pattern model and the probabilistic charging model to the deterministic model. The deterministic model uses all the charging event data directly in the database, approximately 2,786 charging events, to create the weekly charging profile presented in Figure 7.19. Each weekday there is a peak in the number of vehicle charging at 10 am, the profile levels off in the afternoon and gradually increases from 6 pm to 12 am as individuals charge overnight. The profile gradually decreases between 1 am and 8 am as charging events terminate. Considering the use of the vehicles and from observing the trends in Figure 7.19, it is reasonable to assume that the charging times on weekdays are similar, therefore the observations for weekdays are aggregated together. The profiles for Saturday and Sunday differ from weekdays but as the travel pattern model database contains weekend data, the charging event data from weekend days are also aggregated with the weekday data resulting in the profile in Figure 7.20.

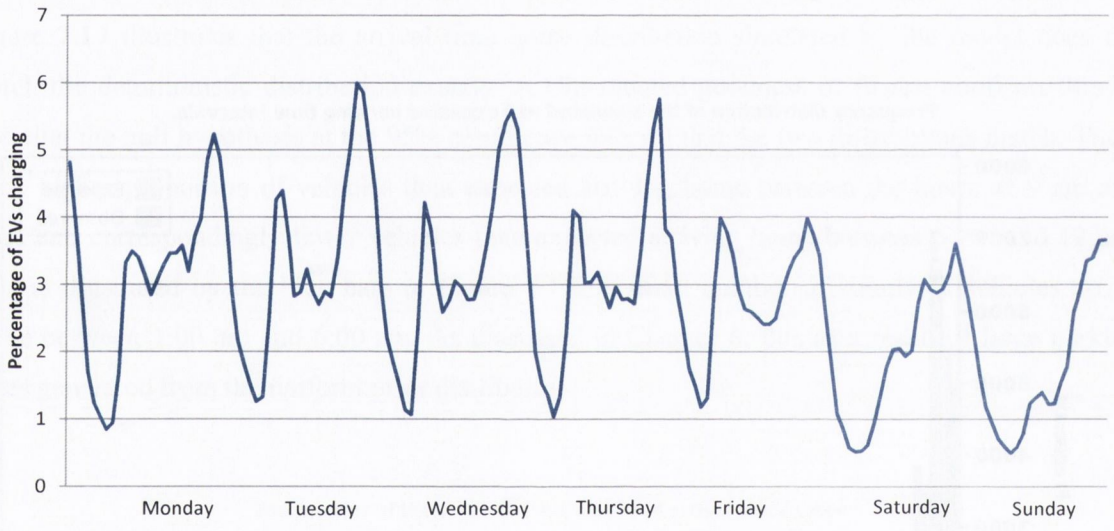

Figure 7.19. Percentage of EVs charging (hourly average).

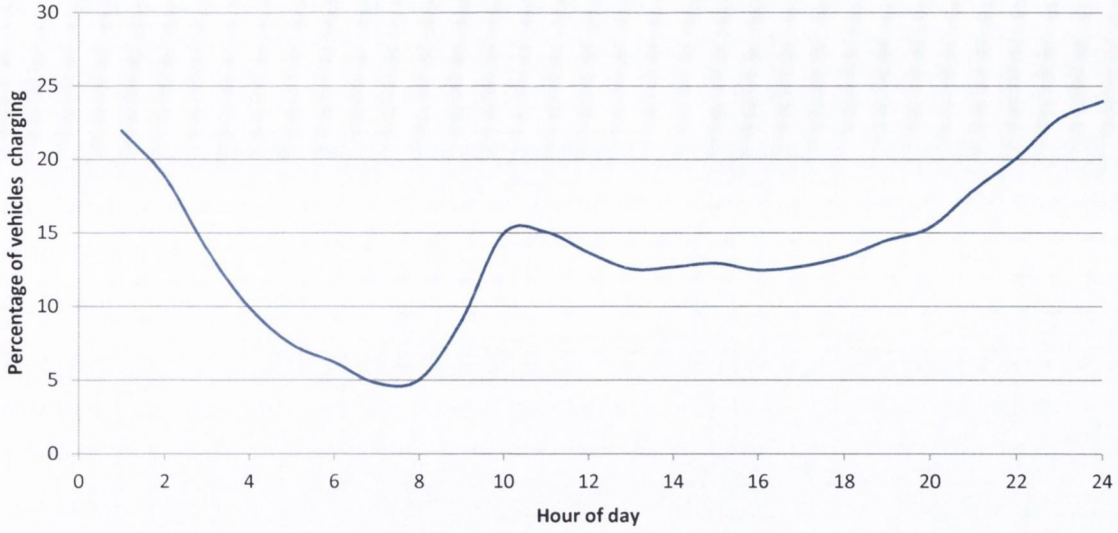

Figure 7.20. Percentage of EVs charging by hour of day (aggregated data).

As discussed previously in Section 7.3.1, the simulation is run for 2,000 EVs and repeated ten times to represent ten 2-day simulations. Figure 7.21 illustrates the simulated charging profile for the second day of each of the 10 days.

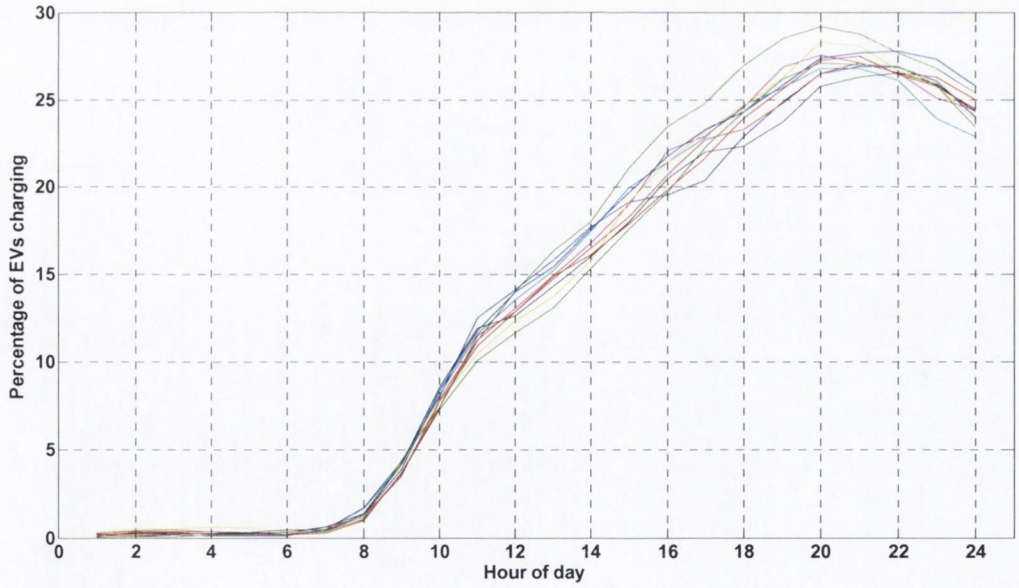

Figure 7.21. The percentage of EVs charging per hour for the second day of the 10 2-day simulations.

The basic principle of a Monte Carlo simulation, uncertainty propagation, is evident in the resulting shapes of the charging profiles. However, the trend of a daily charging profile is not reproduced exactly for each day. There are three points to notice about the simulated charging profiles in Figure 7.21 compared to the deterministic profile in Figure 7.20. The first point is that there is a higher percentage than expected of EVs charging between 1 pm and 6 pm and between 6 pm and 12 am. Secondly, there is a lower percentage of vehicles than expected charging between 12 am

and 8 am. Thirdly, the morning peak in the percentage of vehicle charging is not as large as expected. Each point is addressed separately next.

The source of the error in the simulated charging profiles can be attributed to a number of factors. Regarding point one, the primary source of the error, discussed previously is that the travel pattern model simulates more vehicles arriving home earlier than expected. There is a 0.83 probability that a charging point is available at an overnight destination and there is a 0.55 probability that a vehicle will charge overnight when a charging point is available. As a higher proportion of vehicles arrive home earlier than expected, overnight charging events begin earlier than expected. This explains why the model simulates more vehicles than expected charging between 1 pm and 6 pm. This combined with the natural evening peak in vehicles arriving home and charging accounts for the higher than expected percentage of EVs charging between 6 pm and 12 am. In effect due to more vehicles arriving home earlier than expected the profile of the percentage of EVs charging is shifted forward in the day.

An examination of Figure 7.22, the frequency distribution (binned on a 30 minute time scale) of the expected and simulated charging event start times, supports this reasoning. The model simulates a larger number of charging events than expected in the majority of the 30 minute blocks between 1 pm and 9 pm and fewer charging events than expected beginning between 9.30 pm and 12 am.

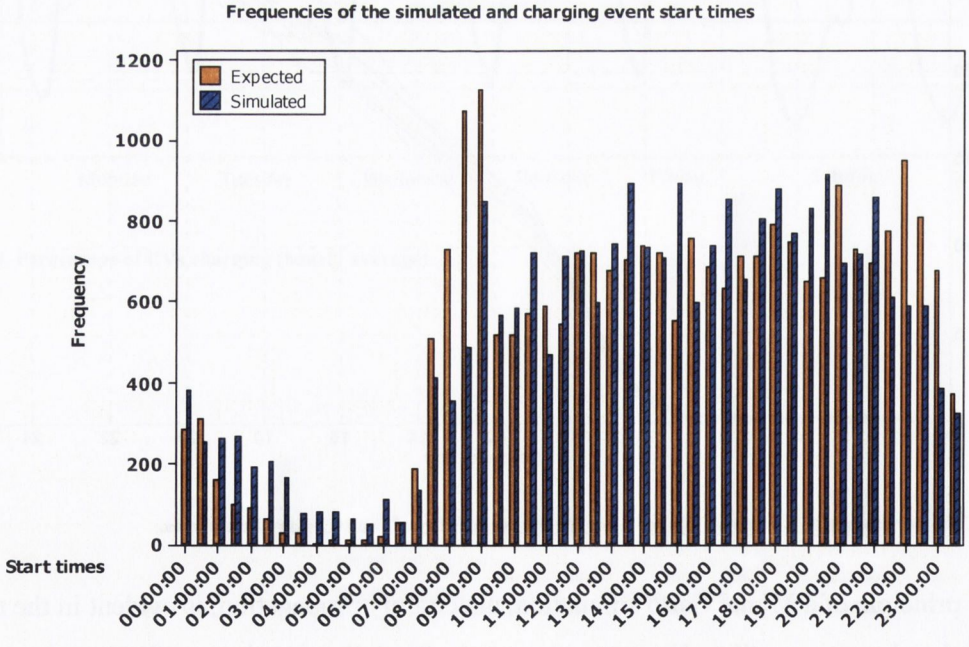

Figure 7.22. Frequencies of the simulated and expected charging event start times (binned on a 30-minute scale).

Correspondingly and in relation to second point, as the simulated overnight charging events begin earlier than expected, the charging events terminate earlier than expected. An examination of Figure 7.23, the frequency distribution of the expected and simulated charging event end times,

confirms this. The model simulates a larger number than expected of charging events terminating between 6.30 pm and 10.30 pm. In the real-world these charging events would be expected to terminate between 12.30 am and 3.30 am.

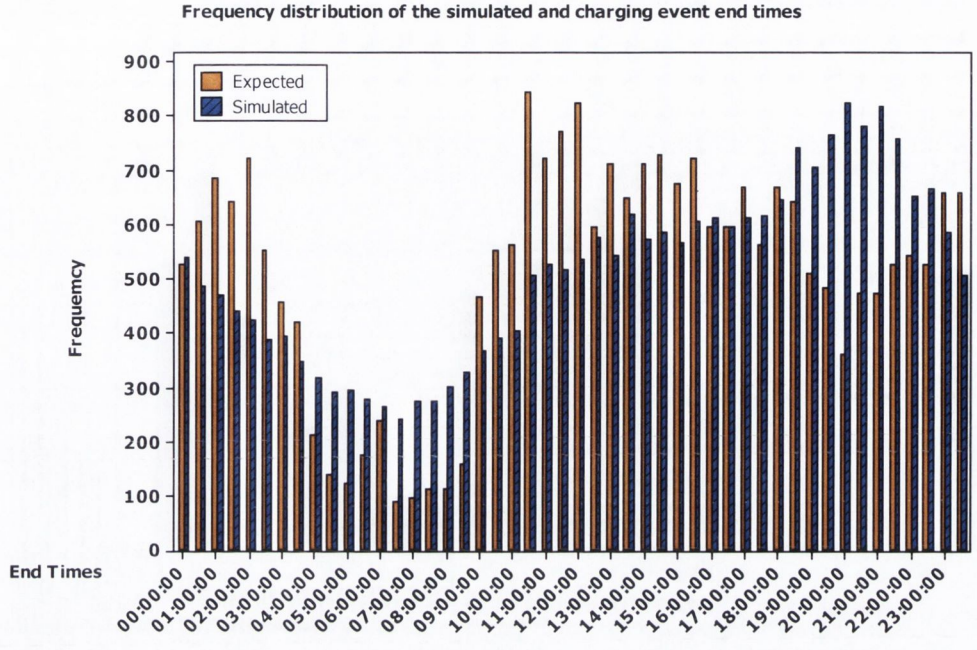

Figure 7.23. Frequencies of the simulated and expected charging event end times (binned on a 30-minute scale).

In relation to the third point, the probabilistic charging model is conditioned on the parking time and the SOC of the battery. The travel pattern model simulates more than expected 0-15 minute parking time intervals between journeys. Therefore, this acts to reduce the calculated probability of charging, as the probability of charging during short parking time intervals is small.

In addition, whilst every attempt was made to replicate real-world battery SOC depletion during trip events and incrementation during charge events, without precise battery SOC measurements it was difficult to replicate the expected SOC of the battery in the model after each event. The SOC measurements in the database which are referenced to calculate the probability of charging are calculated according to the battery gauge display, whereas the model estimates the SOC of the battery after trip and charge events according to Equations 7.1 and 7.2 in Section 7.3.2. Figure 7.24, the frequency distribution of the simulated and the expected SOC of the battery after the first journey of the day, illustrates the difficulty in simulating the exact operation of the battery. After the first journey of the day there are three peaks in the expected SOC of the battery, 87%, 82% and 78%. The aggregated nature of the peaks is as a result of the SOC being calculated from the 16 bars on the battery gauge. The model cannot replicate this behaviour. The model simulates a larger number of vehicles than expected with a SOC of 96%. This also acts to reduce the calculated probability of charging, as the probability of charging is small when the SOC of the battery is high.

Therefore, as the model simulates a larger proportion of vehicles with a higher SOC than expected the number of charging events that is simulated after the first journey of the day is lower than expected. The combination of these two factors acts to reduce the calculated probability of charging upon arrival at a destination and hence there are less charging events than expected at approximately 10 am.

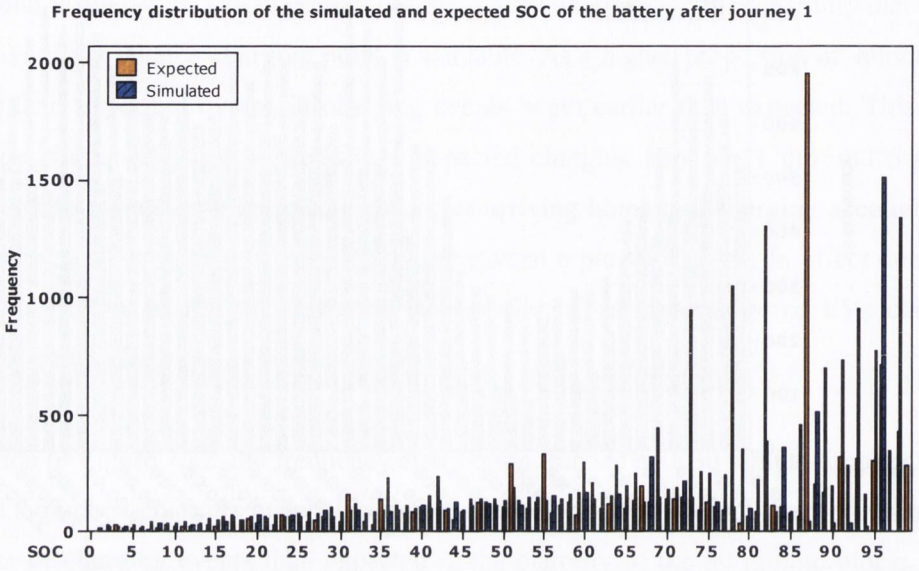

Figure 7.24. Frequencies of the simulated and expected SOC of the batteries after the first journey of the day.

7.10 Conclusions

This chapter extended the stochastic travel pattern model developed in Chapter 6 to translate simulated travel profiles for a fleet of EVs into charging profiles. A number of different methods of modelling charging decision making behaviour were investigated and a probabilistic charging model was incorporated into the travel pattern model and evaluated. At the end of each journey scheduled by the travel pattern model the probability of the availability of a charging point and the probability of charging is computed. A smaller dataset than that used in Chapter 6 was used in this chapter. This in addition to the existing issues regarding the simulation of parking times between two journeys outlined in Chapter 6, had negative implications for the performance of the travel pattern model. As discussed in Chapter 6, the primary source of error in relation to the simulation of parking times is due to the wide bounds on the conditions of the parking time distributions. The result is that more than expected short parking time intervals (0-15 minutes) are simulated in the model. Hence, the model simulates more vehicles arriving home earlier than expected which in turn results in overnight charging events beginning and terminating earlier than expected. In effect the simulated charging profile of a fleet of vehicles is shifted forward in the day. In addition to simulating more vehicles arriving home earlier than expected the simulation of more than expected short parking time intervals between journeys has implications for the charging decision model. The shorter the parking time between two journeys the smaller the probability of charging. Furthermore, without precise SOC measurements it was difficult to replicate in the model the exact

operation of the battery during trip and charge events. The model under predicts the energy consumption of vehicle during trip events. The combination of these two factors in the model, shorter than expected parking times and vehicles with a higher than expected battery SOC result in the model simulating less charging events than expected.

The model is an initial attempt to simulate the stochastic charging patterns of a large fleet of EVs. Further development of the model is needed in order for it to be a viable tool. Both of the sources of error in the model can be addressed. The model is based on data from 12 vehicles operating for 12 months which is a considerably small dataset in the context of the potential size of a national fleet of EVs. An increase in the dataset would allow the bounds on the conditions of the parking times distribution to be narrowed and would reduce the reliance on the assumption of a uniform prior distribution for the parking time distributions. As discussed in Chapter 6, in the cases when data are not retuned from the dataset, the development of an informed prior distribution for parking time simulation would enhance the model. Technical limitations of the data logging equipment used in this study prevented precise SOC measurements from being logged. However, all current EV models transmit large amounts of data relating to the vehicle including precise energy consumption and SOC measurements automatically to servers. Whilst imprecise SOC measurements were an issue in this study, it is unlikely to be an issue going forward.

In the future there will be many advancements in the way that EV charging is controlled with an emphasis on maximising the use of renewable energy and providing power system reserve through vehicle to grid operations. Such a tool could be used in order to analyse the impacts of such measures and to support policy decisions in relation to investment by estimating the potential cost savings associated with a smart grid.

7.11 Areas for further study

As discussed in Chapter 6, incorporating vehicle location into such a model using GPS data would enhance the model. The parking time of a vehicle should ideally be conditioned on the current location. In addition, the availability of a charging point and the probability of charging are also dependent on the current location. However, as discussed previously incorporating location into the model would prevent the aggregation of data as locations are unique to each individual, hence a different stochastic model structure such as a Markov chain would be required.

Separately, at present, the charging of EVs is uncontrolled. The effective CO_2 per kilometre produced by an EV is dependent on the electricity generation mix used to charge the battery. This emphasises the fact that the success of EVs in reducing transport related emissions is highly dependent on the optimal charging of the vehicle. This is in addition to the economic benefits of maximising the use of renewable energy. The efficiency of the energy mix, however, is determined

by the availability of low-emission, or renewable energy sources, such as wind energy. The Irish government have set a national target of deriving 40% of electricity from renewable resources by 2020 (Eirgrid, 2009). As discussed in Chapter 6, the availability of wind energy varies over time, and may even exceed the current demand. Therefore, the intermediate storage of wind energy is required in order to preserve this low-emission energy source and to reduce the effective emissions of the energy mix. Through V2G, EVs could be used as storage devices thus reducing the need for investment in grid expansion or other expensive storage systems such as pump storage. However, it would be difficult to impose restrictions on the mobility of an EV user to accommodate such requirements.

An area of further research would be to develop a methodology and algorithm to shift the charging times of EVs to time intervals of intensive wind energy production. In addition, the batteries should be capable of supplying energy back to the power grid at times where the grid-sided demand is high, in order to avoid CO_2 intensive power plants servicing the demand. Such an energy management approach would need to be flexible to take into account the EV owner's mobility behaviour. The times and locations at which EVs are connected to the grid are wholly conditioned on the EVs owner's mobility patterns.

8 Conclusions

The recent emphasis on fuel efficient vehicles and greenhouse gas emission (GHG) reductions from light duty vehicles (LDV) provide strong impetus for the development of electric vehicles (EV). EVs could make an important contribution to society in terms of reducing GHG emissions, improving urban air quality and reducing our dependence on fossil fuels while at the same time facilitating the future growth of renewable energy sources on the electricity grid. Recognising the potential benefits of EVs, a number of governments worldwide have established clear deployment goals for EVs and have introduced consumer incentives. In Europe, the Irish, Norwegian and Danish governments have set targets to have between 50,000 and 230,000 EVs deployed by 2020. The American government has also set an ambitious target to have one million EVs deployed by 2015 and the Japanese government aims to have 20% of the private car fleet powered by electricity by 2020. Many countries offer subsidies of approximately €5,000 to early purchasers of EVs in an attempt to grow their EV markets and some countries such as Denmark offer additional incentives such as free parking and charging and the use of bus lanes.

The environmental and socioeconomic impacts of EVs on society and the additional demand placed on the electricity grid need to be understood in order to support policy decisions. However, realistic environmental, economic and electricity grid impact studies can only be evaluated if the energy economy, the travel and charging patters of EVs operating in the real-world are understood. In addition, in order to enable the continued development of powertrains and energy storage systems for EVs and to evaluate these developments a better understanding of real-world driving conditions in terms of velocity and acceleration profiles are required.

This thesis presented a number of pieces of research which sought to address these research questions. A detailed discussion and the conclusions drawn from each of the research topics are discussed at length at the end of each chapter. A summary of the key findings and the contribution to the knowledge are presented here.

The literature indicates that EVs are particularly suitable for commuting as driving range restrictions and long charging cycles are not major constraints. In Ireland, a number of studies have found that there is extensive short and long distance car-based commuting in the Greater Dublin Area (GDA). Therefore, in Chapter 2 the potential reduction in road traffic related emissions due to commuting in the GDA in 2020 under different EV market penetration scenarios was evaluated. The results of the analysis showed that the introduction of EVs presents an advantage over a business as usual scenario in terms of reducing emissions. Under the most likely scenario (10% market penetration by the year 2020) the results indicated a net reduction of 3% in CO_2 emissions relative to the business as usual scenario could be achieved. These emissions will most likely account for approximately 2% of the CO_2 emissions from the transport sector in 2020. Urban air

pollutants were individually projected to decrease by up to 11%. The results of the analysis indicate that the time required for EVs to acquire a significant share of the national fleet, suggests that they will have a limited impact on climate change and urban air quality for at least the next decade. However, the analysis supports existing international evidence that EVs are a realistic alternative to internal combustion engine vehicles (ICEV) in the long term and will contribute to emissions reductions.

Many governments have introduced financial consumer incentives to encourage the purchase of EVs. However, EVs present policy makers worldwide with competing goals, the goal to support and encourage the adoption of EVs, while on the other hand to reduce GHG emissions and provide a sustainable transportation system. The loss in tax revenue as a consequence of incentive schemes is becoming a debateable topic. In Chapter 3, a social cost-benefit analysis of the 10% market penetration of EVs in Ireland was undertaken. It analysed the socio-economic costs and benefits of this policy by comparing the environmental benefits, expressed in monetary value, with the associated reduction in tax revenues and the cost of the Irish government's EV grant scheme. The analysis found that by 2020 the 10% market penetration of EVs will result in a social marginal net loss of €324 million or €1,408 per vehicle. The primary reason for this loss is due to losses in all sources of tax revenue compared with the market penetration rates required to achieve significant reduction in emissions. The loss in tax revenue is estimated to be in the region of 0.5% to 1% of total tax revenue in Ireland at 2009 levels. However, this result should be interpreted carefully in light of the assumptions stated in the analysis. The findings of this analysis are in line with a number of international studies which have found that the market penetration of EVs will result in losses in transportation related tax revenues.

In the future, if alternative fuels vehicles achieve mass market penetration, legislative authorities will to need consider alternative funding structures to the current motor and fuel tax mechanism. The current structure could fail to provide adequate revenue to fund and maintain transportation systems. Furthermore, as the overall operational efficiency and range of fuel efficiency of conventional vehicles and alternative fuelled vehicles increases, the use of fuel consumption as a measure of the transportation system use, as we currently do, could become less appropriate. In the future, there will likely be a strong correlation between electricity use and vehicle miles travelled and thus electricity use could serve as a good measure of the usage of a transportation system. Updating existing electricity metres and fee collection mechanisms could facilitate the charging of EV users based on their energy use. In addition, time of use rates and other price signals could be implemented.

Chapter 4 formed the basis of the research presented in Chapter 5. The literature demonstrates that existing driving cycles, which are used in the design, certification and lifecycle evaluation of EVs,

do not emulate real-world driving conditions particularly well and the requirement for realistic real-world driving cycles to be developed has been cited. In Chapter 4, a comprehensive review of existing driving cycle and driving cycle development methodologies for ICEVs and EVs was conducted and the shortcomings of existing driving cycles and driving cycle development methodologies were identified. A four-step modelling approach for developing a set of real-world driving cycles for the GDA was presented. The ability of driving cycles to represent real-world driving conditions was enhanced by improving and combining four important steps in the driving cycle development process: 1) a dynamic statistical analysis of logged driving cycles in order to segment and classify the data was conducted, 2) a driving cycle model that synthesises driving cycles by the application of velocity and acceleration succession probabilities at a second by second level was developed, 3) a number of driving cycle assessment and evaluation procedures were performed to ensure that the developed driving cycles were representative of the original dataset and 4) the developed driving cycles were compared to existing well established worldwide cycles.

The remainder of Chapter 4 detailed the first step in the modelling approach. A methodology for conducting an analysis of real-world vehicle driving cycle data was presented in order to contribute to the knowledge regarding the real-world operating conditions and energy demands of EVs. A driving environment recognition tool, using a neural network technique was developed to identify and segment the driving cycle data in terms of road types and levels of congestion. This facilitated an in depth analysis of real-world driving cycle data. It was determined that EVs almost entirely operate in urban driving conditions and that the energy economy of an EV is highest on short journeys (174 Wh/km) and in urban stop-start driving (437 Wh/km) conditions. These results have implications for life cycle and environmental impact analyses as the real-world energy economy and use of vehicles are critical inputs to these types of analyses and generally cannot be found in scientific literature. Furthermore, this analysis provided an insight into real-world driving conditions that a developed driving cycle should be representative of and hence set a benchmark for the development of the driving cycles presented in Chapter 5.

In Chapter 5 the remaining three-steps of the proposed modelling approach to developing driving cycles were described. Firstly, a Markov-chain driving cycle model developed with real-world data was presented. The model synthesised candidate driving cycles. Secondly, a driving cycle assessment procedure was outlined. A regression analysis was performed to identify driving cycle parameters that are statistically significant in terms of influencing the energy economy of an EV over a driving cycle. When synthesising the driving cycles with the Markov-chain model multiple iterations of the process were performed until the statistical parameters, identified by the regression analysis, matched the mean of the statistical parameters of real-world driving cycles within certain error bounds. This ensured that the developed driving cycles were representative of the real-world

driving cycles in the dataset. In addition, the predicted energy economy values of the developed driving cycles were shown to be representative of real-world energy economy values determined in Chapter 4. In the final step a number of methodologies were used to assess the representativeness of the developed driving cycles and a selection of well-established worldwide driving cycles of the original dataset of recorded real-world driving cycles. The developed driving cycles were also compared to the selection of worldwide cycles.

The developed driving cycles outperformed the selection of worldwide driving cycles with respect to matching the mean of the statistical parameters of the real-world driving cycles. It was found that existing transient cycles were more representative of real-world driving conditions than existing modal cycles such as the New European Driving cycle, which is the current legislative driving cycle in Europe. It was also established that real-world driving conditions differ significantly from existing certification driving cycles developed for emissions testing in America and Japan. They generally consist of lower velocity driving and higher acceleration rates. This implies that these driving cycles may not be suitable for design purposes of EVs. To conclude, the developed driving cycles would aid in the design of EVs that are operating in the GDA and would allow electricity grid analysis, economic and lifecycle studies to be conducted with a higher degree of confidence. Areas for further research in relation to the inclusion of road gradient and air conditionings in driving cycle development are described in detail at the end of Chapter 5.

In terms of evaluating the impacts of EVs on the electricity grid to support policy decisions, in the past the scientific community have used deterministic approaches to model travel and charging patterns of EVs. However, the complexity and stochastic nature of these behaviours suggest that a stochastic model would be more beneficial. Recently, due to the availability of field data, stochastic models have become more popular. Chapters 6 and 7 presented a Monte Carlo simulation approach to simulate the travel patterns and charging profiles of EVs respectively. In Chapter 6, GPS travel data collected during the EV demonstration project were used to derive distributions of travel pattern related variables. The dependence structure between six of the variables was modelled using a non-parametric copula function. The model uses an iterative method of conditional distributions with a Bayesian inference to generate journey schedules by synthesising journey distances, journey times and parking times.

Compared to existing studies this model attempted to synthesise a precise journey schedule on an individual basis, using travel data from EVs placed in actual households, as opposed to modelling journeys to and from the home or the workplace of a fleet of vehicles using data pertaining to travel surveys or data collected by ICEVs. However, whilst the travel patterns simulated by the model were shown to adhere relatively close to the deterministic data, the additional complexity of the model structure adversely affects the performance of the model. Primarily due to a shortage of data,

the model simulates more than expected short parking time intervals (i.e. 5-20 minutes), which results in more vehicles than expected arriving home earlier in the day than expected. This was found to have significant implications for the simulated charging profiles which were modelled in Chapter 7. Overall, the results indicate that the proposed model is a step toward stochastic travel pattern modelling of EVs but future work is needed, specifically with regards to modelling parking times, to fully investigate the usefulness of the current model structure. Areas for further research in relation to modelling the travel patterns of EV are described in detail at the end of Chapter 6.

In general EV electricity grid integration studies either assume definite charging upon arrival at a destination or charging is conditioned upon a set of rules usually related to the state of charge and/or the length of time that the vehicle is parked. Chapter 7 extended the stochastic travel pattern model developed in Chapter 6 to translate the simulated travel profiles for a fleet of EVs into charging profiles. A number of different methods of modelling charging behaviour were investigated and a probabilistic charging model was incorporated into the travel pattern model. At the end of each journey scheduled by the travel pattern model the probability of the availability of a charging point and the probability of charging is computed. Compared to existing models, this model is advantageous in that the probability of charging is computed directly from real-world data. The model could easily be extended to model the probability of charging as a result of different pricing structures at such a time that data becomes available. The charging aspect of the overall model performs satisfactorily, however, the inherent errors in the underlying travel pattern model, which result in vehicles arriving home earlier than expected, in effect results in the simulated charging profiles being shifted forward in time during the day. Therefore, further development of the underlying travel pattern model, as discussed at the end of Chapter 6, is needed in order for it to be a viable tool for analysing the impacts on the electricity grid of large scale EV deployment.

9 Bibliography

Aa Ireland. 2010. *Petrolprices* [Online]. Available: http://www.aaireland.ie/petrolprices/.

Abdollahi, A. D. An Intelligent Control Strategy in a Parallel Hybrid Vehicle. Electric and Hybrid Vehicles, 2006. ICEHV '06. IEEE Conference on, 18-20 Dec. 2006 2006. 1-2.

Alessandrini, A. & Orecchini, F. 2003. A driving cycle for electrically-driven vehicles in Rome. *Proceedings of the Institution of Mechanical Engineers, Part D: Journal of Automobile Engineering,* 217, 781-789.

Ali Ashtari, E. B., Soheil Shahidinejad 2012. Using Large Driving Record Samples and a Stochastic Approach for Real-World Driving Cycle Construction: Winnipeg Driving Cycle. *Transportation Science,* Articles in Advance, pp. 1–14.

Andre, M. 1996. Driving cycle development: Characterization of the methods. *SAE Int. Spring Fuels Lubricants Meet* 1–13.

André, M. 2004. The ARTEMIS European driving cycles for measuring car pollutant emissions. *Science of The Total Environment,* 334–335, 73-84.

Andre, M., Hickman, J., Hassel, D. & Joumard, R. 1995. Driving cycles for emission measurements under european conditions. *SAE Technical Paper Series, the Engineering Society for Advanced Mobility.*

Argonne National Laboratory. 2012. *Autonomie* [Online]. Available: http://www.autonomie.net/ [Accessed January 1st 2012].

Ashtari, A., Bibeau, E. & Shahidinejad, S. 2012a. Using Large Driving Record Samples and a Stochastic Approach for Real-World Driving Cycle Construction: Winnipeg Driving Cycle. *Transportation Science* Articles in Advance, 1-14.

Ashtari, A., Bibeau, E., Shahidinejad, S. & Molinski, T. 2012b. PEV Charging Profile Prediction and Analysis Based on Vehicle Usage Data. *Smart Grid, IEEE Transactions on,* 3, 341-350.

Austin, T. C., Digenova, F. J., Carlson, T. R., Joy, R. W., Gianolini, K. A. & Lee, J. M. 1993. Characterization of driving patterns and emissions from light-duty vehicles in California. Sacramento: California Air Resources Board.

Austrian Institute of Technology. 2013. *Smart Grids model region Salzburg – Building to Grid* [Online]. Available: http://www.ait.ac.at/departments/energy/research-areas/energy-for-the-built-environment/energy-in-buildings/sgms-b2g/?L=1 [Accessed July 25th 2013].

Avere. 2012. Norwegian Parliament extends electric car iniatives until 2018. Available: http://www.avere.org/www/newsMgr.php?action=view&frmNewsId=611&section=&type=&SGLSESSID=mi3rnro4brrhkq4qi69nqcjd61.

Axsen, J. & Kurani, K. S. 2010. Anticipating plug-in hybrid vehicle energy impacts in California: Constructing consumer-informed recharge profiles. *Transportation Research Part D: Transport and Environment,* 15, 212-219.

Barlow, T., Latham, S., Mccrae, I. & Boulter, P. 2009. A reference book of driving cycles for use in the measurement of road vehcile emissions TRL.

Barry, C. 2012. *Using Stepwise Regression to Explain Plant Energy Usage* [Online]. Available: http://blog.minitab.com/blog/real-world-quality-improvement/using-minitab-stepwise-regression-to-explain-plant-energy-usage [Accessed June 1st 2012].

Barth, M., An, F. & Norbeck, J. 1996a. Modal emissions modeling: a physical approach. *Transportation Research Record: Journal of the Transportation Research Board,* 81-88.

Barth, M., Johnston, E. & Tadi, R. 1996b. Using GPS technology to relate macroscopic and microscopic traffic parameters. *Transportation Research Record: Journal of the Transportation Research Board,* 89-96.

Basri, M. 2008. *Medical image classification and symptoms detection using neuro fuzzy* Universiti Teknologi Malaysia.

Bata R, Yacoub Y, Wang Wg, Lyons D, Gambino M & G, R. 1994. Heavy duty testing cycles: Survey and comparison. *International Truck and Bus Meeting and Exposition.* Seattle.

Bergin, A., Conefrey, T., Fitgerald, J. & Kearney, I. 2009. Recovery Scenarios for Ireland. The Economic and

Social Research Institute.

Bergin, A., Conefry, T., Fitz Gerald, J. & Kearney, I. 2010. Recovery Scenarios for Ireland: An Update. Dublin: The Economic and Social Research Institute.
Biehl, M., Ghosh, A. & Hammer, B. 2006. Learning vector quantization: The dynamics of winner-takes-all algorithms. *Neurocomputing,* 69, 660-670.
Big Ladder Software. 2013. *ADVISOR® Advanced Vehicle Simulator* [Online]. Available: http://bigladdersoftware.com/advisor/.
Boldo, E., Medina, S., Tertre, A., Hurley, F., Mücke, H. G., Ballester, F., Aguilera, I. & Eilstein, D. 2006. Health Impact Assessmenton the Benefits of Reducing PM2.5 in 26 European Cities. *European Journal of Epidemiology,* 21, 449-458.
Brady, J. & O'mahony, M. 2011. Introduction of electric vehicles to Ireland: Socioeconomic analysis. *Transportation Research Record: Journal of the Transportation Research Board,* 64-71.
Brady, J. & O'mahony, M. 2011. Travel to work in Dublin. The potential impacts of electric vehicles on climate change and urban air quality. *Transportation Research Part D: Transport and Environment,* 16, 188-193.
Brandewinder, M. 2008. *S-shaped market adoption curve* [Online]. Clear Lines Consulting. Available: http://www.clear-lines.com/blog/post/S-shaped-market-adoption-curve.aspx [Accessed 2009 January 1st].
Brownstone, D. & Train, K. 1999. Forecasting new product penetrationwith flexible substitution patterns. *Journal of Econometrics,* 109–129.
Brzezinski, B., Hart, C. & Enns, P. 2001. Final Facility Specific Speed Correction Factors EPA420-R-01-060. U.S. Environmental Protection Agency.
Cano, J. C. & Nava, P. A. A fuzzy method for automatic generation of membership function using fuzzy relations from training examples. Fuzzy Information Processing Society, 2002. Proceedings. NAFIPS. 2002 Annual Meeting of the North American, 2002 2002. 158-162.
Carlson, T. R. & Austin, T. C. 1997. Development of Speed Correction Cycles. Sacramento, California: Sierra Research, Inc.
Carlsson, F. & Johansson-Stenman, O. 2003. Costs and Benefits of Electric Vehicles, A
2010 Perspective. *Transport Economics and Policy,* 37, 1-28.
Carroll, S. 2011. *RE: iMiEV Data.* Type to BRADY, J.
Central Statistics Office 2007a. Census of Population of Ireland 2006, Place of Work, Census of Anonymised Records (POWCAR)
Users Guide. Dublin, Ireland: Central Statistics Office.
Central Statistics Office 2007b. Transport 2006. Central Statistics Office.
Central Statistics Office 2010. Principle Statistics: Employment and unemployment (ILO) '000s. Dublin,Ireland: Central Statistics Office.
Chen, C., Huang, C., Jing, Q., Wang, H., Pan, H., Li, L., Zhao, J., Dai, Y., Huang, H., Schipper, L. & Streets, D. G. 2007. On-road emission characteristics of heavy-duty diesel vehicles in Shanghai. *Atmospheric Environment,* 41, 5334-5344.
Cleanmpg. 2013. *Mitsubishi's iMiEV "Best in Class" BEV goes on sale in July* [Online]. Available: http://www.cleanmpg.com/forums/showthread.php?t=22506.
Clement-Nyns, K., Haesen, E. & Driesen, J. 2010. The Impact of Charging Plug-In Hybrid Electric Vehicles on a Residential Distribution Grid. *Power Systems, IEEE Transactions on,* 25, 371-380.
Commins, N. & Nolan, A. 2008. The Determinants of Mode of Transport to Work in the Greater Dublin Area. The Economic and Social Research Institute.
Congressional Budget Office 2012. Effects of Federal Tax Credits for the Purchase of Electric Vehicles. Washington: Congress of the united States,Congressional Budget Office.
Dai, Z., Niemeier, D. & Eisinger D. 2008. Driving cycles: A new drive cycle-building method that better represents real world emissions UC Davis: University of California.
Dallinger, D., Krampe, D. & Wietschel, M. 2011. Vehicle-to-Grid Regulation Reserves Based on a Dynamic Simulation of Mobility Behavior. *Smart Grid, IEEE Transactions on,* 2, 302-313.
Delucchi, M. A. & Lipman, T. E. 2001. An analysis of the retail and lifecycle cost of battery-powered electric vehicles. *Transportation Research Part D: Transport and Environment,* 6, 371-404.
Dempsey, N. 2008. Government announces plans for the electrification of Irish motoring. Dublin, Ireland: Department of Transport, Press Release.

Dennehy, E., Howley, M., Ó Gallachóir, B. & Barriscale, A. 2010. Renewable Energy in Ireland 2010 Update. Dublin, Ireland: Sustainable Energy Ireland.
Department of Communications Energy and Natural Resources 2007. National Energy Efficiency Action Plan
for Ireland
2007-2020. Dublin, Ireland: Department of Communications Energy and Natural Resources.
Department of Energy 2011. One Million Electric Vehicles By 2015 Feburary 2011 Status Report. United States of America, Department of Energy,.
Department of Transport 2008. Sustainable Travel and Transport Action Plan. Dublin, Ireland: Department of Transport.
Department of Transport 2009. Irish Bulletin of Vehicle and Driver Statistics 2008. Dublin,
Ireland.: Department of Transport.
Di, W., Aliprantis, D. C. & Gkritza, K. 2011. Electric Energy and Power Consumption by Light-Duty Plug-In Electric Vehicles. *Power Systems, IEEE Transactions on,* 26, 738-746.
Diamond, D. 2009. The impact of government incentives for hybrid-electric vehicles: Evidence from US states. *Energy Policy,* 37, 972-983.
Dieselnet. 2013a. *EPA New York City Cycle (NYCC)* [Online]. Available: http://www.dieselnet.com/standards/cycles/nycc.php.
Dieselnet. 2013b. *Japanese 10-15 Mode* [Online].
Dieselnet. 2013c. *Japanese JC08 Cycle* [Online]. Available: http://www.dieselnet.com/standards/cycles/jp_jc08.php.
Dieselnet. 2013d. *SFTP-SC03* [Online]. Available: http://www.dieselnet.com/standards/cycles/ftp_sc03.php.
Dieselnet. 2013e. *Worldwide Harmonised Test*
Procedure for Light Duty Vehicles
WLTP [Online]. Available: http://www.dieselnet.com/standards/cycles/wltp.php [Accessed January 5th 2013].
Doyle, A. & Adomaitis, N. 2013. Norway shows the way with electric cars, but at what cost? Available: http://www.reuters.com/article/2013/03/13/us-cars-norway-idUSBRE92C0K020130313 [Accessed March 13th 2013].
Draper, M., Rodriguez, E., Kaminsky, P., Sidhu, I. & Tenderich, B. 2008. Economic Impact of Electric Vehicle Adoption in the United States. University of Califorina Berkeley.
Dubarry, M., Svoboda, V., Hwu, R. & Liaw, B. Y. 2007. A roadmap to understand battery performance in electric and hybrid vehicle operation. *Journal of Power Sources,* 174, 366-372.
Duoba, M., Carlson, R. & Bocci, D. 2009. Calculating Results and Performance Parameters
for PHEVs. *SAE Technical Paper 2009-01-1328.*
E. D. Tate, Harpster, M. O. & Peter J. Savagian 2009. The electrification of the automobile: from conventional hybrid, to plug-in hybrids, to extended-range electric vehicles. *SAE Int. J. Passeng. Cars - Electron. Electr. Syst.* .
Easyfitxl. 2013. *Distribution Fitting for Excel* [Online]. Available: http://www.mathwave.com/easyfitxl-distribution-fitting-excel.html [Accessed August 1st 2012].
Eirgrid 2009. National Renewable Energy Action Plan. Dublin ,Ireand: Eirgrid.
Eksin, C., Güzelkaya, M., Yesil, E. & Eksin, B. 2012. Fuzzy Logic approach to mimic decision making behaviour of humans in stock management game. BogaziciUniversity.
Electric Auto Association. 2005. Electric Vehicle History. Available: http://www.eaaev.org/Flyers/eaaflyer-evhistory.pdf.
Electric Power Research Institute 2007. Environmental Assessment of Plug-In Hybrid Electric Vehicles. Electric Power Research Institute.
Electric Vehicles Initiative 2013. Global EV outlook, Understanding the Electric Vehicle Landscape to 2020. Electric Vehicles Initiative.
Environmental Protection Agency 2009a. Air Quality in Ireland 2008 Wexford, Ireland: Environmental Protection Agency.
Environmental Protection Agency 2009b. Irealnd's Greenhouse Gas Emission Projections 2008-2020. Environmental Protection Agency.

Environmental Protection Agency 2009c. Ireland's Greenhouse Gas Emissons in 2008. Environmental Protection Agency.

Esb. 2013. *Electric car charge point map* [Online]. Available: http://www.esb.ie/electric-cars/electric-car-charging/electric-car-charge-point-map.jsp [Accessed January 2013].

Essen, H. & Kampman, B. 2011. Impacts of Electric Vehicles – Summary report. CE Delft.

Esteves-Booth, A., Muneer, T., Kirby, H., Kubie, J. & Hunter, J. 2001. The measurement of vehicular driving cycle within the city of Edinburgh. *Transportation Research Part D: Transport and Environment,* 6, 209-220.

European Association for Electric Vehicles. 2009. Energy consumption, CO2 emissions and other considerations related to Battery Electric Vehicles. Available: http://www.going-electric.org/docs/CO2-energy-electric-vehicles.pdf.

European Climate Assessment and Dataset. 2010. Available: http://eca.knmi.nl/dailydata/customerquery.php [Accessed 15/1/10.

European Commission 2008. A European Economic Recovery Plan. Brussels: European Commission.

European Commission 2009. Promotion of the use of energy from renewable sources. *In:* EUROPEAN COMMISSION (ed.) *Directive 2009/28/EC.*

European Commission. 2013a. *European Green Cars Initiative* [Online]. Brussels: European Commission. Available: http://www.green-cars-initiative.eu/public/.

European Commission. 2013b. *FP7: the future of European Union research policy* [Online]. Available: http://ec.europa.eu/research/fp7/index_en.cfm.

European Commission. 2013c. *Green eMotion* [Online]. European Commission. Available: http://www.greenemotion-project.eu/.

European Environment Agency 2009. EMEP/EEA air pollutant emission inventory guidebook — 2009. Copenhagen, Denmark: European Environment Agency.

Eurostat 2009a. Eurostat yearbook 2009 *In:* IVAN, D., JOHANSSON, AUGIER, A.J., PIIRTO, J., WIELAND U. (ed.). European Commission.

Eurostat 2009b. Motorisation rate - cars per 1 000 inhabitants. European Commission.

Eva, E. 2000. Variability in urban driving patterns. *Transportation Research Part D: Transport and Environment,* 5, 337-354.

Eva, E. 2001. Independent driving pattern factors and their influence on fuel-use and exhaust emission factors. *Transportation Research Part D: Transport and Environment,* 6, 325-345.

Fellah, M., Signh, G., Rousseau, A., Pagerit, S., Nam, E. & Hoffman, G. 2009. Impact of Real-World Drive Cycles on PHEV Battery Requirements. *SAE Paper 2009-01-1383.*

Fellini, R., Michelena, N., Papalambros, P. & Sasena, M. Optimal design of automotive hybrid powertrain systems. Environmentally Conscious Design and Inverse Manufacturing, 1999. Proceedings. EcoDesign '99: First International Symposium On, 1-3 Feb 1999 1999. 400-405.

Fitzgerald, J. D., Hoe, J. & Kearney, I. 2002. A Model for Forecasting Energy Demand and Greenhouse Gas Emissions in Ireland. Dublin: The Economic and Social Research Institute.

Foley, A., Gallachoir, B. O., Leahy, P. & Mckeogh, E. 2009. Electric Vehicles and Energy Storage – a case study on Ireland *Vehicle Power and Propulsion Conference, 2009. VPPC '09. IEEE.* Dearborn, MI

Foley, M. & Mcgory, J. 2011. *The Application of Fuzzy Logic in Determining Linguistic Rules and Associative Membership Functions for the Control of a Manufacturing Process.* Master of Engineering in Pharmaceutical Process Control and Automation, Dublin Institute of Technology.

Fomunung, I., Washington, S. & Guensler, R. 1999. A statistical model for estimating oxides of nitrogen emissions from light duty motor vehicles. *Transportation Research Part D: Transport and Environment,* 4, 333-352.

Forkenbrock, D. J. 2006. Financing local roads – Current problems and new paradigm. *Transportation Research Record: Journal of the Transportation Research Board,* , 8-14.

Frigyik, B. A., Kapila, A. & Gupta, M. R. 2010. Introduction to the Dirichlet Distribution and Related Processes. Department of Electrical Engineering University of Washington.

Gkatzoflias, D., Kouridis, C., Ntziachristos, L. & Samaras, Z. 2007. Computer programme to calculate emissions from road transport – Methodology for the calculation of exhaust emissions. European Environment Agency.

Golob, T. F. & Gould, J. 1998. Projecting use of electric vehicles from household vehicle trials. *Transportation Research Part B: Methodological,* 32, 441-454.

Gonder, J., Markel, T., Thornton, M. & Simpson, A. 2007. Using Global Positioning System Travel Data to Assess Real-World Energy Use of Plug-In Hybrid Electric Vehicles. *Transportation Research Record: Journal of the Transportation Research Board,* 2017, 26-32.

Gong, Q., Midlam-Mohler, S., Marano, V. & Rizzoni, G. 2011. An Iterative Markov Chain Approach for Generating Vehicle Driving Cycles. *SAE International Journal of Engines,* 4, 1035-1045.

Granovskii, M., Dincer, I. & Rosen, M. A. 2006. Economic and environmental comparison of conventional, hybrid, electric and hydrogen fuel cell vehicles. *Journal of Power Sources,* 159, 1186-1193.

Green, R. C., Lingfeng, W. & Alam, M. The impact of plug-in hybrid electric vehicles on distribution networks: a review and outlook. Power and Energy Society General Meeting, 2010 IEEE, 25-29 July 2010 2010. 1-8.

Guner, E. 2003. *Adaptive neuro fuzzy inference system applications in chemical process.*

Hadley, S. & Tsvetkova, A. 2008. Potential Impacts of Plug-in Hybrid

Electric Vehicles on Regional Power

Generation. Oak Ridge National Laboratory, U.S department of Energy

Hall, A. 2012. *Estimating the Impact on Fuel Tax Revenues from a Changing Light Vehicle Fleet with Increased Advanced Internal Combustion Engine Vehicles and Electric Vehicles.* Master of Science in Engineering, The University of Texas at Austin.

Hayashi, Y., Kato, H. & Teodoro, R. V. R. 2001. A model system for the assessment of the effects of car and fuel green taxes on CO2 emission. *Transportation Research Part D: Transport and Environment,* 6, 123-139.

Hellinga, B. 2011. Issues realted to quantifying the environental impacts of transportation strategies using GPS data. Available: http://www.civil.uwaterloo.ca/bhellinga/publications/Publications/ITE%202002%20GPS%20and%20Emissions%20v7.pdf [Accessed 01,01,2012].

Helmers, E. & Marx, P. 2012. Electric cars: technical characteristics and environmental impacts. *Environmental Sciences Europe,* 24, 1-15.

Hennessy, H. & Tol, R. 2010. The Impact of Climate Policy on Private Car Ownership in Ireland. Dublin, Ireland: Economic and Social Research Institute.

Herynkova, H. 2009. *Impact Analysis of Diffusion of Electric Vehicles in Denmark.* Master programme in Economic Growth, Innovation and Spatial Dynamics Master, Lund University.

Hill, G., Blythe, P. T. & Higgins, C. Deviations in Markov chain modeled electric vehicle charging patterns from real world data. Intelligent Transportation Systems (ITSC), 2012 15th International IEEE Conference on, 16-19 Sept. 2012 2012. 1072-1077.

Hollinshead, M. J., Eastman, C. D. & Etsell, T. H. 2005. Forecasting performance and market penetration of fuel cells in transportation. *Fuel Cells Bulletin,* 2005, 10-17.

Horner, A. 1999. The Tiger Stirring: Aspects of commuting in the Republic of Ireland 1981-1996 *Irish Geography* 32, 99-111.

Houses of Parliament 2010. Electric Vehicles Parliamentary offices of science and technology

Hovhannisyan, M. 2013. *Artificial Neural Network* [Online]. Available: http://en.wikipedia.org/wiki/User:Mariam_Hovhannisyan.

Howley, M., Dennehy, E. & Gallachóir, B. Ó. 2009a. Energy in Ireland Key Statistics 2009. Dublin Ireland: Sustainable Energy Ireland.

Howley, M., Dennehy, E. & Ó Gallachóir, B. 2009b. Energy in Transport 2009 Report. Sustainable Energy Ireland.

Hudson, M. B., Hagan, M. T. & Demuth, H. B. 2012. Neural Netowrk Toolbon: Getting started guide. Mathworks.

Hughes, L. & Sundaram, S. 2011. An analysis of electric vehicles and their potential impact on Nova Scotia's passenger vehicle emissions. Energy Research Group, Electrical and Computer Engineering, Dalhousie University, H.

Hung, W. T., Tong, H. Y., Lee, C. P., Ha, K. & Pao, L. Y. 2007. Development of a practical driving cycle construction methodology: A case study in Hong Kong. *Transportation Research Part D: Transport and Environment,* 12, 115-128.

Intergovernmental Panel on Climate Change 2007. Fourth Assessment Report:The Physical Science Basis. Geneva: Intergovernmental Panel on Climate Change,.

Ipcc 2007. Climate Change 2007: Mitigation. Contribution of Working Group III to the Fourth Assessment Report of the Intergovernmental Panel on Climate Change. *In:* [B. METZ, O. R. D., P.R. BOSCH, R. DAVE, L.A. MEYER (ed.). Cambridge: Intergovernmental Panel on Climate Change.

Irish Statute Book 2003. S.I. No. 541/2003. Air Pollution Act, 1987 (Environmental Specifications for Petrol and Diesel fuels) Regulations 2003. Dublin Stationary Office.

Jang, J. S. R. 1993. ANFIS: adaptive-network-based fuzzy inference system. *Systems, Man and Cybernetics, IEEE Transactions on,* 23, 665-685.

Jensen, P. & Bard, J. 2002. *Operations Research Models and Methods*, John Wiley & Sons.

Jeon, S.-I., Jo, S.-T., Park, Y.-I. & Lee, J.-M. 2002. Multi-Mode Driving Control of a Parallel Hybrid Electric Vehicle Using Driving Pattern Recognition. *Journal of Dynamic Systems, Measurement, and Control,* 124, 141-149.

Jiju, A. 2003. *Design of Experiments for Engineers and Scientists*, Butterworth-Heinemann.

Joint Research Centre 2008. Backcasting approach for sustainable
mobility European Commission ,Joint Research Centre,Institute for Environment and Sustainability.

Kamble, S. H., Mathew, T. V. & Sharma, G. K. 2009. Development of real-world driving cycle: Case study of Pune, India. *Transportation Research Part D: Transport and Environment,* 14, 132-140.

Kantor, I., Fowler, M. W., Hajimiragha, A. & Elkamel, A. 2009. Air quality and environmental impacts of alternative vehicle technologies in Ontario, Canada. *International Journal of Hydrogen Energy,* In Press, Corrected Proof.

Keane, E. & Flynn, D. Potential for electric vehicles to provide power system reserve. Innovative Smart Grid Technologies (ISGT), 2012 IEEE PES, 16-20 Jan. 2012 2012. 1-7.

Kendall, G. 2008. Plugged in – The end of the oil age. World Wide Fund for Nature.

Kent, J. H., Allen, G. H. & Rule, G. 1978. A driving cycle for Sydney. *Transportation Research,* 12, 147-152.

Kim, N., Rousseau, A. & Rask, E. 2012. Autonomie model validation with test data for 2010 Toyota Prius. Argonne National Laboratory.

Kohonen, T. 1990. The self-organizing map. *Proceedings of the IEEE,* 78, 1464-1480.

Kousoulidou, M., Ntziachristos, L., Mellios, G. & Samaras, Z. 2008. Road-transport emission projections to 2020 in European urban environments. *Atmospheric Environment,* 42, 7465-7475.

Kristoffersen, T. K., Capion, K. & Meibom, P. 2011. Optimal charging of electric drive vehicles in a market environment. *Applied Energy,* 88, 1940-1948.

Kumar, T. L., Kumar, T. K. & Rajan, K. S. Speech Recognition Using Neural Networks. 2009 International Conference on Signal Processing Systems, 15-17 May 2009 2009. 248-252.

Lee, T.-K. & Filipi, Z. S. 2011. Synthesis of real-world driving cycles using stochastic process and statistical methodology. *International Journal of Vehicle Design,* 57, 17-36.

Lee, T.-K., Prucka, R. G. & Filipi, Z. S. 2009. Real-time estimation of combustion variability for model-based control and optimal calibration of spark ignition engines. *Proceedings of the Institution of Mechanical Engineers, Part D: Journal of Automobile Engineering,* 223, 1361-1372.

Lewis, F. L. 1996. Neural network control of robot manipulators. *IEEE Expert,* 11, 64-75.

Lilienthal, P. & Brown, H. 2007. Tackling climate change in the US. Potential carbon emissions reductions from energy efficiency and renewable energy by 2030.: American Solar Energy Association.

Lin, J. & Niemeier, D. 2002. An exploratory analysis comparing a stochastic driving cycle to California's regulatory cycle. *Atmospheric Environment,* 36, 5759-5770.

Lin, J. & Niemeier, D. A. 2003. Estimating Regional Air Quality Vehicle Emission Inventories: Constructing Robust Driving Cycles. *Transportation Science,* 37, 330-346.

Lipman, T. E. & Delucchi, M. A. 2006. A retail and lifecycle cost analysis of hybrid electric vehicles. *Transportation Research Part D: Transport and Environment,* 11, 115-132.

Lojowska, A., Kurowicka, D., Papaefthymiou, G. & Van Der Sluis, L. From transportation patterns to power demand: Stochastic modeling of uncontrolled domestic charging of electric vehicles. Power and Energy Society General Meeting, 2011 IEEE, 24-29 July 2011 2011. 1-7.

Lojowska, A., Kurowicka, D., Papaefthymiou, G. & Van Der Sluis, L. 2012. Stochastic Modeling of Power Demand Due to EVs Using Copula. *Power Systems, IEEE Transactions on,* 27, 1960-1968.

Maibach, M., Schreyer, C., Sutter, D., Van Essen, H. P., Boon, B. H., Smokers, R., A, S., Doll, C., Pawlowska, B. & Bak, M. 2009. Handbook on estimation of external costs in the transport sector. European Commission DG TREN.

Martín-Valdivia, M. T., Ureña-López, L. A. & García-Vega, M. 2007. The learning vector quantization algorithm applied to automatic text classification tasks. *Neural Networks,* 20, 748-756.

Mathworks. 2012. *Learning Vector Quantization Networks* [Online]. Available: http://www.mathworks.co.uk/help/nnet/ug/learning-vector-quantization-networks.html.

Mathworks. 2013. *anfis and the ANFIS Editor GUI* [Online]. Available: http://www.mathworks.co.uk/help/fuzzy/anfis-and-the-anfis-editor-gui.html [Accessed October 2012].

Mayeres, I. & Proost, S. 2001. Should diesel cars in Europe be discouraged? *Regional Science and Urban Economics,* 31, 453-470.

Mayor of London 2009. An Electric Vehicle Delivery Plan for London.

Greater London Authority.

Michel, A. 2004. The ARTEMIS European driving cycles for measuring car pollutant emissions. *Science of The Total Environment,* 334-335, 73-84.

Montazeri-Gh, M. & Fotouhi, A. 2011. Traffic condition recognition using the -means clustering method. *Scientia Iranica,* 18, 930-937.

Morgenroth, E. L. W. 2001. Analysis of the Economic, Employment and Social Profile of the Greater Dublin Region (Dublin and Mid East Regions). The Economic and Social Research Institute.

Morgenroth, E. L. W. 2002. Commuting In Ireland: An Analysis of Inter-County Commuting Flows. The Economic and Social Research Institute.

Mullan, J., Harries, D., Bräunl, T. & Whitely, S. 2011. Modelling the impacts of electric vehicle recharging on the Western Australian electricity supply system. *Energy Policy,* 39, 4349-4359.

Mulvaney, P. 2010a. Transformation of Transportation. *Transport Ireland conference.* Dublin, Ireland.

Mulvaney, P. 2010b. Transformation of Transportation. *Future Transport Fuel Forum.* Dublin, Ireland.

Musardo, C., Rizzoni, G. & Staccia, B. A-ECMS: An Adaptive Algorithm for Hybrid Electric Vehicle Energy Management. Decision and Control, 2005 and 2005 European Control Conference. CDC-ECC '05. 44th IEEE Conference on, 12-15 Dec. 2005 2005. 1816-1823.

Nababan, E. B., Hamdan, A. R., Hasan, M. K. & Mohamed, H. Fuzzy membership function in determining statistical process control position. Engineering Management Conference, 2004. Proceedings. 2004 IEEE International, 18-21 Oct. 2004 2004. 1066-1070 Vol.3.

Nagelhout, D. & Ros, J. P. M. 2009. Electric driving – Evaluating transitions based on system options. Netherlands Environmental Assessment Agency.

Namdoo, K., Kwon, J. & Rousseau, A. 2010. Trade-off between Multi-mode Powertrain Complexity and Fuel Consumption. *The 25th World Battery, Hybrid and Fuel Cell Electric Vehicle Symposium & Exhibition.* Shenzhen, China.

Nissan Ireland. 2012. *Nissan Leaf Specifications* [Online]. Available: http://www.nissan.ie/vehicles/leaf/?gclid=CKrjs6etibYCFcyV4QodRSQA5w.

Norris, J. 1998. *Markov Chains*, Cambridge University Press.

O'leary, B. 2009. Air Quality in Ireland 2008. Environmental Protection Agency.

Oecd 2010. REDUCING TRANSPORT GREENHOUSE GAS EMISSIONS: Trends & Data 2010. Organisation for Economic Co-operation and Development.

Papaefthymiou, G. & Kurowicka, D. 2009. Using Copulas for Modeling Stochastic Dependence in Power System Uncertainty Analysis. *Power Systems, IEEE Transactions on,* 24, 40-49.

Pardoe, I. 2012. *Applied Regression Modeling*, John Wiley & Sons.

Parks, K., Denholm, P. & Markel, T. 2007. Costs and Emissions Associated with Plug-In Hybrid Vehicle Charging in the Xcel Energy Colorado Service Territory. National Renewable Energy Laboratory.

Pashajavid, E. & Golkar, M. A. Placing parking lot of plug-in electric vehicles within a distribution grid considering high penetration level of photovoltaic generation. Integration of Renewables into the Distribution Grid, CIRED 2012 Workshop, 29-30 May 2012 2012. 1-4.

Passier, G., Conte., F. V., Smets, S., Badin, F., Brouwer, A., Alaküla, D., Santini, M., Alexander, A. & Alexander, M. 2007. Status Overview of Hybrid and Electric Vehicle technology (2007). International

Energy Agency.

Patil, R., Adornato, B. & Filipi, Z. S. 2009. Impact of Naturalistic Driving Patterns on PHEV Performance and System Design. *SAE Paper 2009-01-2715.*

Qiuming, G., Yaoyu, L. & Zhong-Ren, P. 2008. Trip-Based Optimal Power Management of Plug-in Hybrid Electric Vehicles. *Vehicular Technology, IEEE Transactions on,* 57, 3393-3401.

Rakha, H., Dion, F. & Sin, H.-G. 2001. Field Evaluation of Energy and Emission Impacts of Traffic Flow Improvement Projects using GPS Data: Issues and Proposed Solutions. *Transportation Research Record: Journal of the Transportation Research Board,* No. 1768, 210-223.

Ramgulam, A. 2006. *UTILIZATION OF ARTIFICIAL NEURAL NETWORKS IN THE OPTIMIZATION OF HISTORY MATCHING.* Masters, The Pennsylvania State University

Rask, E. & Rousseau, A. 2012. Evaluating Real World Drive Cycles to Support APRF Technology Evaluations. *2012 DOE Hydrogen Program and Vehicle Technologies.* Argonne National Laboratory.

Riches, E. 2010. *Track Tested: 2010 Mitsubishi i MiEV vs. Mitsubishi i* [Online]. edmunds.com. Available: http://www.edmunds.com/car-reviews/track-tests/track-tested-2010-mitsubishi-i-miev-vs-mitsubishi-i.html [Accessed June 1st 2012].

Ross, T. 2004. *Fuzzy Logic with Engineering Applications*, John Wiley & Sons

Ltd.

Rouwendal, J. & De Vries, F. 1999. The taxation of drivers and the choice of car fuel type. *Energy Economics,* 21, 17-35.

Samaras, C. & Meisterling, K. 2008. Life Cycle Assessment of Greenhouse Gas Emissions from Plug-in Hybrid Vehicles: Implications for Policy. *Environmental Science & Technology* 42, 3170-3176

Sandy Thomas, C. E. 2009. Transportation options in a carbon-constrained world: Hybrids, plug-in hybrids, biofuels, fuel cell electric vehicles, and battery electric vehicles. *International Journal of Hydrogen Energy,* 34, 9279-9296.

Scottish Executive 2005. Migration and Commuting in Urban and Rural Scotland – Statistics from Census 2001. Edinburgh.: The Scottish Government.

Shahidinejad, S., Bibeau, E. & Filizadeh, S. 2010. Statistical Development of a Duty Cycle for Plug-in Vehicles in a North American Urban Setting Using Fleet Information. *Vehicular Technology, IEEE Transactions on,* 59, 3710-3719.

Shahidinejad, S., Filizadeh, S. & Bibeau, E. 2012. Profile of Charging Load on the Grid Due to Plug-in Vehicles. *Smart Grid, IEEE Transactions on,* 3, 135-141.

Shankar, R., Marco, J. & Assadian, F. A methodology to determine drivetrain efficiency based on external environment. Electric Vehicle Conference (IEVC), 2012 IEEE International, 4-8 March 2012 2012. 1-6.

Sheskin, T. 2010. *Markov Chains and Decision Processes for Engineers and Managers*, Taylor & Francis Group.

Shiau, C.-S. N., Samaras, C., Hauffe, R. & Michalek, J. J. 2009. Impact of battery weight and charging patterns on the economic and environmental benefits of plug-in hybrid vehicles. *Energy Policy,* 37, 2653-2663.

Simmons, R., Browning, B., Yilu, Z. & Sadekar, V. Learning to Predict Driver Route and Destination Intent. Intelligent Transportation Systems Conference, 2006. ITSC '06. IEEE, 17-20 Sept. 2006 2006. 127-132.

Simpson, A. 2006. Cost-Benefit Analysis of Plug-In Hybrid Electric Vehicle Technology. *22nd International Battery, Hybrid and Fuel Cell Electric Vehicle Symposium and Exhibition (EVS-22).* Yokohama, Japan

National Renewable Energy Laboratory.

Sioshansi, R. & Denholm, P. 2010. The Value of Plug-In Hybrid Electric Vehicles as Grid Resources. *The Energy Journal,* 0, 1-24.

Smit, R. 2006. *An examination of congestion in road traffic emission models and their application to urban road networks.* PhD, Griffith University

Smith, W. J. 2010. Plug-in hybrid electric vehicles--A low-carbon solution for Ireland? *Energy Policy,* 38, 1485-1499.

Society of the Irish Motor Industry 2010a. National vehicle statistics. Dublin, Ireland: Society of the Irish Motor Industry.

Society of the Irish Motor Industry. 2010b. *National Vehicle Statistics* [Online]. Dublin,

Ireland. Available: http://www.simi.ie/statistics/national_vehicle_statistics.aspx.

Sundstrom, O. & Binding, C. 2012. Flexible Charging Optimization for Electric Vehicles Considering Distribution Grid Constraints. *Smart Grid, IEEE Transactions on,* 3, 26-37.

Sustainable Energy Authority Ireland. 2010. *Electric Vehicle Grant Scheme* [Online]. Available: http://www.seai.ie/Grants/Electric_Vehicle_Grant_Scheme/.

Takagi, T. & Sugeno, M. 1985. Fuzzy identification of systems and its applications to modeling and control. *Systems, Man and Cybernetics, IEEE Transactions on,* SMC-15, 116-132.

Tate, E., Harpster, M. & Savagian, P. 2009. The Electrification of the Automobile: From Conventional Hybrid, to Plug-in Hybrids, to Extended-Range Electric Vehicles. *SAE Int. J. Passeng. Cars - Electron. Electr. Syst.,* 1.

The Department of Fiance 2009. Ireland – Stability Programme update. Dublin, Ireland: The Department of Fiance.

The Society of Irish Motor Industry. 2010. *Taxation* [Online]. Available: http://www.simi.ie/taxation/introduction.aspx.

Tong, H. Y. & Hung, W. T. 2010. A Framework for Developing Driving Cycles with On-Road Driving Data. *Transport Reviews,* 30, 589-615.

Tzirakis, E., Pitsas, K., Zannikos, F. & Stournas, S. 2006. Vehicle emissions and driving cycles: comparison of the athens driving cycle (ADC) with ECE-15 and European driving cycle (EDC). *Global NEST* 8, 282-290.

U.S. Environmental Protection Agency. 2012 *MOBILE6 Vehicle Emission Modeling Software* [Online]. Available: http://www.epa.gov/otaq/m6.htm [Accessed October 1st 2012].

United Nations Economic Commission for Europe 2005. Regulation No. 101 Geneva: United Nations Economic Commission for Europe,.

United States Congress 2009. American Recovery and Reinvestment Act of 2009. United States Congress,.

United States Environmental Protection Agency 1993. Federal Test Procedure Review Project. United States Environmental Protection Agency.

United States Environmental Protection Agency. 2013. *Regulations* [Online]. Available: http://www.epa.gov/lawsregs/regulations/.

University of Southern Denmark. 2012. *Module 4: Residual analysis* [Online]. University of southern denmark. Available: http://statmaster.sdu.dk/courses/st111/module04/.

Vermot Energy Investment Corporation 2012. Alternative Fuel Vehicle User Fee Options. Vermot: Vermot Energy Investment Corporation

Volkswagen. 2008. Green power via the electric socket will drive the cars of tomorrow. No. 3, July–August 2008. Available: http://www.volkswagenag.com/vwag/vwcorp/info_center/en/publications/2008/10/p_news_3_2008.-bin.acq/qual-BinaryStorageItem.Single.File/VW_PN_2008_03_englisch.pdf.

Vose, D. 2008. *Risk analysis : a quantitative guide*, Wiley.

Walsh, J., Foley, R., A, K. & Mcelwain, A. 2006. Origins, destinations and catchments: mapping travel to work in Ireland in 2002. *Statistical and Social Inquiry Society of Ireland,* XXXV, pp1-55.

Wang, Q., Huo, H., He, K., Yao, Z. & Zhang, Q. 2008. Characterization of vehicle driving patterns and development of driving cycles in Chinese cities. *Transportation Research Part D: Transport and Environment,* 13, 289-297.

Wang, R. 2013. *Learning Vector Quantization (LVQ)* [Online]. Available: http://fourier.eng.hmc.edu/e161/lectures/nn/node16.html [Accessed March 1st 2013].

Weiller, C. 2011. Plug-in hybrid electric vehicle impacts on hourly electricity demand in the United States. *Energy Policy,* 39, 3766-3778.

Whitefoot, J. W., Ahn, K. & Papalambros, P. Y. 2010. The Case for Urban Vehicles: Powertrain Optimization of a Power-Split Hybrid for Fuel Economy on Multiple Drive Cycles. *ASME Conference Proceedings,* 2010, 197-204.

World Energy Council 2010. Global Transport Scenarios 2050. World Energy Council

Zaccardi, J. & Le Berr, F. 2012. Analysis and choice of representative drive cycles for light duty vehicles – case study for electric vehicles. *Mechanical Engineers, Part D: Journal of Automobile Engineering,* 0, 1-13.

Appendix A: Private car fleet composition

Table 1. Private car fleet composition in 2010 by fuel type and technology class.

Sector	Subsector	Technology	Percentage of fleet
Passenger Cars	Gasoline <1,4 l	ECE 15/04	0.83%
Passenger Cars	Gasoline <1,4 l	PC Euro 1 - 91/441/EEC	2.51%
Passenger Cars	Gasoline <1,4 l	PC Euro 2 - 94/12/EEC	10.95%
Passenger Cars	Gasoline <1,4 l	PC Euro 3 - 98/69/EC Stage2000	20.21%
Passenger Cars	Gasoline <1,4 l	PC Euro 4 - 98/69/EC Stage2005	14.09%
Passenger Cars	Gasoline <1,4 l	PC Euro 5 (post 2005)	1.32%
Passenger Cars	Gasoline <1,4 l	PC Euro 6	0.00%
Passenger Cars	Gasoline 1,4 - 2,0 l	ECE 15/04	0.38%
Passenger Cars	Gasoline 1,4 - 2,0 l	PC Euro 1 - 91/441/EEC	1.17%
Passenger Cars	Gasoline 1,4 - 2,0 l	PC Euro 2 - 94/12/EEC	4.27%
Passenger Cars	Gasoline 1,4 - 2,0 l	PC Euro 3 - 98/69/EC Stage2000	11.40%
Passenger Cars	Gasoline 1,4 - 2,0 l	PC Euro 4 - 98/69/EC Stage2005	10.42%
Passenger Cars	Gasoline 1,4 - 2,0 l	PC Euro 5 (post 2005)	0.50%
Passenger Cars	Gasoline 1,4 - 2,0 l	PC Euro 6	0.00%
Passenger Cars	Gasoline >2,0 l	ECE 15/04	0.02%
Passenger Cars	Gasoline >2,0 l	PC Euro 1 - 91/441/EEC	0.06%
Passenger Cars	Gasoline >2,0 l	PC Euro 2 - 94/12/EEC	0.35%
Passenger Cars	Gasoline >2,0 l	PC Euro 3 - 98/69/EC Stage2000	1.02%
Passenger Cars	Gasoline >2,0 l	PC Euro 4 - 98/69/EC Stage2005	1.31%
Passenger Cars	Gasoline >2,0 l	PC Euro 5 (post 2005)	0.01%
Passenger Cars	Gasoline >2,0 l	PC Euro 6	0.00%
Passenger Cars	Diesel <2,0 l	PC Euro 1 - 91/441/EEC	0.84%
Passenger Cars	Diesel <2,0 l	PC Euro 2 - 94/12/EEC	1.81%
Passenger Cars	Diesel <2,0 l	PC Euro 3 - 98/69/EC Stage2000	4.51%
Passenger Cars	Diesel <2,0 l	PC Euro 4 - 98/69/EC Stage2005	7.09%
Passenger Cars	Diesel <2,0 l	PC Euro 5 (post 2005)	2.34%
Passenger Cars	Diesel <2,0 l	PC Euro 6	0.00%
Passenger Cars	Diesel >2,0 l	PC Euro 1 - 91/441/EEC	0.06%
Passenger Cars	Diesel >2,0 l	PC Euro 2 - 94/12/EEC	0.22%
Passenger Cars	Diesel >2,0 l	PC Euro 3 - 98/69/EC Stage2000	0.73%
Passenger Cars	Diesel >2,0 l	PC Euro 4 - 98/69/EC Stage2005	1.42%
Passenger Cars	Diesel >2,0 l	PC Euro 5 (post 2005)	0.19%
Passenger Cars	Diesel >2,0 l	PC Euro 6	0.00%

Table 2. Projected private car fleet composition in 2020 by fuel type and technology class.

Sector	Subsector	Technology	Percentage of fleet
Passenger Cars	Gasoline <1,4 l	ECE 15/04	0.00%
Passenger Cars	Gasoline <1,4 l	PC Euro 1 - 91/441/EEC	0.00%
Passenger Cars	Gasoline <1,4 l	PC Euro 2 - 94/12/EEC	0.42%
Passenger Cars	Gasoline <1,4 l	PC Euro 3 - 98/69/EC Stage2000	2.65%
Passenger Cars	Gasoline <1,4 l	PC Euro 4 - 98/69/EC Stage2005	5.12%
Passenger Cars	Gasoline <1,4 l	PC Euro 5 (post 2005)	6.16%
Passenger Cars	Gasoline <1,4 l	PC Euro 6	17.24%
Passenger Cars	Gasoline 1,4 - 2,0 l	ECE 15/04	0.00%
Passenger Cars	Gasoline 1,4 - 2,0 l	PC Euro 1 - 91/441/EEC	0.00%
Passenger Cars	Gasoline 1,4 - 2,0 l	PC Euro 2 - 94/12/EEC	0.17%
Passenger Cars	Gasoline 1,4 - 2,0 l	PC Euro 3 - 98/69/EC Stage2000	1.63%
Passenger Cars	Gasoline 1,4 - 2,0 l	PC Euro 4 - 98/69/EC Stage2005	3.75%
Passenger Cars	Gasoline 1,4 - 2,0 l	PC Euro 5 (post 2005)	2.30%
Passenger Cars	Gasoline 1,4 - 2,0 l	PC Euro 6	6.82%
Passenger Cars	Gasoline >2,0 l	ECE 15/04	0.00%
Passenger Cars	Gasoline >2,0 l	PC Euro 1 - 91/441/EEC	0.00%
Passenger Cars	Gasoline >2,0 l	PC Euro 2 - 94/12/EEC	0.01%
Passenger Cars	Gasoline >2,0 l	PC Euro 3 - 98/69/EC Stage2000	0.15%
Passenger Cars	Gasoline >2,0 l	PC Euro 4 - 98/69/EC Stage2005	0.47%
Passenger Cars	Gasoline >2,0 l	PC Euro 5 (post 2005)	0.09%
Passenger Cars	Gasoline >2,0 l	PC Euro 6	0.31%
Passenger Cars	Diesel <2,0 l	PC Euro 1 - 91/441/EEC	0.00%
Passenger Cars	Diesel <2,0 l	PC Euro 2 - 94/12/EEC	0.07%
Passenger Cars	Diesel <2,0 l	PC Euro 3 - 98/69/EC Stage2000	0.66%
Passenger Cars	Diesel <2,0 l	PC Euro 4 - 98/69/EC Stage2005	2.69%
Passenger Cars	Diesel <2,0 l	PC Euro 5 (post 2005)	11.34%
Passenger Cars	Diesel <2,0 l	PC Euro 6	33.59%
Passenger Cars	Diesel >2,0 l	PC Euro 1 - 91/441/EEC	0.00%
Passenger Cars	Diesel >2,0 l	PC Euro 2 - 94/12/EEC	0.01%
Passenger Cars	Diesel >2,0 l	PC Euro 3 - 98/69/EC Stage2000	0.11%
Passenger Cars	Diesel >2,0 l	PC Euro 4 - 98/69/EC Stage2005	0.54%
Passenger Cars	Diesel >2,0 l	PC Euro 5 (post 2005)	0.90%
Passenger Cars	Diesel >2,0 l	PC Euro 6	2.78%

Appendix B: ISus concordance table

Diesel						Petrol					
Tax[a]	ISus	VRT[b]		MT[c]		Tax[a]	Isus	VRT[b]		MT[c]	
		bef	aft	bef	aft			bef	aft	bef	aft
A	A	22.5%	14%	165	104	A	A	22.5%	14%	165	104
B	B	22.5%	16%	165	156	B	B	22.5%	16%	165	156
B	D	22.5%	16%	275	156	B	D	22.5%	16%	275	156
B	E	25%	16%	320	156	C	E	25%	20%	320	302
B	F	25%	16%	343	156	D	F	25%	24%	343	447
B	G	25%	16%	428	156	D	G	25%	24%	428	447
C	H	25%	20%	550	302	E	H	25%	28%	550	630
E	I	30%	28%	800	550	F	I	30%	32%	800	1050
G	J	30%	36%	1150	2100	G	J	30%	36%	1150	2100

Figure 1. Concordance table.

This table shows how the engine size classes in the ISus car model (A-J) are transformed into emissions bands (A-G). The concordance table used to create emissions bands is based on actual sales in 2008-2009.

Table 1. ISus engine size classes.

Engine size	ISus engine size class
<900 cc	A
900-1000cc	B
C	C
1001-1300 cc	D
1301-1400 cc	E
1401-1500 cc	F
1501-1600 cc	G
1601-2000 cc	H
2001-2400 cc	I
>2400 cc	J

Appendix C: Modelled EV powertrain specifications

Table 1. Specifications of the modelled powertrain

Parameter	
12 volt battery mass	18 kg
Constant power loss	200 W
Vehicle body mass	1525 kg
Vehicle cargo mass	136 kg
Vehicle centre of gravity	0.5 m
Coefficient of drag	0.29
Frontal area of vehicle	2.27 m^2
Number of cells in the ultra-capacitor pack connected in parallel	2
Number of cells connected in series	96
Max capacity of the energy storage system	66 Ah
Max Power of the energy storage system	468 W
Final drive ratio	7.94
Coefficient of regen for the motor	1
Motor controller mass	25.6 kg
Maximum current of the motor	616.4 A
Motor mass	64.2 kg
Efficiency	95%
Mass of the torque coupling	10 kg
Torque coupling ratio	1.6
Mass per wheel	30 kg
Radius of wheel	0.317
Maximum braking torque of the vehicle	2000 Nm

Appendix D: Distributions available in EasyfitXL

- Bernoulli
- Beta
- Binomial
- Burr
- Cauchy
- Chi-Squared
- Dagum
- Discrete Uniform
- Erlang
- Error
- Error Function
- Exponential
- F
- Fatigue Life
- Frechet
- Gamma
- Generalized Extreme Value
- Generalized Gamma
- Generalized Logistic
- Generalized Pareto
- Geometric
- Gumbel Max
- Gumbel Min
- Hyperbolic Secant
- Hypergeometric
- Inverse Gaussian
- Johnson SB
- Johnson SU
- Kumaraswamy
- Laplace
- Levy
- Logarithmic
- Logistic
- Log-Gamma
- Log-Logistic
- Log-Pearson 3 (LP3)
- Lognormal
- Negative Binomial
- Nakagami
- Normal
- Pareto
- Pareto 2 (Lomax)
- Pearson 5
- Pearson 6
- Pert
- Poisson
- Phased Bi-Exponential
- Phased Bi-Weibull
- Power Function
- Rayleigh
- Reciprocal
- Rice
- Student's t
- Triangular
- Uniform
- Wakeby
- Weibull

Appendix E: Driving cycles included in the assessment analysis

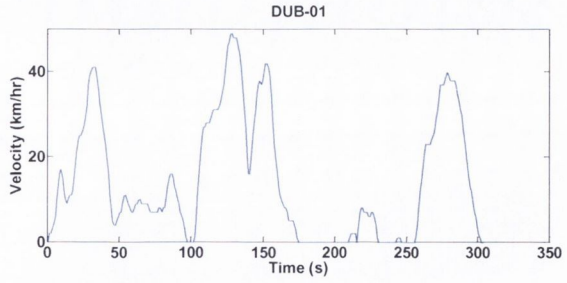

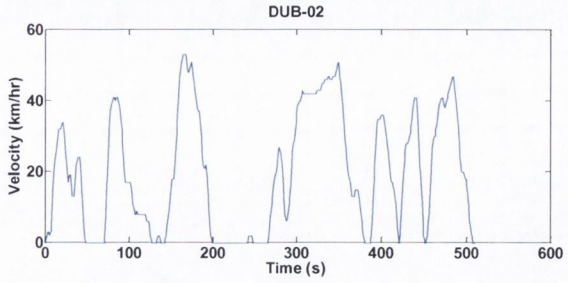

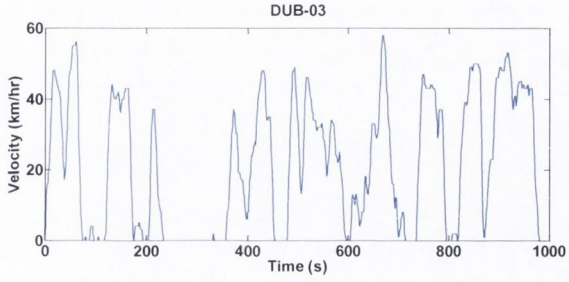

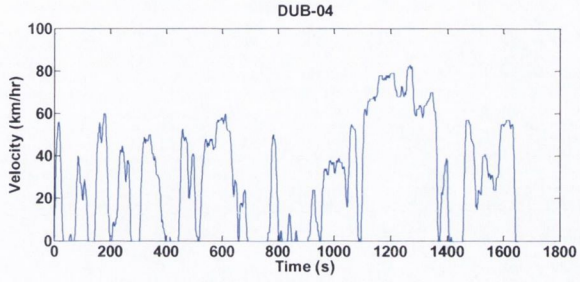

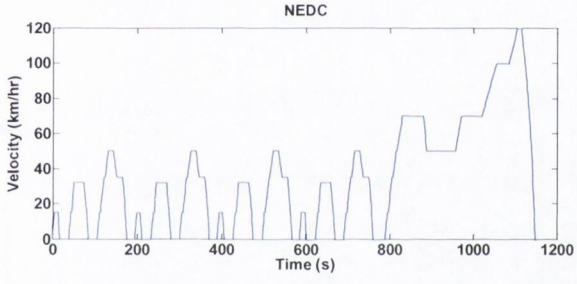

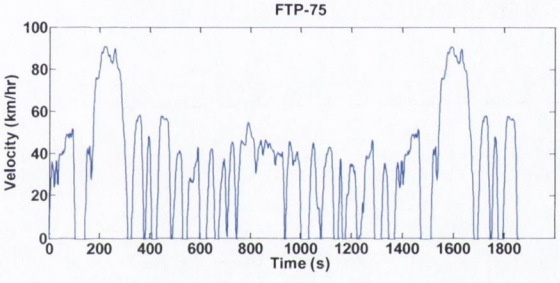

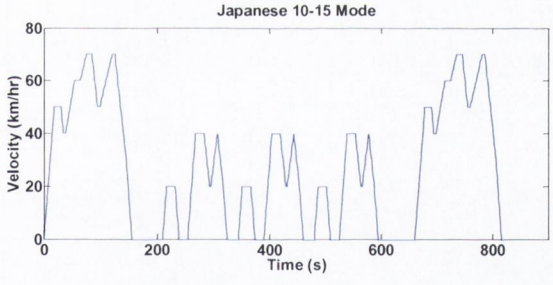

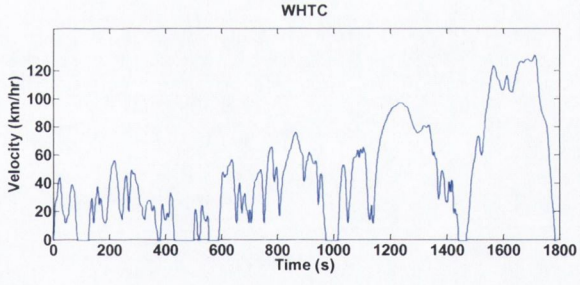

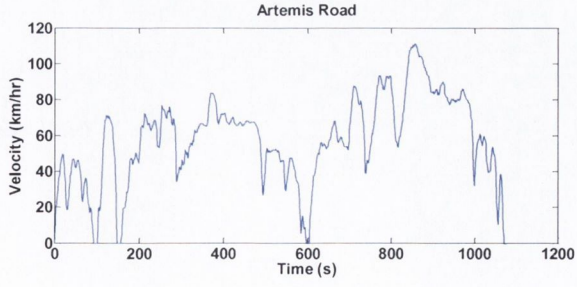

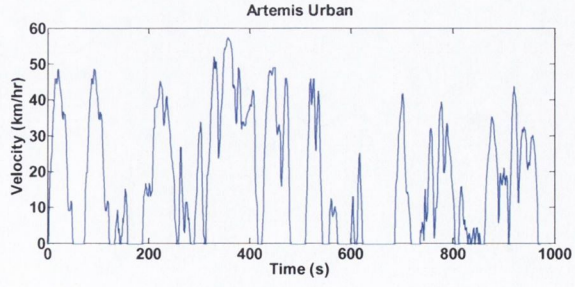

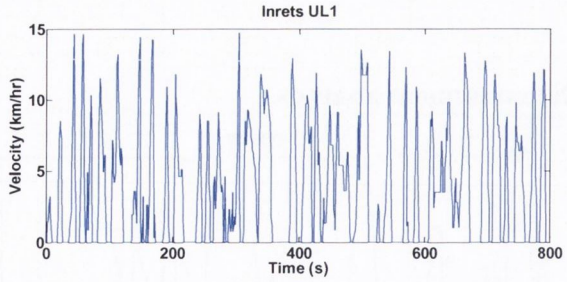
Inrets UL1
Velocity (km/hr)
Time (s)

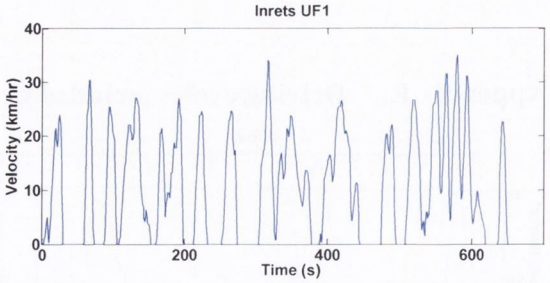
Inrets UF1
Velocity (km/hr)
Time (s)

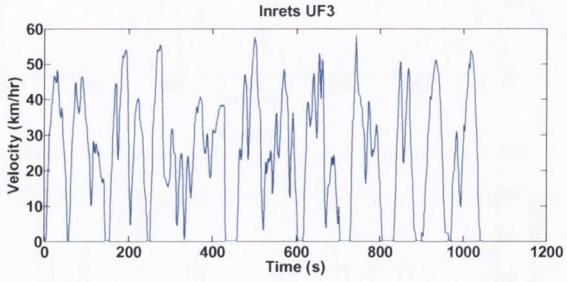
Inrets UF3
Velocity (km/hr)
Time (s)

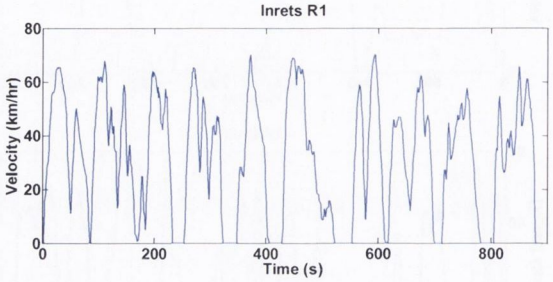
Inrets R1
Velocity (km/hr)
Time (s)

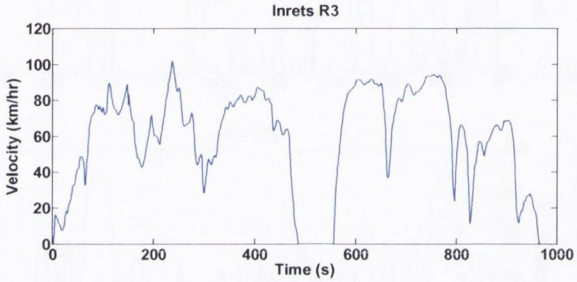
Inrets R3
Velocity (km/hr)
Time (s)

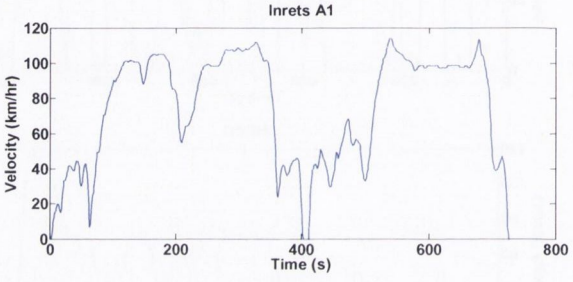
Inrets A1
Velocity (km/hr)
Time (s)

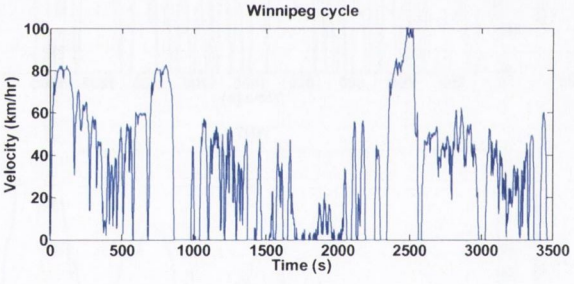
Winnipeg cycle
Velocity (km/hr)
Time (s)

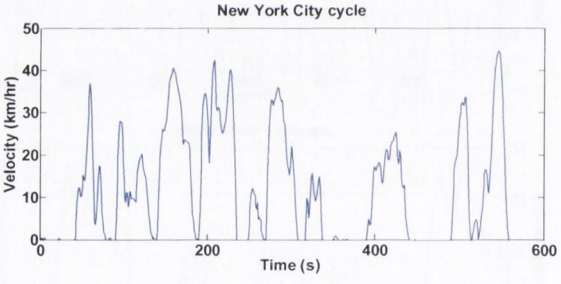
New York City cycle
Velocity (km/hr)
Time (s)

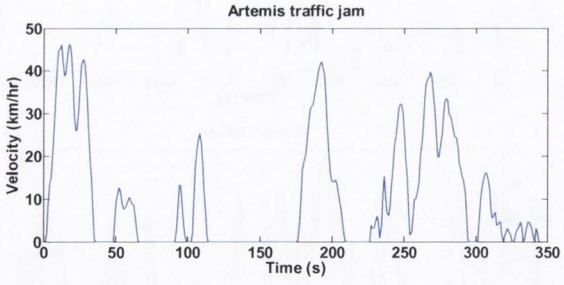
Artemis traffic jam
Velocity (km/hr)
Time (s)

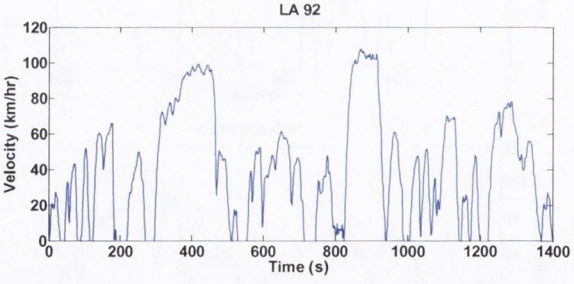
LA 92
Velocity (km/hr)
Time (s)

Appendix F: Contribution to the Chi-Square value by journey distance

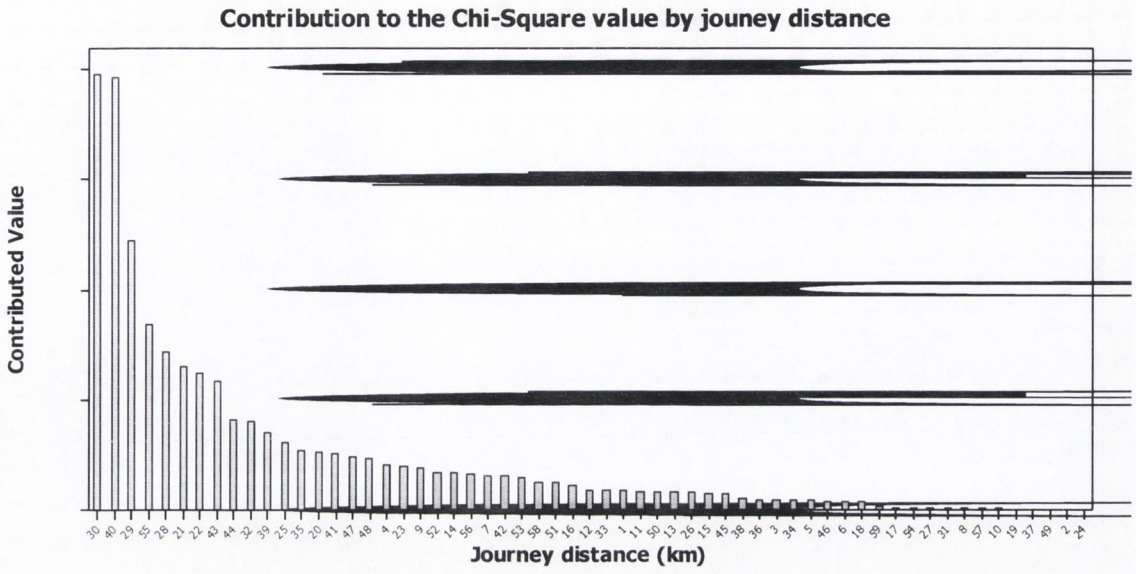

Figure 1. Contribution to the Chi-Square value by journey distance.

Appendix G: The observed and expected frequencies of the parking time intervals

Table 1. The observed and expected frequencies of the parking time intervals.

Category	Observed Frequency	Global Proportion	Expected Frequency	Percentage Difference
0	5493	0.088842	5048.79	9
5	7085	0.121314	6894.17	3
10	3835	0.064752	3679.81	4
15	2795	0.045963	2612.01	7
20	2157	0.040759	2316.31	-7
25	1872	0.032183	1828.95	2
30	1586	0.031894	1812.53	-12
35	1604	0.026884	1527.78	5
40	1610	0.032376	1839.91	-12
45	1367	0.024475	1390.88	-2
50	1078	0.022259	1264.94	-15
55	908	0.019272	1095.18	-17
60	1151	0.020428	1160.89	-1
65	908	0.01773	1007.57	-10
70	849	0.017537	996.62	-15
75	841	0.016381	930.9	-10
80	822	0.017344	985.66	-17
85	654	0.015225	865.19	-24
90	685	0.013586	772.1	-11
95	631	0.015032	854.24	-26
100	760	0.013394	761.15	0
105	639	0.01243	706.39	-10
110	602	0.012141	689.96	-13
115	647	0.011563	657.11	-2
120	551	0.009828	558.54	-1
125	411	0.009058	514.74	-20
130	401	0.007323	416.17	-4
135	431	0.007034	399.74	8
140	377	0.006841	388.79	-3
145	314	0.006552	372.36	-16
150	320	0.006938	394.27	-19
155	299	0.006167	350.46	-15
160	248	0.0053	301.18	-18
165	345	0.007323	416.17	-17
170	349	0.005974	339.51	3
175	197	0.004914	279.27	-29
180	288	0.005781	328.55	-12
185	281	0.005011	284.75	-1
190	312	0.005107	290.22	8
195	241	0.004529	257.37	-6
200	329	0.006071	344.98	-5
205	294	0.004914	279.27	5
210	272	0.006167	350.46	-22
215	307	0.0053	301.18	2
220	281	0.005396	306.65	-8

225	249	0.005107	290.22	-14
230	254	0.005107	290.22	-12
235	244	0.004529	257.37	-5
240	220	0.005396	306.65	-28
245	300	0.004047	229.99	30
250	188	0.003469	197.13	-5
255	250	0.002891	164.28	52
260	167	0.001927	109.52	52
265	157	0.00212	120.47	30
270	218	0.00318	180.71	21
275	189	0.002505	142.37	33
280	193	0.003662	208.08	-7
285	186	0.002794	158.8	17
290	136	0.002024	114.99	18
295	130	0.001542	87.61	48
300	106	0.001156	65.71	61
305	144	0.001445	82.14	75
310	71	0.000867	49.28	44
315	143	0.001253	71.19	101
320	120	0.001734	98.57	22
325	92	0.001542	87.61	5
330	130	0.001927	109.52	19
335	123	0.001734	98.57	25
340	110	0.001349	76.66	43
345	85	0.000964	54.76	55
350	86	0.000675	38.33	124
355	55	0.000964	54.76	0
360	76	0.001253	71.19	7
365	145	0.001542	87.61	66
370	85	0.001445	82.14	3
375	94	0.001253	71.19	32
380	78	0.000964	54.76	42
385	72	0.000867	49.28	46
390	101	0.001156	65.71	54
395	65	0.000964	54.76	19
400	101	0.000867	49.28	105
405	104	0.001542	87.61	19
410	122	0.00106	60.24	103
415	116	0.001156	65.71	77
420	105	0.000867	49.28	113
425	73	0.000867	49.28	48
430	57	0.001156	65.71	-13
435	64	0.000578	32.86	95
440	89	0.00106	60.24	48
445	72	0.00106	60.24	20
450	76	0.001445	82.14	-7
455	92	0.001349	76.66	20
460	110	0.001927	109.52	0
465	79	0.001156	65.71	20
470	69	0.000771	43.81	57

475	121	0.001831	104.04	16
480	68	0.000867	49.28	38
485	55	0.00106	60.24	-9
490	100	0.001734	98.57	1
495	126	0.00106	60.24	109
500	70	0.00106	60.24	16
505	81	0.000964	54.76	48
510	88	0.001156	65.71	34
515	70	0.000771	43.81	60
520	74	0.001253	71.19	4
525	50	0.000867	49.28	1
530	101	0.000964	54.76	84
535	60	0.001156	65.71	-9
540	83	0.000771	43.81	89
545	86	0.000867	49.28	75
550	59	0.000675	38.33	54
555	69	0.000482	27.38	152
560	45	0.000675	38.33	17
565	75	0.001253	71.19	5
570	97	0.001445	82.14	18
575	80	0.00106	60.24	33
580	97	0.001253	71.19	36
585	94	0.001156	65.71	43
590	39	0.000482	27.38	42
595	41	0.00106	60.24	-32
600	87	0.001253	71.19	22
605	36	0.000867	49.28	-27
610	55	0.000771	43.81	26
615	28	0.000578	32.86	-15
620	46	0.000964	54.76	-16
625	40	0.000867	49.28	-19
630	33	0.000578	32.86	0
635	30	0.000482	27.38	10
640	64	0.000964	54.76	17
645	49	0.000771	43.81	12
650	43	0.000675	38.33	12
655	70	0.000771	43.81	60
660	49	0.000578	32.86	49
665	28	0.000675	38.33	-27
670	8	0.000193	10.95	-27
675	6	0.000096	5.48	9
680	35	0.000289	16.43	113
685	19	0.000385	21.9	-13
690	10	0.000289	16.43	-39
695	33	0.000482	27.38	21
700	7	0.000289	16.43	-57
705	52	0.000867	49.28	6
710	101	0.000867	49.28	105
715	83	0.001253	71.19	17
720	70	0.000771	43.81	60

Appendix H: The theory of fuzzy logic

This appendix provides an overview of fuzzy logic, fuzzy logic models and adaptive Neuro-Fuzzy Inference.

1.1 Fuzzy set

In classical sets, a set can be represented by enumerating all its elements:

$$A = \{a_1, a_2, a_3 \ldots, a_n\} \tag{1}$$

If these elements $a_i (i = 1, \ldots., n)$ of A are together a subset of the universal base set X, the set A can be represented for all elements $x \epsilon X$ by its characteristic function

$$\mu_A(x) \begin{cases} 1 & if\ x \epsilon A \\ 0 & otherwise \end{cases} \tag{2}$$

In classical set theory $\mu_A(x)$ can only have the values 0 (false) and 1 (true). This is known as a crisp set. Fuzzy sets are non-crisp sets, for which a characteristic function can also be defined. This function is a generalisation of Equation 2 and is called a membership function. The membership of a fuzzy set is described by the membership function $\mu_A(x)$ of A which associates to each element $x_0 = X$ a grade of membership $\mu_A(x_o)$. In contrast to classical set theory a membership function $\mu_A(x)$ of a fuzzy set can have a value in the normalised closed interval [0 1]. Therefore, each membership function maps elements of a given universal base set X which is itself a crisp set, into real numbers in [0,1]. The notation for the membership function, $\mu_A(x)$ of a fuzzy set A is (Cano and Nava, 2002):

$$A = \{(x, \mu_A(x)) | x \epsilon A, \mu_A(x) \epsilon\ [0,1]\ \} \tag{3}$$

Each fuzzy set is uniquely defined by one particular membership function. Figure 1 illustrates the differences in the crisp and fuzzy sets.

Figure 1. Membership functions of a crisp set and a fuzzy set.

1.2 Membership functions

The membership function $\mu_A(x)$ describes the membership of the elements x of the base set X in the fuzzy set A, whereby for $\mu_A(x)$ a large number of functions are available, such as triangular, gaussian and bell-shaped. Linear functions, such as triangular or trapezoidal functions are the most popular. The grade of membership $\mu_A(x)$ of a membership function describes which grade it belongs to in the fuzzy set A. This value is in the unit interval [0 1], as shown in Figure 2.

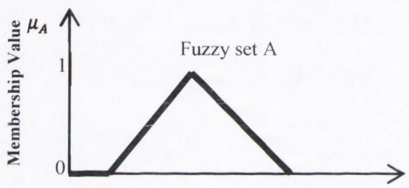

Figure 2. Membership grades of a fuzzy set.

Triangular membership function

Figure 3 illustrates a triangular membership function where a, b and c represent the x coordinates of the three vertices of $\mu_A(x)$ in the fuzzy set A. The coordinate, a, is defined as the lower boundary in set A whose degree of membership is zero. The coordinate, c, is defined as the upper boundary whose degree of membership is also zero and the coordinate, b, is the third apex of the triangle whose degree of membership is one (Ross, 2004). Equation 4 is the formula used to calculate the degree of membership for any element, x, in a fuzzy set A (Nababan et al, 2004).

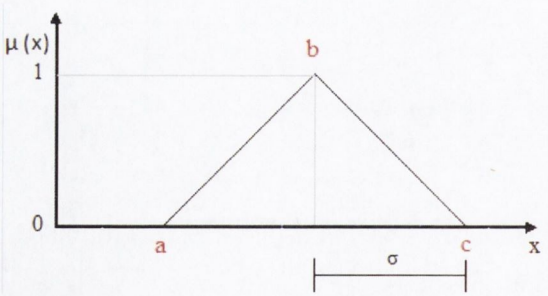

Figure 3. Triangular membership function (Foley and McGory, 2011).

$$\mu(x) = \begin{cases} 0 & if\ x < a \\ 1 + \dfrac{x-b}{0.5\sigma} & if x < b \\ 1 + \dfrac{x-b}{0.5\sigma} & if\ b < x < c \\ 0 & if\ x > c \end{cases} \quad (4)$$

Gaussian membership function

The Gaussian member function is another popular example of a membership function (Ross, 2004), represented by

$$Gaussian\ \mu(x) = \left[\frac{1}{2}\left(\frac{x-b}{\sigma}\right)^2\right] \quad (5)$$

where x is the input variable, b, is the centre of the membership function and σ is the constant that represents the width of the membership function. Gaussian fuzzy membership functions are quite common with regards to fuzzy logic systems. Figure 4 illustrates a typical Gaussian membership function.

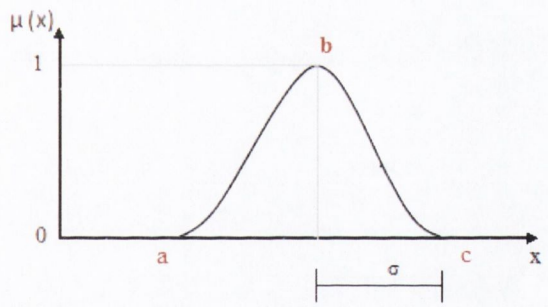

Figure 4. Gaussian membership function (Foley and McGory, 2011).

1.3 Fuzzy set operations

Three set operations that are frequently used in fuzzy logic systems are the union, intersection and complement operations. The union and intersection operators are the fundamental building blocks that compute the fuzzy if-then rules. Both these operators operate in a similar fashion as Boolean logic to perform a calculation. The union operator uses the Boolean term 'OR', whereas the intersection operator uses the term 'AND' when executing the fuzzy rules (Ross, 2004). The following example describes the fuzzy set operations for three fuzzy sets A, B and C:

For a given element, x, of the universe Z the operations union, intersection and complement are defined for fuzzy sets A, B and C as follows (Ross, 2004):

- $Union\ (OR)$: $\mu_{A\cup B} = \mu_A(x) \cup \mu_b(x)$
- $Intersection\ (AND)$: $\mu_{A\cap B} = \mu_A(x) \cap \mu_b(x)$
- $Complement(NOT)$: $\mu_{\bar{A}(x)} = 1 - \mu_A(x)$

Venn diagrams for these fuzzy operations are shown below in Figure 5. The operations shown in these diagrams are based on a triangular membership function, as discussed in the previous section.

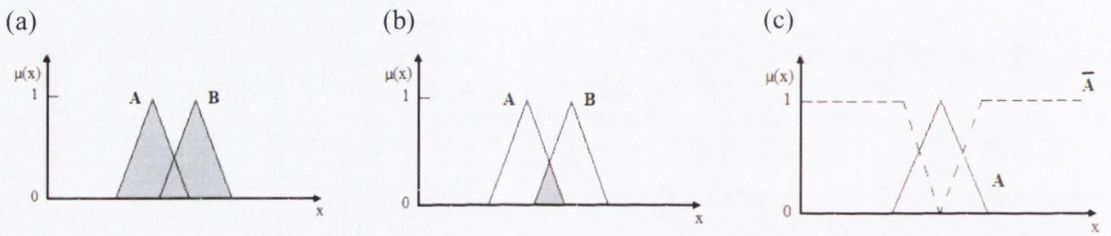

Figure 5. (a) union (OR) of fuzzy set A and B, (b) intersection (AND) of fuzzy set A and B, (c) complement (NOT) of fuzzy set A (Ross, 2004).

Any fuzzy set (A, B or C) defined in the universe Z is a subset of that universe. According to classical set theory, the membership value of any element that exists in the null set (ϕ) is 0. Also, any element that exists in the whole set Z will have a membership value of 1. The notation for these ideas can be defined as follows (Ross, 2004):

$$A \subseteq Z \Rightarrow \mu_A(x) \leq \mu_A(x), \qquad For\ all\ x \in Z, \mu_\phi(x) = 0 \qquad For\ all\ x \in Z, \mu_Z(x) = 1 \tag{6}$$

1.3.1 Fuzzy Intersection

In fuzzy logic, the intersection (AND) is calculated using t-norms. A t-norm operator is a form of binary operation used in multi-valued logic. A t-norm is a function (Ross, 2004):

$$T: [0,1]\ x\ [0,1] \rightarrow [0,1] \tag{7}$$

Where the following conditions are satisfied

- $Commutativity$: $t(a,b) = t(b,a)$
- $Associativity$: $t\big(a, t(b,c)\big) = t(t(a,b),c)$
- $Monotonicity$: $t(a,b) \leq t(c,d);\ \ if\ a \leq c\ and\ b \leq d$
- $Identity$: $the\ number\ 0\ acts\ as\ an\ identidy\ element\ so\ that\ t(a,1) = a$

The most commonly adopted t-norm in fuzzy logic is the minimum. Therefore, the intersection of two fuzzy sets A and B both with respective membership functions $\mu_A(x)$ and $\mu_B(x)$ can be represented as follows (Ross, 2004):

$$\mu_{A\cap B}(x) = \min(\mu_A(x), \mu_B(x)) \tag{8}$$

1.3.2 Fuzzy Union

The union (OR) is calculated using t-conorms, also referred to as s-norms. t-conorms, or snorms, are dual to t-norms under the order-reversing operation which assigns $1 - x$ on [0, 1]. S-norms are used to represent logical disjunction in fuzzy logic and union in fuzzy set theory. Given a t-norm, the complementary conorm is defined as (Ross, 2004):

$$s(a, b) = 1 - s(1 - a, 1 - b) \tag{9}$$

- $Commutativity: s(a, b) = s(b, a)$
- $Associativity: s\big(a, s(b, c)\big) = s(s(a, b), c)$
- $Monotonicity: s(a, b) \leq s(c, d);\ \ if\ a \leq c\ and\ b \leq d$
- $Identity: the\ number\ 0\ acts\ as\ an\ identidy\ element\ so\ that\ s(a, 0) = a$

The most commonly adopted s-norm in fuzzy logic is the maximum. Therefore, the union of two fuzzy sets A and B both with respective membership functions $\mu_A(x)$ and $\mu_B(x)$ can be represented as follows (Ross, 2004):

$$\mu_{A\cap B}(x) = \max(\mu_A(x), \mu_B(x)) \tag{10}$$

1.4 Components of a fuzzy system

Fuzzy inference process contains different stages such as fuzzification of the input variables, application of fuzzy operators in the antecedent, implication from the antecedent to the consequent, aggregation of the consequents across the rules, and defuzzification. There are basically four components in the fuzzy logic system, (1) fuzzification, (2) inference engine, (3) rule base and (4) defuzzification. Figure 6 illustrates the components of a fuzzy system.

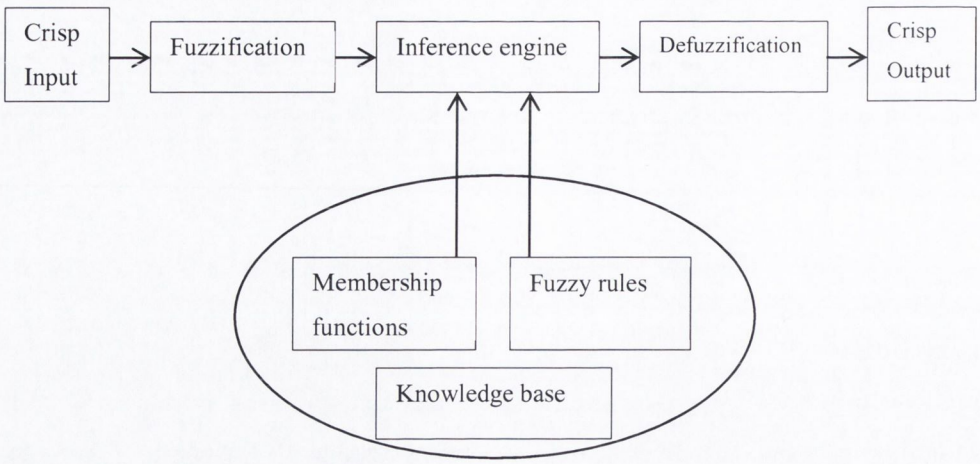

Figure 6. Components of a fuzzy logic system.

The first step in the process is to take the inputs and determine the degree to which they belong to each of the appropriate fuzzy sets via membership functions. Fuzzification is used to convert each piece of input data to degrees of membership by a lookup in one or several membership functions. The fuzzification block matches the input data with the conditions of the rules to determine how well the condition of each rule matches a particular input. There is a degree of membership for each linguistic term that applies to an input variable.

A fuzzy rule base consists of a set of fuzzy if-then rules. It is the heart of the fuzzy system in the sense that all other components are used to implement these rules. Inference engine implies the combination of certain rules into a mapping from a fuzzy rule base to get an output corresponding to the inferred rules. There are two ways in which to infer with a set of rules, composition based inference and individual rule based inference. In composition based inference, all rules in the fuzzy rule base are combined into a single fuzzy relation which is then viewed as a single fuzzy if-then rule. The fuzzy operators $\cap$ (AND) and $\cup$ (OR) are the most common type of inference used. In individual rule base inference, each rule in the fuzzy rule base determines an output fuzzy set and the output of the whole fuzzy inference engine is the combination of many individual fuzzy sets. The combination can be taken either by union or by intersection.

The last step of the process is defuzzification. In this step a fuzzy set (the aggregate output fuzzy set) is reduced to a single numbered output. Without defuzzification, the final output from the inference stage would remain a fuzzy set. In most applications, there is a requirement for a crisp signal. It is not a unique operation as different methods are possible. The most common methods are centre of gravity (CoG), centre of singleton (CoS), maximum membership, weight average and mean-max membership method. The method supported in Matlab is the CoG method.

The CoG method is a technique for finding a crisp value (u) from the mid-point of the output fuzzy set using a weighted average of the membership grades. Suppose, there exists a fuzzy set within a discrete universe, and $\mu(x_i)$ is its membership value in the membership function. The following expression can be used to represent the weighted average of the elements in the support set (Ross, 2004):

$$u = \frac{\sum_i \mu(x_i) x_i}{\sum_i \mu(x_i)} \tag{11}$$

1.5 Models used in Fuzzy Systems

The most commonly used fuzzy logic systems are the Mamdani-type and the Takagi–Sugeno type systems. In the case of a Mamdani-type fuzzy inference system, both premise and consequent (then) parts of a fuzzy if-then rule are fuzzy propositions. In the case of a Takagi–Sugeno-type fuzzy inference system where the premise part of a fuzzy rule is a fuzzy proposition, the consequent part is a mathematical function, usually a zero or first-degree polynomial function.

1.5.1 The Mamdani Model

The Mamdani model uses rules where by the antecedent and the consequent are both fuzzy. Consider the following two rule system:

- Rule 1: If x is $A1$ and y is $B1$
- Rule 2: If x is $A2$ and y is $B2$

where A_1, A_2, B_1, B_2, C_1 and C_2 from the expression above are fuzzy sets. Figure 7 illustrates how a Mamdani model takes two inputs x and y, applies the two rules in order to come to a logical solution based on these inputs.

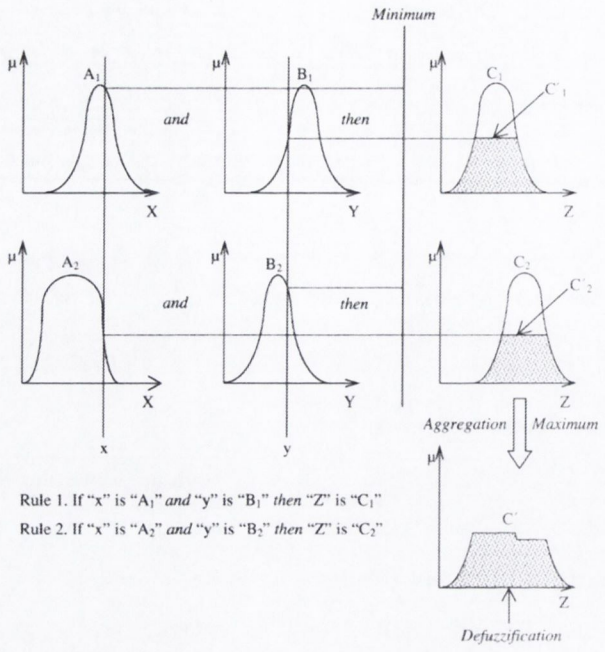

Figure 7. A Mamdani model for two inputs.

For the given values x and y (as depicted in Figure 7), the following is the typical step by step procedure carried out (Foley and McGory, 2011):

(a) For the value x find the membership values associated with fuzzy sets A1 and A2

(b) For the value y find the membership values associated with fuzzy sets B1 and B2

(c) For each rule, stated above, take the minimum of the membership values in Ai and Bi

(d) Use this value to truncate the fuzzy set $c_i (i = 1,2)$ to produce a new set c_i' (i=1,2)

(e) For each value of z in the truncated sets, take the maximum to produce the final output fuzzy set

(f) Optionally, defuzzify the output set to produce a single, or crisp, number

1.5.2 The Takagi-Sugeno Model

A Takagi-Sugeno model is another popular fuzzy logic model. This model type is discussed in greater detail in Section 1.6 as it is the model used in adaptive neuro-fuzzy inference systems. However, a brief explanation is provided in this section. The Takagi-Sugeno model also uses if-then rules similar to the Mamdani model. They are presented in the following form:

- If x is A and y is B, Then $z = f(x, y)$

where A and B are fuzzy sets and z is a crisp function in x, y. The function in the consequent can be any function. However, in a first order Tageaki-Sugeno model the function normally takes the form:

- $f(x, y) = px + qy + r$

where p, q and r are constants. In this particular model, the fuzzy rules contain a fuzzy antecedent and a crisp consequent. The two rules appear in the form:

- Rule 1: If x is A_1 and y is B_1, Then $z_1 = p_1x + q_1y + r_1$
- Rule 2: If x is A_2 and y is B_2, Then $Z_2 = p_1x + q_2y + r_2$

For each input, x and y, the membership values are found in A_1, A_2, B_1 and B_2. For each rule, the antecedent "AND" is then found by taking the minimum of the membership grades in each rule. This operation yields two weighting values, w_1 and w_2, both of which are associated to each function z_1 and z_2. A weighted average of the two functions, z_1 and z_2, produces the final output (Equation 12). Figure 8 illustrates the reasoning mechanism for this Sugeno model.

$$z = \frac{w_1 z_1 + w_2 z_2}{w_1 + w_2} \tag{12}$$

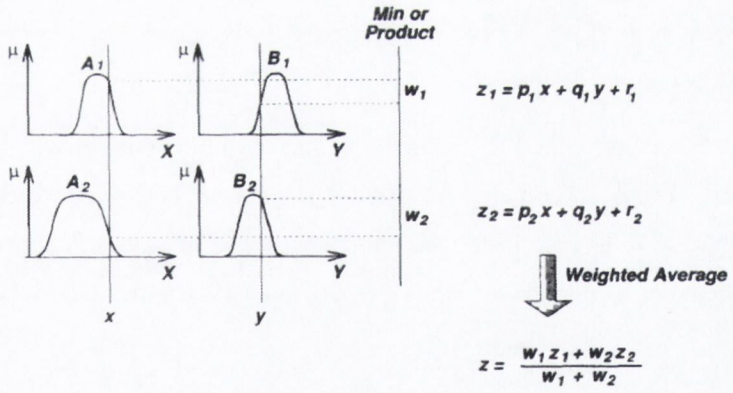

Figure 8. Takagi-Sugeno fuzzy inference system (Takagi and Sugeno, 1985).

1.6 Adaptive Neuro-Fuzzy Inference System

Adaptive Neuro-Fuzzy Inference Systems (ANFIS) are fuzzy systems, which use neural network theory in order to determine their properties (fuzzy sets and fuzzy rules) by processing data samples. Neuro-fuzzy systems harness the power of fuzzy logic and neural networks, by using the properties of neural networks in tuning rule-based fuzzy systems that approximate the way humans' process information. The membership functions in the model are tuned using either an algorithm that operates on a "backpropagation" principal or in combination with a least squares estimation method. ANFIS are a highly efficient means for developing a learned fuzzy model structure because this technique develops membership function parameters that best allow the

fuzzy inference system to track the input/output data. Ultimately, ANFIS operates on the principle that fuzzy systems can be formulated and trained using data from existing real-world processes.

Using a network structure that operates similar to that of a neural network, the input data values are mapped across a layered network, through input membership functions and their associated parameters, and then through output membership functions and their associated parameters in order to obtain a desired output. The parameters associated with both input and output membership functions change during the learning process.

The successful implementation of ANFIS has been reported in many engineering disciplines. Eksin et al (2012) developed an ANFIS model to understand human decision making behaviour in a stock management context. Basri (2008) developed a neuro fuzzy model for MRI image classification and tumour detection. Guner (2003) investigated the use of an adaptive neuro-fuzzy pH controller in a distillation system.

To present the ANFIS architecture, two fuzzy if-then rules based on a first order Sugeno model are considered:

- Rule 1: If x is A_1 and y is B_1, then $f_1 = p_1x + q_1y + r_1$
- Rule 2: If x is A_2 and y is B_2, then $f_2 = p_2x + q_2y + r_2$

where x and y are the inputs, A_i and B_i are the fuzzy sets, f_i are the outputs within the fuzzy region specified by the fuzzy rule, p_i, q_i and r_i are the design parameters that are determined during the training process. The ANFIS architecture to implement these two rules is shown in Figure 9, in which a circle indicates a fixed node, whereas a square indicates an adaptive node.

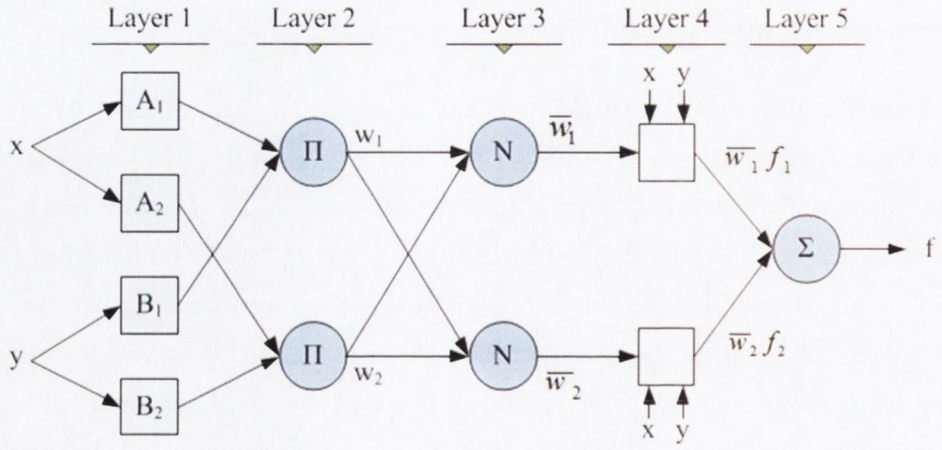

Figure 9. ANFIS architecture (Jang, 1993).

In order to train this particular network both a forward pass and a backward pass is performed over the system. The forward pass propagates the input vector through the network layer by layer in ascending order (Foley and McGory, 2011). The backwards pass, takes the error and sends it back through the network using backpropogation. The following describes how each layer operates:

Layer 1:

In the first layer, all the nodes are adaptive nodes. The outputs of layer 1 are the fuzzy membership grade of the inputs, which are given by (Foley and McGory, 2011):

$$O_i^1 = \mu_{A_i}(x) \quad for\ i=1,2 \tag{13}$$

$$O_i^1 = \mu_{B_{i-2}}(y) \quad for\ i=3,4 \tag{14}$$

where x is the input to node i, and A_i (or B_{i-2}) are a linguistic labels associated with this node. In other words, O_i^1 is the membership grade of a fuzzy set A, of a fuzzy set that contains the elements A_1, A_2, B_1 and B_2. The membership function for A can be any appropriate membership function, such as the triangular or gaussian. When the parameters of membership function changes, chosen membership function varies accordingly, thus exhibiting various forms of membership functions for a fuzzy set A. For example, if the bell shaped membership function is employed, $\mu_{A_i}(x)$ is given by (Foley and McGory, 2011):

$$\mu_{A_i}(x) = \frac{1}{1 + \left|\frac{x - c_i}{a_i}\right|^{2b_i}} \tag{15}$$

Where a_i, b_i and c_i are the parameters of the membership function, governing the bell shaped functions accordingly.

Layer 2:

Each node in this layer is a fixed node. An incoming signal from the previous layer is multiplied with another signal from the previous layer to produce the output of the second layer. The outputs of this layer can be represented as (Foley and McGory, 2011):

$$O_i^2 = w_i = \mu_{A_i}(x).\mu_{B_i}(y), \qquad i = 1,2 \tag{16}$$

Each node in this layer represents the so-called firing strength of the rules.

Layer 3:

In the third layer, the nodes are also fixed nodes. They are labelled with N, indicating that they play a normalization role to the firing strengths from the previous layer. The outputs of this layer are represented according to the following equation (Foley and McGory, 2011):

$$O_i^3 = \overline{w}_i = \frac{w_i}{w_1 + w_2}, \qquad i = 1,2 \tag{17}$$

The outputs, O_i^3 are the so-called normalized firing strengths as they play a normalisation role to the firing strength from the previous layer.

Layer 4:

All nodes in this layer are adaptive nodes with a node function of the form (Foley and McGory, 2011):

$$O_i^4 = \overline{w}_i f_i = \overline{w}_i (p_i x + q_i y + r_i) \tag{18}$$

From the equation above, the output of each node in this layer is the product of the normalised firing strength and a first order polynomial (for a first order Sugeno model).

Layer 5:

There is only one fixed node, labelled S that computes the overall output as the summation of all incoming signals. The overall output, O_i^5 the overall output of the model is given by (Foley and McGory, 2011):

$$O_i^5 = \sum_{i=1}^{2} \overline{w}_i f_i = \frac{\sum_{i=1}^{2} w_i f_i}{w_1 + w_2} \tag{19}$$

It can be observed that there are two adaptive layers in this ANFIS architecture, namely the first layer and the fourth layer. In the first layer, there are three modifiable parameters $\{a_i, b_i, c_i\}$, which are related to the input membership functions. These parameters are the so-called premise parameters. In the fourth layer, there are also three modifiable parameters $\{p_i, q_i, r_i\}$, pertaining to the first order polynomial. These parameters are so-called consequent parameters

1.6.2 Learning algorithm of ANFIS

The task of the learning algorithm for this architecture is to tune all the modifiable parameters, namely $\{a_i, b_i, c_i\}$ and $\{p_i, q_i, r_i\}$ to make the ANFIS output match the training data. When the premise parameters a_i, b_i, and c_i of the membership function are fixed, the output of the ANFIS model can be written as:

$$f = \frac{w_1}{w_1 + w_2} f_1 + \frac{w_2}{w_1 + w_2} f_2 \tag{20}$$

Substituting Equation 17 into Equation 20 yields

$$f = \overline{w}_1 f_1 + \overline{w}_2 f_2 \tag{21}$$

Substituting the fuzzy if then rules into Equation 21, it becomes

$$f = \overline{w}_1 (p_1 x + q_1 y + r_{1)} + \overline{w}_2 (p_2 x + q_2 y + r_2) \tag{22}$$

After rearrangement, the output can be expressed as

$$f = (\overline{w}_1 x) p_1 + (\overline{w}_1 y) q_1 + (\overline{w}_1) r_1 + (\overline{w}_2 x) p_2 + (\overline{w}_2 y) q_2 + (\overline{w}_2) r_2 \tag{23}$$

which is a linear combination of the modifiable consequent parameters p_1, q_1, r_1, p_2, q_2. The least squares method can be used to identify the optimal values of these parameters easily. When the premise parameters are not fixed, the search space becomes larger and the convergence of the training becomes slower. A hybrid algorithm combining the least squares method and the gradient descent method is adopted to solve this problem. The hybrid algorithm is composed of a forward pass and a backward pass. The least squares method (forward pass) is used to optimise the consequent parameters with the premise parameters fixed. Once the optimal consequent parameters are found, the backward pass starts immediately. The gradient descent method (backward pass) is used to optimally adjust the premise parameters corresponding to the fuzzy sets in the input domain. The output of the ANFIS is calculated by using the consequent parameters found in the forward pass. The output error is used to adapt the premise parameters by means of a standard backpropagation algorithm. It has been proven that this hybrid algorithm is highly efficient in training the ANFIS (Ross, 2004).

Appendix I: Publications

Introduction of Electric Vehicles to Ireland

Socioeconomic Analysis

John Brady and Margaret O'Mahony

The objective of this study was to undertake a social cost–benefit analysis of the proposed deployment of 230,000 electric vehicles in Ireland by 2020. The study analyzed the socioeconomic costs and benefits of this policy by comparing the environmental benefits, expressed in monetary values, with the associated reduction in tax revenues and the cost of the government's electric vehicle grant scheme. The study found that the 10% penetration of annual sales by electric vehicles by 2020 would result in a monetary loss of approximately €324 million (US$ 457 million) for the government (0.5% to 1% of total tax revenue expressed at 2009 levels). The primary reason for this shortfall would be a loss in all sources of tax revenue as a result of the electric vehicle penetration rates required to achieve an appreciable reduction in greenhouse gas emissions.

In November 2008, the minister for transport in Ireland announced a government target of 10% (230,000 vehicles) of the private-car fleet to be powered by electricity by 2020 (*1*). In order to ensure the early availability of electric vehicles (EVs) for the Irish market, the government signed memorandums of understanding with a Renault–Nissan alliance and Mitsubishi Motors. Under the terms of the agreements, the car manufacturers will supply battery electric vehicles (BEVs), and the government will introduce policies and incentives to support the widespread adoption of EVs and will support the development of a nationwide charging infrastructure.

The imminent commercial deployment of EVs has the potential to address issues such as climate change, oil dependence, and air quality. However, common to all new technologies, EVs face barriers to adoption, such as lack of knowledge by potential users, low consumer risk tolerance, and high initial production costs (*2*). In an attempt to address some of these market barriers, it has become common for governments to introduce financial consumer incentives to encourage the purchase of EVs. Despite the proliferation of such incentive programs, their efficiency in actually promoting the purchase of EVs is unclear and the programs are often the subject of public and political debate. One argument put forward by Carlsson and Johansson-Stenman is that "even though EVs may not be socially beneficial today, they probably will be tomorrow and that the introduction of EVs is a long process that must start today" (*3*).

Cost–benefit analysis is a useful tool for comparing the positive and negative effects of different activities or projects. Large uncertainties and simplified assumptions are generally associated with a cost–benefit analysis. A common criticism of published research in this area is the outdated data on EV technology and the electrical generation mix on which they are based. However, Carlsson and Johansson-Stenman argue that cost–benefit analysis can be a valuable tool for policy-making decisions provided that a detailed presentation of the assumptions made is outlined (*3*).

The objective of this study is to examine the socioeconomic costs and benefits of the proposed deployment of EVs in Ireland by 2020. This objective is achieved by comparing the environmental benefits, expressed in monetary values, with the associated reduction in tax revenues and the cost of the government's EV grant scheme. This comparison is particularly important in countries with high fuel taxes, as is the case with most European countries.

COST–BENEFIT ANALYSIS OF EVs

The concept of a social cost–benefit analysis is commonly used by policy decision makers to measure the social benefits of a proposed project in monetary terms and to compare them with its costs. Carlsson and Johansson-Stenman attempted to calculate the costs and benefits of both EVs and hybrid EVs and the private and societal costs attached to them (*3*). The study was conducted from a Swedish perspective for 2010, and rather than focusing on manufacturing and maintenance costs, the primary objective was to estimate all relevant cost elements while simultaneously highlighting the effect of changed tax revenues. The social benefits and costs of replacing internal combustion engine (ICE) vehicles with EVs was defined as the "difference between the benefit in terms of decreased external costs and the cost in terms of reduced taxation." In this context "external costs" refers to environmental costs. Consequently, the social marginal net benefit (MNB) can be calculated according to the following equation derived by Carlsson and Johansson-Stenman (*3*):

$$\text{MNB} = \Delta\text{MD} - \Delta R \quad (1)$$

where ΔMD is the decrease in marginal damage, or external costs from replacing one ICE vehicle with an EV, and ΔR is the associated decrease in tax revenues.

The analysis revealed that BEVs would be socially unprofitable primarily because the taxes applied to them are heavily subsidized compared with those for ICE vehicles. Hybrid electric vehicles were found to be socially and privately profitable without subsidies, especially for city-based delivery trucks. Herynkova conducted a similar analysis for Denmark for 2020 (*4*) on the basis of the Carlsson and Johansson-Stenman (*3*) social cost–benefit analysis equation. It was found that from a purely financial perspective EVs are not socially profitable since their reduction in environmental costs is by far offset by the decrease in tax revenues. However, vehicles in

Department of Civil, Structural, and Environmental Engineering, Trinity College Dublin, Museum Building, College Green, Dublin 2, Ireland. Corresponding author: M. O'Mahony, margaret.omahony@tcd.ie.

Transportation Research Record: Journal of the Transportation Research Board, No. 2242, Transportation Research Board of the National Academies, Washington, D.C., 2011, pp. 64–71.
DOI: 10.3141/2242-08

Denmark are subject to a particularly high registration tax of 180% and a value-added tax (VAT) of 25%.

Forkenbrock points out that the rising fuel efficiency of vehicles such as hybrid electric vehicles will result in reduced revenue from motor fuel taxes and, as the motor fuel tax becomes less productive, governments will have to change the ways in which they finance road infrastructure (*5*). Although BEVs do not directly consume fossil fuel, a study by Gonder et al. suggests that plug-in hybrids (PHEVs) will also result in substantial petroleum displacement, which further strengthens the concept that motor fuel taxes will be significantly reduced as a result of the deployment of EVs in national private vehicle fleets (*6*). Earlier research by Delucchi and Lipman presented a detailed life-cycle cost analysis for BEVs and found that the performance and cost of batteries must be significantly reduced in order for BEVs to become competitive (*7*). More recently, Granovskii et al. performed an economic and environmental comparison of ICE vehicles, EVs, and hydrogen fuel cell vehicles (*8*). It was shown that if electricity generated by a gas turbine engine with an efficiency of 50% to 60% was used to charge a BEV with a high-capacity battery, an EV would be advantageous. Lipman and Delucchi (*9*) provide a detailed and comprehensive life-cycle cost analysis of HEVs based on significant modifications to a previous model presented by Delucchi and Lipman (*7*). It was found that combining advanced vehicle improvements with mild vehicle hybridization provides the least-cost hybrid vehicle option, with life-cycle costs close to those of baseline vehicles.

VEHICLE TAX SYSTEM IN IRELAND

In 2006 the total contribution from all motor-related sources to the Irish exchequer was over €5.5 billion ($7.76 billion in U.S. 2010 dollars; €1 = $1.41). The main contributors were vehicle registration taxes (VRTs), annual motor taxes, and excise duty on fuels, which accounted for €1,257.5 ($1,775) million, €879.7 ($1,241) million, and €2,042.3 ($2,882) million, respectively (*10*). Income from VAT receipts and revenue from road tolls also contributed significantly. Since July 2008, VRTs and annual motor tax rates have been linked directly to the specific carbon dioxide (CO_2) emissions (CO_2 g/km) of the vehicle and have been applied as a percentage of the open market selling price (OMSP), as shown in Table 1. In addition, as shown by the range applied across the tax bands, the purchasing signal promoting lower-emitting cars is strong. VRT rates vary from 14% on the purchase price for cars with CO_2 emissions of up to 120 g/km to 36% for cars with CO_2 emissions greater than 225 g/km. However, under current legislation, BEVs are exempt from VRTs and PHEVs are entitled to up to €2,500 ($3,528) off the VRT payable on new-vehicle registration. Vehicles with emissions in the 0 to 120 g/km category are subject to annual motor taxes of €104 ($147).

Since April 2010, a government grant has been available toward the purchase price of BEVs and PHEVs. BEVs with an OMSP greater than €20,000 ($28,220) are eligible for a €5,000 ($7,053) governmental grant, whereas PHEVs with an OMSP greater than €18,000 ($25,391) are eligible for a €2,500 grant (*11*). The incentive for BEVs with an OMSP less than €20,000 will range from €2,000 ($2,821) for vehicles priced between €14,000 ($19,746) and €15,000 ($21,156) to €4,500 ($6,347) for those priced between €19,000 ($26,792) and €20,000. Excise duties of 54.34 cents/L (76.67 US cents/L) and 44.95 cents/L (63.38 US cents/L) are applied to unleaded gasoline- and diesel-fueled vehicles, respectively. These duties include the new carbon tax introduced in 2010 and are subject to VAT at 21%. A reduced VAT rate of 13.5% is levied on electricity utility bills.

TABLE 1 CO_2-Based Vehicle Registration and Road Tax Bands

Emission Band	Specific CO_2 Emissions (g/km)	VRT (% of OMSP)	AMT (€)
A	≤120	14	104
B	>120–140	16	156
C	>140–155	20	302
D	>155–170	24	447
E	>170–190	28	630
F	>190–225	32	1,050
G	>225	36	2,100

NOTE: AMT = annual motor tax.

METHODOLOGY AND KEY ASSUMPTIONS

Two different scenarios were explored: a business-as-usual scenario and an EV scenario, in which the 10% EV target is achieved and 230,000 vehicles are deployed. Carlsson and Johansson-Stenman's (*3*) social cost–benefit analysis equation was employed; however, an additional parameter was included to account for the Irish government's EV grant scheme. Thus the equation is expanded to the following:

$$MNB = \Delta MD - \Delta R - G \quad (2)$$

where

ΔMD = total decrease in marginal damage, or external costs, from replacing ICE vehicles with EVs;
ΔR = associated decrease in tax revenues; and
G = cost of BEV grant scheme.

The general assumptions made in this analysis are also detailed. These assumptions provide a natural benchmark case, since it is not known whether economic or technical parameters such as prices, taxes, and vehicle characteristics will fluctuate over the next decade.

Vehicle Parameters

Two particular vehicles, which are due to be released in 2011 and 2012, were taken as representative of EVs: the Nissan Leaf (a BEV) and the Toyota Prius (a PHEV). Fourteen ICE vehicle models were taken to represent conventional vehicles. Each of the seven road tax bands (A to G) were allocated two representative vehicles, one gasoline and one diesel. The characteristics of each vehicle are based on published specifications. However, the price of the PHEV has yet to be released and is assumed to be competitive with a similar-sized car. Table 2 shows both the actual and the assumed technical and economic parameters of each vehicle. It is recognized that future passenger vehicle requirements are difficult to predict, and so these values are hypothetical indicators that enable the calculation of resource consumption in a range of areas such as fuel consumption and electricity supply. This calculation in turn allows the estimation of projected tax revenue from a variety of sources.

TABLE 2 Technical and Economic Parameters

Vehicle	Emission Band	Fuel Type	Engine Size (L)	CO_2 Emissions (g/km)	Fuel Consumption (L/100 km)	OMSP (€)	Battery Capacity (kW-h)
Toyota Aygo	A	Petrol	1.0	106	4.5	10,670	—
Volkswagen Polo Trendline	A	Diesel	1.2	92	3.4	17,000	—
Nissan Leaf	A	Electric	—	0	0	29,995	24
Toyota plug-in Prius	A	Electric–petrol	1.8	89	3.9	30,000	5.2
Toyota Auris	B	Petrol	1.3	139	5.9	18,945	—
Volkswagen Jetta Trendline	B	Diesel	1.6	122	4.7	21,700	—
Toyota Avensis	C	Petrol	1.6	152	6.5	24,165	—
Volkswagen Passat CC	C	Diesel	2.0	146	6.1	38,520	—
Toyota Verso	D	Petrol	1.6	161	6.8	29,040	—
Volkswagen Tiguan	D	Diesel	2.0	164	6.4	35,760	—
Toyota RAV4	E	Petrol	2.0	174	7.4	28,695	—
Nissan X-Trail	E	Diesel	2.0	179	6.8	37,170	—
Mercedes-Benz S-Class	F	Petrol	3.0	200	7.6	98,600	—
Nissan Qashai+2	F	Diesel	2.0	209	7.9	38,785	—
Mercedes-Benz SL-Class	G	Petrol	3.5	236	8.8	136,635	—
Toyota Land Cruiser	G	Diesel	3.0	243	9.1	36,735	—

NOTE: — = not applicable.

Emissions Calculation

The potential reduction in tailpipe greenhouse gas emissions was calculated by using the COPERT 4 computer model (*12*). The COPERT 4 model is part of the *Atmospheric Emission Inventory Guidebook* from the European Monitoring and Evaluation Program and the Core Inventory of Air Emissions and is recommended by the European Environment Agency to calculate national emission inventories (*13*). Over 20 European member states including Ireland use the COPERT 4 model.

The greenhouse gases considered are carbon dioxide (CO_2), methane, and nitrous oxide, which can each be described in the form of carbon dioxide equivalent (CO_{2eq}), where CO_2 is given the value of 1 CO_{2eq} (*14*). The actual weighting used to convert methane and nitrous oxide to CO_{2eq} depends on the particular global warming potential lifetime used. In this study it is taken as 100 years, and as such methane and nitrous oxide assumed weightings of 25 and 298 (*14*). The other main pollutants related to traffic (particulate matter, nonmethane volatile organic compounds, and nitrogen oxides) are also evaluated. The external costs of the tailpipe emissions in euros per tonne are estimated on the basis of the European Commission's handbook of external costs in the transport sector (*15*).

The temperature data required for the COPERT model were from the *European Climate Assessment and Dataset* (*16*). For the period 2006 to 2008, the 2005 advanced fuel specification provided by COPERT 4 was used. However, for the period 2009 to 2020, although an advanced fuel specification is provided by COPERT 4 for 2009-stage fuel, the fuel specifications defined in the Air Pollution Act of 1987 were utilized instead (*17*). The only difference is that the 2009-stage fuel specifications have a reduced sulfur content from 50 parts per million (ppm) to 10 ppm. The polycyclic aromatic hydrocarbon value given in the Irish statutes is by mass and not by volume as demanded by COPERT 4, so the default figure was used instead.

The COPERT 4 methodology is based on average speeds and corresponding average speed emission factors to calculate vehicle emissions (*18*). It includes a total of 37 different classes of gasoline passenger cars. A given car belongs to one of three different subsectors depending on the cylinder volume (<1.4 L, 1.4 to 2.0 L, and >2.0 L), and each subsector contains 12 to 14 different technology classes, reflecting the various stages of the European Union exhaust regulation (e.g., Euro 1, Euro 2). For diesel passenger cars there are two different subsectors (<2.0 L and >2.0 L), each containing seven different technology classes. A mix of urban (30% of total distance), rural (50% of total distance), and highway (20% of total distance) driving was considered with average speeds of 40 km/h (rural), 60 km/h (urban), and 100 km/h (highway).

Future Size and Breakdown of Private Car Fleet

In 2008 there were 1,924,281 private cars registered in Ireland, of which 3,579 (0.15%) were classified as EVs (*19*). The ISus private car stock model, developed by the Economic and Social Research Institute of Ireland, was used to make assumptions about the future size and breakdown of the private car fleet (*20*). The model, which is driven by forecasts on the economy and the population, is constructed from a long history of data sales and has been calibrated to recent data on the actual stock. The model distinguishes cars by fuel type, engine size, and age and projects that there will be approximately 2.2 million private cars in Ireland in 2020. Because taxation levels are calculated on the basis of emissions per kilometer rather than engine size, concordances constructed by the Economic and Social Research Institute are used to transform engine sizes into emissions bands. The concordance tables used are based on actual sales in 2008 to 2009 (*20*).

From new-vehicle registration statistics of the Society of Irish Motor Industry over the period 2000 to 2007, approximately 158,309 new cars are registered in Ireland each year. Because of the deterioration of the economy, new car registrations significantly decreased to 151,607 (−18%) and 57,460 (−62%) in 2008 and 2009, respectively. Early indications for 2010 (June) suggest a recovery in the industry with a 45% increase in sales (67,864) in the same period in 2009 (*21*).

For this study, it was assumed that the industry would return to the position where it otherwise would have been by 2020 before the global economic recession and that there will be approximately 158,000 new cars registered in Ireland in 2020.

Annual Passenger Car Kilometers

In 2009 the average annual kilometers for passenger cars was 16,708 km (*22*). Cars with a small engine size typically tend to travel less than the average annual mileage. For example, cars with an engine size of less than 1.4 L traveled approximately 13,000 km in 2009. For this study, the results of the distance model of the Economic and Social Research Institute were adopted, which projects the distance traveled for each engine size for a given year (*20*). The model accounts for changes in the composition of the car stock and is driven by the elasticity estimate and change in the relative price of fuel.

For this study it was assumed that PHEVs are viable substitutes for all ICE vehicles with an engine size between 1.4 and 2.0 L, but that BEVs will only replace engine sizes less than 1.4 L because of their limited driving range. The EVs are assumed to be distributed evenly across both fuel types and engine sizes and hence will have a similar annual mileage.

According to Smith (*23*), the fraction of passenger-car kilometers completed by a PHEV in the electric driving mode is dependent on the trip length, fleet penetration, kinematic profile, and the vehicle's characteristics such as its all-electric range. From an analysis of Irish passenger-car trip length distributions and assuming one overnight charge per 24-h period, Smith estimates that 67% of passenger-car kilometers could be completed by PHEVs with an all-electric range of 40 km (*23*). For simplicity, in this study, the same estimate was used.

Electrical Energy Requirements of EVs

In order to quantify the potential electrical requirements of the EV fleet, it is first necessary to quantify the energy required to move a vehicle. Smith developed a model to determine the minimum theoretical energy required to move a given vehicle a fixed distance over a specific drive cycle (*23*). The model was then used to calculate the minimum energy requirement, in kilowatt-hours per kilometer (kW-h per km), of a range of vehicles representative of the Irish passenger-car fleet operating over a selection of legislative and real-world drive cycles. From this analysis it was assumed that the electrical energy requirement of a PHEV would be 0.209 kW-h/km.

In a review of transport options to alleviate the effects of climate change, such as urban air pollution and oil dependence, Thomas reports that under optimum conditions, the average fuel economy of a BEV is 2.6 times greater than that of an ICE vehicle, giving a specific energy consumption of 0.26 kW-h/km (*24*). However, Foley et al. report that under real-world driving conditions, the specific energy consumption is 10 to 25 kW-h/70 km (*25*). The electric energy requirement of a BEV was assumed to be 0.209 kW-h/km.

Size of EV Fleet

The accurate prediction of the market penetration of EVs includes great uncertainties and depends on a multitude of influencing factors. In this study the rate of penetration is estimated by using a logistic *S*-curve.

The shape of the curve is determined by specifying two years and the expected market penetration of EVs for those particular years. If it is assumed that EV sales commence in 2011, that 28% and 90% market penetration is achieved by 2020 and 2035, respectively, and that the average number of sales per year is 158,000, 44,240 EV sales are estimated in 2020 (Figure 1). Cumulative sales over the period 2011–2020 are calculated to be 231,474, which compares with the government target of 230,000. Market penetration refers to the penetration of annual sales; penetration of the entire car fleet would take significantly longer.

In the reviewed studies the range of conceivable market penetration scenarios varies widely. The majority of studies estimate the market penetration of EVs, but few differentiate between PHEVs and BEVs. It was assumed that PHEVs would become widely available in the near future and that rapid growth would lead to mass commercialization. However, mass market production of BEVs is not expected for a number of years because of the premium price and limited consumer acceptance with regard to recharging times and driving range. The Irish electricity utility, the Electricity Supply Board, which is responsible for the development of the national EV charging infrastructure, forecast that in 2020 the EV fleet in

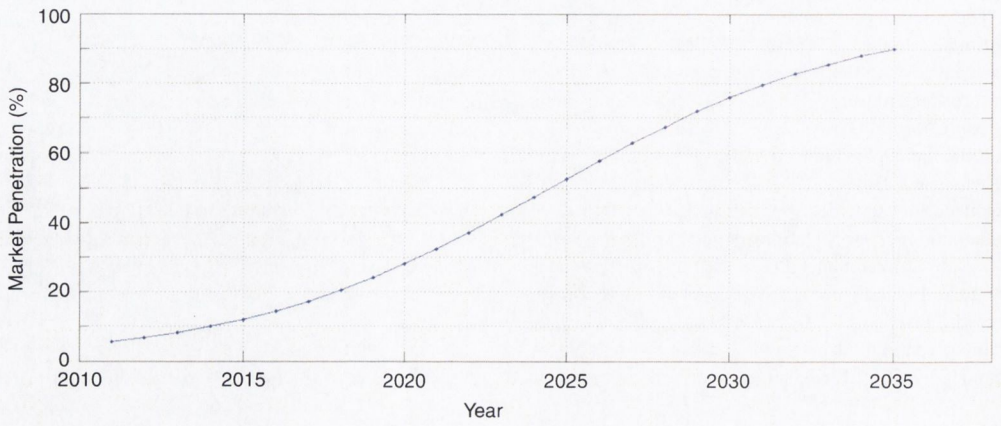

FIGURE 1 Projected EV market penetration.

Ireland will consist of 70% PHEVs and 30% BEVs (*26*). For this study, the same makeup was assumed and sales in 2020 were assumed to be of a similar nature.

Tax and Electricity Rates

As previously discussed, under current legislation PHEVs are entitled to up to €2,500 off the VRT payable upon a new vehicle registration, and BEVs are exempt from the VRT. It is assumed that this policy will be extended to 2020. The excise duties and VAT applied to fuels are assumed to remain unchanged in 2020. Furthermore, annual motor tax rates were assumed to be similar to those in 2010.

It is understood that the Electricity Supply Board will introduce a special night electricity rate under which customers will be able to charge their cars (*27*). However, since details of such rates have yet to be released, it was assumed that the rate would be similar to the Electricity Supply Board's current night saver tariff. Under this rate customers living in urban areas are charged a reduced rate of €0.0745 (excluding VAT) per kilowatt hour of electricity consumed.

RESULTS

Monetary Cost of CO_2 Emissions from Electricity Generation

Assuming that the electrical power requirements of a PHEV and a BEV are 0.209 kW-h/km and 0.25 kW-h/km, respectively, and that 67% of the annual passenger-car kilometers of a PHEV will be completed in the electric driving mode, it was estimated that the total electrical power requirement of EVs in 2020 would be 244 GW-h. In calculating the emissions produced from electricity generation, it is assumed that 40% of the electricity mix will come from renewables and that the electricity CO_2 emission intensity factor will be 393 g/kW-h in 2020 (*26*). On the basis of these assumptions, the total energy-related CO_2 emissions associated with electricity generation is projected to be 235 kilotonnes.

The European Commission prescribes a monetary value of €40/tonne of CO_2. This value equates to a monetary loss of €9.39 ($13.24) million for CO_2 emissions from the generation of the electricity required to power EVs.

Monetary Benefit of Reduced Tailpipe Emissions

Table 3 presents the estimate of total emissions (CO_{2eq}, particulate matter, nonmethane volatile organic compounds, nitrogen oxides) for each scenario and the calculated monetary benefit. The largest benefit will be as a result of decreased CO_{2eq} emissions. The business-as-usual or baseline CO_{2eq} emissions for 2020 from the private-car fleet are projected to be 5.93 megatonnes (Mt) CO_{2eq}. Under the EV scenario it is expected that this amount will decrease to 5.36 Mt CO_{2eq}, a saving of 570,000 t CO_{2eq} and a monetary benefit of €22.8 ($32.09) million. Overall, the total reduction in CO_2 emissions and other types of pollutants would equal a monetary benefit of €31.27 ($44.02) million.

Estimated Vehicle Registration and Motor Tax Revenue

The 2020 vehicle procurement is based on an average of 158,000 new registrations per year and the progressive development in sales of EVs between 2010 and 2020. The expected VRT revenue in 2020 under the business-as-usual scenario and EV scenario is projected to be €857 ($1,208) million and €759 ($1,070) million, respectively.

The annual motor tax rates for each road tax band are presented in Table 1. Currently the annual motor tax rate for both BEVs and PHEVs is €104. Under the EV scenario, the value is calculated by assuming that the passenger-car fleet consists of 230,000 EVs and that the remainder of the fleet consists of ICE vehicles. Taking these factors into account, the expected annual motor tax revenue in 2020 under the business-as-usual scenario and EV scenario is projected to be €859 ($1,211) million and €824 ($1,162) million, respectively. From the introduction of EVs, the calculations indicate a monetary loss of €98 ($138) million and €35 ($49) million in VRT and annual motor tax revenue, respectively.

Estimated Cost of Governmental EV Grant Scheme

In a worst-case scenario the OMSP of all BEVs and PHEVs purchased in 2020 will be greater than €20,000 ($28,193) and €18,000 ($25,374), respectively. Under this scenario, the EV grant scheme could potentially cost the government €143.77 ($203) million.

Estimated Fuel Tax Revenue

The fuel economy of the vehicles is based on the specifications provided in Table 2. BEVs are powered solely by electricity. Hence they consume no fossil fuel, and it is assumed that 67% of the annual passenger-car kilometers of a PHEV will be completed in the electric driving mode. On the basis of these factors, approxi-

TABLE 3 Emission Results

		EV Scenario		BAU Scenario		
Pollutant	External Cost (€/tonne)	Emissions	Monetary Cost (€ millions)	Emissions	Monetary Cost (€ millions)	Monetary Benefit (€ millions)
CO_{2eq} (Mt)	40	5.36	214.4	5.93	237.2	22.80
NO_x (t)	3,800	5,920	22.50	6,394	24.30	1.80
NMVOC (t)	700	1,361	0.95	1,530	1.07	0.13
$PM_{2.5}$ (t)	126,200	391	49.34	422	53.26	3.92
PM_{10} (t)	50,500	623	31.46	675	34.09	2.63
Total			318.65		349.92	31.27

NOTE: NMVOC = nonmethane volatile organic compound; PM = particulate matter.

mately 875 and 1,235 ML of gasoline and diesel, respectively, will be consumed in 2020 under the EV scenario. Assuming that excise duties of 54.34 cents/L and 44.95 cents/L are applied to unleaded gasoline- and diesel-fueled vehicles, respectively, the corresponding fuel tax revenues in 2020 under the business-as-usual scenario and EV scenario are projected to be €1.09 ($1.54) billion and €1.03 ($1.45) billion, respectively. The calculations suggest a potential loss in fuel tax revenue of €60 ($84) million.

Estimated VAT Revenue

In July 2010, the average price per liter of gasoline and diesel in Ireland was 133.3 cents/L and 124.9 cents/L, respectively (*28*). Assuming similar prices in 2020 and that fuel will be subject to a VAT at 21%, the expected VAT revenue from fuel consumption under the business-as-usual scenario and EV scenario is projected to be €308.95 ($435.47) million and €291.43 ($410.56) million, respectively. The calculations indicate that the reduced fuel consumption associated with the introduction of EVs will result in a reduction of €17.52 ($24.68) million in VAT revenue.

The operation of EVs will result in increased electricity consumption and hence increased VAT revenue. With a VAT rate of 13.5% levied on electricity utility bills, this increased consumption will yield approximately €6.00 ($8) million in VAT revenue.

Social Marginal Net Benefit of EVs

Table 4 presents a summary of the benefits of reduced environmental damage with the costs associated with the losses in fuel tax revenue and the government BEV grant scheme. From the results, it is clear that the deployment of EVs in Ireland will lead to a net benefit in terms of environmental costs (€26 million or $36 million).

TABLE 4 Summary of Social Marginal Net Benefit

	Business-as-Usual Scenario	EV Scenario
Total Marginal (Environmental) Damage (MD) (€ millions)		
CO_2 emissions from electricity generation	na	5
Tailpipe emissions (CO_{2eq}, NO_x, NMVOC, $PM_{2.5}$, PM_{10})	350	319
Total	350	324
Tax Revenue (R) (€ millions)		
VRT	857	759
Motor tax	859	824
Fuel tax	1,091	1,030
VAT from fuel sales	309	291
VAT from electricity consumption	na	6
Total	3,116	2,910
Benefit of Reduced Emissions (€ millions)		
Total marginal benefit (ΔMD)	na	26
Total tax revenue loss (ΔR)	na	206
Cost of governmental EV grant scheme (G)	na	144
Social marginal net benefit (MNB) (MNB = ΔMD − ΔR − G)	na	−324
Social marginal net benefit per EV (€)	na	−1,408

NOTE: na = not applicable; NO_x = nitrogen oxide.

However, this benefit will be offset by the projected losses in tax revenue and the cost of the government's EV grant scheme. The total tax revenue is projected to decrease by 6.6% from €3,116 ($4,389) million to €2,910 ($4,098) million under the business-as-usual and EV scenarios, respectively, a loss of €206 ($289) million. However, the total exchequer taxation receipts for 2009 were €32,570 ($45,859) million (*29*), which indicates that on the basis of 2009 levels this loss will likely only be in the region of 0.5% to 1% of the government's total tax revenue. Including the likely cost of the EV grant scheme (€144 million or $203 million), the overall indication is that the deployment of EVs is not socioeconomically beneficial and results in a social marginal net loss of €324 ($456) million. The potential loss per EV is approximately €1,408 ($1,982).

STUDY LIMITATIONS

This study is relatively narrow in scope in that it does not include a full life-cycle analysis of an EV and the full range of operating costs. Rather the study is meant to contribute to a better understanding of the potential implications for tax revenue of the replacement of ICE vehicles with EVs and also to estimate the environmental benefits. It is intended to expand over time to become a broader social cost–benefit analysis model that will include multiple time frames, different government incentive scenarios, market penetration, and fuel and electricity price scenarios. It will also incorporate energy consumption and EV travel data collected from household EV trials.

The results are based on a number of critical assumptions, some of which are rather uncertain. Above all, the focus is on the year 2020, since this year has been identified by the Irish government as a significant target year to have 230,000 EVs deployed. Although emissions benefits may not be significant by this time, they will continue to increase after 2020, whereas social costs in terms of incentives and VRT tax breaks will most likely have been discontinued. In addition, only a single market penetration scenario was run in which a certain percentage of new car sales each year are electric. The model used does not allow for examination of whether EVs replace old high-emitting vehicles or whether they are only purchased by environmentally concerned consumers who already own a vehicle with relatively low emissions. A discrete choice model of consumer preferences to assess the impact of the consumer on EV purchases similar to that used by Brownstone and Train (*30*) would be required. Instead assumptions are made about the vehicle engine sizes that EVs will replace and how certain targets will be reached in terms of market share of sales.

In this study the market penetration of EVs was estimated with a logistic *S*-curve, but in reality it is likely to be a function of a number of factors such as fuel price, the purchase price of the vehicles after government subsidies, and the relative utility of EVs compared with ICE vehicles. The last factor would be difficult to estimate considering that EVs are not yet available on the market. Because of fuel price volatility, no projections were attempted for the future price of fuel or electricity. Current incentives and tax rates were assumed to remain static. However, vehicle production may become commercially viable before 2020, leading to a reduction in retail prices, which in turn may lead to the termination of government incentives and VRT tax breaks before 2020. In addition, the future composition of the EV fleet was assumed to consist of 30% BEVs and 70% PHEVs. This composition is important because each vehicle type is entitled to different incentives and has different performance characteristics in relation to fuel consumption and electrical power requirements. The CO_2 emission intensity of the electrical

generation system in 2020 was taken to be 393 g/kW-h, assuming that the government target of 40% electricity generation from renewable sources by 2020 is achieved. The COPERT 4 model used to estimate emissions from the passenger-car fleet is based on international averages and as such may be subject to some error in the emissions calculated. Finally, the introduction of grants and tax incentives may cause economic activity to slow in the private sector. The level of impact that this scenario could have on the wider economy is unknown and is beyond the scope of this study.

AREAS FOR FURTHER STUDY

This study provides a host of possible new directions for future research. First, it could be extended as noted earlier by including a comprehensive analysis of the full life-cycle costs to society of EVs. The extent of emission reductions depends on what vehicles types are replaced by EVs. A discrete choice model of consumer preferences as described earlier would facilitate a more realistic representation of market penetration.

There is a need to quantify the disutility to the consumer associated with the usability of an EV in terms of the limited driving range and lack of recharging infrastructure. As a starting point, one could estimate the disutility of the costs associated with the installation of home recharging equipment and garage space requirements.

A further analysis would be possible when EVs come to market. It would be useful to integrate a more careful assessment of travel patterns and how these affect both BEV and PHEV miles driven in the electric driving mode. This evaluation would be possible through EV trials and would allow a better analysis of the emissions and fuel consumption savings. Additional sensitivity analysis on the assumed fuel efficiency of EVs and fuel and electricity prices would also provide insights and eliminate ambiguity. A comparison of multiple time frames of different lengths would benefit an analysis of this type to monitor how the social net benefit changes over time.

CONCLUSIONS AND RECOMMENDATIONS

This study presents a simplified social cost–benefit analysis of the adoption of EVs in Ireland. The authors found that by 2020 the 10% adoption of EVs will result in a social marginal net loss of €324 million ($456 million) or €1,408 ($1,982) per EV. The primary reason for this loss is due to losses in all sources of tax revenue compared with the EVs' penetration rates required to achieve an appreciable reduction in emissions. This loss of €206 million ($289 million) is in the region of 0.5% to 1% of total tax revenue in Ireland at 2009 levels. However, this result should be interpreted carefully in light of the assumptions and study limitations outlined. Critically this analysis focuses on the year 2020, which would be in the early stages of a transition from ICE vehicles to EVs. At this time costs in terms of incentives and VRT tax breaks are highest to encourage adoption, and the benefits in terms of reduced emissions are lowest because of low fleet penetration.

A similar analysis conducted over a longer time frame could possibly yield a positive social net benefit. Furthermore, it is difficult to predict when the current government incentive scheme and VRT tax break will be terminated. Combined, these account for 77% (€242 million or $341 million) of losses, which if discontinued before 2020 could result is a positive outcome in the short term. However, this analysis suggests that even if current government incentives and VRT tax breaks are continued to 2020, the short-term social cost of EVs will be close to that of the business-as-usual scenario. The transition from ICE vehicles to EVs will be a lengthy process, and therefore, assuming reasonable anticipated technological progress after 2020, increased market penetration, and the termination of government incentives, the full social lifetime costs of EVs will most likely surpass the short-term losses and could well be lower than the full social lifetime costs of ICE vehicles. However, as both new EV and ICE vehicle designs and concepts continue to emerge, continued research is needed in this area.

ACKNOWLEDGMENTS

The authors thank the Program for Research in Third-Level Institutions for funding this research and the Economic and Social Research Institute for providing the ISus car model data.

REFERENCES

1. Department of Communications, Energy, and Natural Resources. *Government Announces Plans for the Electrification of Irish Motoring.* Dublin, Ireland, Nov. 2008. http://www.dcenr.gov.ie/Press+Releases/2008/Government+announces+plans+for+the+electrification+of+Irish+motoring.htm. Accessed Dec. 1, 2009.
2. Diamond, D. The Impact of Government Incentives for Hybrid-Electric Vehicles: Evidence from U.S. States. *Energy Policy,* Vol. 37, 2009, pp. 972–983.
3. Carlsson, F., and O. Johansson-Stenman. Costs and Benefits of Electric Vehicles: A 2010 Perspective. *Transport Economics and Policy,* Vol. 37, 2003, pp. 1–28.
4. Herynkova, H. *Impact Analysis of Diffusion of Electric Vehicles in Denmark.* Master's thesis. Lund University, Lund, Sweden, 2009.
5. Forkenbrock, D. J. Financing Local Roads: Current Problems and New Paradigm. In *Transportation Research Record: Journal of the Transportation Research Board, No. 1960,* Transportation Research Board of the National Academies, Washington, D.C., 2006, pp. 8–14.
6. Gonder, J., T. Markel, A. Simpson, and M. Thornton. Using Global Positioning System Travel Data to Assess the Real-World Driving Energy Use of Plug-In Hybrid Electric Vehicles. In *Transportation Research Record: Journal of the Transportation Research Board, No. 2017,* Transportation Research Board of the National Academies, Washington, D.C., 2007, pp. 1–11.
7. Delucchi, M. A., and T. E. Lipman. An Analysis of the Retail and Lifecycle Cost of Battery-Powered Electric Vehicles. *Transportation Research,* Vol. 6D, 2001, pp. 371–404.
8. Granovskii, M., I. Dincer, and M. A. Rosen. Economic and Environmental Comparison of Conventional, Hybrid, Electric and Hydrogen Fuel Cell Vehicles. *Journal of Power Sources,* Vol. 159, 2006, pp. 1186–1193.
9. Lipman, T. E., and M. A. Delucchi. A Retail and Lifecycle Cost Analysis of Hybrid Electric Vehicles. *Transportation Research,* Vol. 11D, 2006, pp. 115–132.
10. Society of the Irish Motor Industry. *Motor Industry Related Taxation.* Dublin, Ireland. http://www.simi.ie/taxation/introduction.aspx. Accessed March 10, 2010.
11. Sustainable Energy Authority of Ireland. *Electric Vehicle Grant Scheme.* Sligo, Ireland. http://www.seai.ie/Grants/Electric_Vehicle_Grant_Scheme. Accessed April 12, 2010.
12. Gkatzoflias, D., C. Kouridis, and L. Ntziachristos. *COPERT 4: Computer Programme to Calculate Emissions from Road Transport.* European Environment Agency, Brussels, Belgium, 2007.
13. Kousoulidou, M., L. Ntziachristos, G. Mellios, and Z. Samaras. Road-Transport Emission Projections to 2020 in European Urban Environments. *Atmospheric Environment,* Vol. 42, Oct. 2008, pp. 7465–7475.
14. *Fourth Assessment Report: The Physical Science Basis.* Working Group I, Intergovernmental Panel on Climate Change, Geneva, 2007.
15. *Handbook on Estimation of External Costs in the Transport Sector.* European Commission DG TREN, Brussels, Belgium, 2008.
16. Royal Netherlands Meteorological Institute. *European Climate Assessment and Dataset.* De Bilt, Netherlands. http://eca.knmi.nl/dailydata/customquery.php. Accessed Jan. 15, 2010.

17. Irish Statute Book. *Air Pollution Act, 1987 (Environmental Specification for Petrol and Diesel Fuels) Regulations 2003.* S.I. No. 541/2003. Stationery Office, Dublin, Ireland, 2003.
18. Gkatzoflias, D., C. Kouridis, L. Ntziachristos, and Z. Samaras. *Computer Programme to Calculate Emissions from Road Transport: Methodology for the Calculation of Exhaust Emissions.* European Environment Agency, Brussels, Belgium, 2007.
19. *Irish Bulletin of Vehicle and Driver Statistics 2008.* Department of Transport, Dublin, Ireland, 2009.
20. Hennessy, H., and R. S. J. Tol. *The Impact of Climate Policy on Private Car Ownership in Ireland.* Working Paper 342. Economic and Social Research Institute, Dublin, Ireland, 2010.
21. Society of the Irish Motor Industry. *National Vehicle Statistics.* Dublin, Ireland. http://www.simi.ie/statistics/national_vehicle_statistics.aspx. Accessed June 10, 2010.
22. *Energy in Transport 2009 Report.* Sustainable Energy Authority Ireland, Dublin, 2009.
23. Smith, W. J. Plug-in Hybrid Electric Vehicles: A Low-Carbon Solution for Ireland? *Energy Policy,* Vol. 38, 2010, pp. 1485–1499.
24. Thomas, S. Transportation Options in a Carbon-Constrained World: Hybrids, Plug-in Hybrids, Biofuels, Fuel Cell Electric Vehicles, and Battery Electric Vehicles. *International Journal of Hydrogen Energy,* Vol. 34, 2009, pp. 9279–9296.
25. Foley, A., H. Daly, E. McKeogh, and B. Ó Gallachoir. Quantifying the Energy and Carbon Emission Implications of a 10% Electric Vehicles Target. In *Proc., International Energy Workshop,* June 20–23, 2010, Stockholm, Sweden.
26. Mulvaney, P. Transformation of Transportation. Presented at Transport Ireland Conference, Dublin, Ireland, April 29, 2010.
27. Electric Vehicle Deal Agreed. *Irish Times,* May 5, 2010. http://www.irishtimes.com/newspaper/breaking/2010/0524/breaking61.html. Accessed May 24, 2010.
28. AA Ireland. *Irish Petrol Prices: June 2011.* http://www.aaireland.ie/petrolprices. Accessed July 4, 2010.
29. *Ireland—Stability Programme Update.* Department of Finance, Dublin, Ireland, 2009.
30. Brownstone, D., and K. Train. Forecasting New Product Penetration with Flexible Substitution Patterns. *Journal of Econometrics,* Vol. 89, 1999, pp. 109–129.

The Social and Economic Factors of Transportation Committee peer-reviewed this paper.

Transportation Research Part D 16 (2011) 188–193

Contents lists available at ScienceDirect

Transportation Research Part D

journal homepage: www.elsevier.com/locate/trd

Notes and comments

Travel to work in Dublin. The potential impacts of electric vehicles on climate change and urban air quality

John Brady *, Margaret O'Mahony

Centre for Transportation Research, Simon and Perry Building, Trinity College, Dublin 2, Ireland

ARTICLE INFO

Keywords:
Electric vehicles
Urban air quality
Greenhouse gases

ABSTRACT

The Irish government has outlined plans for 10% of the national road fleet to be powered by electricity by 2020. The objective of this paper is to evaluate the potential reduction in road traffic related emissions due to commuting in the Greater Dublin Area under different electric vehicle market penetration scenarios. The results indicate that the introduction of electric vehicles offers the potential for reductions in all road traffic related emissions. However, the time required for electric vehicles to acquire a significant share of the fleet, suggests that they will have a limited impact on climate change and urban air quality for at least the next decade.

1. Introduction

In November 2008, the Irish Minister for Transport announced a target for 10% (230,000 vehicles) of the private car fleet to be powered by electricity by 2020 (Dempsey, 2008) as part of the initiative to address issues of climate change, oil dependence and air quality. Typically commuter's are particularly suited to electric vehicle (EV) use due to the repetitive nature and fixed distances of their trips and because their vehicles are available for recharging either during daytime or overnight (Turrentine et al., 1992).

In 2008, transport in Ireland accounted for 21.3% of national greenhouse gas (GHG) emissions; an increase of 176% over 1990 levels (Environmental Protection Agency, 2009). This increase can be attributed to a period of unprecedented economic growth, which led to an increase in vehicle numbers, the purchase of larger vehicles, and greater reliance on private cars for commuting. These trends are particularly noticeable in the Greater Dublin Area (GDA),[1] which saw an increase in employment by 48.9% and private car registrations by over 60% between 1996 and 2006 (Central Statistics Office, 2007a). Furthermore, in 2006, 51.8% of commuters in the GDA travelled to work by car, an increase of 5% on 1996 levels (Commins and Nolan, 2008). Morgenroth (2001) utilized data supplied by the Irish Revenue Commissioners to estimate the extent of the commuting belt around Dublin and concluded that it extends beyond the GDA and that a substantial number of individuals commute long distances from counties outside the GDA; the "Outer Belt" region in Fig. 1.

Numerous studies have explored the potential environmental benefits of EVs. The Electrical Power Research Institute (2007) and the Natural Resources Defence Council compared plug-in hybrid vehicles (PHEV) to hybrid vehicles (HEV) and ICEVS using specific electricity generating technologies and concluded that regardless of the electricity supply, PHEVs and HEVs would result in a net decrease in GHG emissions of between 28% and 67% relative to ICEVs. Lilienthal and Brown (2007) estimated the potential carbon dioxide (CO_2) emissions reduction through the introduction of PHEVs into individual states in the US and determined that use of PHEVs would reduce emissions in 49 states and on average by 42% per mile

* Corresponding author. Tel.: +353 858232116.
E-mail address: bradyj7@tcd.ie (J. Brady).

[1] Defined as Dublin City and the surrounding counties of Fingal, Dun Laoghaire-Rathdown, South Dublin, Kildare, Wicklow and Meath.

1361-9209/$ - see front matter © 2010 Elsevier Ltd. All rights reserved.
doi:10.1016/j.trd.2010.09.006

Fig. 1. Commuter belt for Dublin City. *Source*: Morgenrath (2001).

driven, with that reductions if a larger proportion electricity came from renewable sources rather than coal. In the Irish car fleet, Smith (2010) examined the potential benefits of PHEVs in terms of reducing the primary energy requirement (PER) and CO_2 emissions of passenger cars and found that the electricification could reduce the PER and CO_2 emissions by 50% per km.

2. Methodology

2.1. Fleet emission

The details of regular work trips were sourced from the Place of work Census of Anonymised Records (POWCAR) (Central Statistics Office, 2007b). It derives from the data gathered in the 2006 Irish census and provides information on 1,834,472 regular work trips.

The ISus private car stock model, developed by the Economic and Social Research Institute (ESRI) of Ireland (Hennessy and Tol, 2010), is used to derive assumptions about the future composition of the private car fleet. The model, which is driven by forecasts on the economy and the population, is constructed from a history of passenger car sales calibrated to recent data on the actual stock, and distinguishes cars by fuel type, engine size and age. The current composition of the Irish private car fleet is presented in Table 1.

The potential reduction in tailpipe GHG emissions was calculated using the COPERT 4 computer model, which is part of the EMEP/CORINAIR Atmospheric Emissions Inventory Guidebook and is recommended by the European Environment Agency to calculate national emission inventories (Kousoulidou et al., 2008). The COPERT 4 methodology is based on average speeds and corresponding average speed emission factors to calculate vehicle emissions (Gkatzoflias et al., 2007). It includes 37 classes of gasoline passenger cars. A given car belongs to one of three "subsectors" depending on the cylinder volume (<1.4 L, 1.4–2.0 L and >2.0 L), and each subsector contains 12–14 "technology classes", reflecting the various stages of the EU exhaust regulation (EURO 1, EURO 2, etc.). For diesel cars there are two subsectors (<2.0 L and > 2.0 L), each containing seven technology classes. A mix of urban (14% of distance), rural (9% of distance) and highway (76% of distance) driving is

Table 1
Irish private car fleet composition.

Engine size (L)	Fuel	Number of vehicles	Private car fleet (%)
<1.4	Gasoline	963,044	49.9
1.4–2.0		543,080	28.1
>2.0		53,251	2.8
<2.0	Diesel	320,073	16.6
>2.0		50,571	2.6
Total		1930,019	100

considered with average speeds of 40 km/h (rural), 60 km/h (urban) and 100 km/h (highway). The vehicles are allocated to European emission standards on the basis of their age and application dates of the standards in Ireland.

The temperature data required for the COPERT models is sourced from the European Climate Assessment and Dataset (2010). For 2006–2008, the 2005 advanced fuel specification provided by COPERT 4 is used. However, for the 2009–2020, despite there being an advanced fuel specification provided by COPERT 4 for 2009 stage fuel, the fuel specifications defined in the Air Pollution Act 1987 are utilized (Irish Statue Book, 2003). The only difference being that the 2009 stage fuel specifications, have a reduced sulphur content from 50 ppm (ppm) to 10 ppm. The polycyclic aromatic hydrocarbon value given in the Irish Statutes is in % m/m, and not in % v/v as demanded by COPERT 4, so the default figure was used.

2.2. Employment and passenger car kilometres in the GDA

In 2006, it is estimated that 223,578 individuals travelled to work in Dublin by car. Based on the Central Statistics Office (2010) employment statistics for the nation between 2006 and 2009 and future employment projections by the ESRI (Bergin et al., 2010), the number of individuals who will potentially travel to work by car to Dublin in 2020 is forecast. Under a low growth scenario, the ESRI predict that annual employment will increase by 1.9% and 0.9% between 2011 and 2015 and between 2015 and 2020. By applying the national employment statistics to the GDA, we estimate that about 226,300 people will travel to work by car to Dublin in 2020, of which approximately 156,800 will belong to households with two or more vehicles.

Since we are concerned with annual emissions, the daily trip kilometres are calculated on an annual level, assuming that an individual completes a daily return work trip in a 220 day year. The average distance travelled to work in Dublin was 15.3 km in 2006, which equates to an average annual distance of 6732 km per individual.

2.3. Potential electric vehicle market penetration

The main uncertainty of the study is without any doubt the estimation of the future market penetration of EVs into the motor industry. The accurate prediction of market penetration includes great uncertainties and depends on a multitude of influencing factors (i.e. fossil fuel price, national incentive schemes and new developments in EV technology). In this study the rate of market penetration was estimated using a logistic *S*-curve. This methodology is in keeping with other studies, which have used *S*-curves to predict the market penetration of new technologies. These include Draper et al. (2008), who employed *S*-curves to predict the economic impact of EV adoption in the United States and Smith (2010), who utilized *S*-curves to predict the penetration of PHEVs into the Irish car market.

The shape of the curve is determined by specifying 2 years and the expected market penetration of EVs at those particular years. Assuming that EV sales commence in 2011 and that 90% market penetration is achieved by 2035 we explore the reduction in emissions under three different market penetration scenarios, 'high', 'medium' and 'low' (Fig. 2). In this case, market penetration refers to the penetration of annual sales – penetration of the entire car fleet would take significantly longer. Un-

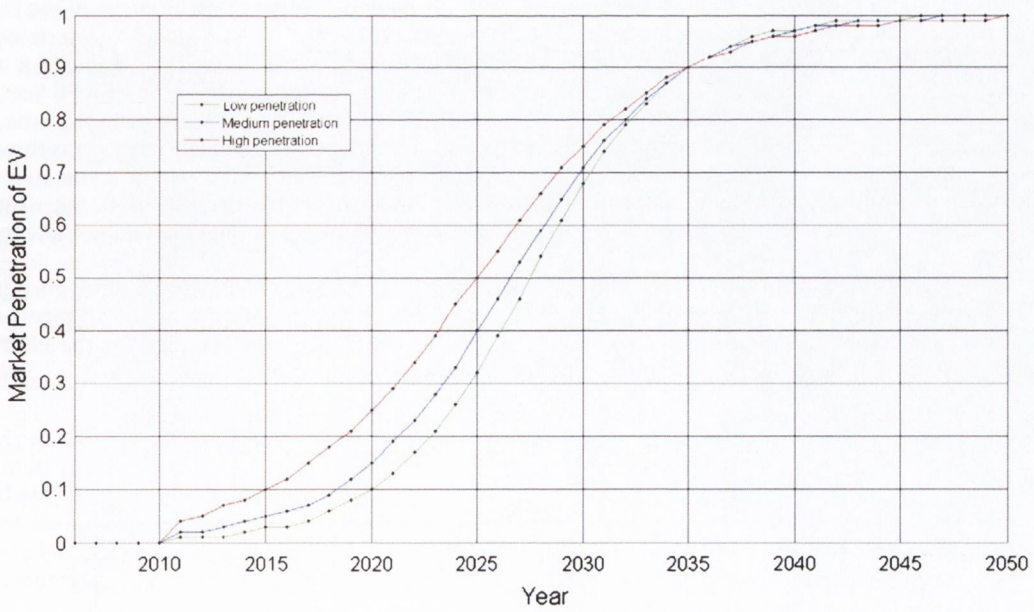

Fig. 2. Projected EV market penetration under three scenarios 'high', 'medium' and 'low'.

der the 'high' penetration scenario it is assumed that EVs will achieve 25% market share by 2020; under the 'medium' and 'low' scenarios, a share of 15% and 10% respectively. A Business as Usual (BAU) or baseline scenario was also investigated.

From the analysis of the Society of Irish Motor Industry's (2010) new vehicle registration statistics over 2000–2007, an average of 79,512 new cars were registered in the GDA per annum. Due to the deterioration of the economy, new car registrations significantly decreased to 63,557 and 26,265 in 2008 and 2009. Early indications for June 2010 suggest a recovery in the industry with a 42% increase in sales over the same period in 2009. We assume that the industry will return to its position where it otherwise would have been by 2020, prior to the global economic recession and that there will be approximately 79,500 new cars registered in the GDA each year up to, and including, 2020.

Numerous studies have shown that the proportion of households with at least two cars is considerably higher in rural than in the urban areas largely because individuals living in cities have better access to a more frequent public transport system (Commins and Nolan, 2009; Scottish Executive, 2005). Only 65% of households own two or more vehicles in the GDA. Based on the technical features such as the driving range achievable by current EV models it is likely that EVs will only be purchased with the intention of becoming a household's secondary vehicle. Therefore we assume that only households with two or more cars would consider purchasing an EV. This reduces the potential market to some 51,700 sales per year.

Due to the extended driving range achievable by PHEVs, we assume that PHEVS are viable substitutes for all ICEVs with an engine size between 1.4 and 2.0 L, but that battery electric vehicles (BEV) will only replace ICEVs with an engine size less than 1.4 L, which have a lower than average annual mileage (Howley et al., 2009a). In the case of PHEVs, the fraction of the trip completed in all electric driving (ED) mode is difficult to determine. According to Smith (2010) and Parks et al., (2007) the fraction of the trip completed in ED mode is dependent on trip length, the kinematic profile, driving habits and the PHEV operational mode. Smith (2010) reports that some current PHEV models such as the Chevrolet Volt and Volkswagen VW "twindrive" have 100% performance capacity and are capable of travelling 40 km or more in ED mode (Tate et al., 2008; Volkswagen AG., 2008). It is expected that in the future all PHEV models will have 100% performance capacity in ED mode and that the combustion engine will only serve as a means of extending the driving range. In 2006, 93% of commuters travelled less than 40 km to work in Dublin. Therefore for simplicity it is assumed that all trips to work are completed in ED mode and hence produce no tailpipe emissions.

The range of market penetration scenarios is large (Simpson, 2006; Clement et al., 2008). The majority of studies estimate the market penetration of EVs, but few differentiate between PHEVs and BEVs. We assume that PHEVs will become widely available in the near future and that rapid growth will lead to mass commercialisation. We do not, however, expect mass market penetration of BEVs for a number of years due to the premium price and limited consumer acceptance with regard to recharging times and driving range. The Irish Electricity Utility, the Electricity Supply Board, which is responsible for the development of the national EV charging infrastructure, forecast that in 2020 the EV fleet in Ireland will consist of 70% PHEVs and 30% BEVs (Mulvaney, 2010). Table 2 presents the projected composition of the commuter fleet in 2020 under each of the investigated scenarios.

2.4. Energy requirement of electric vehicles and the emission intensity of the national grid

In estimating the potential GHG and urban air quality benefits from the deployment of EVs, it is necessary to account for the emissions impact of electricity generation. In order to quantify the potential electrical requirement of the EV fleet, it is first necessary to quantify the energy required to move a vehicle. Smith (2010) developed a model to determine the minimum theoretical energy required to move a given vehicle a fixed distance over a specific drive cycle and used it to calculate the minimum energy requirement (MER), in W h km^{-1}, of a range of vehicles representative of the Irish PC fleet, operating over a selection of legislative and real-world drive cycles. A MER of 105 W h km^{-1} for a PHEV on an Irish drive cycle was calculated. Allowing for inefficiencies between the wall socket/tyre–road interface (75%) and efficiency gains through regenerative braking (60%), this increases to 140 W h km^{-1} and is referred to as the wall socket electrical energy requirement (WSER). Losses that occur during the generation, transmission and distribution of electricity must also be taken into account. The Irish electricity supply efficiency is expected to be 67% in 2020. We therefore expect the WSER to translate to a primary energy requirement (PER) of 0.209 kW h km^{-1}.

Thomas (2009) reports that under optimum conditions, the average fuel economy of a BEV is 2.6 times greater than that of an ICE engine, giving a specific energy consumption of 0.26 kW h km^{-1}. However, Foley et al. (2010) report that under real-world driving conditions specific energy consumption is 10–25 kW h/70 km. We assume that the electric energy requirement of a PHEV and a BEV is 0.209 kW h km^{-1} and 0.25 kW h km^{-1} respectively.

Table 2
Projected composition of the commuter fleet.

Technology	BAU	High	Medium	Low
ICEV	226,300	161,398	193,037	206,186
BEV	0	19,471	9979	6034
PHEV	0	45,431	23,284	14,080
Total	226,300	226,300	226,300	226,300

Table 3
Emission results.

Pollutant	2010	BAU 2020	% Change from 2010	High Scenario	% Change from BAU 2020	Medium Scenario	% Change from BAU 2020	Low Scenario	% Change from BAU 2020
Tailpipe CO_2	337,102	317,700	−6	248,678	−22	282,316	−11	296,296	−7
Grid CO_2	–	–	–	37,999	–	19,475	–	11,776	–
Net CO_2	337,102	317,700	−6	286,677	−10	301,791	−5	308,072	−3
CH_4	28.54	13.02	−54	11.38	−13	12.18	−6	12.51	−4
N_2O	5.24	7.03	34	4.42	37	5.69	−19	6.22	11
CO	3,384.65	828.60	−76	713.85	−14	769.75	−7	792.99	−4
VOC	376.71	113.37	−70	94.26	−17	103.57	−9	107.44	−5
NO_X	283.79	200.50	−29	148.80	−26	172.38	−14	182.19	−9
NO_2	41.46	13.30	−68	13.16	−1	13.23	−0.54	13.25	−0.34
$PM_{2.5}$	29.93	21.30	−29	15.90	−25	18.53	−13	19.62	−8
PM_{10}	42.31	35.12	−17	25.76	−27	30.32	−14	32.22	−8

Note: All values are in tonnes.

In 2008 the carbon intensity of the Irish electricity supply was 582 g CO_2/kW h (Howley et al., 2009b). Wind generation is steadily growing and accounted for 10% of electricity generation in 2009 and overall, the share of electricity generated from renewable energy sources accounted for 14.4% (Dennehy et al., 2010).[2] The high levels of growth in wind generation are expected to continue into the next decade as the Irish government have set a national target of deriving 40% of electricity from renewable resources by 2020. Taking into account the combined measures of increasing the share of renewable generation and improvements in the overall efficiency of the electricity supply, we assume that the carbon intensity of the electricity supply will be 393 g CO_2/kW h in 2020.

3. Results

Current emissions levels for 2010, and projected emissions under three EV market penetration scenarios and a BAU scenario 2020 were estimated in this study. Table 3 presents both the estimated tailpipe emissions and the emissions due to electricity generation for each of the scenarios investigated. The results show that each of the EV scenarios examined would realise a net reduction in CO_2 emissions and tailpipe air pollutants. BAU or baseline CO_2 emissions for 2020 are projected to be 318 Kt CO_2, a 6% reduction on 2010 levels. The 'high' and 'medium' market penetration scenarios demonstrate that a net reduction in CO_2 emissions of 10% and 5% could be achieved. Under the most likely scenario of 10% market penetration, the findings suggest a possible a net reduction of 3% in CO_2 emissions.

The results for the BAU scenario suggest that there will be significant reductions in CO, VOC, PM, NO_2 and NO_X emissions in 2020, without the introduction of EVs to the fleet. These reductions can be attributed, the introduction of Euro 5 and Euro 6 emissions standards, which have stricter limits on pollutant emissions and the retirement of older higher pollutant emitting vehicles from the fleet. The greatest reduction is, consequently, predicted for CO (76%) and VOCs have a similar expected evolution (70%). The results also showed considerable reductions of 68% and 54% for NO_2 and CH_4 emissions respectively. The Euro 5 and 6 emissions standards will require NO_X emissions to be reduced by 25–50%, therefore a 29% reduction in NO_X emissions is as expected.

The introduction of EVs exhibits superiority in further reducing all road traffic related emissions. A comparison between the EV adoption scenarios examined demonstrates that the 'high' adoption scenario would result in the largest decrease in overall emissions. Under the most probable scenario, a 10% market penetration by the 2020, the results indicate a modest reduction in emissions. A further 8% reduction on the BAU scenario for $PM_{2.5}$ and PM_{10} is observed. Globally, VOCs contribute to the formation of ozone (O_3) which can lead to the production of photochemical smog in urban areas. Whilst Ireland does not experience smog pollution, the introduction of EVs could further reduce emissions by 5%. By 2020, NO_X emissions are expected to decrease by a further 9% relative to the BAU scenario. Projected reductions in CO and NO_2 emissions are the lowest at 4% and <1%.

4. Conclusions

Our study shows that the introduction of EVs presents an advantage over the BAU case in every aspect of their emissions. Under the most likely scenario the results indicate a net reduction of 3% in CO_2 emissions relative to the BAU case could be achieved. These results are only mildly encouraging as the CO_2 emissions emitted from commuting in Dublin will most likely only account for approximately 2% of the CO_2 emissions from the transport sector in 2020. Urban air pollutants are individually projected to decrease by up to 11% under the most likely 'low' market penetration scenario. Due to the displacement of tailpipe emissions from densely populated areas to remote electricity generation sites, moderate pollution exposure benefits

[2] This suggests that Ireland has surpassed the mandatory EU interim target of 13.2% for 2010 as outlined in the EU Directive (2009/28/EC).

could be realised. The results thus indicate that the time required for electric vehicles to acquire a significant share of the fleet means they will have limited impact on climate change and urban air quality for at least the next decade but supports existing evidence that EVs are a realistic alternative to ICEVs in the long term and can contribute to emissions reductions.

Acknowledgements

The authors would like to thank the programme for research in third level institutions (PRTLI IV) for funding this research, the Economic and Social Research Institute and the Society for the Irish Motors Industry for providing the ISus car model data and the vehicular sales data. The author would also like to thank the Central Statistics Office of Ireland for providing the POWCAR dataset. The authors would like to thank the referees for their helpful suggestions to improve the original manuscript.

References

Bergin, A., Conefry, T., Fitz Gerald, J., Kearney, I., 2010. Recovery Scenarios for Ireland: An Update. The Economic and Social Research Institute, Dublin.
Central Statistics Office, 2007a. Transport 2006. CSO, Dublin.
Central Statistics Office, 2007b. Central Statistics Office, Census of Population of Ireland 2006, Place of Work, Census of Anonymised Records (POWCAR) Users Guide, CSO, Dublin.
Central Statistics Office, 2010. Principle Statistics: Employment and Unemployment (ILO) '000s. CSO, Dublin.
Clement, K., Heasen, E., Driesen, K., 2008. The impact of charging plug-in hybrid electric vehicles on the distribution grid. In: Proceedings 2008–4th IEEE BeNeLux Young Researchers Symposium in Electrical Power Engineering, Eindhoven.
Commins, N., Nolan, A., 2008. The Determinants of Mode of Transport to Work in the Greater Dublin Area. ESRI Working Paper No. 268. The Economic and Social Research Institute, Dublin.
Commins, N., Nolan, A., 2009. Car Ownership and Mode of Transport to Work in Ireland. ESRI Working Paper No. 310. The Economic and Social Research Institute, Dublin.
Dempsey, N., 2008. Government Announces Plans for the Electrification of Irish Motoring. Department of Transport, Dublin (Press Release, 26 November 2008).
Dennehy, E., Howley, M., Ó Gallachóir, B., Barriscale, A., 2010. Renewable Energy in Ireland 2010 Update. Sustainable Energy Ireland, Dublin.
Draper, M., Rodriguez, E., Kaminsky, P., Sidhu, I., Tenderich, B., 2008. Economic Impact of Electric Vehicle Adoption in the United States. University of California, Berkeley.
Electric Power Research Institute, 2007. Environmental Assessment of Plug-In Hybrid Electric Vehicles. Electric Power Research Institute, University of California, Davis.
Environmental Protection Agency, 2009. Ireland's Greenhouse Gas Emissions in 2008. Environmental Protection Agency, Wexford.
European Climate Assessment and Dataset, 2010. <http://eca.knmi.nl/dailydata/customerquery.php> (accessed 15.01.10).
Foley, A.M., Leahy, P.G., McKeogh, E.J., Ó Gallachóir, B.P., 2010. Quantifying displaced carbon dioxide emissions from electric vehicles in Ireland, Proceedings of the Irish Transport Research Network 2010, University College Dublin.
Gkatzoflias, D., Kouridis, C., Nlziachristos, L., 2007. COPERT 4: Computer Programme to Calculate Emissions from Road Transport. European Environmental Agency. Brussels.
Hennessy, H., Tol., R., 2010. The Impact of Climate Policy on Private Car Ownership in Ireland. Working Paper No. 342. Economic and Social Research Institute, Dublin.
Howley, M., Dennehy, E., Gallachóir, B.Ó., 2009a. Energy in Transport 2009 Report. Sustainable Energy Ireland, Dublin.
Howley, M., Ó Gallachóir, B., Dennehy, E., 2009b. Energy in Ireland Key Statistics 2009. Sustainable Energy Ireland, Dublin.
Irish Statute Book, S.I. No. 541/2003. Air Pollution Act, 1987 (Environmental Specifications for Petrol and Diesel fuels) Regulations 2003. Stationary Office, 2003, Dublin.
Kousoulidou, M., Ntziachristos, L., Mellios, G., Samaras, Z., 2008. Road-transport emission projections to 2020 in European urban environments. Atmospheric Environment 42, 7465–7475.
Lilienthal, P., Brown, H., 2007. Tackling Climate Change in the U.S.: Potential Carbon Emissions Reductions from Plug-in Hybrid Electric Vehicles by 2030. American Solar Energy Association.
Morgenroth, E.L.W., 2001. Analysis of the Economic, Employment and Social Profile of the Greater Dublin Region (Dublin and Mid East Regions). The Economic and Social Research Institute, Dublin.
Parks, K., Denholm, P., Markel, T., 2007. Costs and Emissions Associated with Plug-In Hybrid Vehicle Charging in the Xcel Energy Colorado Service Territory. National Renewable Energy Laboratory.
Scottish Executive, 2005. Migration and Commuting in Urban and Rural Scotland – Statistics from Census 2001. The Scottish Government. Edinburgh.
Simpson, A., 2006. Cost–benefit analysis of plug-in hybrid electric vehicle technology. In: Proceedings of the 22nd International Battery, Hybrid and Fuel Cell Electric Vehicle Symposium and Exhibition. Yokohama.
Smith, W.J., 2010. Plug-in hybrid electric vehicles – a low-carbon solution for Ireland? Energy Policy 38, 1485–1499.
Tate, E.D., Harpster, M.O., Savagian, P., 2008. The electrification of the automobile: from conventional hybrid, to plug-in hybrids, to extended-range electric vehicles. SAE Technical Paper Series 2008-01-0458.
Thomas, S., 2009. Transportation options in a carbon-constrained world: Hybrids, plug-in hybrids, biofuels, fuel cell electric vehicles, and battery electric vehicles. International Journal of Hydrogen Energy 34, 9279–9296.
Volkswagen, AG., 2008. Green power via the electric socket will drive the cars of tomorrow. P:News No. 3, July–August 2008, p. 7. Available from: <http://www.volkswagenag.com/vwag/vwcorp/info_center/en/publications/2008/10/p_news_3_2008.-bin.acq/qual-BinaryStorageItem.Single.File/VW_PN_2008_03_englisch.pdf>.
Turrentine, T., Lee Gosselin, M., Kurani, K., Sperling, D., 1992. A Study of Adaptive and Optimizing Behavior for Electric Vehicles Based on Interactive Simulation Games and Revealed Behavior of Electric Vehicle Owners. UCTC No. 130. University of California Transportation Center. University of California at Berkeley.